Author:
Gold, Vicki Anne Munro

Title:
The SecA ATPase reaction cycle and its consequence in protein translocation.

The SecA ATPase Reaction Cycle and its Consequence in Protein Translocation

Vicki Anne Munro Gold

A dissertation submitted to the University of Bristol in accordance with the requirements of the degree of Doctor of Philosophy in the Faculty of Medical and Veterinary Sciences.

Department of Biochemistry

January 2008

Word Count: 55,501

Some text bound close to the spine.

Abstract

Molecular motors have evolved to interconvert chemical energy and mechanical work. They have been exploited to drive a number of processes that are central to cell biology, such as protein translocation. In bacteria, the SecA motor ATPase associates with a ubiquitous channel SecYEG where it drives the post-translational secretion of pre-proteins across the plasma membrane. In spite of the recent progress within the field, there are several disputed and outstanding aspects of the reaction mechanism.

Steady-state analysis revealed an inhibitory allosteric binding site for magnesium, which exerted a strong influence on the turnover and affinity for ATP. The inhibited and activated forms of the enzyme were studied by analytical ultracentrifugation; both of them were dimers that interconvert via a large conformational change. ADP was found to inhibit the ATPase activity in a competitive manner, stabilising the steady-state complex SecA-ADP and preventing the rate-limiting release of the product. SecA in this state binds to solubilised SecYEG with low affinity, but turnover is dramatically increased in the presence of the *E. coli* solubilised bilayer lipid cardiolipin, found to be specifically bound to the SecYEG complex.

Activation of SecA was achieved in the presence of SecYEG associated with membranes containing cardiolipin. However, a yet further increase in activity was reached in the presence of the same proteoliposomes, together with the pre-protein substrate proOmpA. The substrate induced stimulation coincidental with a switch of the steady-state complex to SecA-ATP, where ATP hydrolysis is now the rate limiting step. This information has been used to build a kinetic model of pre-protein translocation through the SecYEG channel by the SecA motor ATPase.

Acknowledgements

A number of people have offered help and advice to me throughout the course of my PhD that I would like to acknowledge.

Firstly, Professor Tony Clarke and Dr Gus Cameron for all of their assistance in data fitting, invaluable discussions and for helping me to understand enzyme kinetics a little better.

Thanks also go to Professor Steve Halford and Professor Dek Woolfson for use of their Analytical Ultracentrifuges. For teaching me the technique and the complexities of data analysis, I would particularly like to acknowledge Dr Emma Longman and Dr Lucy Catto.

I would especially like to thank my supervisor Dr Ian Collinson, for all of his ideas, support and encouragement. I am also grateful to Dr Alice Robson and all who have helped us in lab C100 over the last three years.

Finally I wish to thank all members of my family who have always encouraged and supported me throughout.

Authors Declaration

I declare that the work in this dissertation was carried out in accordance with the Regulations of the University of Bristol. The work is original, except where indicated by special reference in the text, and no part of the dissertation has been submitted for any other academic award. Any views expressed in the dissertation are those of the author.

SIGNED....V.M.Addy.....

DATE....31/01/08.....

Table of Contents

Table of Figures

Table of Tables

Table of Equations

Abbreviations

CL	Cardiolipin
DOPE	1,2-Dioleoyl-sn-Glycero-3-Phosphoethanolamine
DOPG	1,2-Dioleoyl-sn-Glycero-3-[Phospho-rac-(1-glycerol)]
DDM	n-Dodecyl β-D-maltoside
DTT	Dithiothreitol
ER	Endoplasmic Reticulum
FRET	Fluorescence Resonance Energy Transfer
HEPES	4-(2-hydroxyethyl)-1-piperazineethanesulfonic acid
HPLC	High Performance Liquid Chromatography
IMVs	Inner Membrane Vesicles
IRA	Internal Regulator of ATPase Activity
LB	Luria-Bertani
MESG	2-amino-6-mercapto-7-methylpurine riboside
NBF	Nucleotide Binding Fold
PC	Phosphatidylcholine
PE	Phosphatidylethanolamine
PEP	Phosphoenolpyruvate
PG	Phosphatidylglycerol
PK/LDH	Pyruvate Kinase / Lactate Dehydrogenase
PNP	Purine Nucleoside Phosphorylase
RB	Reconstitution Buffer
SDS-PAGE	Sodium Dodecyl Sulfate - Polyacrylamide Gel Electrophoresis
SD	Standard Deviation
SE	Standard Error
SRP	Signal Recognition Particle
TB	Transfer Buffer
TK buffer	50 mM triethanolamine, pH 7.5, 50 mM KCl
TKM buffer	50 mM triethanolamine, pH 7.5, 50 mM KCl, 2 mM $MgCl_2$
TLC	Thin Layer Chromatography
TM	Transmembrane

Chapter 1

Introduction

1.1 Protein Translocation

The cell is defined and compartmentalised by membranes composed of hydrophobic lipid bilayers that pose a barrier to hydrophilic solutes, including polypeptides. The majority of proteins are synthesised in the cytosol, thus many of them need to negotiate this barrier posed by the membrane. The targeting and passage of proteins through, or in the case of membrane proteins, into the membrane is a process that requires the assistance of complex proteinaceous energy transducing machines; this is generally referred to as protein translocation.

1.1.1 The nature of the lipid membrane

The lipid membrane was proposed to form a bilayer of amphipathic molecules with polar headgroups on the exterior and hydrophobic fatty acid tails facing inwards (Gorter et al., 1925). The polar hydrophilic surface of the membrane had been proposed to interact with water, where as the hydrophobic interior was impermeable to polar molecules (Langmuir, 1917). This explained how the membrane structure could act as such a permeability barrier.

With the development of electron microscopy techniques, both inner and outer membrane leaflets could be visualised, between which was an internal intermembrane space (Robertson, 1959). Some years following, the fluid mosaic model predicted that proteins may either be peripherally attached to the membrane by weak attachments,

or may form an integral part of the membrane, either adsorbed to the surface or spanning the entire width (Singer and Nicolson, 1972). The nature of membrane spanning domains was found to be hydrophobic, explaining their stability within the amphipathic lipid structure (Unwin and Henderson, 1984).

1.1.2 The signal sequence hypothesis

In 1971 a hypothesis was advanced, suggesting that nascent protein chains emerging from ribosomes in the cytosol would carry an N-terminal sequence of amino acids that would be recognised by a factor mediating its targeting to the endoplasmic reticulum (ER) membrane (Blobel and Sabatini, 1971). One seminal experiment subsequently discovered that mouse myeloma mRNA encoded a polypeptide 1.5 kDa larger than the mature immunoglobulin light chain (Milstein et al., 1972). This work culminated in a detailed version of the signal sequence hypothesis for passage of proteins across the ER (Blobel and Dobberstein, 1975). A number of other organelles were also shown to have the ability to import externally added protein substrates, such as the mitochondria (Maccecchini et al., 1979), and the chloroplast (Chua and Schmidt, 1978), as well as the bacterial envelope (Chen and Tai, 1985; Muller and Blobel, 1984).

1.1.3 Proteins can be translocated in a folded or unfolded manner

The majority of protein translocation concerns proteins presented in an unfolded conformation. However, folded proteins and even oligomeric complexes can be imported into the peroxisome (McNew and Goodman, 1994), the chloroplast (Clark and Theg, 1997) and through the nuclear pores (Dworetzky and Feldherr, 1988; Feldherr et al., 1984). The Sec (Secretion) pathway is conserved within all three domains of life and is restricted to unfolded protein import (Arkowitz et al., 1993). However, folded titin and dihydrofolate reductase domains can be presented in tertiary structure and subsequently unfolded in the bacterial system (Arkowitz et al., 1993; Nouwen et al., 2007).

Bacteria have developed a specialised system for the transport of folded proteins, mainly those which must bind redox cofactors in the cytosol (Berks, 1996). The TAT (Twin-Arginine Translocation) system was originally discovered in the chloroplast, where translocation of pre-proteins is driven by the pH difference across the thylakoid membrane (Mould and Robinson, 1991). This system exports proteins with an invariant twin-arginine motif present in the signal sequence (Berks, 1996). Translocation can also occur across multiple membranes simultaneously. For example the Type III secretion system of pathogenic bacteria can inject proteins across both plasma membranes and a target cell plasma membrane through a single translocase (Cornelis, 2006).

The multiple protein import machineries are often unrelated, but they do share general operational principles. In most cases, pre-proteins engaged with either the ribosome or a chaperone protein bind to a specific receptor on the target membrane, transfer the pre-protein to an import channel where it is translocated either completely across the membrane, or laterally into it by an energy transducing reaction. Of these systems, only the Sec pathway is ubiquitous.

1.2 The Sec Translocation Complex

The Sec pathway is found in the plasma membrane of bacteria and archaea (SecY) and in the ER of eukaryotic cells (Sec61). Two modes of translocation (co- and post-translational) converge on the Sec complex, which is a highly versatile and dynamic structure capable of conducting large substrates both laterally into, and across the membrane (Robson and Collinson, 2006).

The majority of proteins that are destined for secretion by the Sec complex carry an N-terminal signal sequence, which is recognised by specific targeting factors (Walter and Blobel, 1981). Exceptions to this rule include some membrane proteins, which can be translocated without assistance from a such a sequence (Dalbey et al., 1995). Instead, insertion into the membrane is mediated by signals contained within the first transmembrane segment (Monne et al., 1999; Nilsson et al., 2000).

The important features of the Sec pathway signal sequence are the N-terminal positive charge, thought to increase translocation efficiency (Akita et al., 1990), and a hydrophobic core region with a threshold hydrophobic density (Doud et al., 1993; von Heijne, 1985). Primary sequence homology is extremely variable, yet these general features remain across the three domains of life (Pohlschroder et al., 1997). The attributes which direct a pre-protein to either the co- or post-translational route are assumed to be due to the hydrophobicity, however these pathways are not necessarily mutually exclusive (Facey et al., 2007; Karamyshev and Johnson, 2005; Kebir and Kendall, 2002; Peterson et al., 2003; Qi and Bernstein, 1999). Those proteins with a greater hydrophobic charge tend to utilise the co-translational route, whereas signal sequences with a smaller hydrophobic core are more often associated with the post-translational pathway (Beck et al., 2000; Huber et al., 2005; Karamyshev and Johnson, 2005; Lee and Bernstein, 2001; Müller et al., 2001; Neumann-Haefelin et al., 2000; Valent et al., 1998; Yi et al., 2004).

1.2.1 Co-translational translocation

The event of co-translational translocation occurs by essentially the same mechanism in every cell. The ribosome-nascent chain complex is targeted to the membrane courtesy of the signal recognition particle (SRP) and its receptor (Gilmore and Blobel, 1983; Walter et al., 1981) (Figure 1-1). The SRP is composed of one or more proteins and an RNA molecule. *E. coli* SRP is composed of a single polypeptide named Fifty-four homologue (Ffh) as it is homologous to SRP54, one of the GTP binding peptide components of the eukarytotic SRP (Römisch et al., 1989). The SRP receptor (SR) in *E. coli* is FtsY in the cytoplasmic membrane; the eukaryotic counterpart is found on the ER membrane. Polypeptide components of SRP and SR are GTPases, indicating a regulatory and targeting role for the GTP binding domains (Walter and Johnson, 1994).

SRP binds to the emerging signal sequence on the ribosome nascent chain and this complex is relayed to the membrane by virtue of the SR (Gilmore et al., 1982; Luirink et al., 1994). In eukaryotes SRP binding has the ability to arrest protein synthesis, enabling sufficient time for diffusion to the ER membrane (Halic et al., 2004; Walter and Blobel, 1981). The SRP and SR associate in their GTP bound forms (Egea et al., 2004; Focia et al., 2004; Miller et al., 1993) and subsequent reactions that are not fully understood deliver the translating ribosome to the SecY/Sec61 complex (Neuhof et al., 1998; Song et al., 2000). Finally, the SRP and SR dissociate on GTP hydrolysis (Connolly et al., 1991).

In the ribosome-Sec complex associated state, the ribosomal polypeptide exit site is located in close vicinity to the Sec channel pore (Beckmann et al., 2001), enabling protein translocation to be driven by the concomitant chain elongation (Gorlich et al., 1992; Görlich and Rapoport, 1993). GTP hydrolysis by the ribosome during translation provides the energy requirement for translocation, thus eliminating the requirement for a specific motor protein to provide the driving force. This method of translocation is responsible for transport and subsequent insertion of most membrane proteins in bacteria (Karamyshev and Johnson, 2005; Neumann-Haefelin et al., 2000).

In eukaryotic cells, the ribosome maintains the permeability barrier of the membrane in the cytosol by interaction with Sec61 (Crowley et al., 1994a). Within the lumen of the ER, the pore is thought to be sealed by BiP, an Hsp70 homologue, which notably has a key role in eukaryotic post-translational translocation. (Haigh and Johnson, 2002; Hamman et al., 1998). When BiP is in an ADP-bound conformation, the Sec61 channel is sealed, where as on ATP binding the channel is opened (Alder et al., 2005). The BiP seal is disrupted once the nascent chain reaches 70 amino acid residues in length, enabling the protein to pass directly into the lumen (Crowley et al., 1994b; Hamman et al., 1998).

1.2.2 Post-translational translocation

In contrast to co-translational translocation, the post-translational route in eukaryotes and prokaryotes operate by entirely different mechanisms. Both however require interaction with cytosolic chaperones after release from the ribosome, to maintain pre-proteins in a translocation competent state.

1.2.2.1 Eukaryotes

In eukaryotes the post-translational import into the ER lumen relies on the motor ATPase BiP (Kar2p in yeast). This acts by preventing the retrograde transport of a substrate by using ATP to effectively pull the polypeptide chain in a ratchet-like mechanism (Matlack et al., 1999; Misselwitz et al., 1999; Panzner et al., 1995; Rapoport et al., 1999). Movement of the polypeptide across the membrane results when ATP-bound BiP binds to the luminal J domain of a membrane component Sec63 (Brodsky and Schekman, 1993). This stimulates the ATPase and enables interaction with the incoming polypeptide chain (Matlack et al., 1999). The pre-protein is prevented from backsliding, and after the chain has translocated a sufficient distance, another BiP molecule can bind. The result is a mechanism likened to a Brownian ratchet (Matlack et al., 1999).

1.2.2.2 Prokaryotes

Bacteria have adopted a different method, which pushes proteins across the SecY channel by employing a cytosolic motor protein ATPase SecA (Brundage et al., 1990; Hartl et al., 1990) (Figure 1-1). To maintain a translocation competent conformation of the pre-protein and to prevent premature folding and aggregation, a cytosolic component SecB is required (de Keyzer et al., 2002; Hartl et al., 1990; Kusters et al., 1989; Weiss et al., 1988). The mechanism of bacterial post-translational translocation forms the basis of this study and will be discussed in some detail in the following sections.

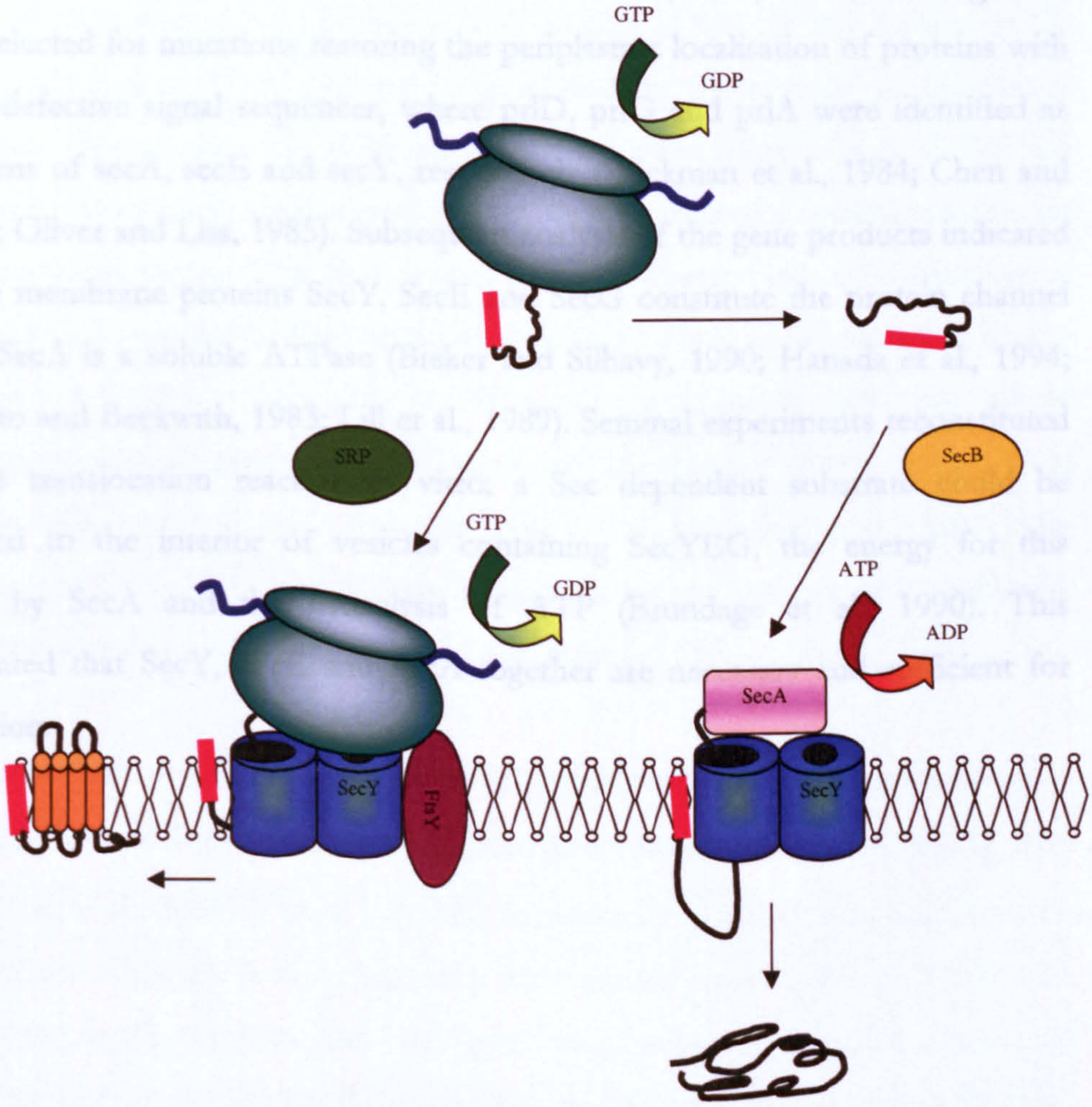

Figure 1-1. Co- and post-translational translocation in bacteria.

Schematic overview of protein translocation and membrane protein insertion through the SecYEG complex in bacteria. Nascent chains possessing an N-terminal signal sequence (red) emerge from the ribosome (green) and are localized to the SecY complex (blue). This occurs either co-translationally by the signal recognition particle (SRP) and its receptor (FtsY; left) or alternatively, pre-proteins can be presented post-translationally by SecA and SecB (right).

1.3 Identification of the Sec Protein Translocation Pathway

Elements of the Sec pathway were identified during the 1980's through different genetic screens conducted with *E. coli*. The genes essential to secretion were distinguished through two main genetic approaches. Conditional-lethal mutations associated with a generalised protein-secretion defect facilitated the identification of the genes secA, secB, secE and secY (Emr et al., 1981; Kumamoto and Beckwith, 1983; Oliver and Beckwith, 1981; Oliver and Beckwith, 1982). The second genetic strategy selected for mutations restoring the periplasmic localisation of proteins with secretion-defective signal sequences, where prlD, prlG and prlA were identified as allelic forms of secA, secE and secY, respectively (Brickman et al., 1984; Chen and Tai, 1985; Oliver and Liss, 1985). Subsequent analysis of the gene products indicated that three membrane proteins SecY, SecE and SecG constitute the protein channel and that SecA is a soluble ATPase (Bieker and Silhavy, 1990; Hanada et al., 1994; Kumamoto and Beckwith, 1983; Lill et al., 1989). Seminal experiments reconstituted the entire translocation reaction in vitro; a Sec dependent substrate could be transported to the interior of vesicles containing SecYEG, the energy for this provided by SecA and the hydrolysis of ATP (Brundage et al., 1990). This demonstrated that SecY, SecE and SecA together are necessary and sufficient for translocation.

1.4 The SecY Channel

1.4.1 Structure and oligomeric state of the resting channel

Images recorded by electron cryo-microscopy contain enough detail to reconstruct low-resolution structural information of large biological macromolecules (Crowther et al., 1996). The first pictures of the mammalian Sec complex revealed an oligomeric assembly of an estimated 3-4 complexes with an area of low density formed at the interface (Hanein et al., 1996). This pore aligned with the polypeptide exit channel of the ribosome (Beckmann et al., 1997; Menetret et al., 2000; Morgan et al., 2002), and at the time it was naturally concluded that together they formed a continuous conduit for protein translocation. The first crystal structure determined to a significantly higher resolution was that of the membrane bound *E. coli* SecYEG complex, with a monomeric molecular weight of 74 kDa. Electron microscopy and image reconstruction revealed all 15 of the predicted transmembrane (TM) α-helices, 10 in SecY, 3 in SecE and 2 in SecG (Breyton et al., 2002; Collinson et al., 2001). The arrangement of the SecYEG protomers seen in the resting state on the membrane was that of a dimer in a so-called 'back-to-back' arrangement.

The breakthrough came with the solution of a high resolution X-ray structure of a monomeric archaeal SecYEβ complex in detergent solution, also in its resting state (van den Berg et al., 2004) (Figure 1-2). The sequence of the SecY complex from *M. jannaschii* shares about 20 % homology with the bacterial counterpart and 30 % with the eukaryotic Sec61 complex, and has three fewer helices compared to the *E. coli* version. The most surprising result of this work was the observation of a hydrophilic restriction point in the centre of the monomer. This narrow pore is held closed by a short reinserted loop (the 'plug') and a girdle of hydrophobic side chains.

The most conserved residues in SecY line the channel (van den Berg et al., 2004). The *prl* phenotype is characterised by a diminished requirement for functional signal

peptides (Bieker et al., 1990; Derman et al., 1993), reduced dependence on the proton-motive force, increased translocation rates and increased affinity for SecA by SecYEG (Nouwen et al., 1996; van der Wolk et al., 1998) and weakened SecYEG subunit association (Duong and Wickner, 1999). These mutations therefore modulate the channel function, and importantly map the putative protein path in the centre of SecY (van den Berg et al., 2004).

This putative channel is conveniently located next to the signal sequence binding pocket between TM2 and TM7 (Cannon et al., 2005; Plath et al., 1998), and the pore itself has been shown to form cross-links with mature regions of a translocating pre-protein (Cannon et al., 2005). The periphery of the monomeric complex in its observed state is too hydrophobic to form a protein channel by association with other monomers. Therefore the structure predicts that the protein path is formed through the centre of a single copy of SecY and not at the interface of a larger assembly.

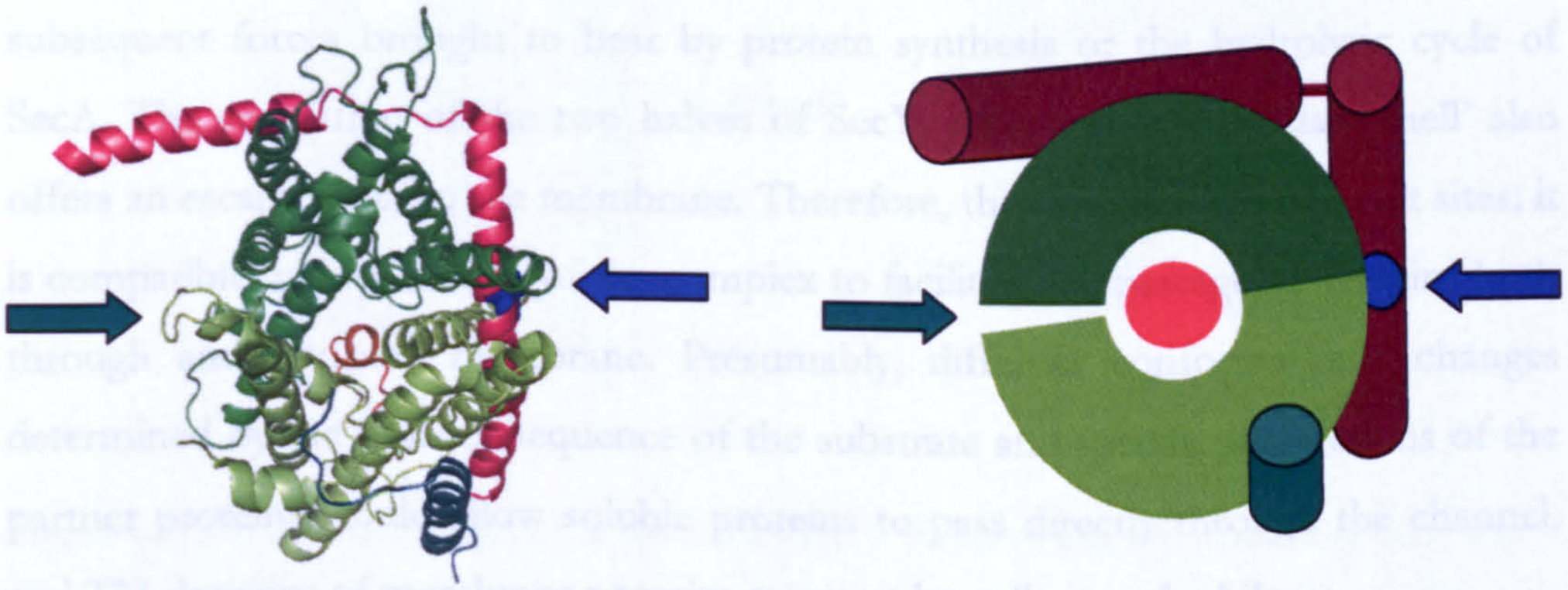

Figure 1-2. Ribbon and schematic representation of the detergent solubilised monomeric *Methanococcus jannaschii* SecYEβ complex, viewed from the cytosolic face (van den Berg et al., 2004).

Transmembrane helices 1-5 are coloured in light green, helices 6-10 dark green, the 'plug' orange, SecE red and Secβ (SecG) is shown in sea green. The crosslinking site between two SecYEGs in the dimer induced by incorporation of the equivalent *E. coli* cysteine (L106C) is indicated in blue, close to the blue arrow. The green arrow denotes the position of the lateral gate.

1.4.2 The active SecY channel

The channel pore is formed between two distinct halves of the SecY protein (helices 1-5 and 6-10) (Figure 1-2). SecE has been proposed to form a clamp to maintain these in close proximity and to keep the channel closed. Release of this grip may bring about a widening of the channel, which has been reported to form an opening of 40 Å (Hamman et al., 1997). The closed state of the channel suggests a pore diameter of 5-8 Å (van den Berg et al., 2004) which is too narrow for the passage of an alpha-helix, however molecular dynamics simulations show that a helix could indeed be transported through (Gumbart and Schulten, 2006). This would require concomitant displacement of the plug domain to a location at the periphery of the complex, in addition to a widening of the central pore to accommodate the substrate protein. These conformational changes are presumably directed by the combination of the association of the partner protein (the ribosome or SecA), insertion of the signal sequence, binding of the translocation substrate (Tam et al., 2005) and subsequent forces brought to bear by protein synthesis or the hydrolytic cycle of SecA. The separation of the two halves of SecY, comparable to a 'clam-shell' also offers an escape route to the membrane. Therefore, the structure has two exit sites; it is compatible with the ability of the complex to facilitate the passage of proteins both through and into the membrane. Presumably, different conformational changes determined by the primary sequence of the substrate and specific interactions of the partner proteins would allow soluble proteins to pass directly through the channel, and TM domains of membrane proteins to move laterally into the bilayer.

The SecG subunit is non-essential for *in vitro* translocation or viability (Hanada et al., 1994; Nishiyama et al., 1994; Nishiyama et al., 1993). Original lines of evidence suggested that the SecA hydrolytic cycle is facilitated by membrane topology inversion of SecG (Nishiyama et al., 1996), but this has been recently disproved by covalent linkage of SecY to SecG whereby translocation was still fully functional (van der Sluis et al., 2006b). SecG has subsequently been shown to assist in the later stages of the SecA ATPase reaction, following the initiation stage of translocation (Duong and Wickner, 1997a). Thus the precise function of this subunit is as yet unresolved.

1.4.3 The importance of the plug domain

The structure of the open state of the SecY channel has not been determined in detail, however, there are a few indicators which imply how it may form. The plug has been shown to cross-link to the C-terminus of SecE, approximately 20Å away from the position identified in the structure (Flower et al., 1995; Harris and Silhavy, 1999; Tam et al., 2005) identifying a potential pocket which it can inhabit during protein translocation (Figure 1-3). A careful inspection of the membrane bound dimer (Breyton et al., 2002) in comparison to the detergent solubilised monomer (van den Berg et al., 2004), indicates that the plug moves about 6 Å towards the outside, and the lateral gate for membrane protein insertion is partially open. In this context, although closed, the channel may be primed for protein translocation (Bostina et al., 2005).

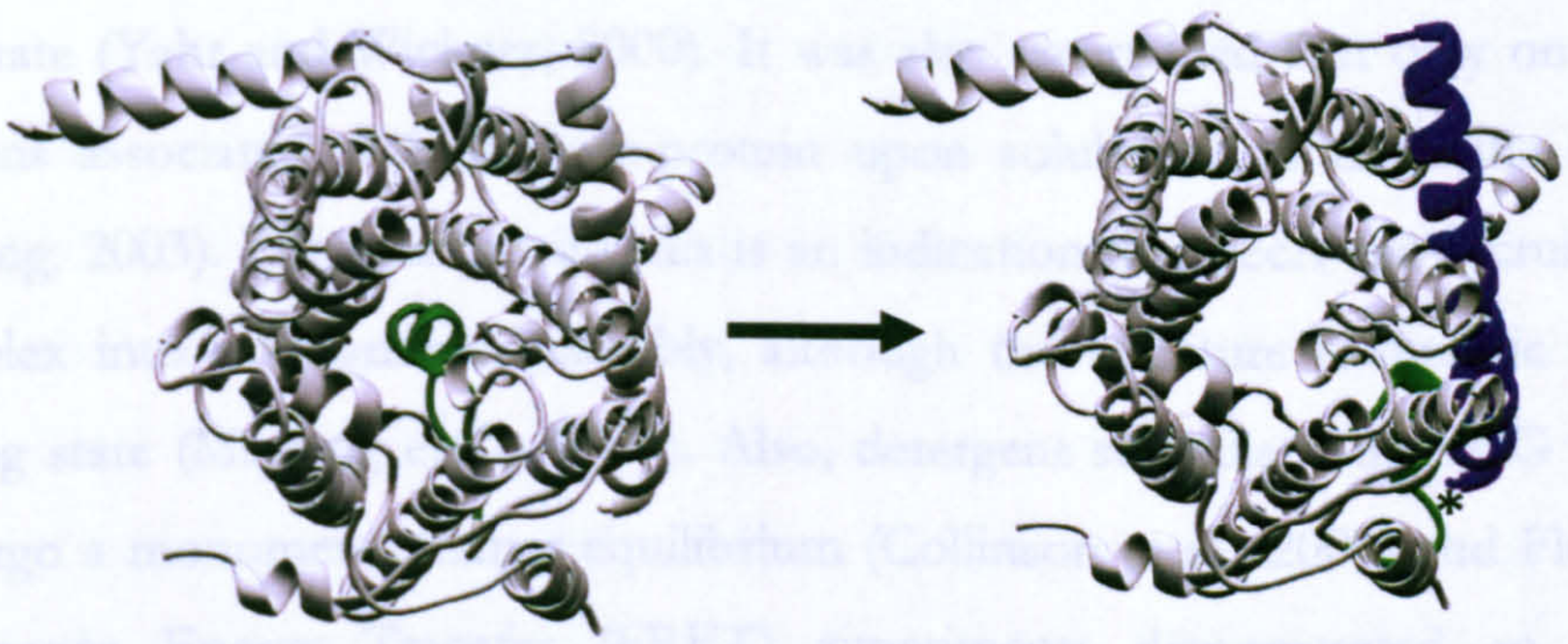

Figure 1-3. Ribbon representation of the channel pore in the closed and open state (van den Berg et al., 2004).

Left; all helicies in *M. jannaschii* SecYEβ are shown in grey, with the exception of the plug which is shown in green. Right; modelled movement of the plug domain towards SecE. The star indicates where the cysteine cross-link forms between the plug and the C-terminus of SecE in *E. coli*.

Locking the plug within the centre of the channel inactivates the translocon (Maillard et al., 2007), but the functionality of the complex is retained by removal of this structure, which results in a *prl*-like phenotype (Li et al., 2007; Maillard et al., 2007). This indicates that the plug is not the only determinant for channel opening. Regulation of the channel is infact maintained in the absence of the plug due to

formation of a new structure from neighbouring residues (Li et al., 2007), maintaining the overall architecture but lacking many interactions, explaining the altered phenotype. Thus the pore ring alone is insufficient to seal the channel, and mutations within this also result in transient channel opening (Saparov et al., 2007). Therefore both the pore ring and the plug domain are collectively likely to serve as the barrier for ions and water (Saparov et al., 2007; van den Berg et al., 2004).

1.4.4 The native state of SecYEG is a dimer

One puzzling aspect of the translocation channel is the active oligomeric state. The monomer appears to provide all of the components for translocation: the signal sequence binding site, the protein-pore, exposed cytosolic loops for partner protein interaction and two potential exit sites. There is also biochemical evidence in support of this particular arrangement, in the context of both the membrane and pre-protein substrate (Yahr and Wickner, 2000). It was also ascertained that only one SecYEG remains associated with the pre-protein upon solubilisation from the membrane (Duong, 2003). Discordant with this is an indication that SecA can recruit the SecY complex into a tetrameric assembly, although the structure is dimeric when in a resting state (Manting et al., 2000). Also, detergent solubilised SecYEG appears to undergo a monomer-tetramer equilibrium (Collinson et al., 2001) and Fluorescence Resonance Energy Transfer (FRET) experiments demonstrated an oligomeric arrangement of two or more subunits in the membrane (Mori et al., 2003; Scheuring et al., 2005). The mammalian Sec61 counterpart is a tetramer while engaged with ribosomes, and the organization of the protomers within this tetramer is a dimer of dimers arranged side-by-side (Menetret et al., 2005).

Notwithstanding this, the widely held consensus is that the bacterial channel is a dimer in its native state, illustrated using a variety of techniques such as cross-linking, native gel electrophoresis, electron cryo-microscopy and analytical ultracentrifugation (Bessonneau et al., 2002; Breyton et al., 2002; Collinson et al., 2001; Mitra et al., 2005; Scheuring et al., 2005; Tam et al., 2005; Tziatzios et al., 2004). Even a covalently linked SecYEG dimer created by fusion of SecY genes was functional both *in vivo* and *in vitro* (Duong, 2003). The reasons for the existence of high oligomeric states are

not entirely clear. It may be for simple reasons of stability; the complex may exist in the membrane with two independent active sites, as many other soluble and membrane proteins do (*e.g.* bacteriorhodopsin (Maillard et al., 2007)) for indeterminate reasons. Alternatively, the dimeric and tetrameric assemblies might be required to provide a large enough platform for the association of the larger partner proteins. This idea has recently been demonstrated in *E. coli* by means of disulphide cross-linking, which established that SecA transfers the pre-protein substrate into a single SecY channel, via direct interaction with the adjacent SecY complex (Osborne and Rapoport, 2007). Specific inter-subunit interactions might also be required to support a dynamic process required for the reaction. Finally, the mechanism might rely on the partner proteins or substrate to introduce an asymmetric element important for the reaction, to generate a single active protomer.

The 'back-to-back' orientation observed by electron cryo-microscopy of the membrane bound form has also been detected biochemically. In this particular SecYEG dimer, the C-terminal TM domain of SecE is located at the interface and the lateral gate for membrane protein insertion (between TM2 & TM7) point in opposite directions and toward the lipid bilayer (Bostina et al., 2005; Breyton et al., 2002; van den Berg et al., 2004) (Figures 1-2 and 1-4). Cysteine mutagenesis experiments have been employed to probe some of the interactions that the SecY complex makes, and they identify residues in SecE that were close to the equivalent helix in the neighbouring monomer (Kaufmann et al., 1999; Veenendaal et al., 2001). This cross-link is enhanced by conditions that promote a productive association of the partner protein SecA (Kaufmann et al., 1999). This cross-linked dimer retained the capacity to tightly bind and activate SecA, but had lost the ability to couple ATP hydrolysis to the work of translocation (Kaufmann et al., 1999). A careful inspection of the position of the respective side chains reveal that, although close, they point away from each another (Figure 1-4). The association of SecA may have perturbed them and brought them closer together, and thus more amenable to cross-linking. The formation of a disulphide in this position would bring about a considerable distortion of the two helices. It is conceivable that this imposed distortion and restriction on the motility at the dimer interface may have had a minor affect on the association with SecA, but a disastrous one for the energy coupling process.

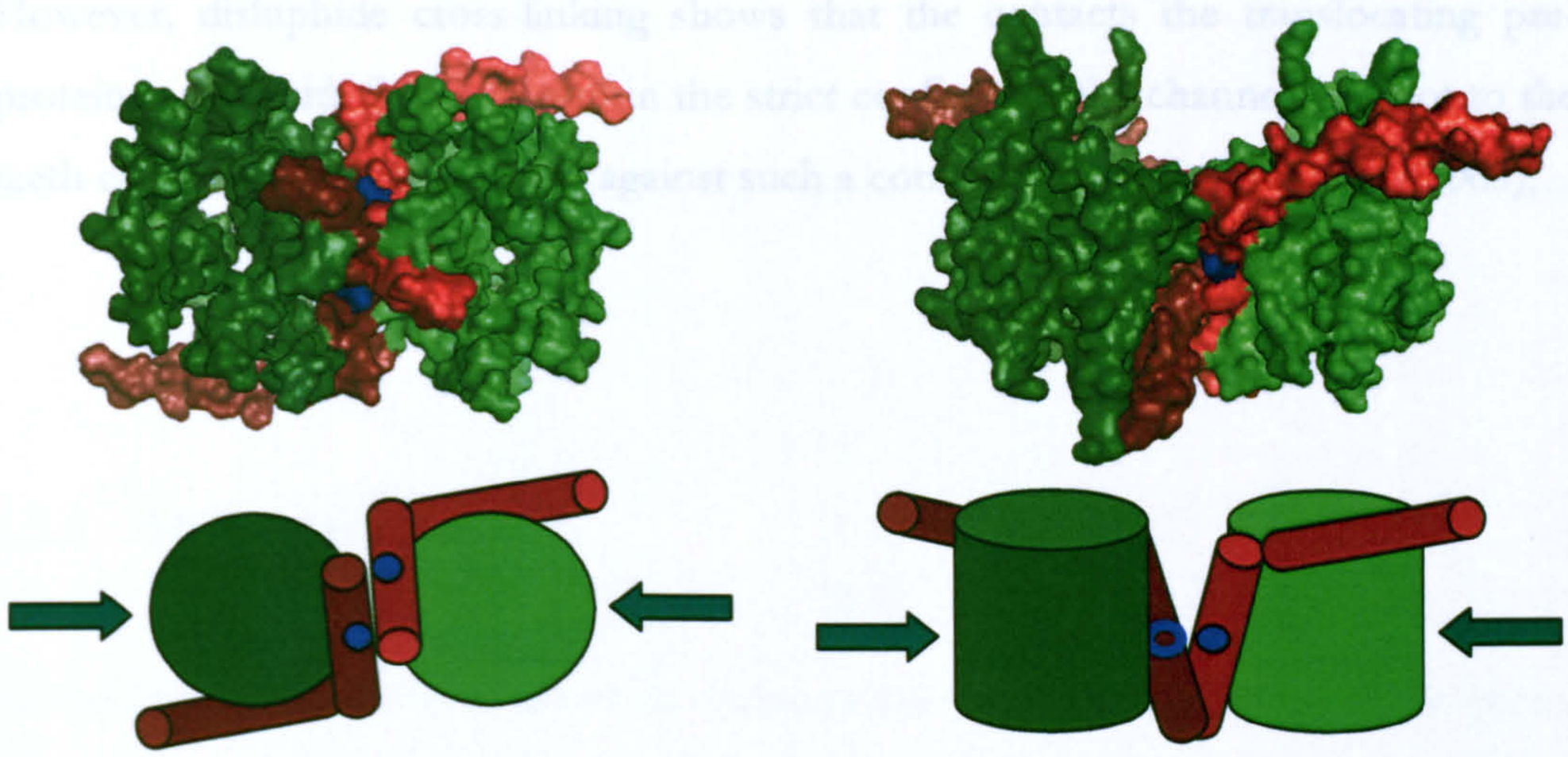

Figure 1-4. Space filling representation of the dimeric membrane-bound *E. coli* atomic model (Bostina et al., 2005).

SecY and SecE are coloured green and red, respectively. The green arrows denote the position of the lateral gate. The *E. coli* cysteine cross-link (L106C) is shown in blue. The distance between the two cysteines is 18.5 Å, contrasting to the 2.05Å disulphide bond length. Left; view from the periplasmic face of the membrane. Right; view in the plane of the membrane. Simplified cartoon views have been drawn underneath; the open blue circle (SecE; right) denotes that the cysteine is on the other side of TM3 in SecE.

A recent study by cryo-electron microscopy has revealed the *E. coli* channel in an active state (Mitra et al., 2005). A SecYEG dimer was observed in association with an actively translocating ribosome in the vicinity of the polypeptide exit site. The map was of insufficient detail to resolve clear and individual TM domains, but could be used to fit the high-resolution structure into the electron density and make some predictions on the arrangement and conformational changes that had occurred. On the basis of normal mode-based flexible fitting and the calculated correlation coefficients for various fits, the 'back-to-back' structure of the SecYEG structure (Breyton et al., 2002) was rejected in favour of a new 'front-to-front' model. This arrangement places the same TM domain of SecE on the opposite side of the membrane complex, and the two lateral gates face each other. This proposal has been used as a foundation for a model of translocation incorporating both monomers of SecYEG in a single translocation cycle; in this context it has been suggested that the channels open at the dimer interface to form a consolidated

environment for protein transport (Mitra and Frank, 2006; Mitra et al., 2005). However, disluphide cross-linking shows that the contacts the translocating pre-protein makes with SecY are within the strict confines of the channel, but not to the teeth of the 'clam-shell', arguing against such a corroboration (Cannon et al., 2005).

1.5 Energy Transduction by SecA during Post-translational Translocation

1.5.1 Molecular motors

Molecular motors have evolved to interconvert chemical energy and mechanical work. They have been exploited to drive a number of processes that are central to cell biology, such as protein folding and degradation, DNA coiling, ATP synthesis and protein translocation. One particular group of motor proteins include the RecA-like motor ATPases, with a common structural domain first seen in the DNA recombination enzyme RecA (Story and Steitz, 1992). ATPases catalyse the dephosphorylation of adenosine triphosphate (ATP) to adenosine diphosphate (ADP) and an inorganic phosphate (Pi). Energy is released by this decomposition reaction and is used to fuel essential processes in the cell.

1.5.2 RecA-like motor ATPases

RecA-like motor ATPases are characterised by the Walker A and B motifs that form the catalytic site (Story and Steitz, 1992; Walker et al., 1982) (Figure 1-5). The RecA domain forms a β-strand structure, which is flanked on both sides by α-helices (Story and Steitz, 1992). The Walker A motif contains the highly conserved sequence A/GXXXXGKT/S (X is any residue), and forms a loop around the nucleotide, called the Phosphate-loop (P-loop) (Saraste et al., 1990; Walker et al., 1982). The Walker B motif takes the form of the hydrophobic β-strand sequence ϕϕϕϕDE (where ϕ is any hydrophobic residue) (Walker et al., 1982).

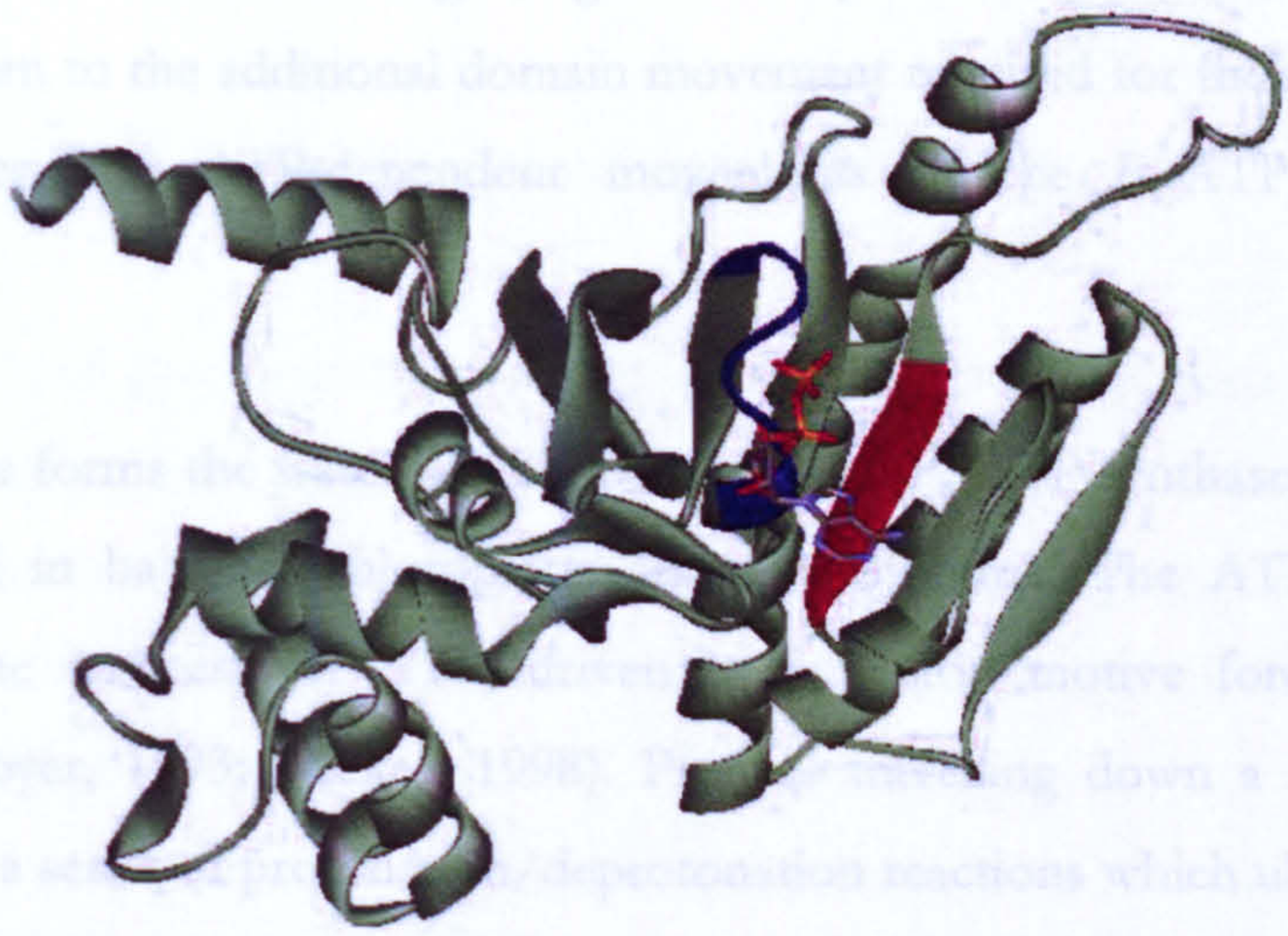

Figure 1-5. Organisation of the Walker A and B motifs in RecA-ADP.

Ribbon representation of RecA-ADP showing the Walker A motif (P-loop) in blue (^{66}GPESSGKT^{74}) and the Walker B motif (^{140}VIVVD^{144}) in red, bound to an ADP molecule (Story and Steitz, 1992).

The structure of the F_1-ATPase in complex with ADP and aluminium fluoride shows the β- and γ-phosphates of ATP to be co-ordinated by the Walker A motif (Menz et al., 2001). Negatively charged residues in the Walker B motif co-ordinate the Mg^{2+} cofactor required for hydrolysis, assisted by the hydroxyl of the T/S in the Walker A motif (Menz et al., 2001). Generally, a glutamate or aspartate residue in the Walker B motif activates the attacking water molecule by polarisation, uniquely in the case of F_1-ATPase this is actually found in an adjacent and distinct subunit (Menz et al., 2001).

Sequence similarity in RecA-like proteins is low, they all belong to different families of the P-loop ATPases (AAA+ ATPases, the ABC family, and helicase superfamilies I, II, and III) which include the F_1-ATPase, the DNA helicase PcrA and SecA (Ye et al., 2004). These ATPases can contain different numbers of RecA-like motifs; SecA contains two within a single polypeptide chain (Hunt et al., 2002). These are known as the nucleotide binding folds (NBFs), the interface of which provides the binding site for ATP (Soultanas and Wigley, 2000; Ye et al., 2004).

RecA-like motor ATPases undergo large ATP dependent conformational changes and couple them to the additional domain movement required for their function. Of these examples, the ATP-dependent movements of the F_1-ATPase are best understood.

The F_1-ATPase forms the water soluble part of the F_1F_0 ATP synthase, a ubiquitous enzyme found in bacteria, chloroplasts and mitochondria. The ATP synthase is involved in the synthesis of ATP, driven by a proton motive force across the membrane (Boyer, 1993; Walker, 1998). Protons travelling down a concentration gradient cause a series of protonation/deprotonation reactions which ultimately drive rotation of specific subunits in the F_0 transmembrane domain (Elston et al., 1998). This sequentially forces different conformations on the catalytic domains, resulting in the synthesis and release of ATP.

The F_1 component can also perform the reverse reaction; ATP is hydrolysed and the structure acts as a rotary motor. F_1 forms a hexameric ring of α- and β- subunits, all with RecA-like domains, surrounding a γ-subunit (Abrahams et al., 1994). The three β-subunits hydrolyse ATP sequentially, causing a conformational change within these domains that pushes the γ-subunit (Boyer, 1993; Menz et al., 2001). This leads to a 90° rotation of the γ-subunit, followed by a further 30° on ADP release (Yasuda et al., 2001). The α-subunits do not hydrolyse ATP due to the lack of a water-polarising molecule (Abrahams et al., 1994; Ye et al., 2004).

Similar to the other RecA-like ATPases like F_1, the key step for energy transduction in SecA must be the conformational change regulated by ATP binding, hydrolysis and product release in the NBF. It is how these movements are relayed through the enzyme and to their partners, which provides the power stroke, and holds the key to understanding the reaction mechanism.

1.5.3 Structure of the SecA nucleotide binding fold

NBFs 1 and 2 of SecA exhibit a strong homology to the superfamily I and II helicases, and all of the DEAD (Asp-Glu-Ala-Asp) box helicase motifs (I through VI) are found in SecA (Hunt et al., 2002; Koonin and Gorbalenya, 1992; Sianidis et al., 2001). The Walker box sequences A (motif II) and B (motif V) form NBF1 (Mitchell and Oliver, 1993).

NBF1 forms a high affinity binding site ($K_{d[ADP]}$ = 150 nM), and it was originally proposed that NBF2 forms a second site of low affinity ($K_{d[ADP]}$ = 300 μM) (Mitchell and Oliver, 1993). However, nucleotide binding has not been directly demonstrated to this second site, and the Walker box sequences have diverged from the canonical. Gel filtration studies have suggested that one binding site for ADP exists per dimer (Schmidt et al., 2000), where as Isothermal Titration Calorimetry (ITC) demonstrated two molecules of ADP bound per one SecA dimer (den Blaauwen et al., 1999). Assays employing nitrocellulose filtration determined the binding affinity for ATP at one site to be tight, but negligible for the putative second (Zito et al., 2005). Moreover, none of the structures identify a second nucleotide binding site within a single protomer (Hunt et al., 2002; Osborne et al., 2005; Papanikolau et al., 2006). NBF2 has however been shown to be important for translocation (Economou et al., 1995; Mitchell and Oliver, 1993) and indeed for ATP hydrolysis (Karamanou et al., 1999). This leads to the conclusion that although NBF1 forms the high affinity site for nucleotide, binding and hydrolysis is probably facilitated by residues in NBF2.

1.5.4 SecA structure and oligomeric state

SecA is a soluble protein of 102 kDa and exists in solution in a monomer-dimer equilibrium ($K_{d[SecA\text{-}SecA]}$ = 250-500 nM) (Woodbury et al., 2002); under physiological conditions it is predominantly dimeric in either the presence or absence of nucleotide (Akita et al., 1991; Driessen, 1993; Shilton et al., 1998; Woodbury et al., 2002). This equilibrium is sensitive to temperature, protein concentration and the ionic strength of the surrounding medium (Bu et al., 2003; Driessen, 1993; Woodbury et al., 2002).

Of the six published SecA crystal structures, five of them are dimeric (Hunt et al., 2002; Papanikolau et al., 2007; Sharma et al., 2003; Vassylyev et al., 2006; Zimmer et al., 2006) and one is monomeric (Osborne et al., 2004). The protomers of each dimer all have a similar structure, the major differences being at the dimer interface. Interestingly, the structure from *T. thermophilus* is in a parallel conformation (Vassylyev et al., 2006), in contrast to all of the other structures which are packed in an anti-parallel or intertwined fashion (Hunt et al., 2002; Osborne et al., 2004; Sharma et al., 2003; Vassylyev et al., 2006; Zimmer et al., 2006) (Figure 1-6). In the monomeric form, domain movements not seen in the other structures result in the opening of a groove that may be the pre-protein binding site (Musial-Siwek et al., 2006; Osborne et al., 2004) (Figure 1-7).

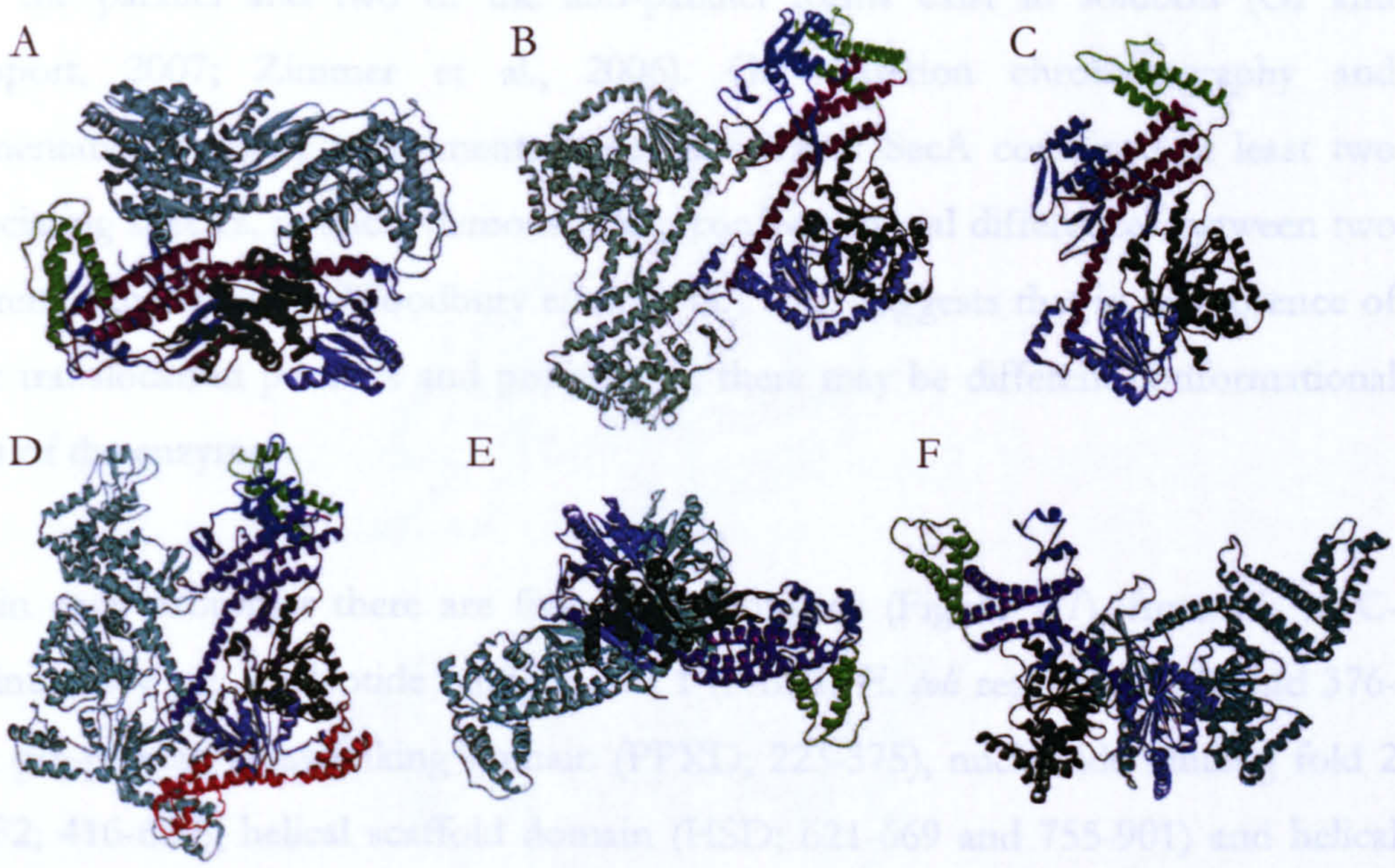

Figure 1-6. The six SecA crystal structures.

(A) *B. subtilis* antiparallel dimer (Hunt et al., 2002) (B) *M. tuberculosis* antiparallel dimer (Sharma et al., 2003), (C) *B. subtilis* monomer (Osborne et al., 2004), (D) *T. thermophilus* parallel dimer (Vassylyev et al., 2006), (E), *B. subtilis* antiparallel dimer (Zimmer et al., 2006), (F) *E. coli* intertwiner dimer (Papanikolau et al., 2007). Conformations represented by (A), (D) and (E) have been shown to exist in solution.

In *B. subtilis*, the dimer contacts are formed between the N-terminal residues of one protomer, and the C-terminal domain of another (Hunt et al., 2002). On this basis it was proposed that they were required for formation of the physiological dimer. A truncation mutant (SecA-Δ11/N95; the N-terminal 11 residues and C-terminal 70 residues are removed) was shown to be monomeric, supporting this notion (Or et al., 2005). However, in another study the deletion of the C-terminal 40 residues and an N-terminal nonapeptide maintained the SecA dimeric structure (Karamanou et al., 2005).

The structure which represents the physiological state has not been confirmed. It is possible that the oligomeric arrangement observed in the X-ray structures is a consequence of the extreme crystallisation conditions or the lattice contacts and constraints. There is however evidence based on FRET for the existence of the first *B. subtilis* anti-parallel structure in solution (Ding et al., 2003; Hunt et al., 2002). In addition cysteine scanning mutagenesis and cross-linking studies have shown that

both the parallel and two of the anti-parallel forms exist in solution (Or and Rapoport, 2007; Zimmer et al., 2006). Gel filtration chromatography and sedimentation velocity experiments have shown that SecA contained at least two dissociating species, possibly demonstrating conformational differences between two different dimeric states (Woodbury et al., 2002). This suggests that in the absence of other translocation partners and pre-protein, there may be different conformational states of the enzyme.

Within each protomer there are five major domains (Figure 1-7), from N- to C-terminus they are: nucleotide binding fold 1 (NBF1; *E. coli* residues 1-222 and 376-415), pre-protein cross-linking domain (PPXD; 223-375), nucleotide binding fold 2 (NBF2; 416-620), helical scaffold domain (HSD; 621-669 and 755-901) and helical wing domain (HWD; 670-754) (Hunt et al., 2002). In all of the apo- and nucleotide-bound structures, there are essentially no major changes in the structure of the NBFs (Hunt et al., 2002; Osborne et al., 2005; Papanikolau et al., 2006; Sharma et al., 2003; Zimmer et al., 2006). This means that there are missing active states of the complex. The constraints of the crystallisation process or the transient nature of these states may mean that they are difficult to stabilise and visualise in a crystal lattice.

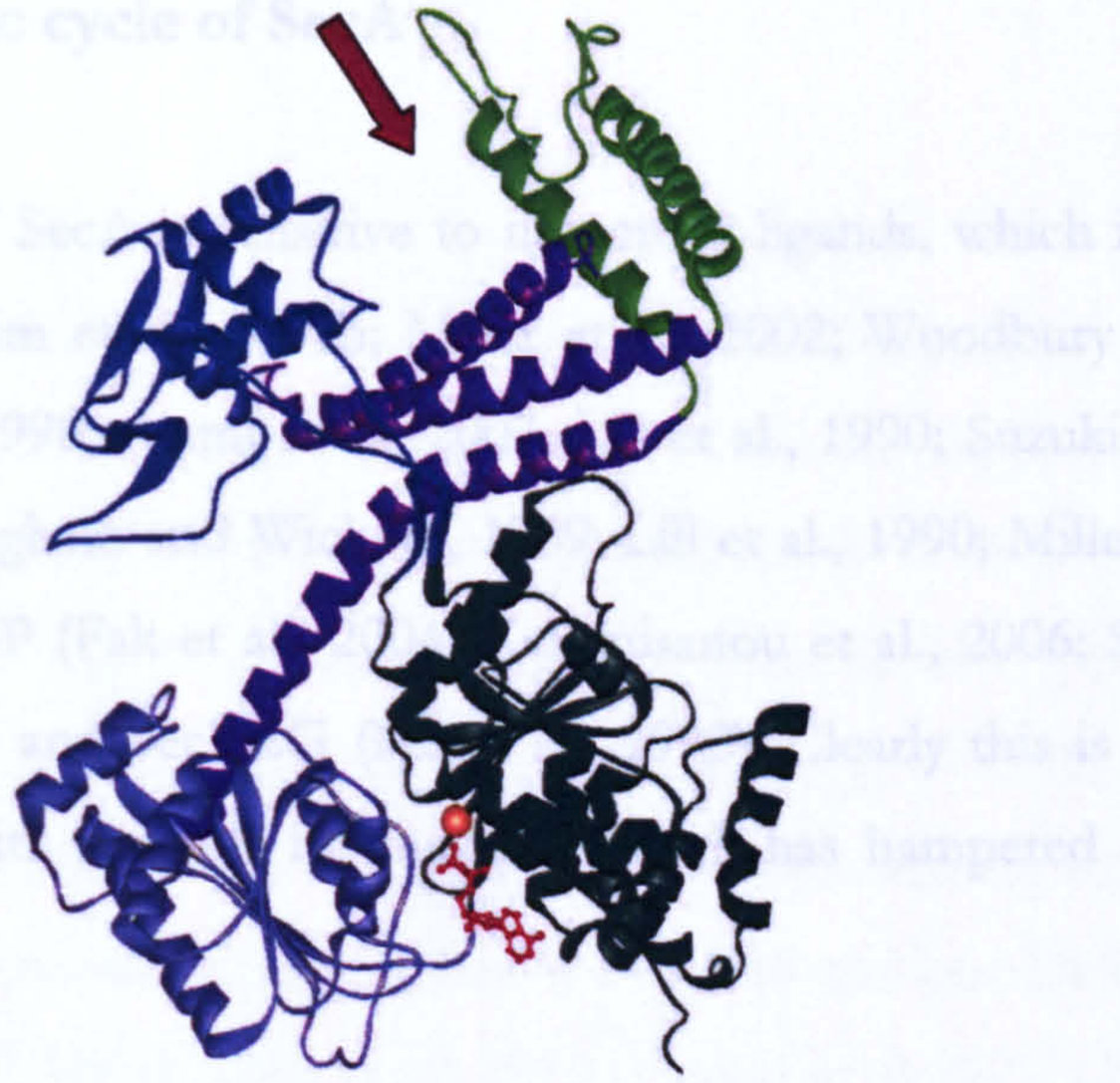

Figure 1-7. The domain organisation of SecA.

Ribbon representation of the monomeric SecA structure (Osborne et al., 2004). From N- to C-terminus the domains are NBF1 (dark green), PPXD (dark blue), NBF2 (pale blue), HSD (purple) and HWD (bright green). The bar at the bottom of this panel shows the locations of these domains in the linear sequence of SecA, and the positions of the IRA sequences (red). The arrow (magenta) denotes the position of the putative polypeptide binding site.

1.5.5 The hydrolytic cycle of SecA

The ATPase activity of SecA is sensitive to numerous ligands, which include: SecB (Fekkes et al., 1999; Kim et al., 2001b; Miller et al., 2002; Woodbury et al., 2000), lipids (Ahn and Kim, 1998; Alami et al., 2007; Lill et al., 1990; Suzuki et al., 1999), signal peptides (Cunningham and Wickner, 1989; Lill et al., 1990; Miller et al., 1998; Wang et al., 2000), ADP (Fak et al., 2004; Keramisanou et al., 2006; Sianidis et al., 2001; Zito et al., 2005) and SecYEG (Lill et al., 1990). Clearly this is an extremely complicated enzyme with multiple interactions, which has hampered our ability to clearly understand it.

Two specific regulatory domains for ATPase activity have been proposed. Disruption of the C-terminus (residues 610-901) leads to an enhanced ATPase activity (Triplett et al., 2001), and deletion of residues 783-795 has the same effect (Karamanou et al., 1999). This region was named Intramolecular Regulator of ATPase activity (IRA1) (Figure 1-7) (Karamanou et al., 1999). The second domain, IRA2 (nearly coincident with NBF2; residues 462-610) controls the nucleotide binding and release occurring at NBF1 (Sianidis et al., 2001). Some residues in NBF2 contact bound ATP, and IRA2/NBF2 interacts with NBF1 and activates ATP turnover (Sianidis et al., 2001). This could explain why NBF2 transpires to be paramount for translocation (Economou et al., 1995; Mitchell and Oliver, 1993) and for ATP hydrolysis (Karamanou et al., 1999).

The ATPase activity has been rudimentally characterised, and subdivided into three categories. Firstly, there is a slow basal activity without substrate or partner protein (endogenous ATPase). Secondly a slightly elevated activity induced by binding to inner membrane vesicles (IMVs) (membrane ATPase), and finally a high activity induced by binding to IMVs and pre-protein (translocation ATPase) (Cunningham and Wickner, 1989; Lill et al., 1989; Lill et al., 1990).

1.5.6 SecA interacts with diverse ligands

1.5.6.1 SecA - SecB

The role of SecB is to maintain cytosolic pre-proteins in a translocation competent conformation, and to assist targeting to the translocation apparatus via SecA (Driessen, 2001; Hartl et al., 1990) (Figure 1-1). SecB binds to cytosolic SecA with low affinity ($K_{d[SecA;\ soluble\ -\ SecB]}$ = 1-2 μM) (den Blaauwen et al., 1997), but with much higher affinity to translocase-bound SecA ($K_{d[SecA;\ translocase\ -\ SecB]}$ = 30 nM) (Breukink et al., 1995; Fekkes et al., 1997; Hartl et al., 1990). The SecB binding site is at the C-terminus of SecA, and contains three conserved cysteines and one histidine/cysteine which coordinate a Zn^{2+} ion (Fekkes et al., 1999; Fekkes et al., 1997; Zhou and Xu, 2003). The far C-terminus is unresolved in the crystal structures of SecA, but a structure of the homotetrameric SecB interacting with two C-terminal domains of SecA indicates the requirement for a dimer of the motor protein at this stage of translocation (Figure 1-8) (Zhou and Xu, 2003). This oligomeric arrangement between a dimer of SecA and a tetramer of SecB has also been shown biochemically by analytical gel filtration (Randall et al., 2005).

Figure 1-8. A SecB tetramer bound to two SecA C-termini.

Ribbon representation of a SecB tetramer (the four subunits are coloured blue, green, orange and yellow), in complex with two SecA C-terminal pepides (red) and two Zn^{2+} ions (purple).

The ATPase activity of SecA is enhanced by binding to SecB (Kim et al., 2001b; Miller et al., 2002), and promotes an exchange between soluble and membrane bound SecA (Woodbury et al., 2000). SecB has also been shown to increase SecA catalytic turnover in the presence of proteoliposomes and the pre-protein substrate proOmpA (Fekkes et al., 1999). It is predicted that the NBFs of SecA are conformationally regulated by SecB, leading to an increase in the ATP hydrolysis step of the catalytic cycle when the two proteins interact (Miller et al., 2002).

1.5.6.2 SecA - lipids

The nature and function of the interaction occurring between SecA and lipids in the inner membrane has been the subject of conflicting reports. The *E. coli* inner membrane contains three major phospholipids, consisting of 58% zwitterionic phosphatidylenthanolamine (PE), and the negatively charged lipids phosphatidylglycerol (PG) and cardiolipin (CL), present at 15% and 10% respectively. Mutants of *E. coli* that are unable to synthesise PG (and consequently CL, which is derived from PG) were found to be defective in translocation of outer membrane proteins across the inner membrane (de Vrije et al., 1988). This was the first demonstration that the major acidic phospholipids are a requirement for translocation.

A large body of subsequent work has demonstrated the dependence of protein translocation for the acidic phospholipids; required for both translocation and elevated SecA ATPase activity (Ahn and Kim, 1998; Alami et al., 2007; de Vrije et al., 1989; Kusters et al., 1991; Lill et al., 1990; Suzuki et al., 1999; van der Does et al., 2000). SecA is thought to interact directly with the membrane, resulting in a conformational change, which is also dependent upon the acidic phospholipid content (Ahn and Kim, 1998; Hendrick and Wickner, 1991; Lill et al., 1990; Shinkai et al., 1991; Ulbrandt et al., 1992). Supporting this, an electron microscopy study identified two structural forms of SecA, only in the presence of an acidic phospholipid environment (Wang et al., 2003).

Acidic phospholipids and some detergents result in the loss of specific inter-molecular cross-links and a change in FRET (Benach et al., 2003; Or et al., 2002; Osborne et al., 2004). These observations were predicted to be due to the induction of SecA monomers, but could equally be the result of a rearrangement to form another of the characterised dimeric structures, or otherwise uncharacterised and active forms of the protein. The latter proposal is consistent with a Small Angle Neutron Scattering (SANS) study, where SecA in lipid vesicles was shown to be a dimer (Bu et al., 2003). The discrepancies may be explained by the fact that the latter

experiment was conducted at a much greater SecA concentration, that would promote dimer formation (Bu et al., 2003; Driessen, 1993; Or et al., 2002; Woodbury et al., 2002). These results are further confounded by the observation that at least two different SecA populations are associated with the inner membrane (Spelbrink et al., 2005). One of these is a stable dimeric population, and the other is either monomeric, or a less stable association of dimer that dissociates upon solubilisation.

There are additional examples of phospholipid mediated regulation of proteins, for example the Ca^{2+}-ATPase is upregulated with increasing PE content in the membrane (Starling et al., 1996), and the glucose-specific permease of the phosphotransferase system requires PG (Erni et al., 1982). Additionally, the acidic phospholipids (particularly CL) of the mitochondrial inner membrane were shown to enable a Mg^{2+} mediated activation of the F_1F_0-ATPase (Ye and Lin, 1990). Also, CL has been shown to be required for the activity of the ADP/ATP carrier (Hoffmann et al., 1994; Pebay-Peyroula et al., 2003).

1.5.6.3 SecA – magnesium

There have been several observations with respect to Mg^{2+} and its effects on the regulation of SecA, which have not been adequately explained. In the optimisation of proteoliposome experiments, an ATPase reaction was noted at low Mg^{2+} (Lill et al., 1990). Secondly, removal of this cation from a binding site, distinct from the NBFs, can result in a 10-fold stimulation of ADP release (Fak et al., 2004). In addition, the activity of SecA and the elevated activity found in a complex of SecA and SecYEG were both stimulated by the removal of Mg^{2+}, which also served to stabilize the latter complex in the presence of ATP (or ATPγS) (Duong, 2003). Mg^{2+} has also been shown to modulate fluorescence anisotropy measurements, as well as the fluorescence observed from intrinsic and extrinsic probes of the enzyme (den Blaauwen et al., 1997; Osborne et al., 2004; van der Wolk et al., 1995). Thus it could be anticipated that the ion may have specific a functional role that is yet to be resolved.

1.5.6.4 SecA - pre-protein substrate

The PPXD was originally identified when pre-protein was cross-linked to various SecA truncates, explicitly identifying the region from residues 267-340 (Kimura et al., 1991). Specifically, residue Tyr326 in this region was required for the pre-protein regulated steps of the translocation cycle (Kourtz and Oliver, 2000). The open groove between the PPXD and HSD/HWD depicted in the monomeric crystal structure (Osborne et al., 2004) (Figure 1-7) was proposed to be a candidate for the pre-protein binding site, which is in agreement with a photoaffinity labelling study localising the signal peptide binding site to the same domain (Musial-Siwek et al., 2006). A region closer to the N-terminus (219-244), known as the substrate specificity domain (SSD) has also been implicated in signal sequence binding (Baud et al., 2002; Triplett et al., 2001; Vrontou et al., 2004).

The signal peptide alone can bind SecA both in solution and in the presence of the lipid bilayer (Wang et al., 2000). In the latter case it has been shown to stimulate the ATPase activity of SecA (Cunningham and Wickner, 1989; Lill et al., 1990; Miller et al., 1998; Wang et al., 2000). Binding of SecA to a signal peptide is weak in solution (K_d = 2.4 μM) (Musial-Siwek et al., 2005; Triplett et al., 2001; Vrontou et al., 2004) increasing to 40 nM in the presence of phospholipid bilayers (Hartl et al., 1990). In addition, pre-protein (proOmpA) association with SecA is stimulated by lipid membranes (Hartl et al., 1990).

Signal peptide is thought to promote a more open state of SecA (Shin et al., 2006) and have a stronger association for a monomer of SecA (Musial-Siwek et al., 2005; Or et al., 2002; Triplett et al., 2001). However, oligomerisation of SecA has also been demonstrated (Benach et al., 2003; Shin et al., 2006). Some of these discrepancies may have resulted from the different SecA-lipid ratios used in the respective studies, as they also have effects on the oligomeric state of the motor (Benach et al., 2003; Musial-Siwek et al., 2005; Or et al., 2002; Osborne et al., 2004).

1.5.6.5 SecA - nucleotide

The ATP bound state of SecA has been shown to be in an extended conformation, whereas the ADP bound form is more compact (Bu et al., 2003; den Blaauwen et al., 1996; Fak et al., 2004; Hunt et al., 2002; Karamanou et al., 1999; Kim et al., 2001a; Sianidis et al., 2001; Song and Kim, 1997). Release of ADP is thought to be the rate limiting step of the steady-state reaction cycle (Fak et al., 2004; Keramisanou et al., 2006; Sianidis et al., 2001; Zito et al., 2005), but under protein translocation conditions both nucleotide binding and release are significantly faster (Natale et al., 2004). The presence or absence of nucleotide does not appear to affect the predominantly dimeric species occurring in solution (Akita et al., 1991; Driessen, 1993; Or et al., 2002; Shilton et al., 1998; Woodbury et al., 2002).

The non-hydrolysable ATP analogue AMP-PNP stabilises the association of SecA and SecYEG and promotes the 'inserted' state of a substrate protein (de Keyzer et al., 2003; Duong, 2003; Economou et al., 1995; Economou and Wickner, 1994; Eichler and Wickner, 1997; Tziatzios et al., 2004). In addition, ATP has been shown to promote an interaction of SecA with membranes (Economou et al., 1995; Economou and Wickner, 1994). In support of this, both the ADP-bound compact SecA structure, and the apoprotein have a low affinity for SecY and the membrane (den Blaauwen et al., 1996; Fak et al., 2004; Hunt et al., 2002; Shilton et al., 1998; Ulbrandt et al., 1992), suggesting that after ATP hydrolysis, SecA may retract from the translocon. This could explain the observed effects of Walker mutations leading to a stable membrane associated form (Mitchell and Oliver, 1993; van der Wolk et al., 1993). However, experiments employing surface plasmon resonance and cross-linking show that ATP induces the release of SecA from SecYEG (de Keyzer et al., 2003; Duong, 2003), and the inhibition of the apparent binding and insertion of SecA into membranes (Breukink et al., 1992). Thus the role of the catalytic cycle, and how this is propagated to translocation is yet to reach a consensus.

1.5.6.6 SecA - SecYEG

The structure of the SecYEG complex indicates that there are loops exposed to the cytosol available for partner protein interaction (Bostina et al., 2005; Breyton et al., 2002; van den Berg et al., 2004), but the precise locations are ill defined. Second site suppressors, cross-linking and peptide scanning experiments map the interaction sites in SecY to TM4, the fifth cytoplasmic loop (C5) and the C-terminal tail (Alami et al., 2007; Matsumoto et al., 2000; Mori and Ito, 2001; Mori and Ito, 2003; Mori and Ito, 2006; Taura et al., 1994; van der Sluis et al., 2006a; Vassylyev et al., 2006).

Both the N-terminal domain (comprising the NBF) and C-terminal domains of SecA have been shown to be important for the interaction with SecYEG (Matsumoto et al., 2000; Matsumoto et al., 1997; Osborne and Rapoport, 2007; Snyders et al., 1997; Vrontou et al., 2004), where as suppressors of the SecY *prl* mutations are located somewhat irregularly throughout the entire SecA structure (Matsumoto et al., 2000). The ATPase activity of SecA is further stimulated above that of lipids alone, by the presence of SecY in vesicles (Lill et al., 1990).

There is evidence to support the fact that the dimer of SecA is an active form when engaged in translocation. The inactivation of a single SecA protomer has a dominant effect on the activity of the dimer, and FRET experiments designed to monitor the appearance of monomers proved negative (Driessen, 1993). However, recent reports have challenged this view. The fact that one of the structures of SecA is a monomer led to suggestion that the dimer might dissociate when activated (Osborne et al., 2004; Zimmer et al., 2006). A crosslinked dimer based on a *B. subtilis* structure (Hunt et al., 2002) had a normal level of basal and lipid ATPase activity, but proOmpA activated ATPase activity (translocation ATPase) was impaired and translocation did not occur (Or and Rapoport, 2007). However, an almost identical crosslinked dimer retained translocation activity (Jilaveanu and Oliver, 2006). Another C-terminally linked dimer was also shown to be active in translocation (de Keyzer et al., 2005). The difficulty with the interpretation of these experiments resides in the fact that intermolecular crosslinking could reduce the conformational flexibility of the molecule. In addition, the C-terminal crosslink is at the highly flexible end of SecA

(Chou et al., 2002; Hunt et al., 2002), and it may not interfere with dissociation of subunits (Or and Rapoport, 2007).

Genetic studies do not provide support for either view. The largely monomeric form of SecAΔ2-11 (an N-terminal deletion mutant) was poorly active in terms of membrane and translocation ATPase and inactive for translocation (Jilaveanu et al., 2005). Yet the further truncated monomeric mutant SecA-Δ11/N95 (the C-terminal 70 residues are also removed) was shown to support the same level of basal, membrane and translocation ATPase activity as the wild type, and could stimulate translocation of 16% of proOmpA in comparison to wild type (Or et al., 2005).

During translocation, a SecA monomer remained associated with a SecYEG protomer and the pre-protein (Duong, 2003) and both monomers and dimers of SecA have been shown to cycle during translocation (Benach et al., 2003). Two further studies identified that both monomers and dimers of SecA were able to associate with covalently linked or antibody stabilised SecYEG dimers in solution, and that the specific oligomeric association was dependent on nucleotide (Duong, 2003; Tziatzios et al., 2004). The antibody stabilised SecYEG dimer binds one SecA molecule in detergent solution, and two in the presence of AMP-PNP (Tziatzios et al., 2004). Recently a single SecYEG complex has been reconstituted into a nano-scale lipid bilayer (nanodisc), and this was shown to dissociate the SecA dimer and interact only with the monomer (Alami et al., 2007). By surface plasmon resonance, two populations of SecA were detected, which dissociated from SecYEG at different rates (de Keyzer et al., 2005). At this stage we must consider that both monomers and dimers of SecA may play important roles in the translocation reaction, and association and dissociation are required to complete the reaction cycle.

1.6 A Model for Post-translational Translocation through SecYEG

SecA resides in the cytoplasm in a stable dimeric ADP-bound state, with a low basal activity (Fak et al., 2004; Keramisanou et al., 2006; Sianidis et al., 2001; Zito et al., 2005). When SecA is targeted to the membrane, interaction with acidic phospholipids and SecY results in an elevation of the ATPase activity during protein translocation (Ahn and Kim, 1998; Alami et al., 2007; de Vrije et al., 1989; Kusters et al., 1991; Lill et al., 1990; Suzuki et al., 1999; van der Does et al., 2000).

SecB, although non-essential (and indeed absent in some bacteria) recognises nascent pre-proteins (Randall and Hardy, 2002) and delivers them to membrane bound SecA (Breukink et al., 1995; Fekkes et al., 1997; Hartl et al., 1990). This interaction involves a dimer of SecA and a tetramer of SecB (Fekkes et al., 1997; Randall et al., 2005; Zhou and Xu, 2003). When translocation commences, SecB is released back into the cytosol (Fekkes et al., 1997).

The catalytic cycle has been proposed to proceed by a multi-step mechanism for translocation via specific SecA insertion and de-insertion events (Economou and Wickner, 1994; Ramamurthy and Oliver, 1997; van der Wolk et al., 1997). The evidence is based upon the observed protease protection of a large 30 kDa domain of SecA while bound by SecY, which is dependent on ATP and pre-protein (Economou and Wickner, 1994; Eichler et al., 1997; Jilaveanu and Oliver, 2007). This fragment could be chased by an excess of unlabelled SecA, leading to the proposal of a cycle alternating between a membrane and cytosolic form (Economou and Wickner, 1994). SecA has also been shown to penetrate the membrane directly (Ulbrandt et al., 1992) and traverse the bilayer (Ahn and Kim, 1994; Kim et al., 1994; Ramamurthy and Oliver, 1997). The C-terminus of SecA was shown to be one region of exposure due to periplasmic labelling and proteolysis accessibility (Kim et al., 1994; Ramamurthy and Oliver, 1997; van der Does et al., 1996). The PMF has been shown to enhance deinsertion (Nishiyama et al., 1999) and protein translocation itself (Schiebel et al., 1991).

Other studies do not support this hypothesis, as they have failed to detect the translocation-dependent dissociation of membrane bound SecA, and show that SecA is permanently associated with the membrane (Chen et al., 1996). Furthermore, the structure and dimensions of the SecY complex seem to be incompatible with this interpretation; SecA is simply too large to fit inside the SecY channel (Breyton et al., 2002; van den Berg et al., 2004). In light of the recent work demonstrating that SecA is bound to a non-translocating SecY copy, and pushes the pre-protein through an adjacent copy (Osborne and Rapoport, 2007), it seems possible that the protection of the 30 kDa fragment is possibly the result of a large conformational change exposing a protease sensitive sequence, or perhaps a partial insertion of the peripherally associated SecA and not necessarily the result of a deep penetration of the enzyme. Clearly there must be large conformational changes to SecYEG and SecA associated with the translocation reaction that are yet to be fully characterised.

There are discrepancies regarding the kinetics of pre-protein translocation. One study suggests that each cycle of ATP binding and hydrolysis results in the translocation of approximately 5 kDa (50 amino acids) of pre-protein (Schiebel et al., 1991; van der Wolk et al., 1997), where as in another study it is estimated that 5 ATP molecules are required to send each amino acid across the membrane (Tomkiewicz et al., 2006). Clearly multiple rounds of ATP binding and hydrolysis are required for translocation to proceed. Once the protein has been fully translocated through the membrane, the enzyme signal peptidase cleaves the signal peptide from the mature protein (Paetzel et al., 2002).

1.7 Accessory proteins to the SecYEG complex

1.7.1 SecDFyajC

Associated with SecYEG is a 93 kDa heterotrimeric membrane protein complex SecDFyajC (Duong and Wickner, 1997a). Genetic screens identified the proteins SecD and SecF as important for protein export (Gardel et al., 1987; Riggs et al., 1988), and also encoded on the same operon is the gene for yajC (Gardel et al., 1990).

The role of this protein complex is however poorly defined. Protein export is diminished but not abolished in host strains deficient in SecD and SecF (Pogliano and Beckwith, 1994). It has been postulated that SecDF is involved in release of proteins from the SecYEG translocon (Matsuyama et al., 1993) and that it can also regulate the SecA membrane cycling reaction (Economou et al., 1995). The complex has been shown to slow the movement of the translocating polypeptide, preventing it from backsliding in the incorrect direction (Duong and Wickner, 1997b). And finally, IMVs which have been depleted of SecD and SecF cannot maintain a proton motive force (PMF), suggesting a potential role in the coupling of the PMF to the translocation reaction (Arkowitz and Wickner, 1994).

1.7.2 YidC

Weakly associated with the Sec complex is a 61 kDa membrane protein yidC (Nouwen and Driessen, 2002; Xie et al., 2006). Integration of certain membrane proteins via the Sec pathway, such as leader peptidase, require this component (Beck et al., 2001; Froderberg et al., 2004; Houben et al., 2004; Samuelson et al., 2000). Little is known regarding the mechanism of integration via yidC, but is postulated to occur by the provision of a lipid protected environment which can assist in folding of the transmembrane domains (Beck et al., 2001).

An essential membrane insertion activity has also been identified which is independent of SecYEG (Nouwen et al., 2001; Samuelson et al., 2000; Serek et al., 2004; Wang et al., 2003; Yi et al., 2004). This is thought to occur occur via SRP and the co-translational pathway (Facey et al., 2007; Okamoto et al., 2002; Serek et al., 2004; van Bloois et al., 2004).

YidC has homologues in both mitochondra and chlroplasts (Oxa1 and Alb3 respectively) (Bellafiore et al., 2002; Bonnefoy et al., 1994; Driessen et al., 2001; Houben et al., 2004; Moore et al., 2000). Both Oxa1 and Alb3 are also responsible for insertion of membrane proteins (Bellafiore et al., 2002; Funes et al., 2004; Hell et al., 2001; Ossenbuhl et al., 2004; Woolhead et al., 2001).

1.8 Concluding Paragraph

This is an extremely complicated field of membrane biology and our current comprehension is thanks to a generation of research on the related eukaryotic, bacterial and archaeal systems studied by both genetic and biochemical means. In spite of this progress in the SecA field, there are several disputed and outstanding aspects of the reaction mechanism. These problems will need to be addressed by a structural determination of an active state of the translocation complex with pre-protein, and by further biophysical studies probing the dynamics of the reaction. Understanding details both on the nature and timing of the conformational changes that derive from the release of chemical energy, and of specific protein-protein interactions holds the key to understanding how they are coupled to protein transport.

1.9 Aims of this study

Much of the SecA literature is conflicting in nature. Somewhat surprisingly, a thorough steady-state analysis of SecA in the context of translocation ligands is absent. In order to resolve some of the confounding issues, and to merge the gaps in our knowledge of the ATPase, my intent was to carry out a comprehensive study of the SecA ATPase by steady-state analysis. To resolve the discrepancies regarding the oligomeric state of SecA, the aim was to perform an analysis by analytical ultracentrifugation.

The first part of this work focused on wild type SecA and the proposed monomeric mutant SecA-Δ11/N95 (Or et al., 2005), with the aim to fully characterise these ATPases in the absence of pre-protein and translocation partners. This would facilitate a thorough understanding of the motor protein in terms of oligomeric state, ATP turnover and product inhibition in solution.

Experiments in the second part of this work explore and dissect the contribution of additional components of the translocation reaction on the ATP hydrolytic cycle of SecA. The majority of previous work in the field revolves around study of the entire translocation process, and little has been done to successfully deconstruct this reaction. The work presented here has enabled the translocation reaction to be dissected and understood at the level of SecA and ATP turnover, revealing novel information which has facilitated a clearer understanding of some of the contradictions in the literature.

Materials and Methods

2.1 Chemicals and Biochemicals

All *E. coli* and synthetic lipids were purchased from Avanti (Alabaster, Alabama, USA). Polyoxyethylene(9)dodecyl ether ($C_{12}E_9$) and n-Dodecyl β-D-maltoside (DDM) were purchased from Anatrace (Maumee, Ohio, USA). All precast gels, molecular weight markers and electrophoresis reagents were bought from either Biorad (Hercules, California, USA) or Invitrogen (Carlsbad, California, USA), and the blotting apparatus from the latter. The EnzChek™ kit was purchased from Molecular Probes (Invitrogen), all chromatographic reagents and media were purchased from GE Healthcare (Chalfont St. Giles, UK) except where indicated, Biobeads were from Biorad, Centriprep centrifugal filters were from Millipore (Billerica, Massachusetts, USA) and all other reagents were acquired from Sigma (St. Louis, Missouri, USA).

2.2 Overexpression and Purification of Translocation Reaction Components

2.2.1 SecA and SecA-Δ11/N95

SecA (wild-type) and SecA–Δ11/N95 were overexpressed respectively from plasmids pT7SecA2 (Or et al., 2002) and pET21Δ11N95 (Or et al., 2005). Both were donated by Professor T. Rapoport (Harvard Medical School, Boston, USA). SecA-Δ11/N95 is truncated both at the C-terminus (70 residue deletion, ending at Val831) and the N-terminus (ΔLeu^{2}-Gly^{11}). Both proteins were extended by a hexahistidine tag at the C-terminus. The plasmid constructs were transformed into competent *E. coli* host cells BL21.19(λDE3) by heat-shock at 42°C, and grown on Luria-Bertani (LB) agar plus 100 μg/ml ampicillin overnight at 37°C.

A colony was inoculated into 100 ml LB medium with 100 μg/ml ampicillin, and grown overnight at 37°C as a pre-culture whilst shaking. 20 ml cells were then transferred into 5 x 5L flasks (2L LB per flask), also containing 100 μg/ml ampicillin, and induced with 1 mM isopropyl 1-thio-β-D-galactopyranoside (IPTG) at mid-log phase of growth (A_{600} ~ 0.8), also whilst shaking at 37°C. After 1.5 hours of induction the cells were pelleted by centrifugation (7200 x *g* for 35 minutes at 4°C; Sorvall RC-3B centrifuge with H-6000A rotor), then resuspended in 200 ml 20 mM Tris-HCl pH 7.5, 100 mM KCl, 2 mM $MgCl_2$ and ruptured by using a cell disruptor (Constant Cell Disruption Systems, Daventry, UK).

Membranes and insoluble material were removed by centrifugation (205,000 x *g* for 30 minutes at 4°C; Coulter Optima L-100 XP ultracentrifuge with 45Ti rotor; Palo Alto, California). Supernatants were then applied to a Ni^{2+}-Sepharose column (Chelating Sepharose fast flow), washed in the same buffer with 25 mM imidazole and SecA was eluted in 300 mM. Proteins were further purified by anion exchange

chromatography in 20 mM Tris-HCl, pH 7.5, 100 mM KCl, 2 mM $MgCl_2$, 1 mM DTT and eluted by a linear gradient (0-1 M KCl) (Q-Sepharose HP XK 26/20 column) (Figures 2-1 and 2-3). Subsequently, a further purification step was used to remove bound nucleotides and Mg^{2+} by gel filtration chromatography (Figures 2-2 and 2-4). A procedure adapted from one used to strip the F_1-ATPase (Lutter et al., 1993) was performed by using a gel filtration column (Superdex 200 HR 26/60) equilibrated in 20 mM Tris-HCl pH 7.5, 100 mM KCl, 1 mM DTT, 50 mM EDTA, 20% (v/v) glycerol. The chromatographic procedure was subsequently repeated in 20 mM Tris-HCl pH 7.5, 100 mM KCl, 1 mM DTT to remove EDTA and glycerol (Figures 2-2 and 2-4), the protein was concentrated to ~ 100 μM (10 mg/ml) using a 50 kDa cut-off centrifugal filter device, and stored at -80°C. Protein quantification by amino acid analysis determined the extinction coefficient to be 99,000 ± 1,980 $M^{-1}cm^{-1}$ for wild-type protein (Alta Bioscience) (Robson et al., 2007).

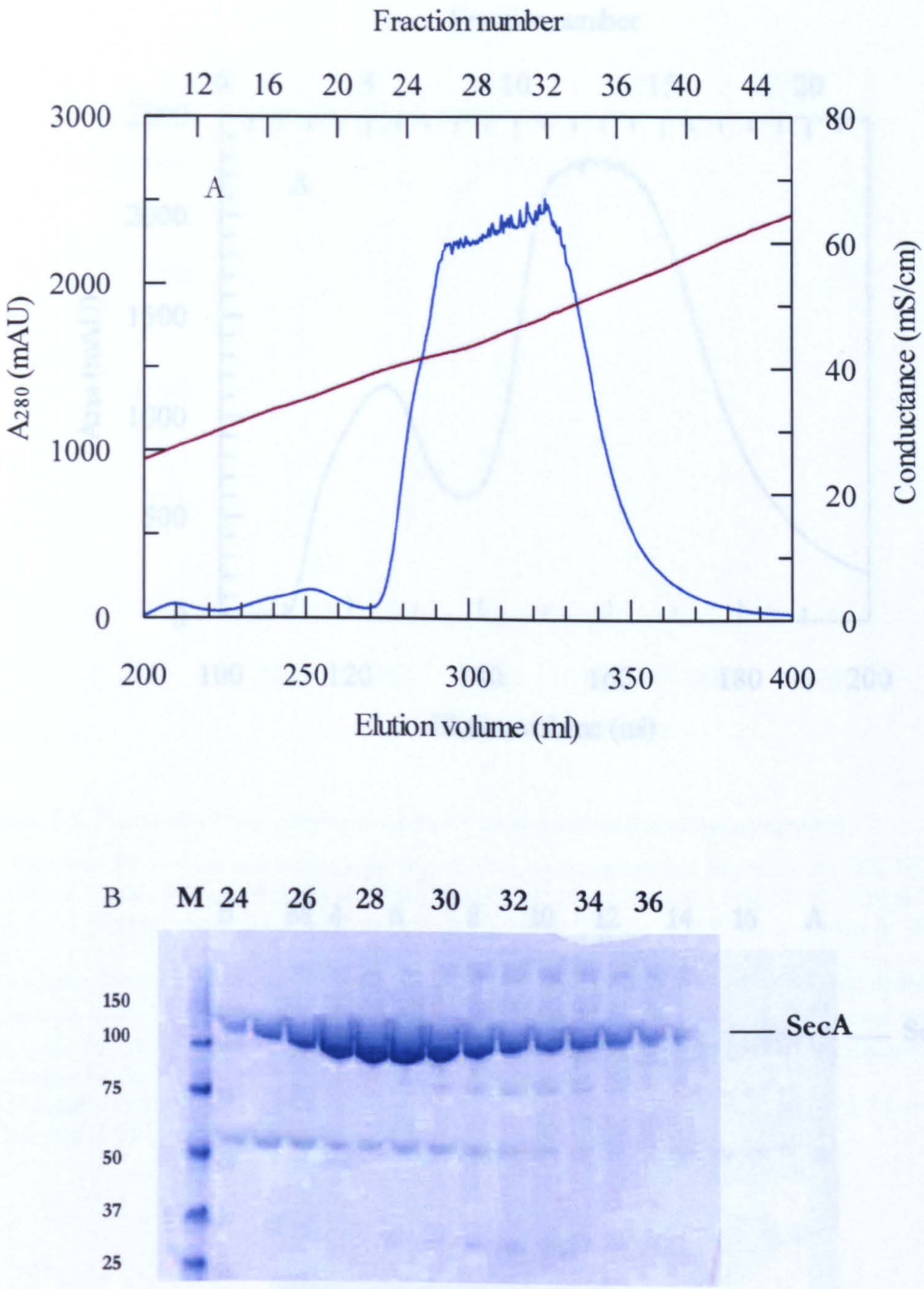

Figure 2-1. Anion exchange chromatography during the purification of SecA.

(A) A Q-Sepharose HP XK 26/20 column was equilibrated in 20 mM Tris-HCl pH 7.5, 100 mM KCl, 2 mM $MgCl_2$ and eluted by a linear gradient (0-1 M KCl). The absorbance at 280 nm is shown by the blue trace, and conductance (mS/cM) by the brown trace.

(B) Samples from across the anion exchange elution profile were applied to an SDS-PAGE gel, and stained with Coomassie blue. The lanes are as follows: M – 10 µl Precision plus markers (molecular weight is shown on the left), 24-37 – 10 µl of the corresponding fractions in (A), Fractions 27 - 31 were selected for further purification.

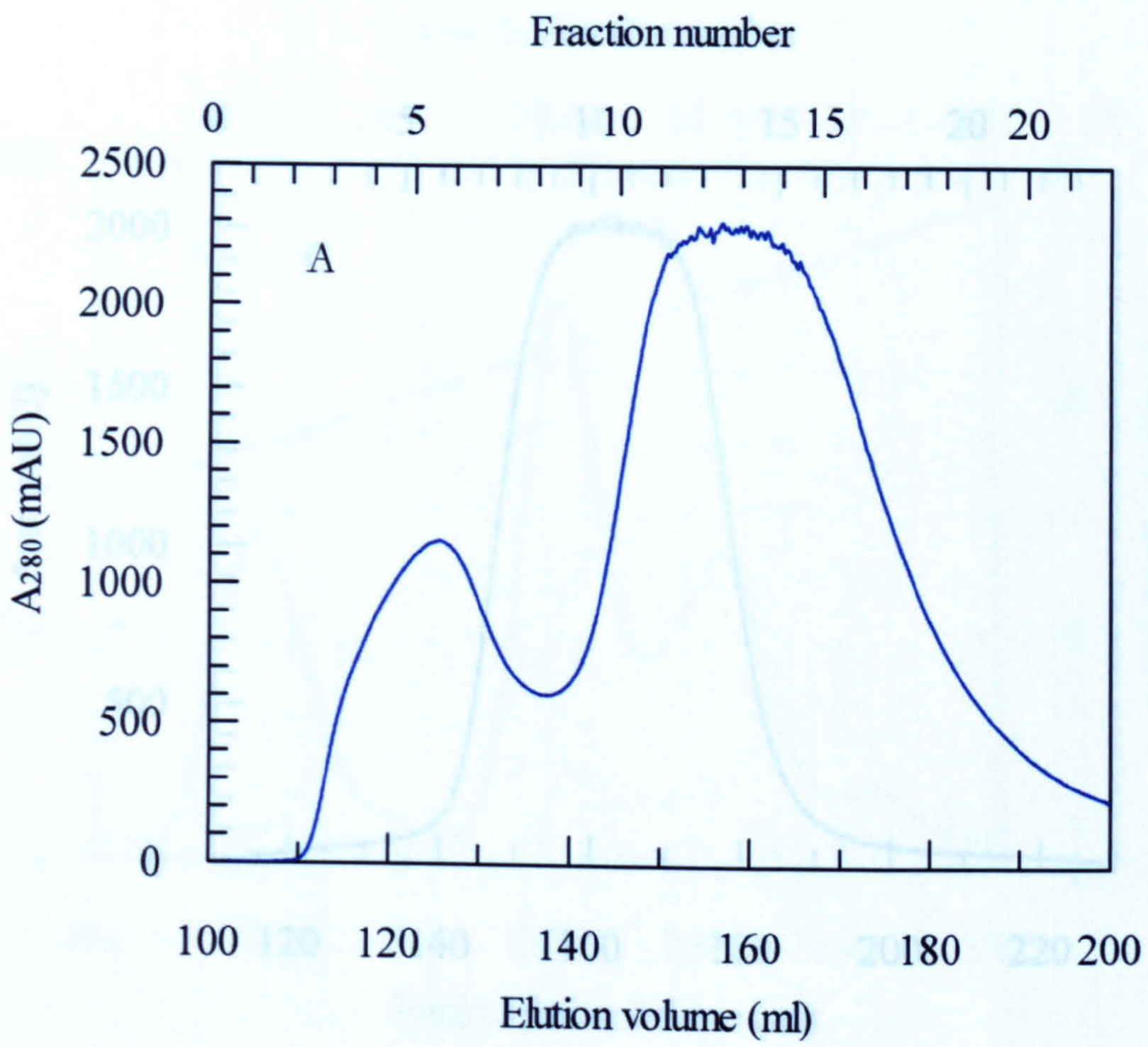
Fraction number
0
5
10
15
20
A
2500
2000
1500
1000
500
0
A280 (mAU)
100
120
140
160
180
200
Elution volume (ml)

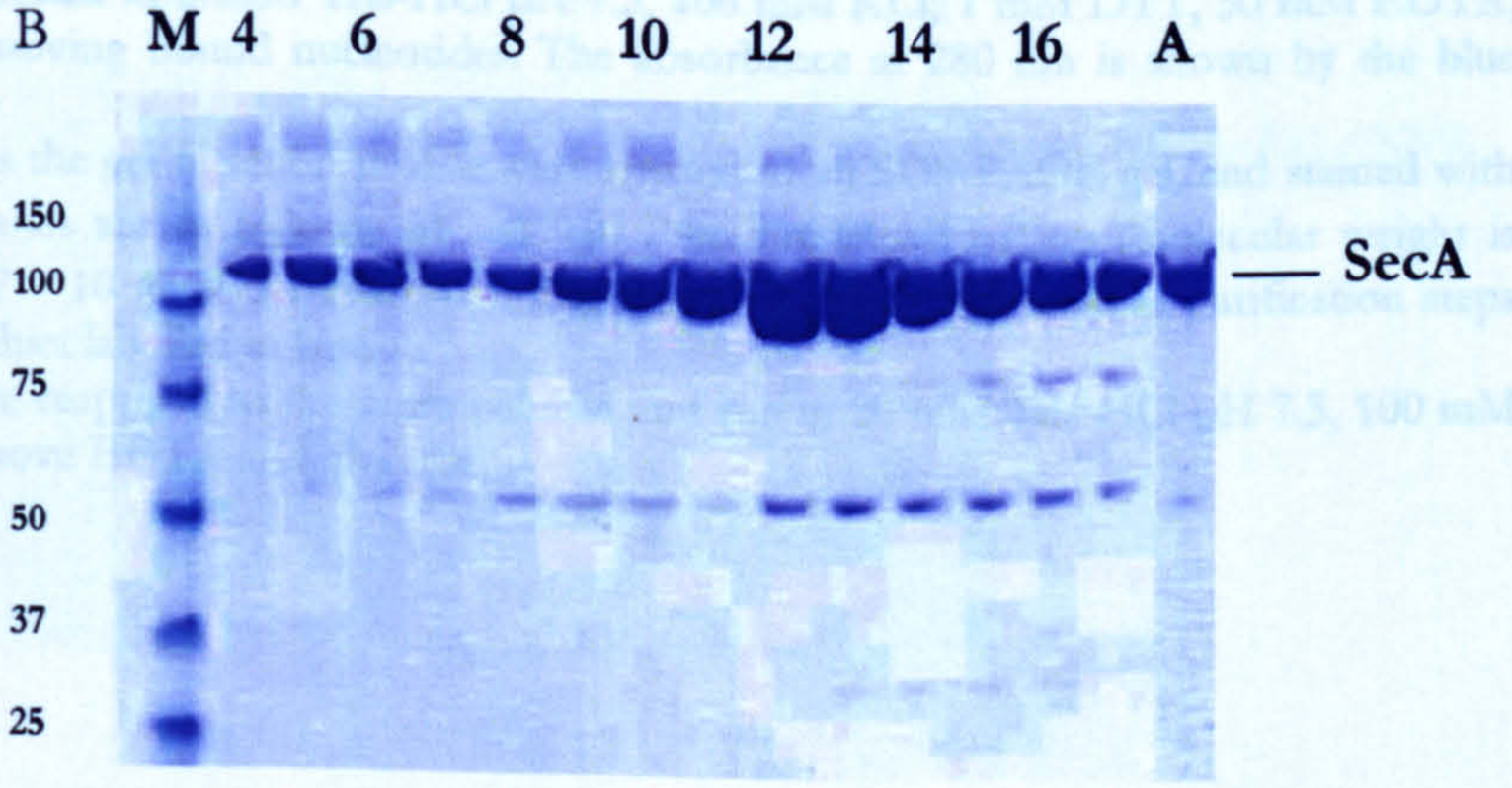
B
M
4
6
8
10
12
14
16
A
150
100
75
50
37
25
SecA

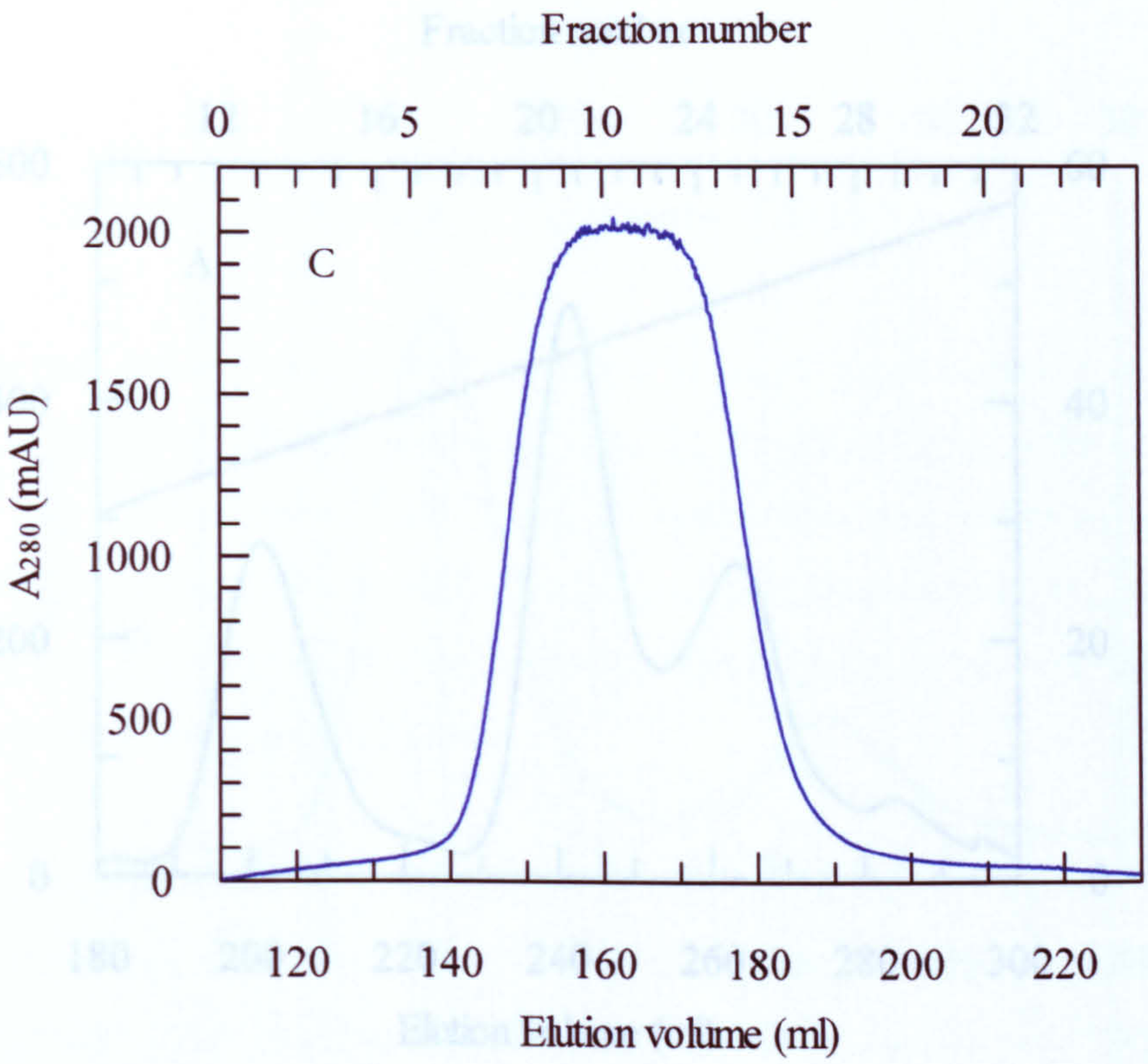

Figure 2-2. Removal of nucleotides from SecA by size exclusion chromatography.

(A) Fractions 27-31 from anion exchange (Figure 2-1) were applied to a Superdex 200 XK 26/60 gel filtration column equilibrated in 20mM Tris-HCl pH 7.5, 100 mM KCl, 1 mM DTT, 50 mM EDTA, 20% (v/v) glycerol, removing bound nucleotides. The absorbance at 280 nm is shown by the blue trace.

(B) Samples from across the gel filtration profile were applied to an SDS-PAGE gel, and stained with Coomassie blue. The lanes are as follows: M – 10 µl Precision plus markers (molecular weight is shown on the left), 4-17 – 10 µl of the corresponding fractions in (A). Subsequent purification steps resulted in the final product labelled in lane A.

(C) Fractions 12-15 were reapplied to the same column and run in 20 mM Tris-HCl pH 7.5, 100 mM KCl, 1 mM DTT to remove EDTA and glycerol.

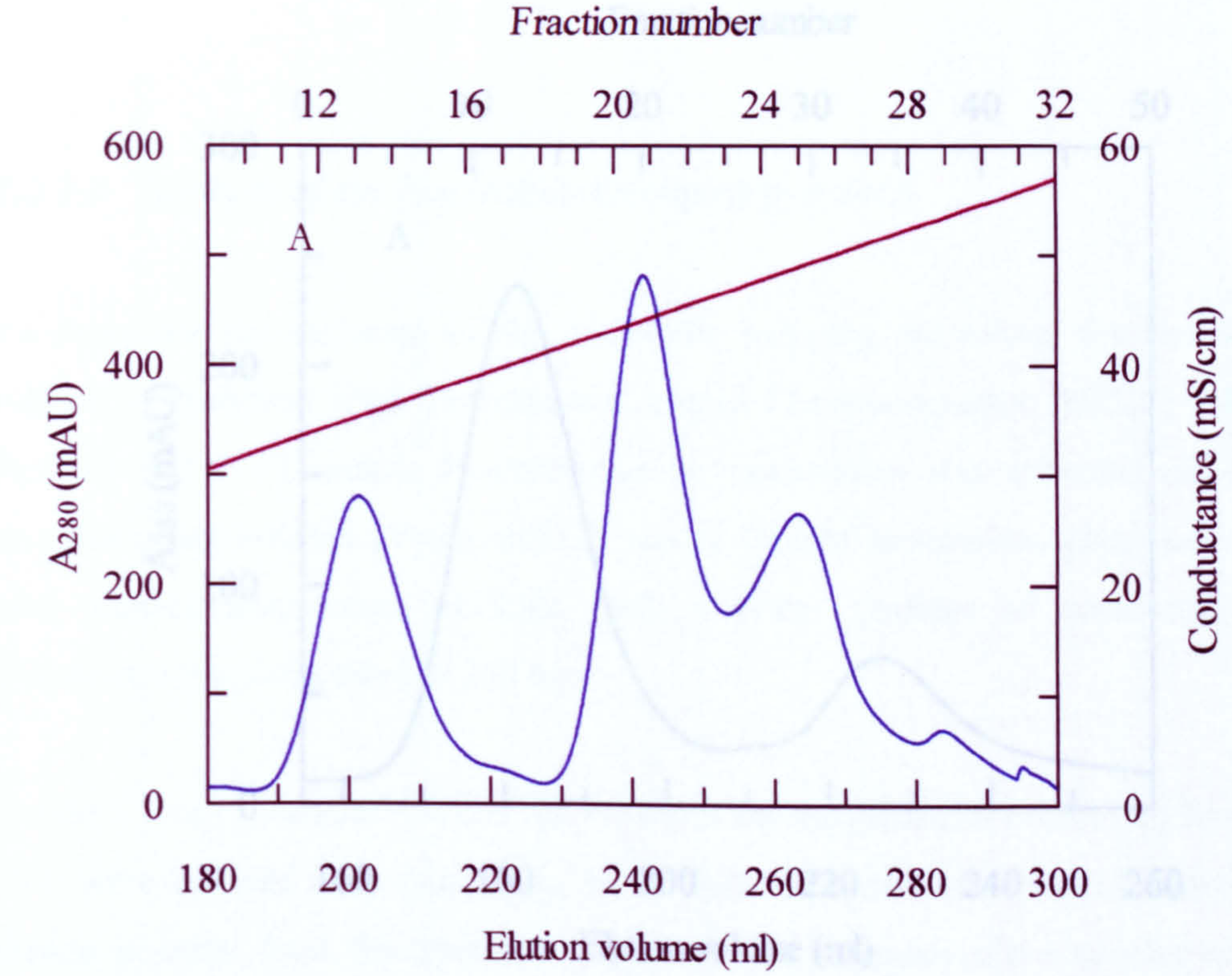

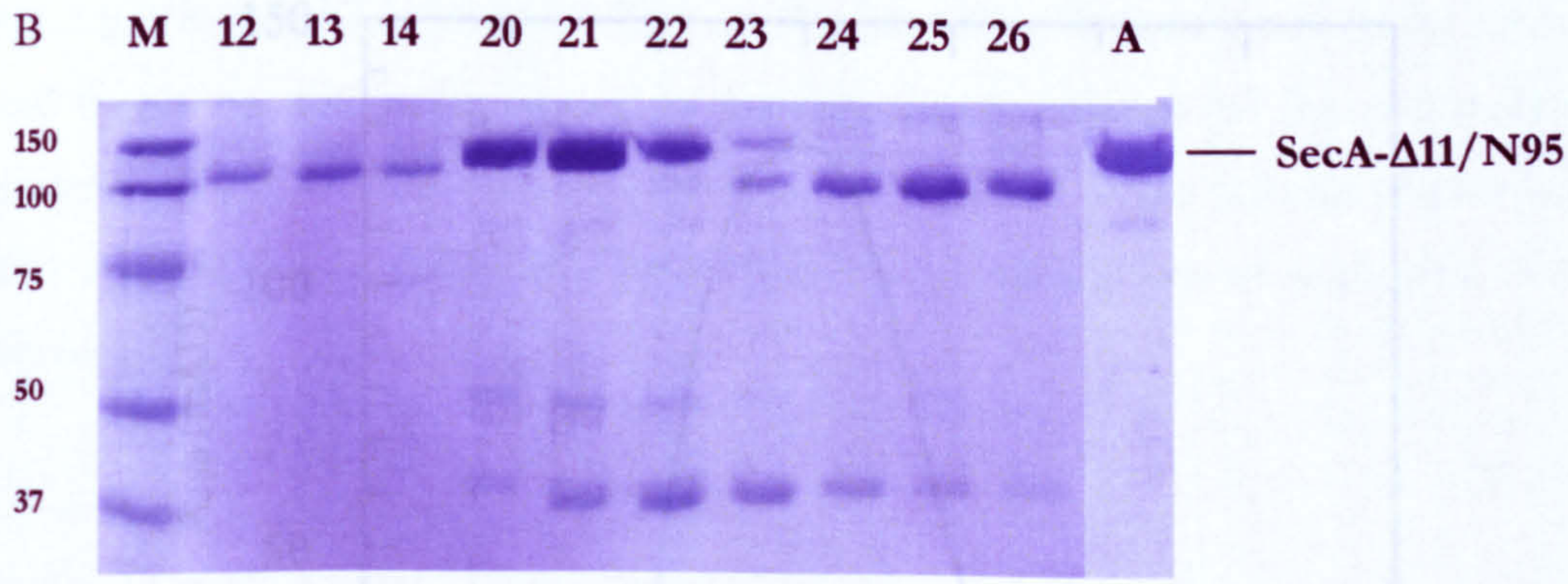

Figure 2-3. Purification of SecA-Δ11/N95 by anion exchange chromatography.

(A) A Q-Sepharose HP XK 26/20 column was equilibrated in 20 mM Tris-HCl pH 7.5, 100 mM KCl, 2 mM $MgCl_2$ and eluted by a linear gradient (0-1 M KCl). The absorbance at 280 nm is shown by the blue trace, and conductance (mS/cM) by the brown trace.

(B) Samples from across the anion exchange elution profile were applied to an SDS-PAGE gel, and stained with Coomassie blue. The lanes are as follows: M – 10 µl Precision plus markers (molecular weight is shown on the left), 12-26 – 10 µl of the corresponding fractions in (A), fractions 20-22 were selected for further purification. Subsequent purification steps resulted in the final product labelled in lane A.

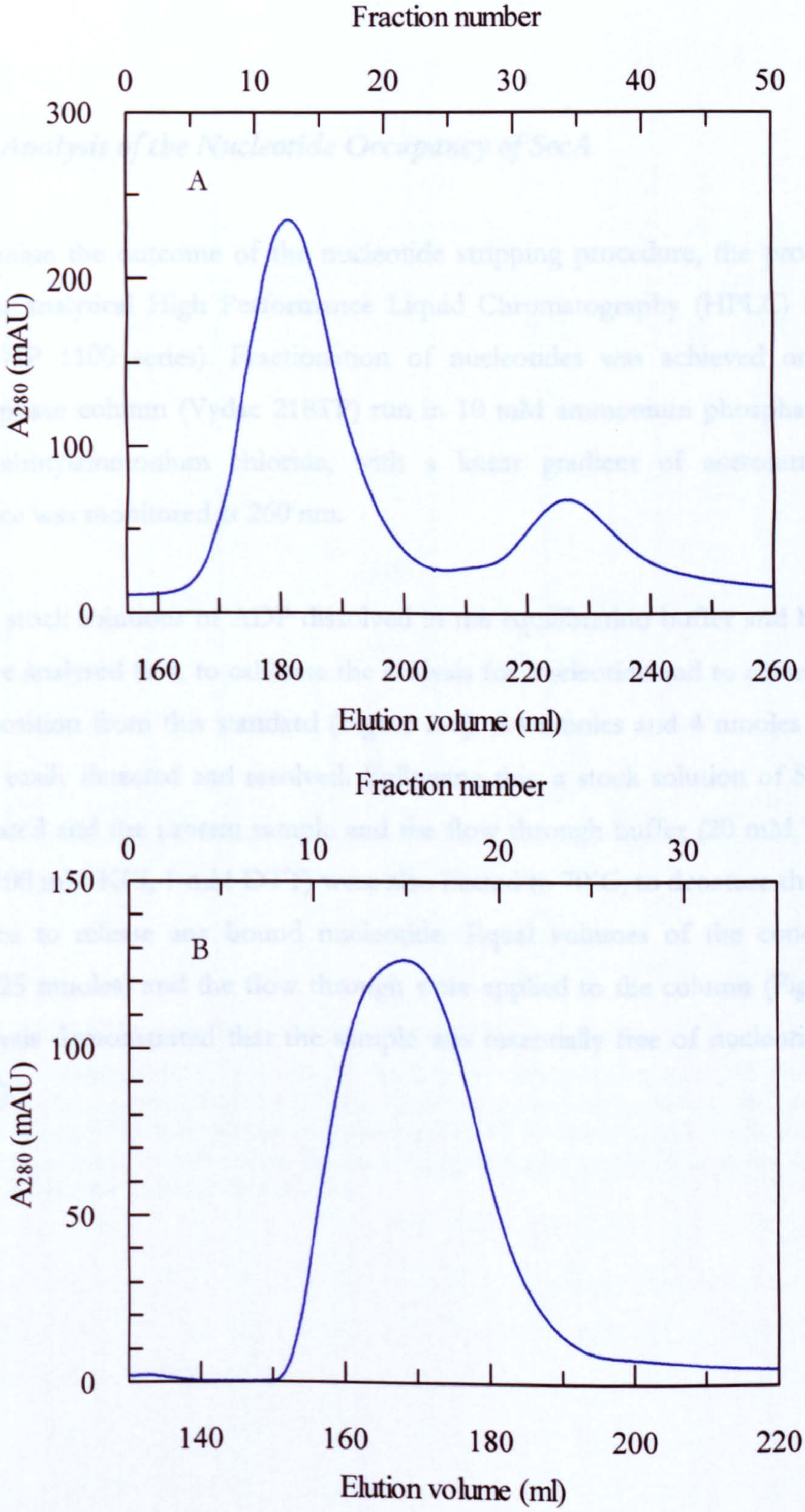

Figure 2-4. Removal of nucleotides from SecA-Δ11/N95 by size exclusion chromatography.

(A) Fractions 20-22 from anion exchange (Figure 2-3) were applied to a Superdex 200 XK 26/60 gel filtration column equilibrated in 20mM Tris-HCl pH 7.5, 100 mM KCl, 1 mM DTT, 50 mM EDTA, 20% (v/v) glycerol, removing bound nucleotides. The absorbance at 280 nm is shown by the blue trace.
(B) Fractions 9-16 in (A) were reapplied to the same column and run in 20 mM Tris-HCl pH 7.5, 100 mM KCl, 1 mM DTT to remove EDTA and glycerol. The absorbance at 280 nm is shown by the blue trace.

2.2.1.1 Analysis of the Nucleotide Occupancy of SecA

To determine the outcome of the nucleotide stripping procedure, the protein was subject to analytical High Performance Liquid Chromatography (HPLC) (Hewlett Packard HP 1100 series). Fractionation of nucleotides was achieved on a C18 reversed-phase column (Vydac 218TP) run in 10 mM ammonium phosphate and 8 mM tetrabutylammonium chloride, with a linear gradient of acetonitrile. The absorbance was monitored at 260 nm.

Standard stock solutions of ADP dissolved in the equilibration buffer and heated to 70°C were analysed first, to calibrate the analysis for nucleotide and to determine the elution position from this standard (Figure 2-5). 0.4 nmoles and 4 nmoles of ADP could be easily detected and resolved. Following this, a stock solution of SecA was concentrated and the protein sample and the flow through buffer (20 mM Tris-HCl pH 7.5, 100 mM KCl, 1 mM DTT) were also heated to 70°C, to denature the protein and hence to release any bound nucleotide. Equal volumes of the concentrated protein (25 nmoles) and the flow through were applied to the column (Figure 2-5). The analysis demonstrated that the sample was essentially free of nucleotide (<1% occupied).

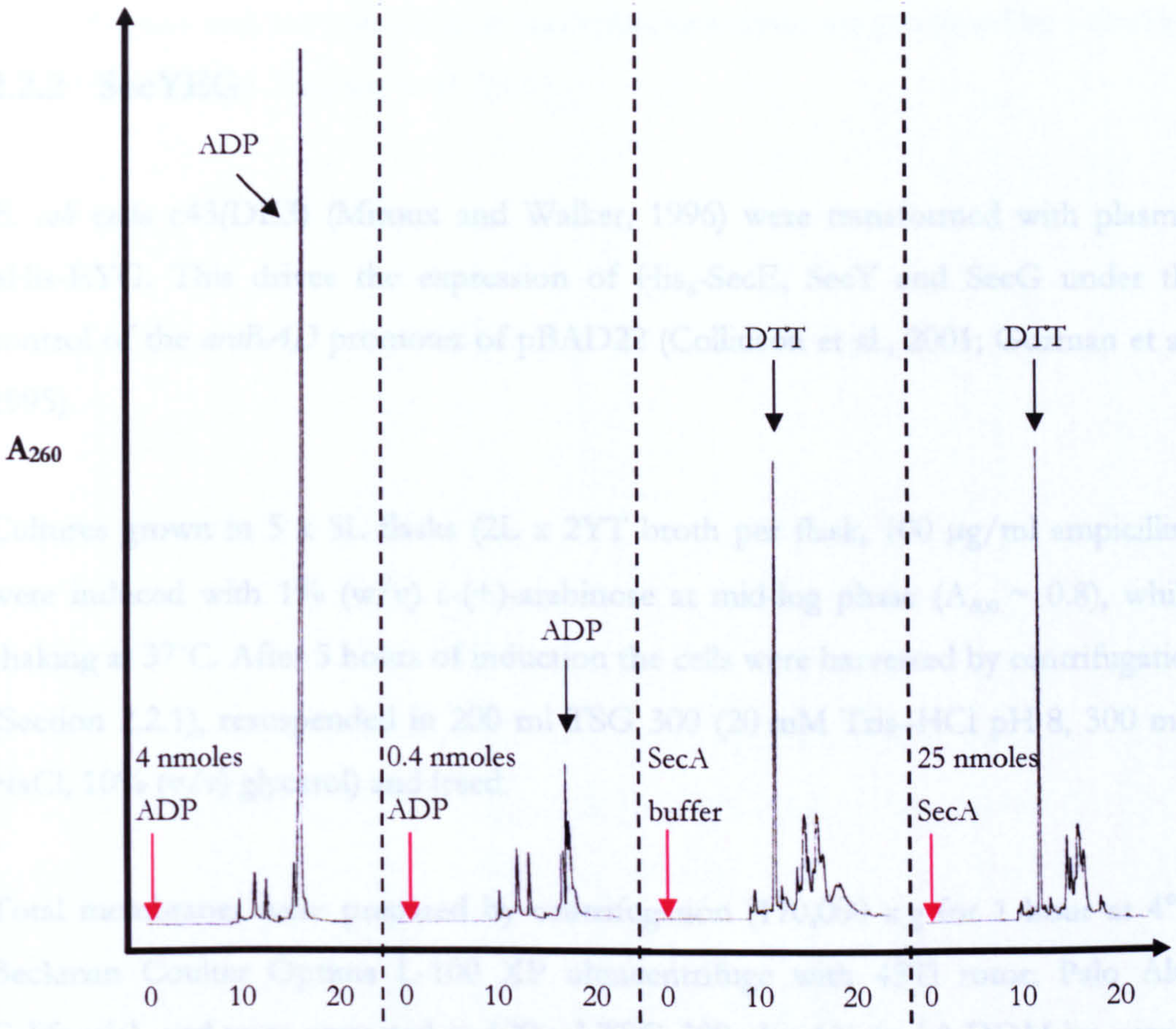

Figure 2-5. Nucleotide analysis of SecA samples by HPLC

Standard stock solutions of ADP (4 and 0.4 nmoles) were analysed first on a C18 reversed-phase column using a linear gradient with acetonitrile. A stock solution of denatured SecA was concentrated, and equal volumes of the flow through (20 mM Tris-HCl pH 7.5, 100 mM KCl, 1 mM DTT) and the concentrated protein (25 nmoles) were separated. The absorbance at 260 nm is shown by the black traces and the injection point by the red arrows.

2.2.2 SecYEG

E. coli cells c43(DE3) (Miroux and Walker, 1996) were transformed with plasmid pHis-EYG. This drives the expression of His_6-SecE, SecY and SecG under the control of the *araBAD* promoter of pBAD22 (Collinson et al., 2001; Guzman et al., 1995).

Cultures grown in 5 x 5L flasks (2L x 2YT broth per flask, 100 μg/ml ampicillin), were induced with 1% (w/v) L-(+)-arabinose at mid-log phase (A_{600} ~ 0.8), whilst shaking at 37°C. After 3 hours of induction the cells were harvested by centrifugation (Section 2.2.1), resuspended in 200 ml TSG 300 (20 mM Tris–HCl pH 8, 300 mM NaCl, 10% (v/v) glycerol) and lysed.

Total membranes were prepared by centrifugation (170,000 x *g* for 1 hour at 4°C; Beckman Coulter Optima L-100 XP ultracentrifuge with 45Ti rotor; Palo Alto, California), and were extracted in 100 ml TSG 300 plus 1% (w/v) DDM by stirring for 1 hour at 4°C. Insoluble material was removed by centrifugation as before.

A Ni^{2+}-Sepharose column (Chelating Sepharose fast flow) was employed to bind the SecYEG complex, which was subsequently washed with TSG 300 containing 25 mM imidazole and 0.1% (w/v) $C_{12}E_9$. This procedure served to exchange the detergent bound to SecYEG, so all subsequent steps were performed in $C_{12}E_9$. SecYEG was eluted in the same buffer plus 300 mM imidazole. Further purification was achieved by simultaneous gel filtration (Superdex 200 XK 26/60 column) and anion exchange (Q-Sepharose HP XK 26/20 column) chromatography in 20 mM Tris–HCl pH 8, 130 mM NaCl and 0.05% (w/v) $C_{12}E_9$ (Figure 2-6). The proteins are thus first separated by gel filtration chromatography, and in the same step contaminants are bound to the anion exchange column whilst SecYEG passes directly through. This procedure demonstrated that the shoulder eluting after the main peak contained mostly the SecE subunit (lanes 8 and 9). The protein was concentrated to ~ 300 μM (20 mg/ml), and stored at -80°C. Protein quantification was carried out by amino acid analysis, revealing an extinction coefficient value of 139,000 ± 23,350 M-1cm-1

(Alta Bioscience, Birmingham, UK) (Robson et al., 2007). The preparation was relatively pure with the exception of two minor contaminants generated by a cleavage in SecY (Collinson, Breyton et al. 2001).

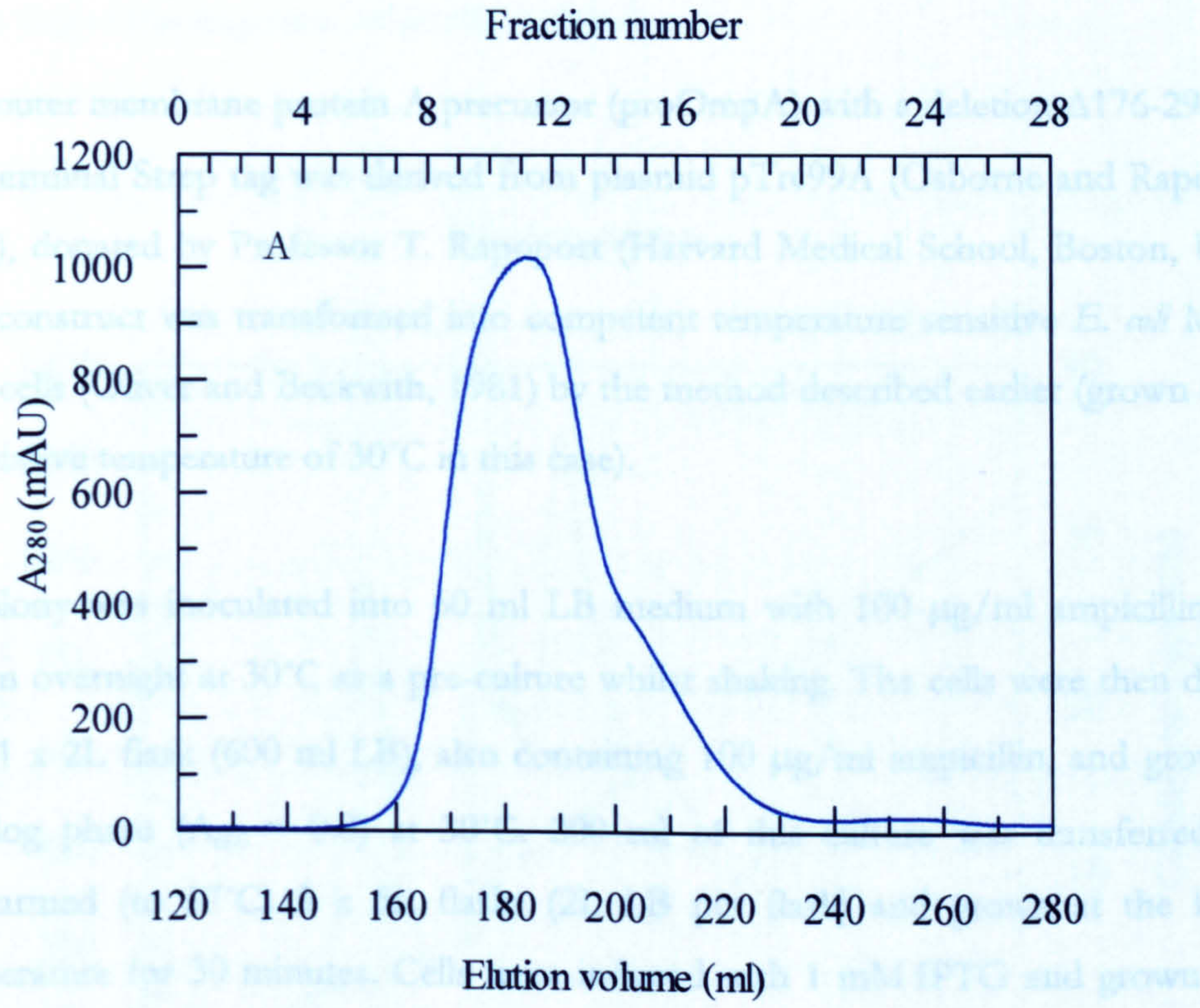

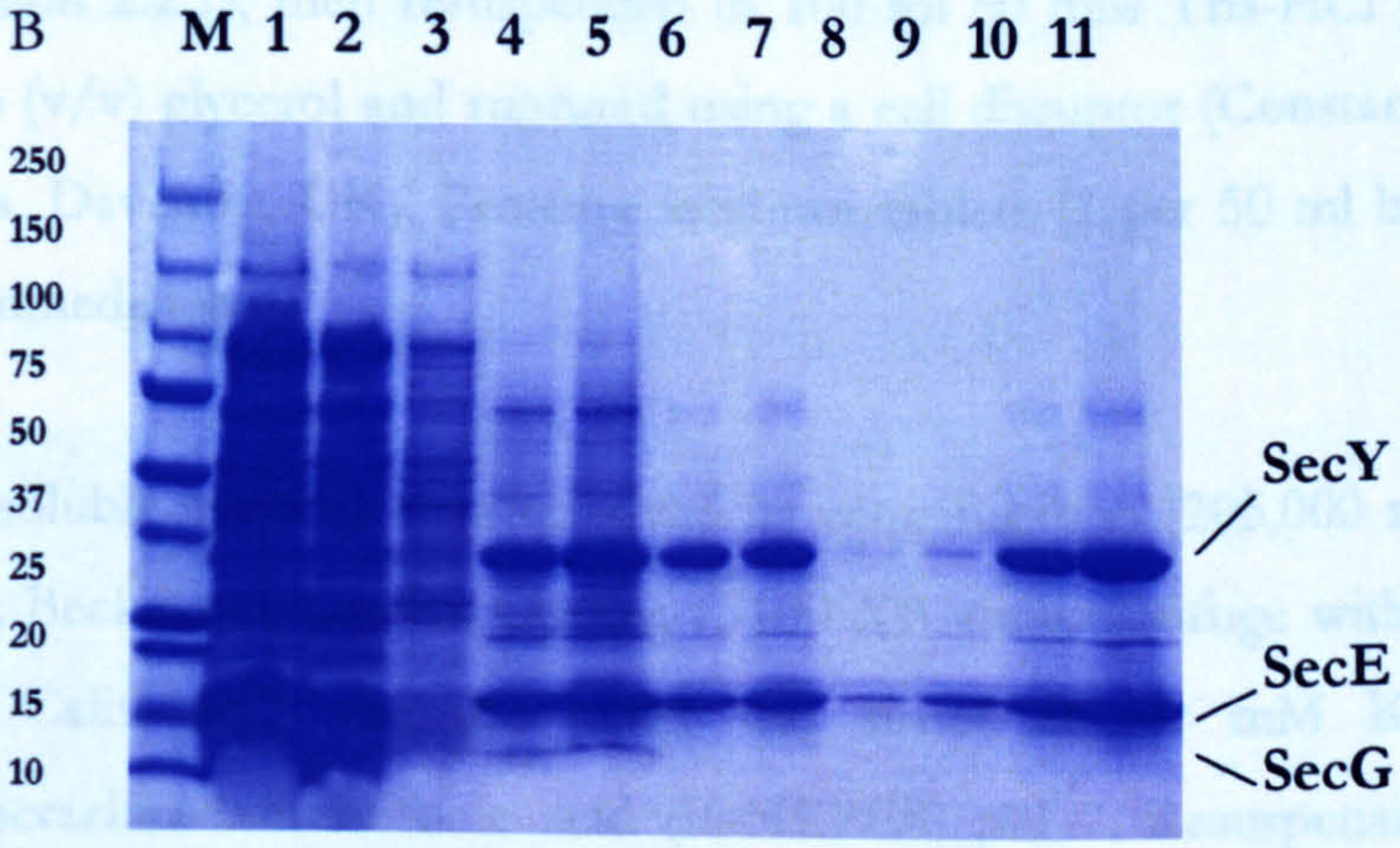

Figure 2-6. Purification of SecYEG.

(A) Gel filtration chromatography using a Superdex 200 XK 26/60 column and anion exchange using a Q-Sepharose HP XK 26/20 column were carried out simultaneously in 20 mM Tris–HCl pH 8, 130 mM NaCl and 0.1% (w/v) $C_{12}E_9$. The absorbance at 280nm is shown by the blue trace.
(B) Samples from various stages of SecYEG purification were applied to an SDS-PAGE gel, and stained with Coomassie blue. The lanes are as follows: 1 – 10 µl Precision plus markers (molecular weight is shown on the left), 2 – 10 µl solubilised membranes, 3 – 6 µl flow through from the Ni^{2+}-affinity column, 4 – 10 µl 25 mM Imidazole Ni^{2+}-affinity column wash, 5 – 5 µl 300 mM Imidazole Ni^{2+}-affinity column eluate, 6 – 10 µl of the same sample, 7 – 5 µl gel filtration and anion exchange eluate (fractions 9-12 in (A)), 8 – 10 µl of the same sample, 9 – 2 µl fraction 16 in (A), 10 – 5 µl of the same sample, 11- 0.5 µl pure concentrated SecYEG, 12 – 1 µl of the same sample.

2.2.3 proOmpA

The outer membrane protein A precursor (proOmpA) with a deletion Δ176-296 and a C-terminal Strep tag was derived from plasmid pTrc99A (Osborne and Rapoport, 2007), donated by Professor T. Rapoport (Harvard Medical School, Boston, USA). The construct was transformed into competent temperature sensitive *E. coli* MM52 host cells (Oliver and Beckwith, 1981) by the method described earlier (grown at the permissive temperature of 30°C in this case).

A colony was inoculated into 60 ml LB medium with 100 μg/ml ampicillin, and grown overnight at 30°C as a pre-culture whilst shaking. The cells were then diluted into 1 x 2L flask (600 ml LB), also containing 100 μg/ml ampicillin, and grown to mid-log phase (A_{600} ~ 0.8) at 30°C. 200 ml of this culture was transferred into prewarmed (to 37°C) 3 x 5L flasks (2L LB per flask) and grown at the higher temperature for 30 minutes. Cells were induced with 1 mM IPTG and grown for a further 2 hours at 37°C. After protein expression, the cells were harvested by centrifugation (Section 2.2.1), then resuspended in 100 ml 50 mM Tris-HCl pH 8, 300 mM KCl, 10% (v/v) glycerol and ruptured using a cell disruptor (Constant Cell Disruption Systems, Daventry, UK). Protease inhibitor tablets (1 per 50 ml broken cells) were added immediately.

Membranes and insoluble material were removed by centrifugation (205,000 x *g* for 30 minutes at 4°C; Beckmann Coulter Optima L-100 XP ultracentrifuge with 45Ti rotor; Palo Alto, California), and the pellet was rinsed in 50 mM K-4-(2-hydroxyethyl)-1-piperazineethanesulfonic acid (K-HEPES) pH 7. Resuspension of the pellet was achieved by use of 50 ml buffer containing 50 mM K-HEPES pH 7, 6M urea and a dounce homogenizer. The suspension was stirred for 20 minutes at room temperature, and the unfolded protein separated by centrifugation (100,000 x *g* for 1 hour at 4°C; Beckmann Coulter Optima L-100 XP ultracentrifuge with 70Ti rotor; Palo Alto, California). The supernatant was then fractionated with an anion exchange column (Q-Sepharose HP XK 26/20 column, GE Healthcare), equilibrated in the same buffer and eluted by a linear gradient (0-1M KCl) (Figure 2-7). The purified protein was concentrated to ~ 80 μM (2 mg/ml), and stored at -80°C.

Protein quantification was carried out using the extinction coefficient calculated according to the sequence, of 49,860 $M^{-1}cm^{-1}$.

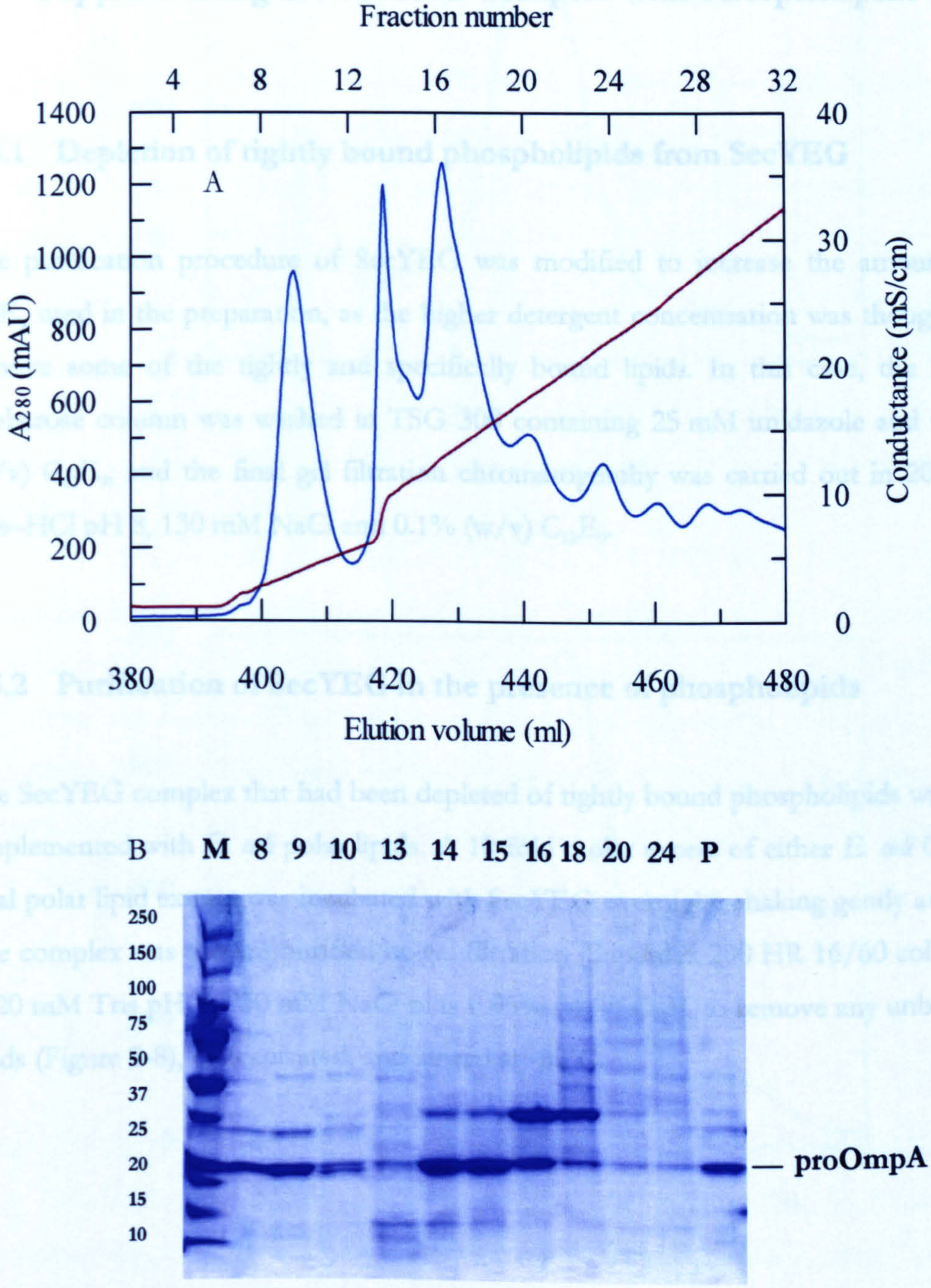

Figure 2-7. Purification of proOmpA.

(A) A Q-Sepharose HP XK 26/20 column was equilibrated in 50 mM K-HEPES pH 7, 6M urea and eluted by a linear gradient (0-1 M KCl). The absorbance at 280 nm is shown by the blue trace, and conductance (mS/cM) by the brown trace.
(B) Samples from across the anion exchange elution profile were applied to an SDS-PAGE gel, and stained with Coomassie blue. The lanes are as follows: M – 10 µl Precision plus markers (molecular weight is shown on the left), 8-24 – 10 µl of the corresponding fractions in (A). Subsequent purification steps performed with fractions 8 and 9 resulted in the final product labelled in lane P.

2.3 Supplementing the SecYEG Complex with Phospholipids

2.3.1 Depletion of tightly bound phospholipids from SecYEG

The purification procedure of SecYEG was modified to increase the amount of $C_{12}E_9$ used in the preparation, as the higher detergent concentration was thought to remove some of the tightly and specifically bound lipids. In this case, the Ni^{2+}-Sepharose column was washed in TSG 300 containing 25 mM imidazole and 0.5% (w/v) $C_{12}E_9$, and the final gel filtration chromatography was carried out in 20 mM Tris–HCl pH 8, 130 mM NaCl and 0.1% (w/v) $C_{12}E_9$.

2.3.2 Purification of SecYEG in the presence of phospholipids

The SecYEG complex that had been depleted of tightly bound phospholipids was re-supplemented with *E. coli* polar lipids. A 10-fold molar excess of either *E. coli* CL or total polar lipid extract was incubated with SecYEG overnight, shaking gently at 4°C. The complex was then re-purified by gel filtration (Superdex 200 HR 16/60 column) in 20 mM Tris pH 8, 130 mM NaCl plus 0.05% (w/v) $C_{12}E_9$ to remove any unbound lipids (Figure 2-8), concentrated, and stored at -80°C.

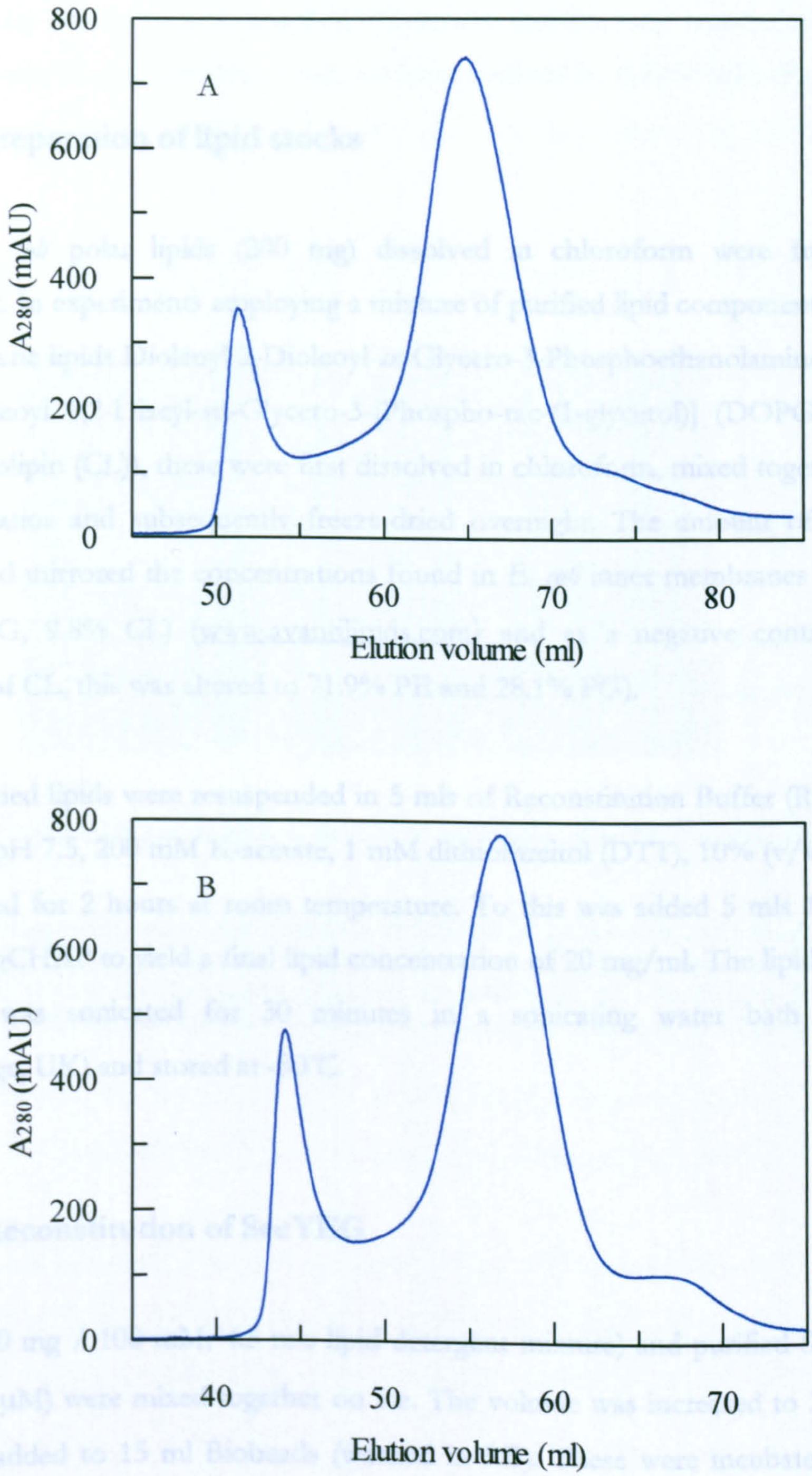

Figure 2-8. Isolation of the lipid supplemented SecYEG complex by gel filtration chromatography.

SecYEG supplemented with (A) *E. coli* CL or (B) total *E. coli* polar lipids was loaded onto a Superdex 200 HR 16/60 in 20 mM Tris pH 8, 130 mM NaCl, 0.05% (w/v) $C_{12}E_9$ to remove any unbound lipids. The absorbance at 280nm is shown by the blue trace.

2.4 Reconstitution of SecYEG into Liposomes

2.4.1 Preparation of lipid stocks

Total *E. coli* polar lipids (200 mg) dissolved in chloroform were freeze-dried overnight. In experiments employing a mixture of purified lipid components (such as the synthetic lipids Dioleoyl 2-Dioleoyl-*sn*-Glycero-3-Phosphoethanolamine (DOPE) and Dioleoyl 1,2-Diacyl-sn-Glycero-3-[Phospho-rac-(1-glycerol)] (DOPG), and *E. coli* Cardiolipin (CL)), these were first dissolved in chloroform, mixed together at the desired ratios and subsequently freeze-dried overnight. The amount of synthetic lipids used mirrored the concentrations found in *E. coli* inner membranes (67% PE, 23.2% PG, 9.8% CL) (www.avantilipids.com) and as a negative control in the absence of CL, this was altered to 71.9% PE and 28.1% PG).

Freeze-dried lipids were resuspended in 5 mls of Reconstitution Buffer (RB; 50 mM HEPES pH 7.5, 200 mM K-acetate, 1 mM dithiothreitol (DTT), 10% (v/v) glycerol) and stirred for 2 hours at room temperature. To this was added 5 mls 12% (w/v) DeoxyBigCHAP to yield a final lipid concentration of 20 mg/ml. The lipid-detergent mixture was sonicated for 30 minutes in a sonicating water bath (CamLab, Cambridge, UK) and stored at -80°C.

2.4.2 Reconstitution of SecYEG

Lipids (90 mg / 100 mM; 4.5 mls lipid-detergent mixture) and purified SecYEG (5 mg / 75 μM) were mixed together on ice. The volume was increased to 30 ml with RB and added to 15 ml Biobeads (washed in RB). These were incubated, shaking gently at 4°C overnight to extract the detergent. The turbid liquid was then run down a gravity filter column to remove all Biobeads, and the liposomes pelleted by centrifugation (205,000 x *g* for 1 hour at 4°C; Beckmann Coulter Optima L-100 XP ultracentrifuge with 45Ti rotor; Palo Alto, California). The pellets were resuspended in 14 mls 50 mM K-HEPES pH 7.5, 1 mM DTT, 10% (v/v) glycerol to yield final stock concentrations of 0.4 mg/ml SecYEG (5.4 μM) and 6.6 mg/ml lipids (7 mM)

and were stored at -80°C. Liposome samples were also made in the absence of SecYEG for use as negative controls. To ensure that the total amount of SecYEG was similar in all reconstitutions, samples were resolved by SDS-PAGE (Figure 2-9).

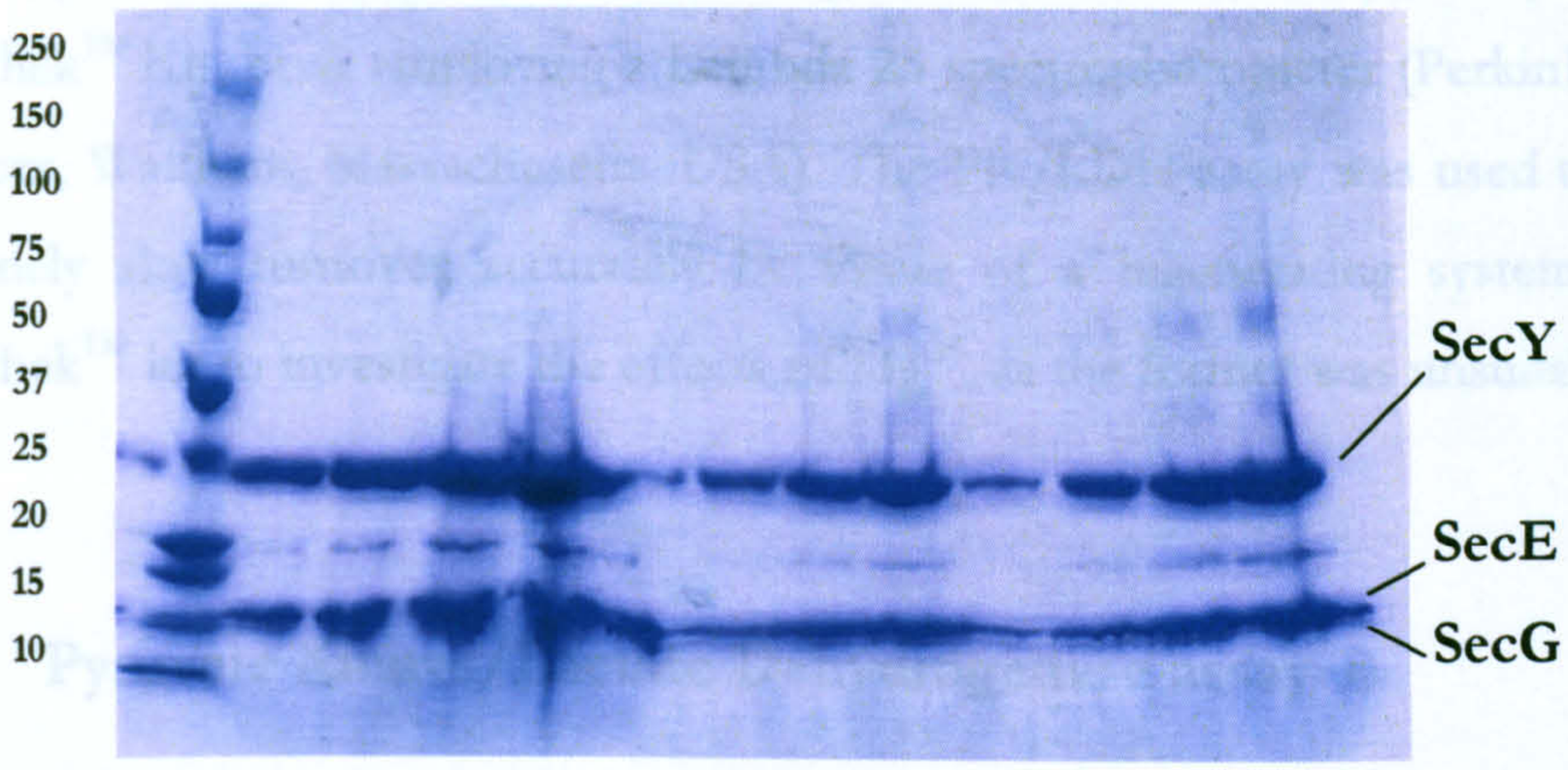

Figure 2-9. Quantification of protein content in reconstituted SecYEG preparations by SDS-PAGE.

Reconstituted proteoliposomes were applied to an SDS-PAGE gel at amounts of 1 μg, 2 μg, 4 μg and 8 μg SecYEG, and stained using Coomassie blue. The lanes were loaded in increasing amounts from left to right: 1-4 - SecYEG reconstituted into *E. coli* polar lipids, 5-8 - SecYEG reconstituted into vesicles of DOPE and DOPG, 9-12 - SecYEG reconstituted into vesicles of DOPE, DOPG and CL.

2.5 Measurement of the Steady-state ATPase Activity of SecA

Steady-state ATPase assays were carried out and monitored at 25°C, either by the linked pyruvate kinase / lactate dehydrogenase (PK/LDH) assay, or by use of the EnzChek™ Kit, both employing a Lambda 25 spectrophotometer (PerkinElmer Life Sciences, Waltham, Massachusetts, USA). The PK/LDH assay was used to measure extremely slow turnover accurately by virtue of a regenerating system, and the EnzChek™ kit to investigate the effects of Mg^{2+}, as the former was unsuitable.

2.5.1 Pyruvate Kinase/Lactate Dehydrogenase assay

The PK/LDH assay measures the release of ADP, via a double linked enzyme system. The final step is conversion of NADH and H^+ to NAD^+, thus a decrease in absorbance at 340 nm is used to monitor reaction progress (Figure 2-10). Standard assay components were 10 units/ml LDH, 7 units/ml PK, 2 mM phosphoenolpyruvate (PEP), and 0.2 mM NADH in TKM buffer (50 mM triethanolamine pH 7.5, 50 mM KCl, 2 mM $MgCl_2$). SecA or SecA-Δ11/N95 (0.3 μM) were used in each reaction, and the assays were initiated by addition of ATP.

The decrease in optical density was converted into ATPase activity where 1 molecule of NADH oxidized to NAD^+ corresponds to the production of 1 molecule of ADP by SecA. This was calculated using the extinction coefficient for NADH of 6,220 $M^{-1}cm^{-1}$.

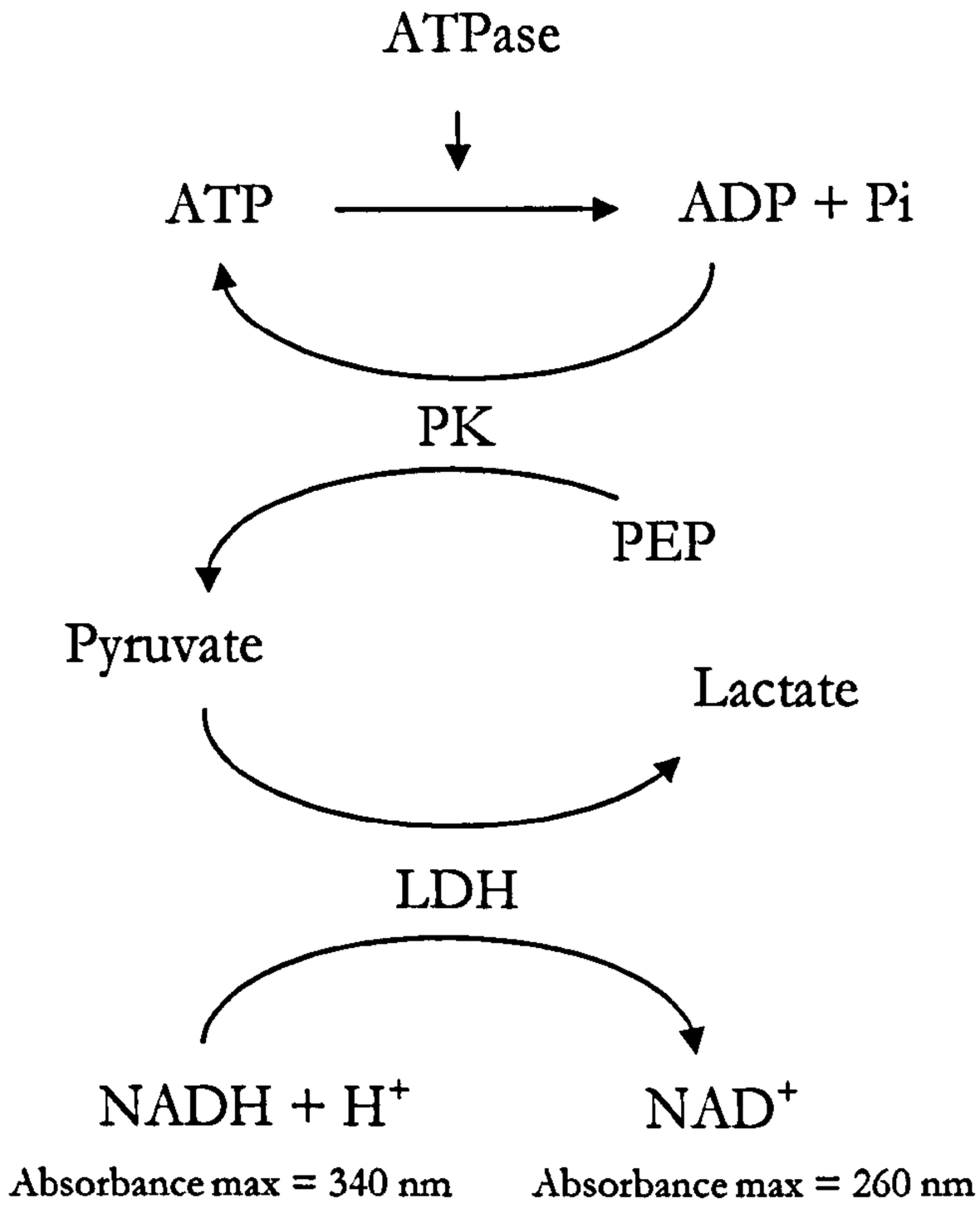

Figure 2-10. PK/LDH assay.

ATP is hydrolysed to ADP and Pi by the ATPase. The released ADP is used in the conversion of PEP to pyruvate by PK, whilst concomitantly regenerating ATP from a Pi donated from PEP. This is coupled by the conversion of pyruvate to lactate by LDH. This step requires NADH, which is oxidised to NAD^+, and which absorbs less strongly at 340 nm.

2.5.2 EnzChek™ assay

The EnzChek™ assay measures the release of Pi , via a single linked enzyme system. The reaction measures the change in absorbance of an added substrate 2-amino-6-mercapto-7-methylpurine riboside (MESG) at 360 nm (Figure 2-11) (Webb, 1992). The standard assay components were 0.2 mM MESG and 1 unit of purine nucleoside phosphorylase (PNP) in TK buffer (50 mM triethanolamine, pH 7.5, 50 mM KCl). 0.3 μM SecA or SecA-Δ11/N95 was used in each reaction, together with ADP, Mg^{2+}, lipids, SecYEG (solubilised in $C_{12}E_9$ or in present in proteoliposomes) and proOmpA at various concentrations, prior to the initiation of the reaction by addition of ATP. In some conditions where the ATPase activity was very high, and thus to maintain the released Pi within the linear range of the assay, the concentration of SecA was reduced to 0.05 μM where indicated.

The increase in optical density was converted into ATPase activity where 1 molecule of MESG phosphorylated corresponds to the production of 1 molecule of Pi by SecA. This was calculated using the extinction coefficient for MESG of 11,000 $M^{-1}cm^{-1}$ (Webb, 1992).

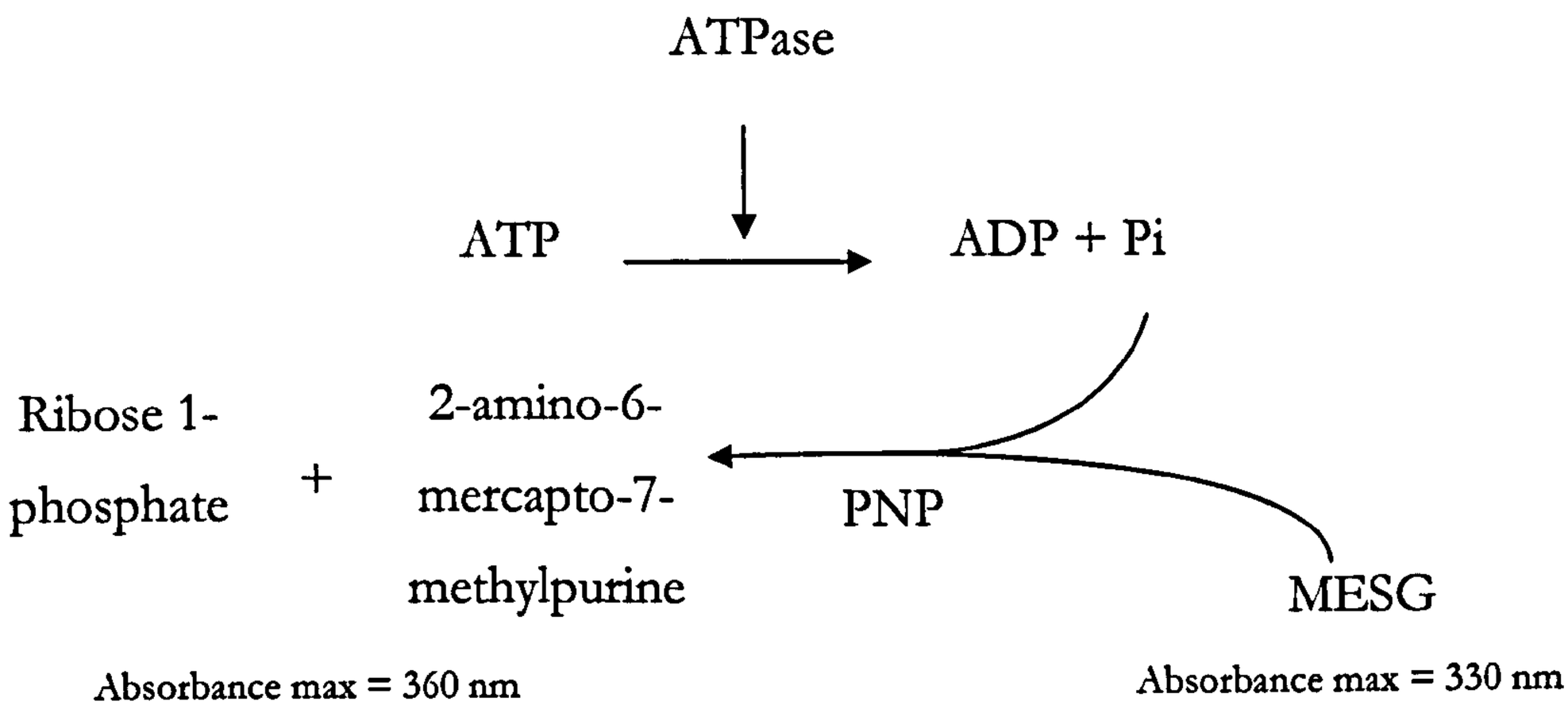

Figure 2-11. EnzChek™ Assay.

ATP is hydrolysed to ADP and Pi by the ATPase. The released Pi is used to convert the guanosine analogue MESG to a purine base product of its reaction, catalysed by PNP. Upon phosphorolysis, MESG generates an increase in absorbance at 360 nm.

2.5.3 Analysis and Curve Fitting of the Steady-state ATPase Activity

2.5.3.1 The Michaelis-Menten equation

The kinetics of ATP turnover were fitted according to the Michaelis-Menten equation, defined as:

$$v = \frac{V\max.[S]}{K_M + [S]}$$

Equation 2-1. The Michaelis-Menten equation.

where v = enzyme velocity, Vmax = maximum enzyme velocity, K_M = Michaelis-Menten constant (the dissociation constant for enzyme-substrate) and $[S]$ = free substrate concentration. Data were fitted using GraFit (Erithacus).

2.5.3.2 Magnesium inhibition

$K_{i(app)}$ values for Mg^{2+} were fitted individually using a hyperbolic inhibition function, defined as:

$$v = Vo - \frac{V\max.[I]}{K_{i(app)} + [I]}$$

Equation 2-2. Hyperbolic inhibition function.

Where v = enzyme velocity, Vo = enzyme velocity at zero concentration of inhibitor, Vmax = maximum enzyme velocity, $[I]$ = free inhibitor concentration and $K_{i(app)}$ = dissociation constant for enzyme-inhibitor. Data were fitted using GraFit (Erithacus).

Binding constants for ATP and allosteric Mg^{2+} to SecA were calculated using a global fit and Monte-Carlo analysis using IGOR software (Wavemetrics), using the following derivation:

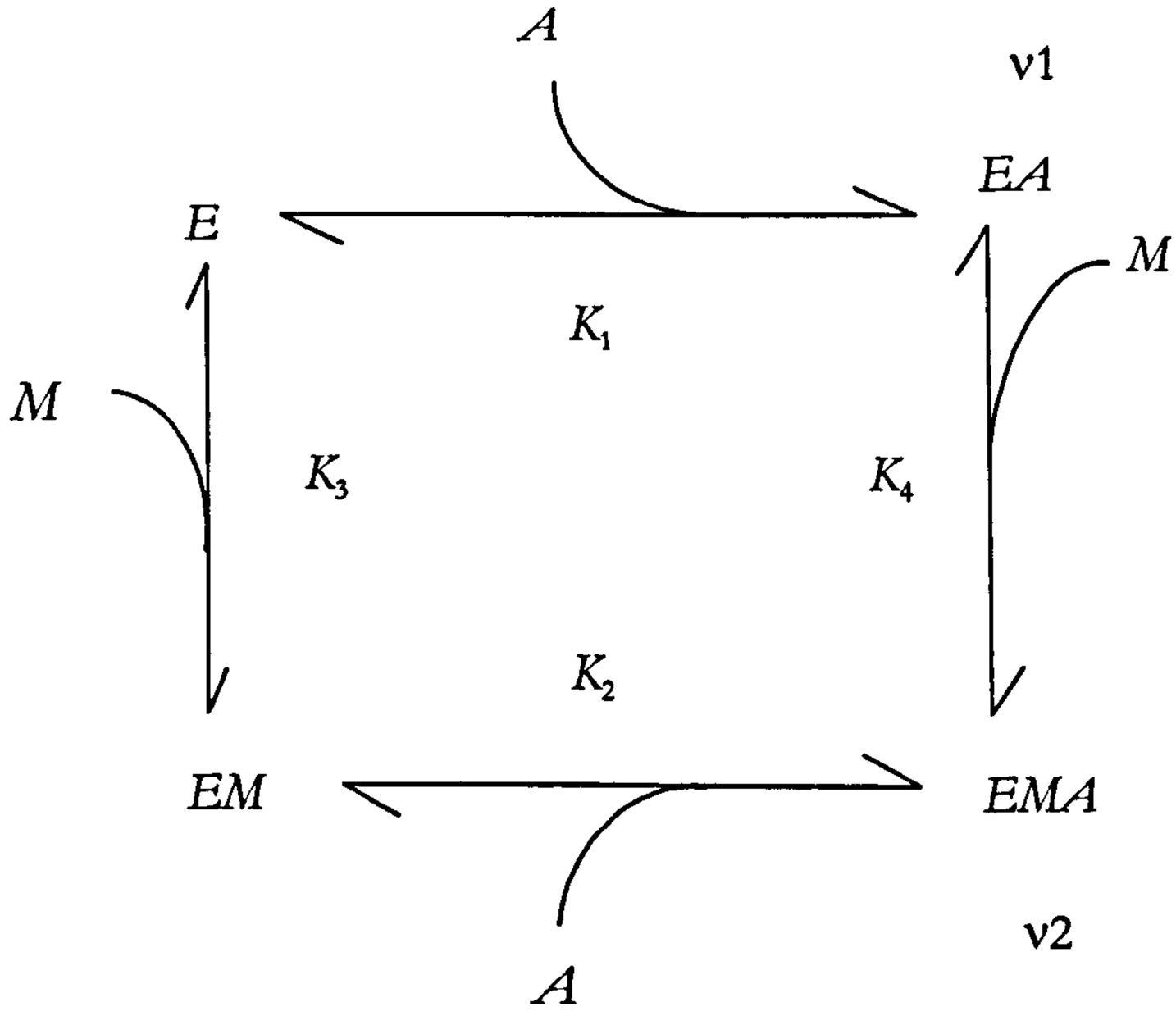

where E = apo enzyme, A= ATP, M = free Mg^{2+} available to bind to an allosteric site, EA = enzyme-ATP complex, EM = enzyme-allosteric Mg^{2+} complex, EMA = enzyme-allosteric magnesium-ATP complex, $K_{1\text{-}4}$ = respective binding constants for A and M and v1-2 = measured velocity. We assume that the Mg^{2+} bound to the catalytic site is always bound to SecA.

Step 1 - Define $K_{1\text{-}4}$:

$$K_1 = \frac{[E][A]}{[EA]} \qquad K_2 = \frac{[EM][A]}{[EMA]} \qquad K_3 = \frac{[E][M]}{[EM]} \qquad K_4 = \frac{[EA][M]}{[EMA]}$$

Step 2 - Incorporate into $\frac{v}{Eo}$ two different states of the enzyme with corresponding different velocities and all possible species:

$$\frac{v}{Eo} = \frac{[EA].v1 + [EMA].v2}{[E] + [EA] + [EM] + [EMA]}$$

Step 3 -Divide by [E]:

$$\frac{v}{Eo} = \frac{\frac{[EA]}{[E]}.v1 + \frac{[EMA]}{[E]}.v2}{1 + \frac{[EA]}{[E]} + \frac{[EM]}{[E]} + \frac{[EMA]}{[E]}}$$

Step 4 - Rearrange *K*:

$K_{1:}$ $\qquad$ $K_{2:}$ $\qquad$ $K_{3:}$

$$\frac{[EA]}{[E]} = \frac{[A]}{K_1} \qquad [EMA] = \frac{[EM][A]}{K_2} \qquad [E] = \frac{K_3[EM]}{[M]} \text{ and } \frac{[EM]}{[E]} = \frac{[M]}{K_3}$$

Step 5 - Substitute and rearrange in terms of $\frac{[EMA]}{[E]}$:

$$\frac{[EMA]}{[E]} = \frac{[EM][A]}{K_2} \cdot \frac{[M]}{K_3[EM]}$$

Step 6 - Simplify:

$$\frac{[EMA]}{[E]} = \frac{[A][M]}{K_2.K_3}$$

Step 7 - Substitute $\frac{[EA]}{[E]}$ and $\frac{[EMA]}{[E]}$ into $\frac{v}{Eo}$:

$$\frac{v}{Eo} = \frac{\frac{[A]}{K_1}.v1 + \frac{[A][M]}{K_2.K_3}.v2}{1 + \frac{[A]}{K_1} + \frac{[M]}{K_3} + \frac{[A][M]}{K_2.K_3}}$$

Step 8 – Incorporation of Mg^{2+}-ATP chelation:

An adjustment had to be made on account of the chelation of Mg^{2+} by ATP. This is defined as:

$$[M] = [Mo]\left(1 - \frac{[Ao]}{[Ao] + K_{ATP\,/\,Mg}}\right)$$

where $[M]$ = free magnesium, $[Mo]$ = total Mg^{2+}-ATP, total ATP = free ATP, thus $[Ao] = [A]$ and $K_{ATP/Mg} = K_{d[Mg2+\cdot ATP]}$.

Step 9 – Substitution of the chelation effect and rearrangement:

Thus substitute $[M]=[Mo]\left(1-\frac{[Ao]}{[Ao]+K_{ATP\,/\,Mg}}\right)$ and $[A] = [Ao]$ into $\frac{v}{Eo}$ and arrange in terms of v to give the parent equation:

$$v=\frac{[Eo]\left(\frac{[Ao]}{K_1}.v1+\frac{[Ao][Mo]\left(1-\frac{[Ao]}{[Ao]+K_{ATP\,/\,Mg}}\right)}{K_2.K_3}.v2\right)}{1+\frac{[Ao]}{K_1}+\frac{[Mo]\left(1-\frac{[Ao]}{[Ao]+K_{ATP\,/\,Mg}}\right)}{K_3}+\frac{[Ao][Mo]\left(1-\frac{[Ao]}{[Ao]+K_{ATP\,/\,Mg}}\right)}{K_2.K_3}}$$

Equation 2-3. Derived equation for global fit of magnesium to an allosteric binding site

2.5.3.3 ADP inhibition

ADP inhibition was fitted using a competitive inhibition function, defined as:

$$v=V\max-\frac{V\max.[I]}{K_{i(app)}+[I]}$$

Equation 2-4. Competitive inhibition function.

Where v = enzyme velocity, Vmax = maximum enzyme velocity, $[I]$ = free inhibitor concentration and $K_{i(app)}$ = apparent dissociation constant for enzyme-inhibitor (ADP).

The actual affinity for ADP, $K_{d[ADP]}$ was calculated by fitting the data to the equation:

$$v = \frac{V\max.[T]}{K_{M[ATP]}(1+\frac{[D]}{K_{d[ADP]}})+[T]}$$

Equation 2-5. Calculation of the affinity of ADP for SecA.

where v = measured velocity, $[T]$ = free ATP substrate concentration, Vmax = maximum enzyme velocity, $K_{M[ATP]}$ = Michaelis-Menten constant (the dissociation constant for enzyme-substrate), $[D]$ = free ADP inhibitor concentration; $K_{d[ADP]}$ = dissociation constant for enzyme-ADP. This incorporates the altered value of $K_{M[ATP]}$ at different Mg^{2+} concentrations. Data were fitted using GraFit (Erithacus).

2.5.3.4 Weak ligand binding

Data for CL and liposome (with and without reconstituted SecYEG) binding to SecA in the presence of total *E. coli* polar lipid proteoliposomes were fitted to a one-site weak ligand binding equation (as the concentration of SecA was significantly below the K_d) with background, defined as:

$$v = \frac{V\max.[L]}{K_d+[L]} + Background$$

Equation 2-6. Weak ligand binding equation.

where v = enzyme velocity, Vmax = maximum enzyme velocity, $[L]$ = free ligand concentration and K_d = dissociation constant for enzyme-ligand. Data were fitted using GraFit (Erithacus).

2.5.3.5 *Tight ligand binding*

Data for proOmpA binding to SecA were fitted to a one-site quadratic tight ligand binding equation (as the concentration of SecA was close to the value of the K_d) with background, defined as:

$$v = V\max\frac{[L]+[Eo]+K_d-\sqrt{([L]+[Eo]+K_d)^2-4[Eo][L]}}{2[Eo]}+Background$$

Equation 2-7. Tight ligand binding equation.

where v = enzyme velocity, Vmax = maximum enzyme velocity, $[L]$ = total ligand concentration, $[Eo]$ = total SecA concentration, and K_d = dissociation constant for enzyme-ligand. Data were fitted using GraFit (Erithacus).

2.5.3.6 *Derivation of the steady-state equation*

In order to determine the effect of proOmpA on the SecA ATPase cycle, the steady-state equation for SecA was derived by the vectorial method (Wong, 1975) as follows:

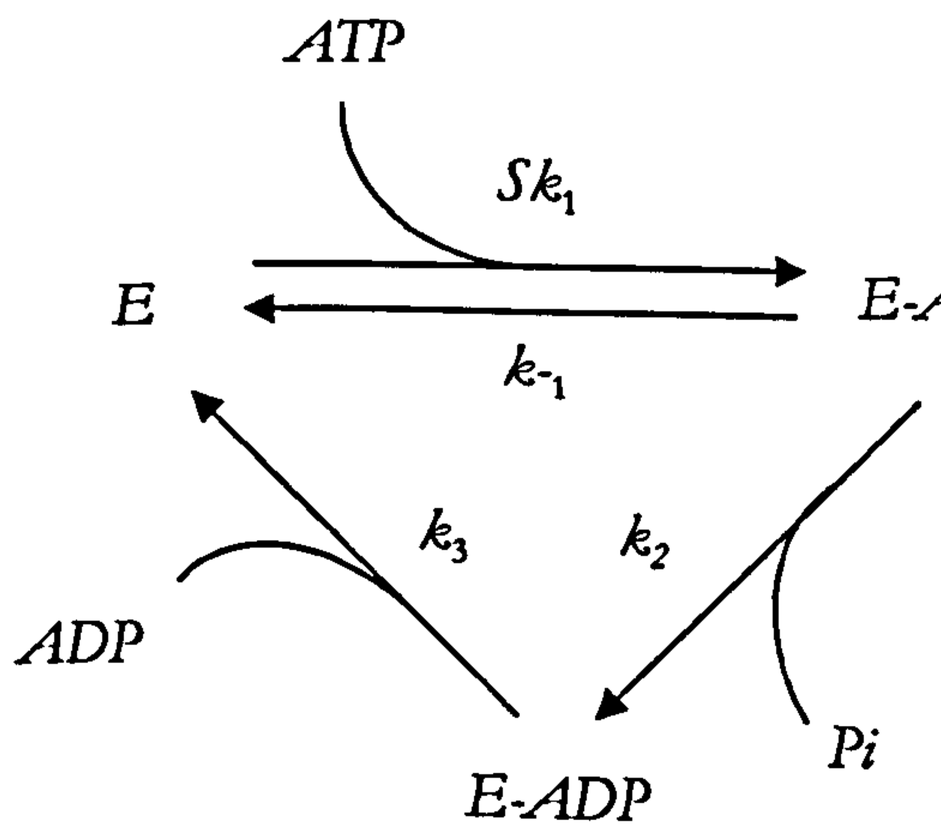

where E = enzyme, S = substrate and k_{1-4} = corresponding rate constants. Bond cleavage and release of *Pi* are shown as one step, as the off rate for *Pi* is extremely fast and not rate-limiting (A. Robson, A. R. Clarke and I. Collinson, unpublished results).

Step 1 – Define all non-cyclic paths that lead to E, E-ATP (ET) and E-ADP (ED):

$E = k_{-1}k_3 + k_2k_3$

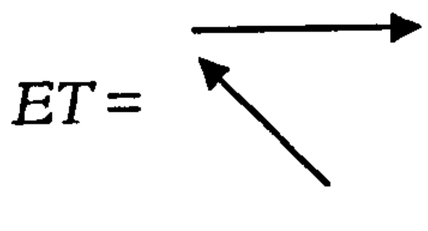

$ET = S_{k1}k_3$

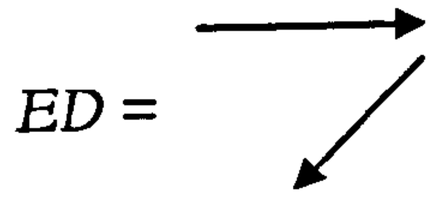

$ED = Sk_1k_2$

Step 2 – Incorporate into $\frac{v}{Eo}$ rate constants and all possible species:

$$\frac{v}{Eo} = \frac{Sk_1k_2k_3}{E + ET + ED}$$

Step 3 – Substitute the denominator in terms of *k*:

$$\frac{v}{Eo} = \frac{Sk_1k_2k_3}{k_{-1}k_3 + k_2k_3 + Sk_1k_3 + Sk_1k_2}$$

Step 4 – Collect together terms in S:

$$\frac{v}{Eo} = \frac{Sk_1k_2k_3}{k_{-1}k_3 + k_2k_3 + S(k_1k_3 + k_1k_2)}$$

Step 5 – Rearrange into Michaelis-Menten form $v = \frac{kcat.[S]}{K_M + [S]}$:

$$\frac{v}{Eo} = \frac{S\dfrac{k_1k_2k_3}{k_1k_3 + k_1k_2}}{\dfrac{k_{-1}k_3 + k_2k_3}{k_1k_3 + k_1k_2} + S}$$

Equation 2-8. SecA steady-state equation

Therefore $k_{cat} = \dfrac{k_1k_2k_3}{k_1k_3 + k_1k_2}$ and $K_M = \dfrac{k_{-1}k_3 + k_2k_3}{k_1k_3 + k_1k_2}$

Step 6 – Simplify by dividing through by k_1, and substitute $K_d = \frac{k_{-1}}{k_1}$:

Therefore $k_{cat} = \dfrac{k_2k_3}{k_3 + k_2}$ and $K_M = \dfrac{K_dk_3 + \dfrac{k_2k_3}{k_1}}{k_3 + k_2}$

Step 7 – Define K_M in the two systems:

In system I (SecA in the presence of SecYEG proteoliposomes, and without proOmpA) ADP release is the rate limiting step (A. Robson, A. R. Clarke and I. Collinson, unpublished results). Thus $k_3 < k_2$. k_1 is also large as this value is determined by enzyme-substrate diffusion.

k_1 = 1-5 x 10^7 $second^{-1}$ (Christensen et al., 1990).

k_2 = 6.00 ± 0.12 $second^{-1}$ (A. Robson, A. R. Clarke and I. Collinson, unpublished results).

k_3 = 0.27 ± 0.01 $second^{-1}$ (15.92 ± 0.62 moles ATP mole $SecA^{-1}$ min^{-1}; this study)

Thus in system I, $\frac{k_2 k_3}{k_1}$ is negligible

Therefore $K_M = \frac{K_d k_3}{k_3 + k_2}$

$$= K_d \frac{k_3}{k_3 + k_2}$$

$$= \frac{K_d(0.27)}{0.27 + 6.00}$$

$$= 0.04 K_d$$

In system II (the presence of both SecYEG proteoliposomes and proOmpA), the increase in k_{cat} must be due to the increased rate of product release, as ADP release is the rate limiting step. In this case k_{cat} = 7.60 ± 0.29 moles ATP mole $SecA^{-1}$ $second^{-1}$ (456.27 ± 17.21 moles ATP mole $SecA^{-1}$ min^{-1}; this study), = k_2, which must now be the rate limiting step.

Thus in system II, $\frac{k_2 k_3}{k_1}$ and $\frac{k_3}{k_3 + k_2}$ are negligible

Therefore $K_M = K_d$

2.6 Analytical Gel Filtration Chromatography

To determine the effect of nucleotides and Mg^{2+} on SecA conformation, analytical gel filtration chromatography was carried out. Experiments were performed with a Superose 6 HR 10/30 column (GE Healthcare), with approximately 10 nmoles of SecA or SecA-Δ11/N95 per experiment, and absorption measured at 280nm. Where the effects of Mg^{2+} were analysed, this was added to a concentration of 2 mM or 20 mM in TK buffer, and compared to no added magnesium or 50 mM EDTA conditions. Where nucleotides (ATP and ADP) were included, these were added to a concentration of 100 μM in the equilibration buffer.

2.7 Analytical Ultracentrifugation

2.7.1 Introduction to the technique

Two very different experiments, sedimentation velocity and sedimentation equilibrium, can be performed with the ultracentrifuge and provide complementary data sets to solve a given problem. When used together in this manner, the technique is an extremely powerful tool for the determination of information regarding the hydrodynamic properties of a molecule. An advantage to these methods include the ability to analyse samples in their native state and free from interactions with a solid support, as can be the case in certain chromatographic techniques.

Sedimentation velocity experiments generate information on the size and shape of molecules in free solution. At the start of an experiment, the protein is uniformly distributed across the centrifuge cell. The solute is then spun at a high angular velocity and as it begins to sediment towards the cell base, a boundary is formed

between the depleted region near the meniscus, and the uniform region below. It is the rate of movement of this boundary that is dependent upon size and shape of the molecule. If a protein self-associates, the apparent rate of sedimentation will increase with increasing concentration.

Sedimentation equilibrium is used to determine accurate values of molecular weight, as well as stoichiometries and association kinetics and their strengths. This technique is independent of the shape of molecules. At the start of the experiment, the uniform solution is centrifuged at a lower speed than is used for sedimentation velocity experiments, until a concentration-dependent equilibrium is reached. This is when the force of sedimentation towards the cell base is equal to that of diffusion in the opposing direction. The result is an exponential distribution of protein towards the cell base that is invariant with time. Measurement of the protein concentration across the cell is used to determine the molecular weight. The distribution is thus dependent upon the absolute molecular weight and also any association behaviour.

2.7.2 Preparation of samples and equipment

SecA stock solutions of wild type and of SecA-Δ11/N95 were dialysed overnight with two buffer changes against either TK or TKM buffers. Where ADP was included, this was added to a concentration of 100 μM. These were subjected to sedimentation velocity and sedimentation equilibrium centrifugation experiments using either an XL-A or XL-I centrifuge (Beckman Instruments; Palo Alto, California) equipped with standard Epon centrepieces, quartz windows and an An-60Ti rotor. This rotor houses 4 holes, 3 of which are for samples and 1 of which is for the counterbalance. The latter enables a calibration of radial distance by the machine, and is used to balance the rotor by virtue of an adjustable mass. 0.4-13 μM SecA or SecA-Δ11/N95 were used and scans recorded at either 230 or 280 nm, to achieve optical density values in the range of 0.2-1. All experiments were carried out at 25°C.

2.7.3 Sedimentation Velocity

The experiments were carried out using three double sector centrepieces per experiment. One sector houses the sample solute and one the reference solvent, enabling the optics on the machine to correct for movement of solvent components and any corresponding absorbance. The sample sector contained 400 µl of sample solute, and the reference sector contained 410 µl of reference buffer. Thus a total of 3 different conditions or protein concentrations could be run simultaneously if required. The samples were spun at 130,000 x *g*, with 3 minute 30 second scan intervals. Acquisition of scans continued until complete sedimentation was achieved.

2.7.4 Sedimentation Equilibrium

Sedimentation equilibrium experiments were carried out using three six sector centrepieces per experiment, three of which contained 110 µl of sample solute, and three of which contained 120 µl of the appropriate reference solvent in the opposite chambers. Thus a total of 9 different conditions or protein concentrations could be analysed simultaneously if required. The smaller radial distance over which sedimentation occurs in the smaller volume six sector centrepieces compared to the double sector centrepieces significantly reduces the time taken to reach an equilibrium. Scans were taken every four hours, until there was no shift in protein distribution across the cell (an equilibrium was usually reached by 16 hours), at speeds of 3000 x *g*, 5,800 x *g* and 8,000 x *g*.

2.7.5 Analytical Ultracentrifugation Data Analysis

2.7.5.1 Sedimentation Velocity analysis

Movement of the boundary that is formed between the region depleted of solute near the meniscus and the uniform region below is used to determine the sedimentation coefficient. The boundary is subject to diffusion, and thus is seen to broaden with time (Figure 2-12). The absorbance of the plateau region decreases over time, in a process known as radial dilution and is attributable to the sector shape of centrepieces.

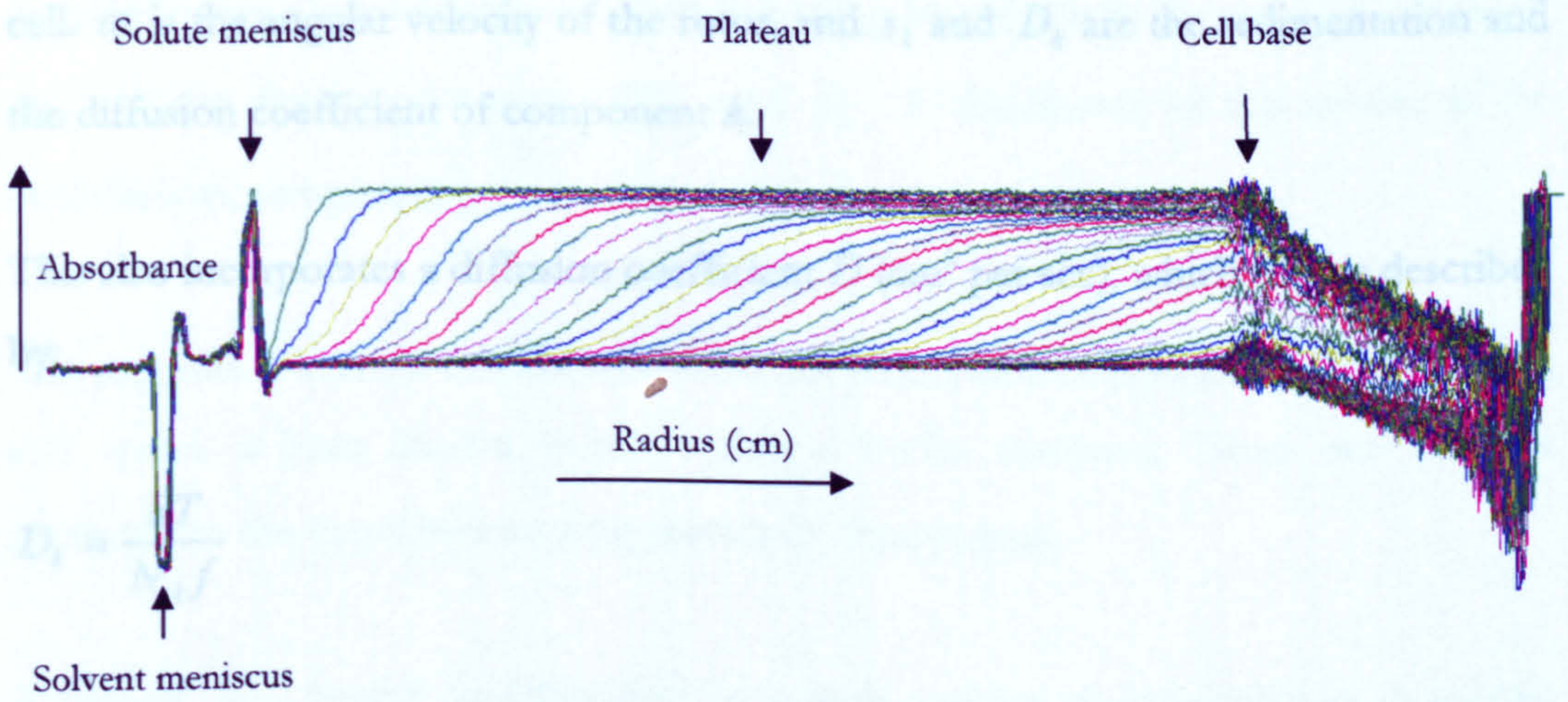

Figure 2-12. Raw data depicting SecA in a sedimentation velocity experiment.

The scans were fitted to determine a sedimentation coefficient *s*. The units of *s* are Svedbergs (S) where 1×10^{-13} seconds equals 1 Svedberg. A finite element solution of the Lamm equation (Lamm, 1929) was used, which uses nonlinear least-squares fitting to obtain this value (Demeler and Saber, 1998). This describes both sedimentation and diffusion processes which occur in the ultracentrifuge cell, and is described in terms of flow, *J* (moles per second per centimetre), which incorporates a change in radial position of the boundary over a period of time.

The Lamm equation in general form is given by:

$$\frac{\partial C_k}{\partial t} + \frac{1}{r}\frac{\partial (rJ_k)}{\partial r} = f_k; \qquad J_k = s_k \omega^2 r C_k - D_k \frac{\partial Ck}{\partial r}$$

Equation 2-9. The Lamm equation

With boundary and initial conditions:

$$J(r_m,t) = J(r_b,t) = 0; \qquad 0 \le t \le T; \qquad C(r,0) = C_0(r)$$

where k = the solute, C = the solute concentration, J = flow, t = time, T = the elapsed time at the end of the experiment, r = the radius from the centre of rotation, and $r_m \le r \le r_b$, where r_m and r_b are the radii of the meniscus and the bottom of the cell. ω is the angular velocity of the rotor, and s_k and D_k are the sedimentation and the diffusion coefficient of component k.

This also incorporates a diffusion coefficient D (cm^2 per sec), which can be described by:

$$D_k = \frac{RT}{N_A f}$$

where R = gas constant, T = temperature, N_A= Avogadro's number and f = frictional coefficient.

In reality, the *c(s)* (sedimentation coefficient distribution) function extends the Lamm equation for sedimentation and diffusion by considering each sedimenting species. The program Ultrascan (Demeler, 2005) was used to fit the data to give *c(s)* versus *s*, which led to determination of a weight average sedimentation coefficient.

The sedimentation coefficient is influenced by the viscosity and density of the solvent (dependent upon T and the buffer composition), and by the concentration of protein, so the value of s is often expressed in terms of sedimentation in a water

solvent at 20°C, and is extrapolated to zero concentration (infinite dilution). This enables relative comparisons to be made between different buffer conditions and temperatures.

The calculation of *s* in terms of water at 20°C is given by:

$$s_{20,w} = s_{obs}\left(\frac{\eta_{T,w}}{\eta_{20,w}}\right)\left(\frac{\eta_s}{\eta_w}\right)\left(\frac{1-\bar{v}\rho_{20,w}}{1-\bar{v}\rho_{T,s}}\right)$$

Equation 2-10. Calculation of $s_{20,w}$

where $s_{20,w}$ = the sedimentation coefficient *s* expressed in terms of sedimentation in water at 20°C, s_{obs} = the measured *s* value from the experiment, $\eta_{T,w}$ and $\eta_{20,w}$ = the viscosities of water at the experimental temperature and at 20°C, η_s and η_w = the viscosities of the solvent and of water at a common temperature, $\bar{v}$ = the partial specific volume (the volume in ml that each gram of solute occupies in solution), $\rho_{20,w}$ = the density of water at 20°C and $\rho_{T,s}$ = the density of the solvent at the experimental temperature.

The program Ultrascan calculates $\bar{v}$ from the amino acid composition of the protein, and η and ρ from known values within a buffer database. These can then be corrected to the experimental temperature by the program.

A plot of $s_{20,w}$ versus concentration of sample enables an extrapolation to infinite dilution (concentration = 0), which yields $s^o_{20,w}$, the limiting sedimentation coefficient as the *y* intercept. This must be corrected for due to non-ideality effects which occur when a molecule is present at very high concentrations. This results in charge effects which may result in repulsion between molecules, and increased viscosity of the solution. $s_{20,w}$ thus varies with concentration, and with pure non-interacting molecules this value will decrease with increasing concentration.

2.7.5.2 *Sedimentation Equilibrium analysis*

When the processes of sedimentation and diffusion reach an equilibrium, the net movement of molecules is equal to zero. The distribution of protein towards the base of the cell increases exponentially (Figure 2-13) and this profile is used to fit the data and yield a molecular weight value.

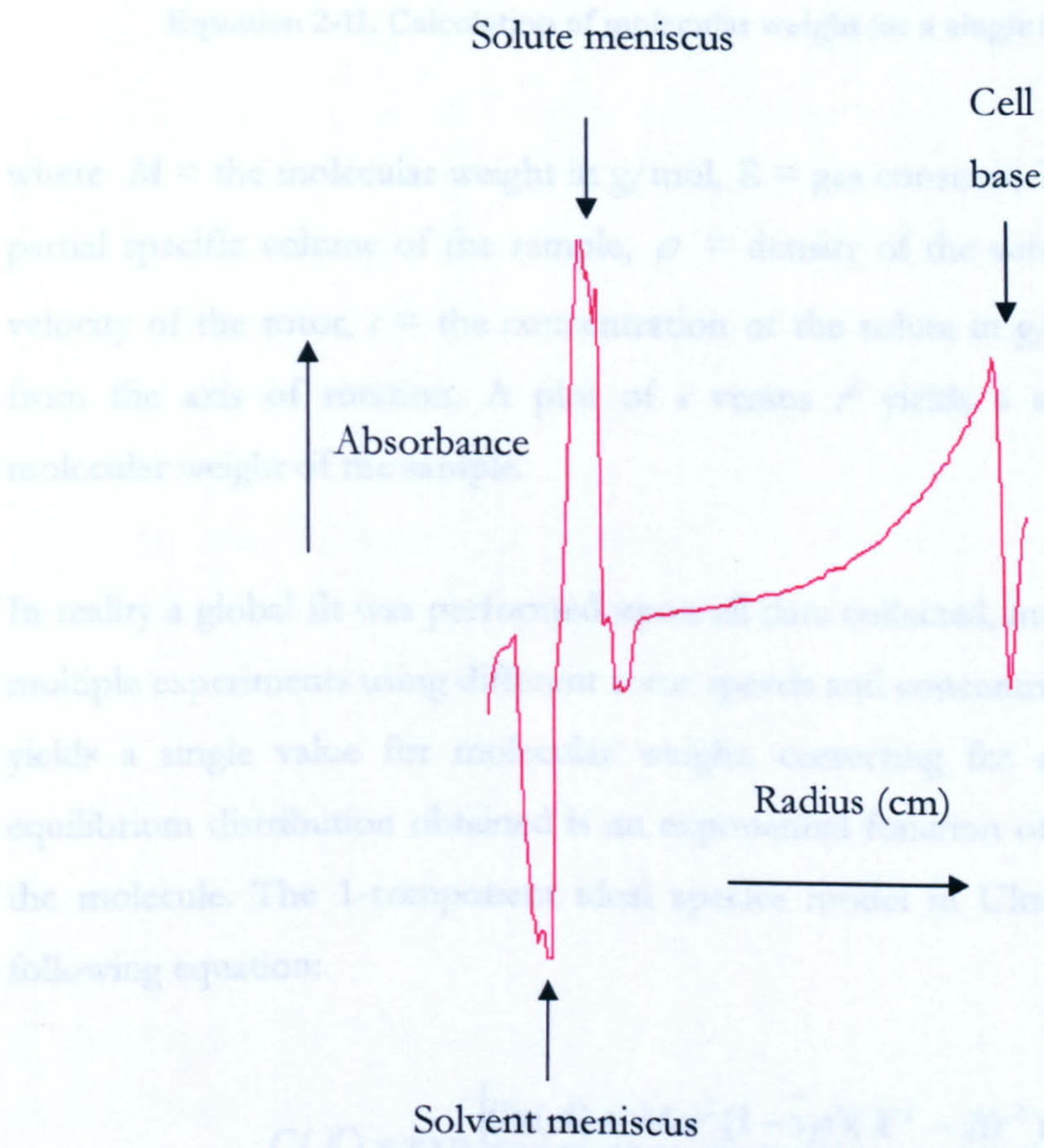

Figure 2-13. Raw data depicting SecA in a sedimentation equilibrium experiment.

The data were again analysed using the Ultrascan program (Demeler, 2005). From the sedimentation velocity data it was known that there was essentially only one species present, thus the data were fitted to 1-component ideal species model, which yielded the best fit. The data were also fitted with monomer-dimer equilibrium models, but the concentration of monomer was found to be too low to determine a $K_{d[SecA\text{-}SecA]}$ value under these conditions. It has been shown that for a single ideal species:

$$M = \frac{2RT}{(1-\bar{v}\rho)\omega^2} \times \frac{\partial(\ln c)}{\partial r^2}$$

Equation 2-11. Calculation of molecular weight for a single ideal species.

where M = the molecular weight in g/mol, R = gas constant, T = temperature, $\bar{v}$ = partial specific volume of the sample, ρ = density of the solvent, ω = the angular velocity of the rotor, c = the concentration of the solute in g/L at radial distance r from the axis of rotation. A plot of c versus r^2 yields a slope proportional to molecular weight of the sample.

In reality a global fit was performed upon all data collected, incorporating data from multiple experiments using different rotor speeds and concentrations of protein. This yields a single value for molecular weight, correcting for any non-ideality. The equilibrium distribution obtained is an exponential function of the buoyant mass of the molecule. The 1-component ideal species model in Ultrascan is fitted to the following equation:

$$C(X) = \exp\frac{\left|(\ln(A) + M\omega^2(1-\bar{v}\rho)(X^2 - Xr^2))\right|}{2RT} + B$$

Equation 2-12. 1-component ideal species model.

Where X = the radius from the centre of rotation for the sample chambers, A = amplitude, M = molecular weight in g/mol, $\bar{v}$ = partial specific volume of the sample, ρ = density of the solvent, Xr = the radius from the centre of rotation for the reference chambers, R = gas constant, T = temperature.

The data were then subjected to a Monte Carlo analysis implemented in Ultrascan (Demeler, 2005), to evaluate the statistical values for all parameters. This works on the basis of a simulation, which generates the equivalent of multiple experiments using a random number generator. Each simulated observation is then fitted to the model and this is then used to assign a confidence to the experimental parameter value.

2.8 Limited Proteolysis of Protein Samples

2.8.1 Preparation of an antibody stabilised complex

To create a stable complex between SecYEG and SecA for proteolysis experiments, an antibody stabilised dimer of SecYEG was used, bound to two SecA molecules. The antibody used was 10A4 (Cocalico, Philadelphia, USA). The presence of this antibody (to an epitope on the periplasmic surface of SecG) results in a stabilisation of a dimer of the SecYEG complex (Tziatzios et al., 2004). Protein components, typically 0.3-1 mg (with SecA in excess over SecYEG and 10A4) were incubated together at room temperature in 20 mM Tris pH 8, 100 mM NaCl, 2 mM $MgCl_2$, 10% (v/v) glycerol, 0.02 % (w/v) DDM, 0.1 mM AMP-PNP. Addition of SecA in the presence of AMP-PNP results in the complex $SecYEG_2.SecA_2.10A4$ (Tziatzios et al., 2004). Size exclusion chromatography was performed with a Superose 6 HR 10/30 column in the same buffer, to separate the large assembly from any unbound species.

2.8.2 Tryptic digests

Tryptic digests were performed to identify changes in the proteolysis pattern of SecA and SecYEG when they are bound together; major changes being indicative of an induced new conformation. SecYEG (2 μM), $SecYEG_2.SecA_2.10A4$ (5 μM) and SecA (2 μM) were subjected to proteolysis using 20 μl of a trypsin-agarose slurry in a 100 μl total reaction volume for 1 minute at room temperature. Trypsin was removed from the reaction by centrifugation in a benchtop microfuge (15,000 x *g* for 2 minutes at 4°C; Beckman Coulter Microfuge 16) and the products were resolved by SDS-PAGE and stained with Coomassie blue.

2.9 Thin Layer Chromatography

Thin Layer Chromatography (TLC) is used to separate compounds within a mixture, based on their individual polarity. The solid phase is a TLC glass plate, coated in a thin layer of silica adsorbent. The mixture is spotted at one end of the plate and is placed into the mobile phase (a pool of solvent) which rises up the plate by capillary action in a chamber with a saturated solvent atmosphere. Individual components will differ in their solubility and strength of adsorption, thus a separation occurs. When the solvent reaches the top of the plate, this is dried and the separated components visualised.

This technique was used to separate individual lipids within a SecYEG preparation, and was performed by D. Hizlan (Max Planck Institute, Frankfurt, Germany) and I. Collinson. 20 mg of *E. coli* PE, PG and CL were spotted onto the TLC plate, with a mobile phase composed of 70% (v/v) chloroform and 25% (v/v) methanol, in a total volume of approximately 20 ml. This was compared to 40 μg of protein samples. After drying, the TLC plate was stained with iodine vapour, producing an orange colour which was readily visualised.

2.10 *In vitro* Protein Translocation Assays

2.10.1 Translocation of proOmpA into SecYEG proteoliposomes

Translocation reactions were carried out at 25°C in TKM buffer. MESG and PNP were also included to keep conditions identical to those used in the kinetics experiments. Complete reactions contained SecA (0.05 μM), proOmpA (0.7 μM) and 36 μl proteoliposomes containing reconstituted SecYEG (or the same volume of empty liposomes) to a final concentration of 1 μM SecYEG and 1.18 mg/ml lipids. Assays were initiated with 1 mM ATP.

After incubation for the desired time, samples were treated with proteinase K to a final concentration of 7 μM (0.2 mg/ml) and left on ice for 45 minutes. All proOmpA that has been successfully translocated into the interior of the proteoliposome will be protected from proteolysis (Figure 2-14). Protease inhibitor AEBSF was then added to a final concentration of 2 mM and this was incubated on ice for 10 minutes. BSA was subsequently added to 15 μM (1 mg/ml), and the protein was precipitated with 20% (v/v) Trichloroacetic acid (TCA) and left on ice for 30 minutes. The protein was pelleted in a benchtop microfuge (15,000 x *g* for 10 minutes at 4°C; Beckman Coulter Microfuge 16), and resuspended in 20 μl SDS-PAGE sample buffer. Samples were heated to 65°C and the proteins were resolved by SDS-PAGE.

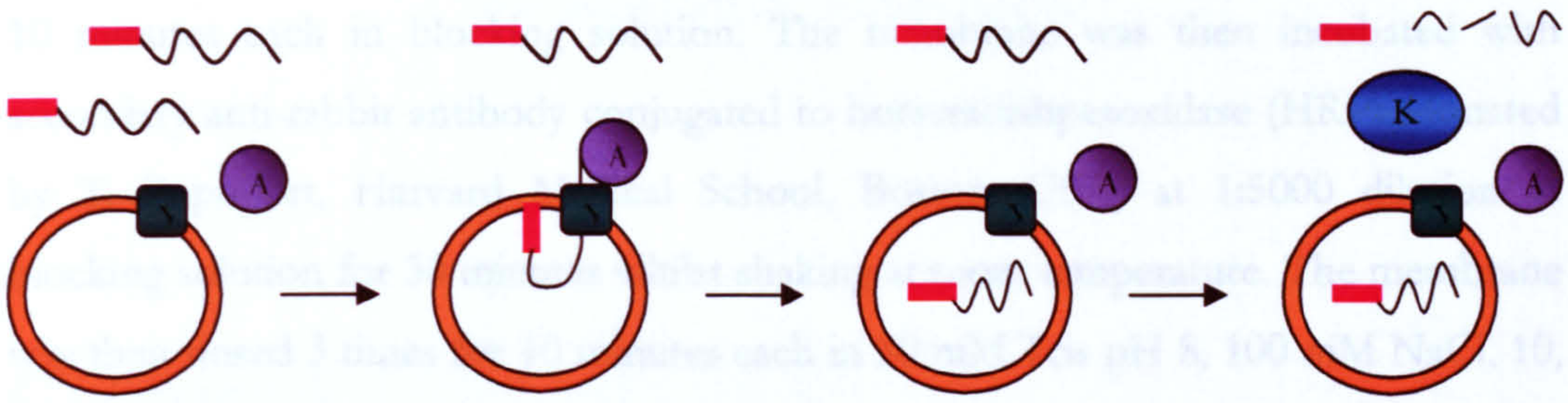

Figure 2-14. *In vitro* translocation assay

Proteoliposomes containing SecYEG (green) are incubated together with SecA (purple), proOmpA (signal sequence red; mature protein black) and ATP. Fully translocated proOmpA is protected from proteinase K (blue) digestion.

2.10.2 Western blot

2.10.2.1 Transfer to PVDF membrane

The gel was removed from the electrophoresis apparatus and rinsed in Transfer Buffer (TB) containing 0.192 M glycine, 25 mM Tris pH 8, 20% (v/v) methanol (Invitrogen, Carlsbad, California, USA). The gel was placed upon 2 sheets of Whatman 3MM paper, also soaked in TB. Soaked Polyvinylidene fluoride (PVDF) membrane was then placed on top of the gel and covered with 2 more sheets of Whatman 3MM paper. The gel was then blotted by use of a 'sandwich assembly' at a current of 100-125 mA (200v constant).

2.10.2.2 Incubation with antibody

The blot was immediately placed into a blocking solution (50 mM Tris pH 8, 100 mM NaCl, 10% (w/v) milk powder, 0.1 % (v/v) Tween) for 1 hour at room temperature whilst shaking gently. Primary rabbit anti-proOmpA antibody (donated by T. Rapoport, Harvard Medical School, Boston, USA) was diluted 1:1000 into blocking solution and incubated with the membrane for 30 minutes whilst shaking at

room temperature. This was then decanted, and the membrane washed 3 times for 10 minutes each in blocking solution. The membrane was then incubated with secondary anti-rabbit antibody conjugated to horseradishperoxidase (HRP) (donated by T. Rapoport, Harvard Medical School, Boston, USA) at 1:5000 dilution in blocking solution for 30 minutes whilst shaking at room temperature. The membrane was then rinsed 3 times for 10 minutes each in 50 mM Tris pH 8, 100 mM NaCl, 10, 0.1 % (v/v) Tween.

2.10.3 Visualising the blot by chemiluminescence

The membrane was placed on a sheet of transparency plastic. 2.5 ml chemiluminescent substrate solution (Invitrogen, Carlsbad, California, USA), was added to the membrane surface and allowed to react for one minute. This was decanted and the membrane covered with a second piece of transparency film. Photographic film was placed upon the membrane and the film allowed to develop for 30 seconds in a developer cassette. The film was developed in a film processor (AGFA Curix 60, Mortsel, Belgium).

Results Chapters

Chapter 3

Kinetic Analysis of SecA

Chapter 4

SecA undergoes a large conformational change that is regulated by magnesium and ADP

Chapter 5

Kinetic modulation of SecA by the protein channel SecYEG

Chapter 6

The ATPase activity associated with protein translocation

Chapter 3

Kinetic Analysis of SecA

3.1 SecA and SecA-Δ11/N95 exhibit the same basal ATPase activities

Kinetic assays were initially carried out in TKM buffer (in the presence of 2 mM $MgCl_2$), due to the ubiquitous requirement of all ATPases for a Mg^{2+} ion as a cofactor for ATP hydrolysis (Section 2.5, Materials and Methods). Preliminary experiments demonstrated an extremely low rate of steady-state hydrolysis under these conditions, thus in order to measure these rates accurately, a regenerating system (the PK/LDH assay) was employed. Both wild type SecA and the proposed monomeric derivative SecA-Δ11/N95 (Or et al., 2005) exhibit a similar level of activity; ATP binding is tight and substrate turnover is slow (Figure 3-1). The data were fitted according to the Michaelis-Menten equation (Equation 2-1, Materials and Methods), revealing values for $K_{M[ATP]}$ and k_{cat} (Table 3-1).

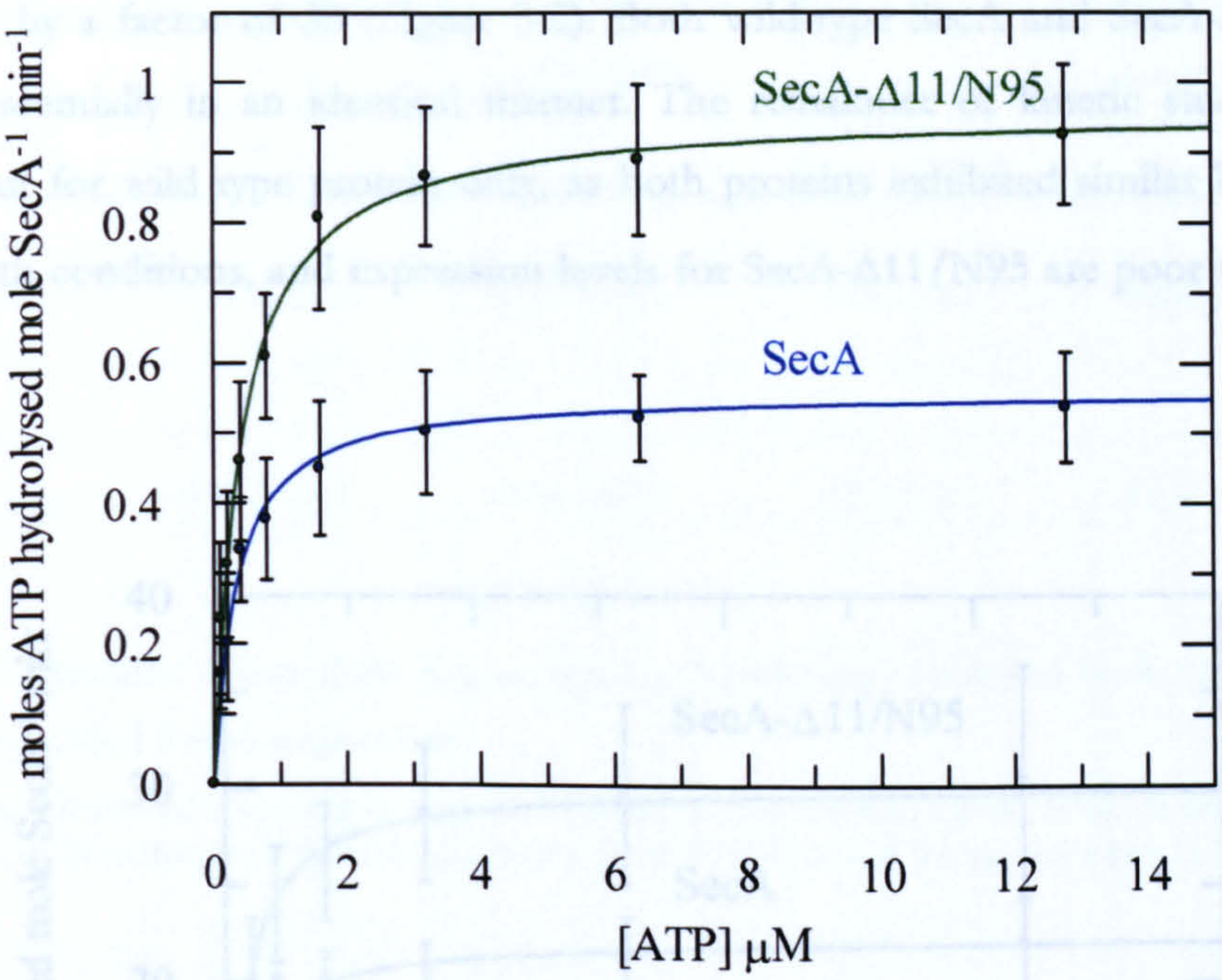

Figure 3-1. Michaelis-Menten plot of SecA and SecA-Δ11/N95 ATPase activity as a function of ATP concentration in the presence of 2 mM magnesium.

The ATPase activities of purified wild type SecA (0.3 μM; blue trace) and SecA–Δ11/N95 (0.3 μM; green trace) were measured with increasing ATP concentrations in TKM buffer, and fitted according to the Michaelis-Menten equation (Equation 2-1, Materials and Methods). Error bars represent Standard Deviation (SD) from 4-6 replicates. The calculated values of $K_{M[ATP]}$ and k_{cat} are shown in Table 3-1.

3.2 Magnesium concentration dramatically alters both the affinity for ATP and the turnover rate

It was observed that the steady-state ATPase activity of SecA was strongly influenced by the concentration of Mg^{2+} in the buffers employed. Thus a titration of ATP was performed for a second time, this time in TK buffer (in the absence of added Mg^{2+}). Due to the dependence for Mg^{2+} on the linking enzyme PK, an alternative system was established, this being the EnzChek™ assay. Turnover rates were significantly faster, thus the requirement for the regenerating system was eliminated.

In the absence of any added Mg^{2+}, the behaviour of SecA is dramatically altered, the affinity for ATP being weakened by approximately 150 fold, and the turnover increased by a factor of 30 (Figure 3-2). Both wild-type SecA and SecA-Δ11/N95 behave essentially in an identical manner. The remainder of kinetic studies were carried out for wild type protein only, as both proteins exhibited similar behaviour under both conditions, and expression levels for SecA-Δ11/N95 are poor (Figure 2-3).

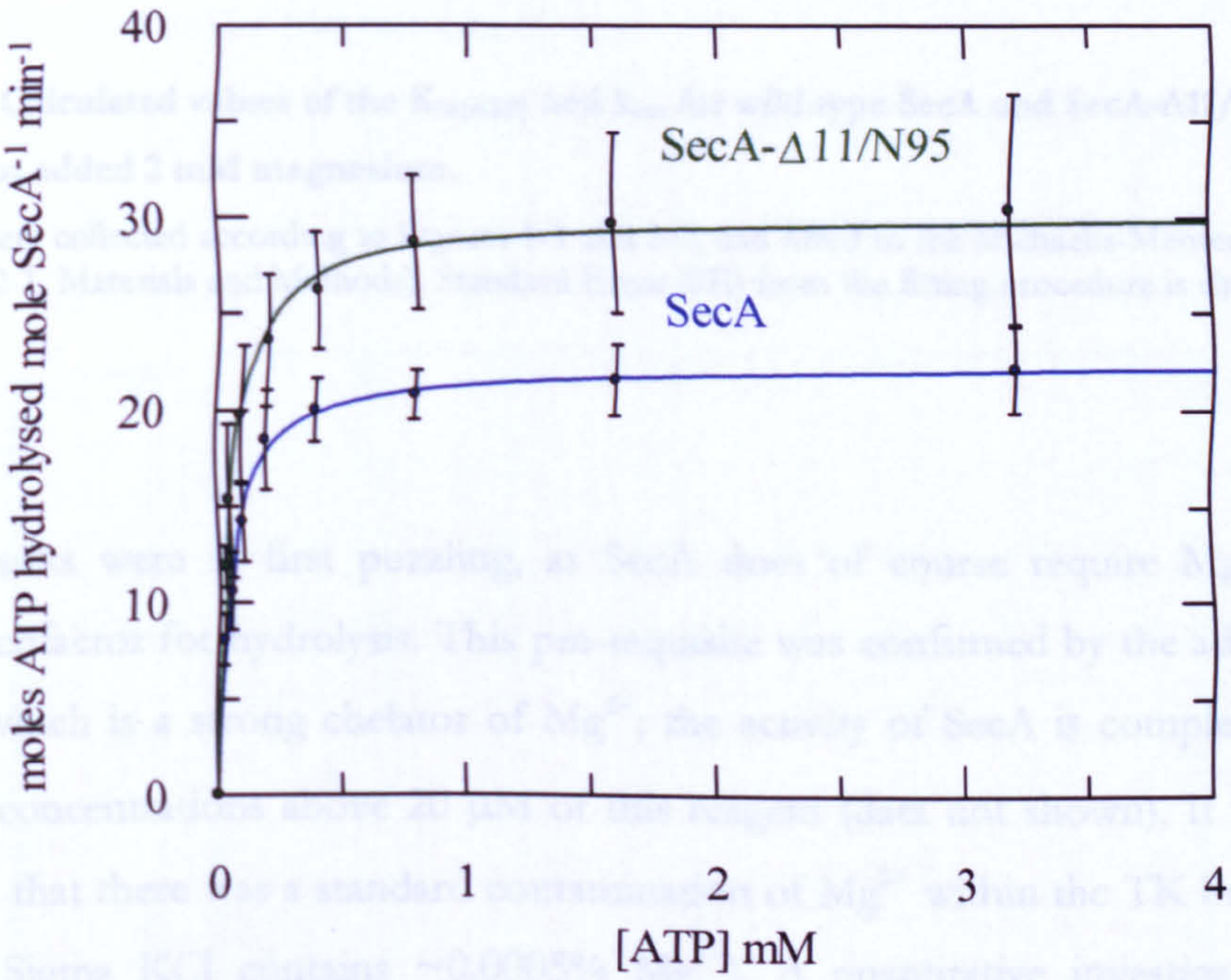

Figure 3-2. Michaelis-Menten plot of ATPase activity as a function of ATP concentration in the absence of added magnesium.

The ATPase activities of purified wild type SecA (0.3 μM; blue trace) and SecA–Δ11/N95 (0.3 μM green trace) were measured with increasing ATP concentrations in TK buffer, and fitted according to the Michaelis-Menten equation (Equation 2-1, Materials and Methods). Error bars represent SD from 4-6 replicates. The calculated values of $K_{M[ATP]}$ and k_{cat} are shown in Table 3-1.

	$K_{M\,[ATP]}$ (μM)	k_{cat} (moles ATP mole SecA^{-1} min^{-1})	$K_{M\,[ATP]}$ (μM)	k_{cat} (moles ATP mole SecA^{-1} min^{-1})
Mg^{2+}	+	+	-	-
SecA	0.32 ± 0.03	0.56 ± 0.01	50.8 ± 3.2	22.36 ± 0.28
SecA–Δ11/N95	0.40 ± 0.03	0.96 + 0.02	47.7 ± 3.7	30.16 ± 0.47

Table 3-1. Calculated values of the $K_{M[ATP]}$ and k_{cat} for wild type SecA and SecA-Δ11/N95 with and without added 2 mM magnesium.

The data were collected according to Figures 3-1 and 3-2, and fitted to the Michaelis-Menten equation (Equation 2-1, Materials and Methods). Standard Error (SE) from the fitting procedure is shown.

These results were at first puzzling, as SecA does of course require Mg^{2+} as an essential cofactor for hydrolysis. This pre-requisite was confirmed by the addition of EDTA, which is a strong chelator of Mg^{2+}; the activity of SecA is completely shut down at concentrations above 20 μM of this reagent (data not shown). It was thus predicted that there was a standard contamination of Mg^{2+} within the TK buffer (for example Sigma KCl contains ~0.0005% Mg^{2+}). A quantitative investigation was subsequently carried out using the technique of Inductively Coupled Plasma – Atomic Emission Spectroscopy (ICP-AES) by Dr. Poon-Chung Choi, Dept. of Earth Sciences, University of Bristol, UK. This determined the residual magnesium concentration in the TK assay buffer to be ~1 μM, approximately 3 times greater than the 0.3 μM SecA concentration used in the experiment. This contaminating Mg^{2+} will subsequently be referred to as 'residual' Mg^{2+}.

Accordingly, the apparent inhibitory effect of Mg^{2+} on ATPase activity was examined in more detail by a Mg^{2+} titration at two different ATP concentrations. The data were fitted to the hyperbolic inhibition function (Equation 2-2, Materials and Methods) to determine values for $K_{i(app)[Mg2+]}$. This value was shown to be relatively unaffected by a 10-fold increase in the concentration of ATP (Figure 3-3). The affinity of Mg^{2+} for

ATP is relatively high ($K_{d[Mg\text{-}ATP]}$ = 20 μM) (Pecoraro et al., 1984), therefore the fact that the inhibition is not strongly coupled to the concentration of ATP indicates that the inhibition occurs via Mg^{2+}, and not by Mg^{2+}-ATP. In other words, it is acting at a location distinct from the nucleotide binding site and the effect is allosteric. Moreover, it can be deduced that Mg^{2+}-ATP is not the substrate for SecA, as the Mg^{2+} required for catalysis must be always bound at the NBF, as hydrolysis can occur when ATP is in great excess over Mg^{2+} (1 mM ATP to 1 μM Mg^{2+}, Figure 3-2). Also, the actual binding affinity for Mg^{2+} at this second allosteric site must be much higher than the affinity the cation has for ATP, given the fact that it remains inhibitory when ATP is more than 500 times in excess.

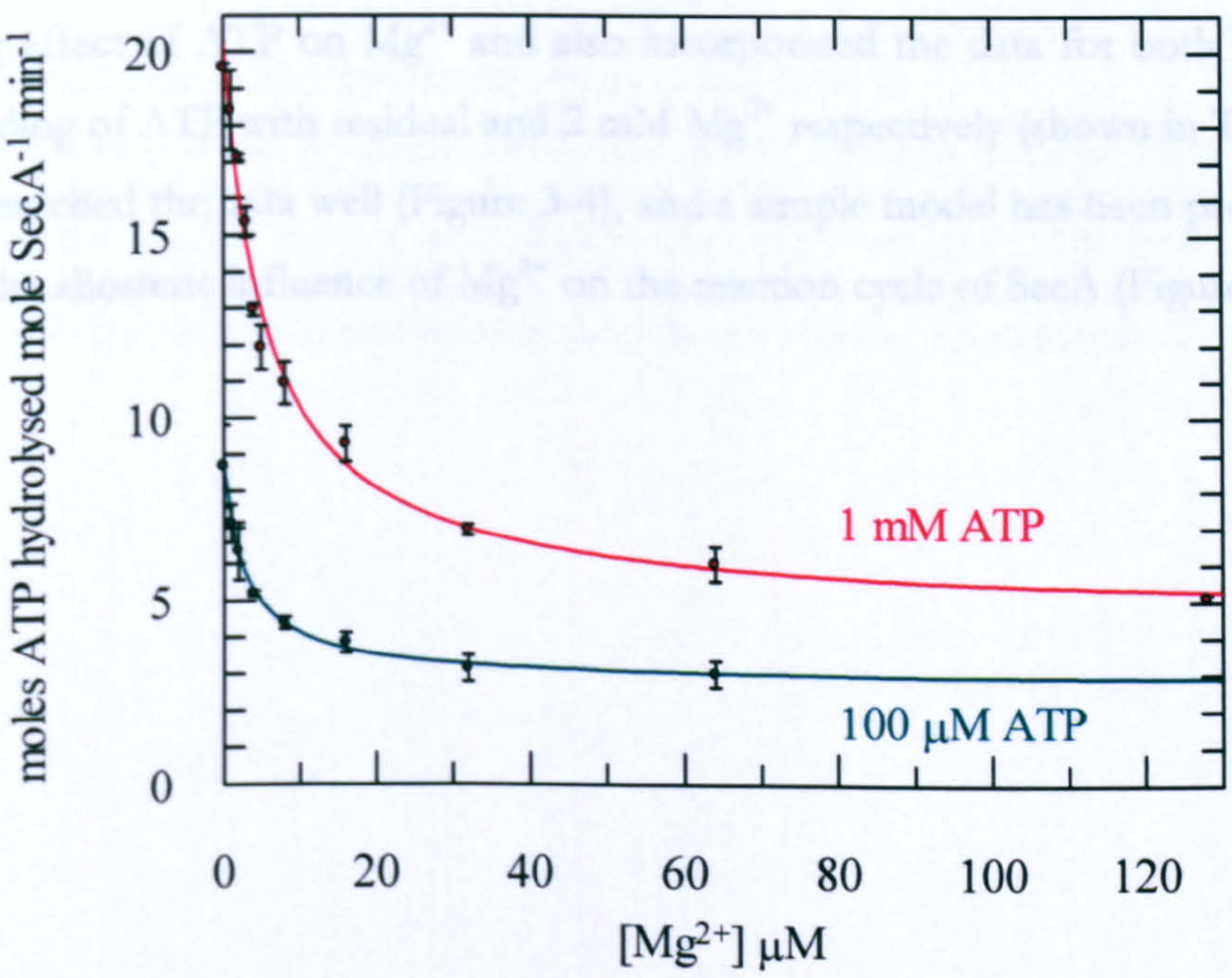

Figure 3-3. Magnesium inhibits the ATPase activity of SecA.

The ATPase activity of SecA (0.3 μM) was measured over a range of Mg^{2+} concentrations, with 1 mM ATP (red trace) and 100 μM ATP (green trace), in TK buffer. Error bars represent SD from 3 replicates. The data were fitted to the hyperbolic inhibition function (Equation 2-2, Materials and Methods) to determine values for $K_{i(app)[Mg2+]}$. These values are shown in Table 2-2.

	$K_{i(app)[Mg2+,\ 1mM\ ATP]}$ (μM)	$K_{i(app)[Mg2+,\ 100\mu M\ ATP]}$ (μM)
SecA	5.8 ± 0.94	2.97 ± 0.22

Table 3-2. Calculated values for $K_{i(app)[Mg2+]}$ in the presence of 1 mM and 100 μM ATP.

The data were collected according to Figure 3-3, and fitted to a hyperbolic inhibition function (Equation 2-2, Materials and Methods). SE from the fitting procedure is shown.

The data were then fitted according to a global fit (Equation 2-3, Materials and Methods), which incorporates a matrix of Mg^{2+} and ATP concentrations and the respective steady-state rate kinetics. This procedure made an adjustment for the chelating effect of ATP on Mg^{2+} and also incorporated the data for both weak and tight binding of ATP with residual and 2 mM Mg^{2+} respectively (shown in Table 3-1). The fit matched the data well (Figure 3-4), and a simple model has been proposed to explain the allosteric influence of Mg^{2+} on the reaction cycle of SecA (Figure 3-5).

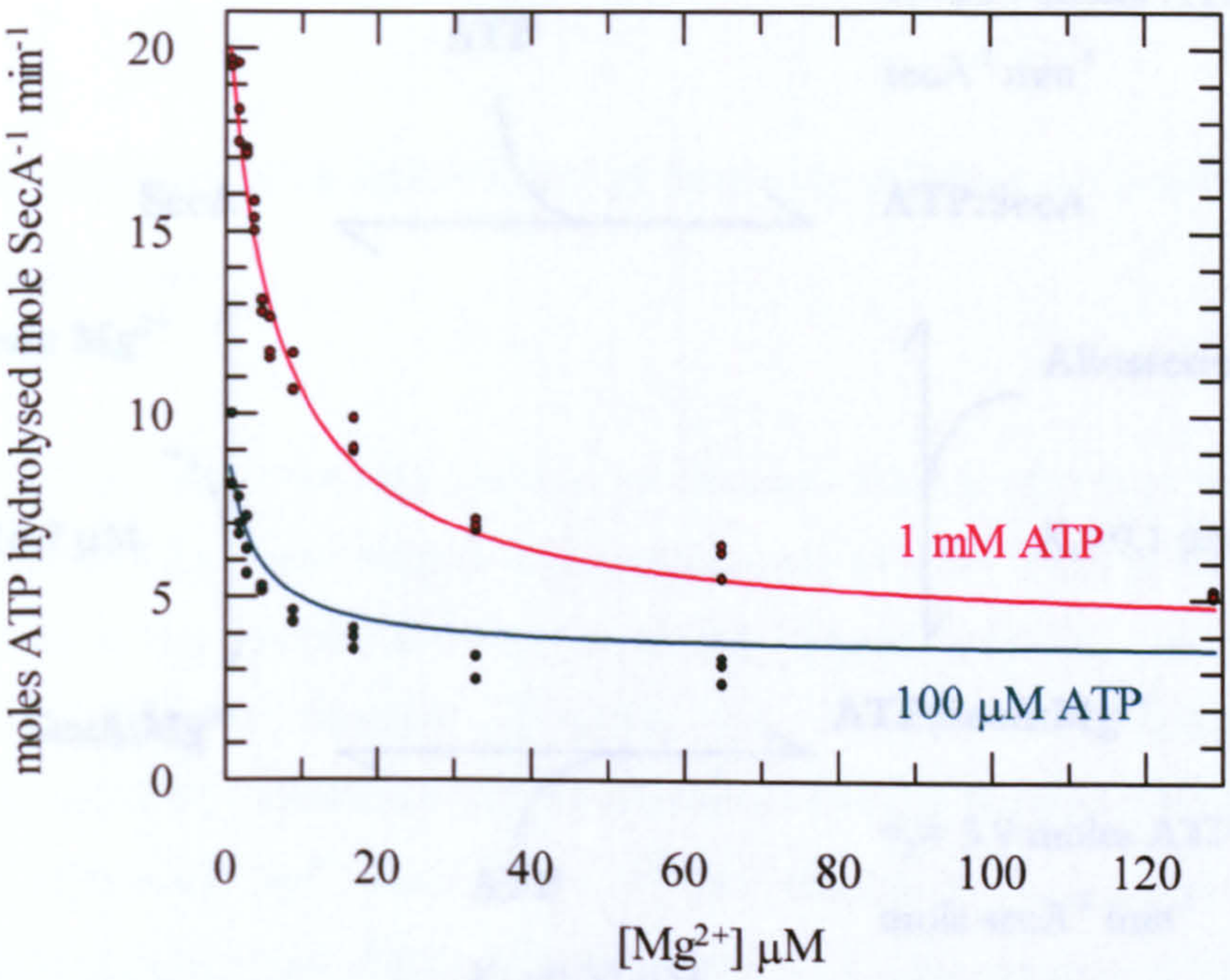

Figure 3-4. Inhibition of ATP turnover by magnesium; global fit

The same data sets as shown in Figure 3-3 were fitted globally (Equation 2-3, Materials and Methods), making an adjustment for the chelation effect of Mg^{2+}-ATP and incorporating the data for both weak and tight binding of ATP by SecA under high and low Mg^{2+} conditions. Data from six different experiments are shown, at 1 mM ATP (red trace) and at 100 μM ATP (green trace). An allowance of 10% was allowed for enzyme concentration between the two separate data sets in the fit.

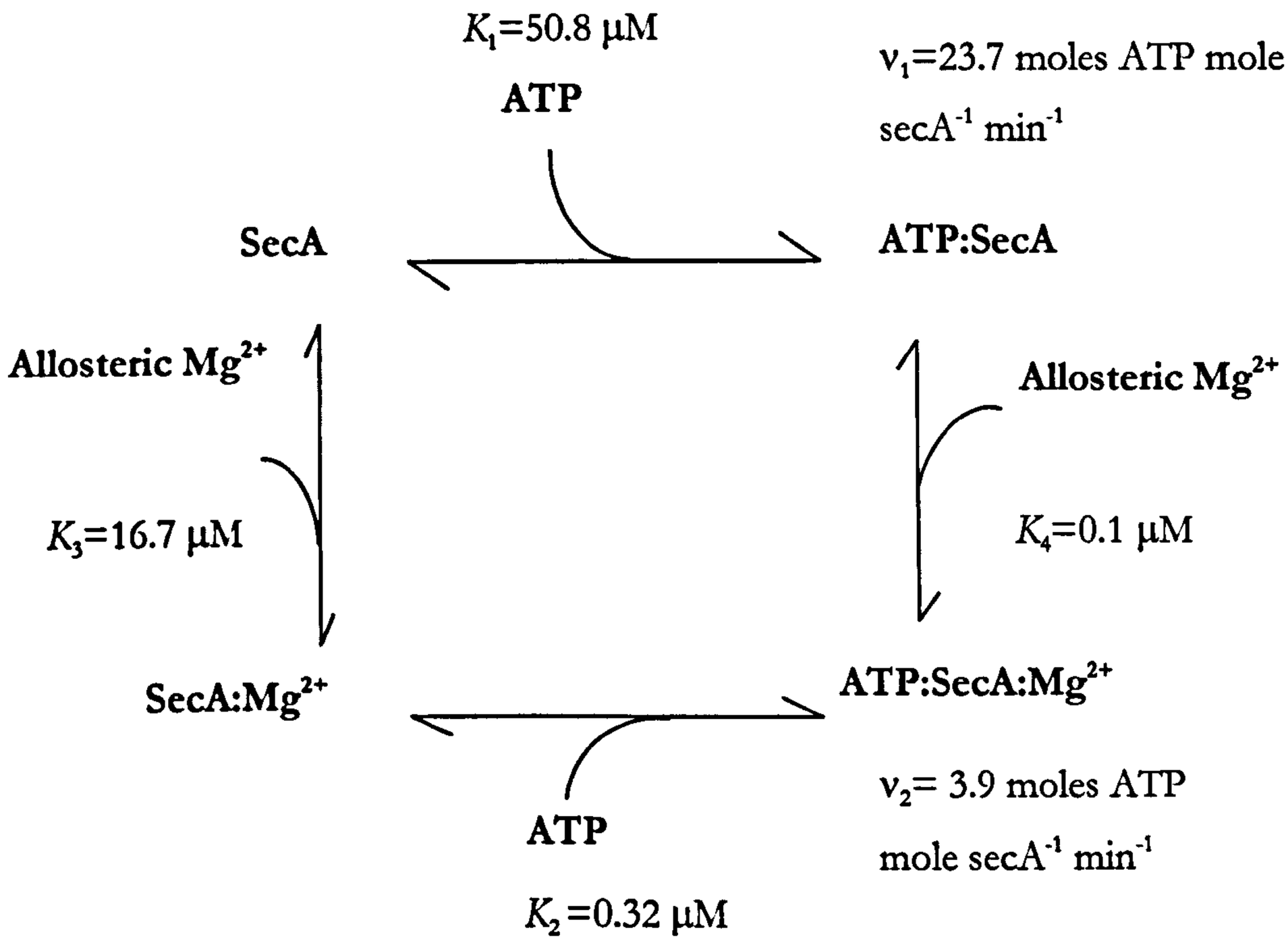

Figure 3-5. The SecA binding cycle for ATP substrate and the non-catalytic regulatory magnesium.

The parameters from the global fit shown in Figure 3-4 were used to construct the kinetic model shown (Equation 2-3, Materials and Methods).

3.3 The competitive inhibition of SecA by ADP is also affected by magnesium

In order to fully understand the reaction mechanism of SecA, effects of the product of the catalytic cycle were studied. The consequence of ADP binding to SecA was studied both in the presence and absence of Mg^{2+} (Figure 3-6). This was fitted to a competitive inhibition function (Equation 2-4, Materials and Methods). The nucleotide exhibited a classic competitive inhibition effect with respect to ATP in the presence of residual Mg^{2+}; there was a 10-fold increase in $K_{i(app)[ADP]}$ at a 10-fold higher ATP concentration (Table 3-3). Only one ATP concentration (100 μM) was used in the absence of any added Mg^{2+}. This is because rates were too slow to be measured accurately at lower ATP concentrations using the non-regenerating EnzChek™ assay, which was a requirement due to the recruitment of ADP by PK as a substrate. At higher ATP concentrations a chelation of Mg^{2+} was observed, which resulted in a slow but discernable increase in steady-state rates. Thus, accurate data fitting procedures could not be performed with confidence.

The affinity of SecA for ADP, given by $K_{d[ADP]}$, was calculated at different concentrations of ATP and Mg^{2+}, taking into account the increased affinity for ATP at the higher Mg^{2+} concentration (Equation 2-5, Materials and Methods, Table 3-3). As with affinity of SecA for ATP, in the presence of 2 mM Mg^{2+} the affinity for ADP was greatly increased, by approximately 200 fold (Tables 3-1 and 3-3). This indicates that both the binding of ATP and ADP is affected by Mg^{2+}.

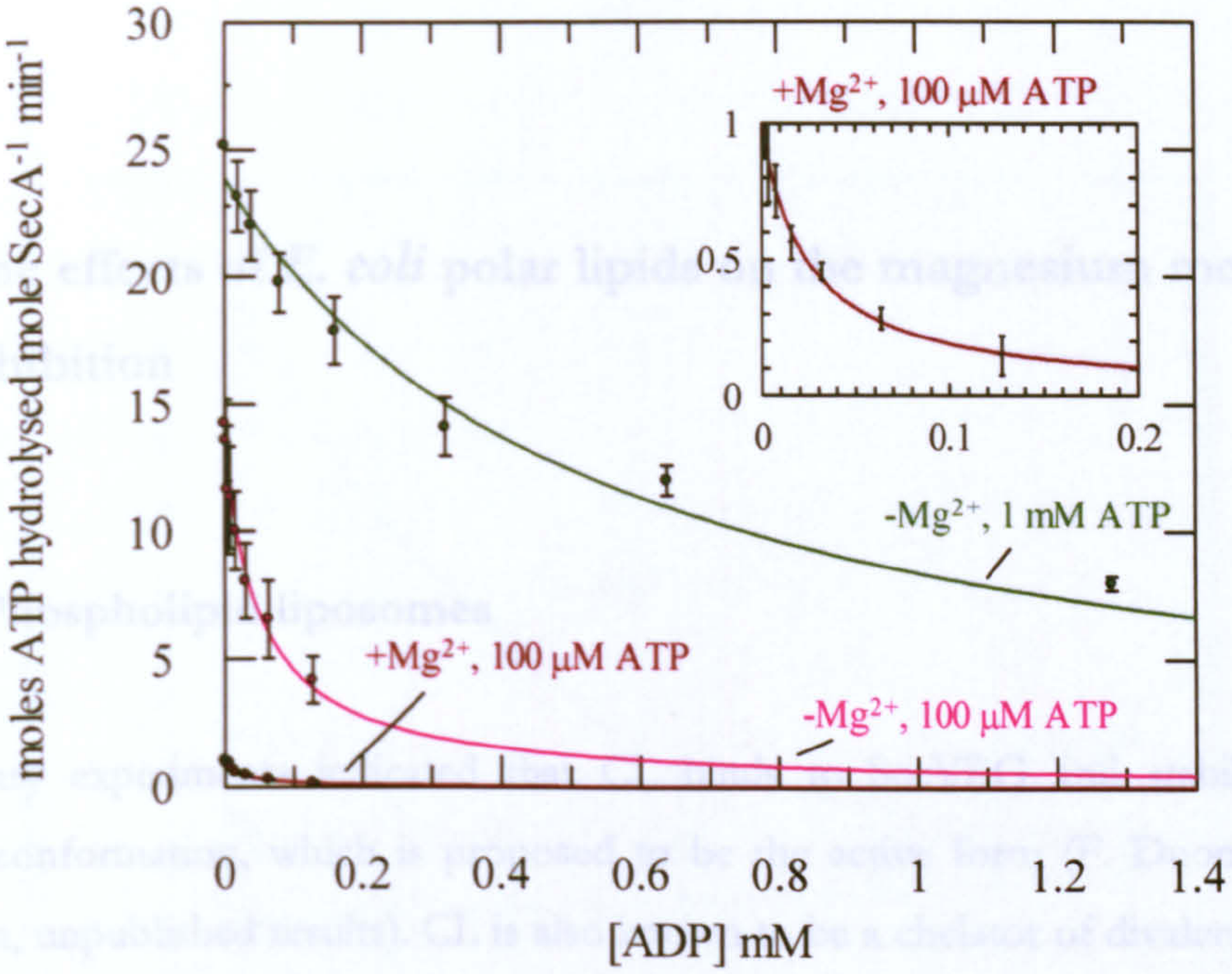

Figure 3-6. The effect of magnesium on competitive product inhibition by ADP.

The ATPase activity of SecA (0.3 µM) was measured with respect to the ADP concentration in TK buffer at both 1 mM ATP (green trace), and 100 µM ATP (pink trace). The experiments were repeated in the presence of 2 mM Mg^{2+} in TKM buffer at 100 µM ATP (inset, brown trace). Error bars represent SD from 4-5 replicates. The data were fitted to a competitive inhibition function (Equation 2-4, Materials and Methods) to determine values for $K_{i(app)[ADP]}$ and subsequently to determine $K_{d[ADP]}$, (Equation 2-5, Materials and Methods) shown in Table 3-3.

SecA	$K_{i(app)[ADP]}$ (mM)	$K_{d[ADP]}$ (µM)
-Mg^{2+}; 1 mM ATP	0.54 ± 0.06	26.25 ± 3.09
-Mg^{2+}; 100 µM ATP	0.051 ± 0.007	17.08 ± 2.21
+Mg^{2+}; 100 µM ATP	0.023 ± 0.001	0.1 ± 0.004

Table 3-3. Calculated values of the $K_{i(app)}$ and K_d for ADP.

The data were collected according to Figure 3-6, and were fitted to a competitive inhibition function (Equation 2-4, Materials and Methods). Actual values for $K_{d[ADP]}$, taking into account the altered $K_{M[ATP]}$ at high concentrations of Mg^{2+}, were calculated by fitting the data in Figure 3-6 to Equation 2-5 as described in Materials and Methods. Standard error (SE) from the fitting procedure is shown.

3.4 The effects of *E. coli* polar lipids on the magnesium mediated inhibition

3.4.1 Phospholipid liposomes

Preliminary experiments indicated that CL binds to SecYEG and stabilises the dimeric conformation, which is proposed to be the active form (F. Duong and I. Collinson, unpublished results). CL is also known to be a chelator of divalent cations (Brenza et al., 1985), mediated by virtue of the negative charges on the polar headgroups. In addition, acidic phospholipids have been shown to be important for protein translocation (Hendrick and Wickner, 1991) and the acidic phospholipids (particularly CL) of the mitochondrial inner membrane were shown to enable a Mg^{2+} mediated activation of the F_1F_0-ATPase (Ye and Lin, 1990). Therefore, it was reasoned that the influence of CL on protein translocation might be an indirect effect mediated by Mg^{2+}, and it was decided to determine the effect of this lipid on the ATPase activity of SecA.

The initial experiment was conducted with phospholipid liposomes, made entirely from *E. coli* CL. The ATPase activity of SecA was measured in the presence of 100 μM ATP in TK buffer (residual concentrations of Mg^{2+}), or TK buffer plus 100 μM Mg^{2+}, or in TKM buffer (containing 2 mM Mg^{2+}) with increasing concentrations of CL (Figure 3-7). In residual Mg^{2+} conditions, a strong inhibition was observed, where as in the presence of high (2 mM) Mg^{2+} a weak stimulation could be perceived. This inhibition effect is presumably due to chelation of the Mg^{2+} required for the hydrolysis of ATP, as CL itself does not seem to inhibit ATPase activity in the presence of Mg^{2+}. As a control to this experiment, the assay was repeated, this time with liposomes composed of total *E. coli* polar lipids (67% PE, 23.2% PG and 9.8% CL) (Figure 3-8). In this case any effect on ATPase activity was insubstantial, indicating a specific effect of CL on SecA.

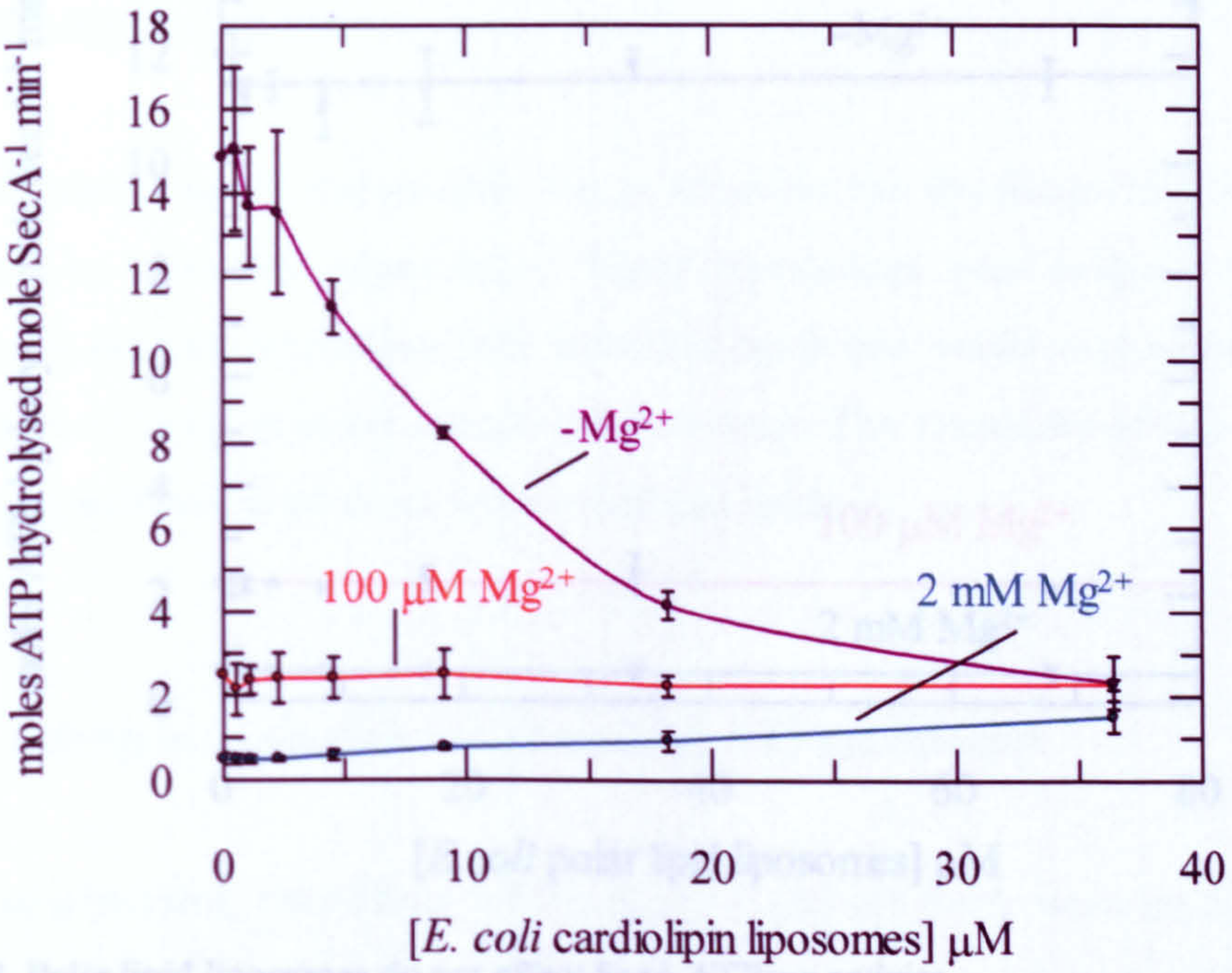

Figure 3-7. The effect of cardiolipin liposomes on SecA ATPase activity is strongly dependent upon the magnesium concentration.

The ATPase activity of SecA (0.3 μM) was measured in the presence of 100 μM ATP in TK buffer with residual Mg^{2+} (purple trace), 100 μM Mg^{2+} (orange trace) or in TKM buffer (2 mM Mg^{2+}; blue trace), with increasing concentrations of CL liposomes. Error bars represent SD from 3-4 replicates.

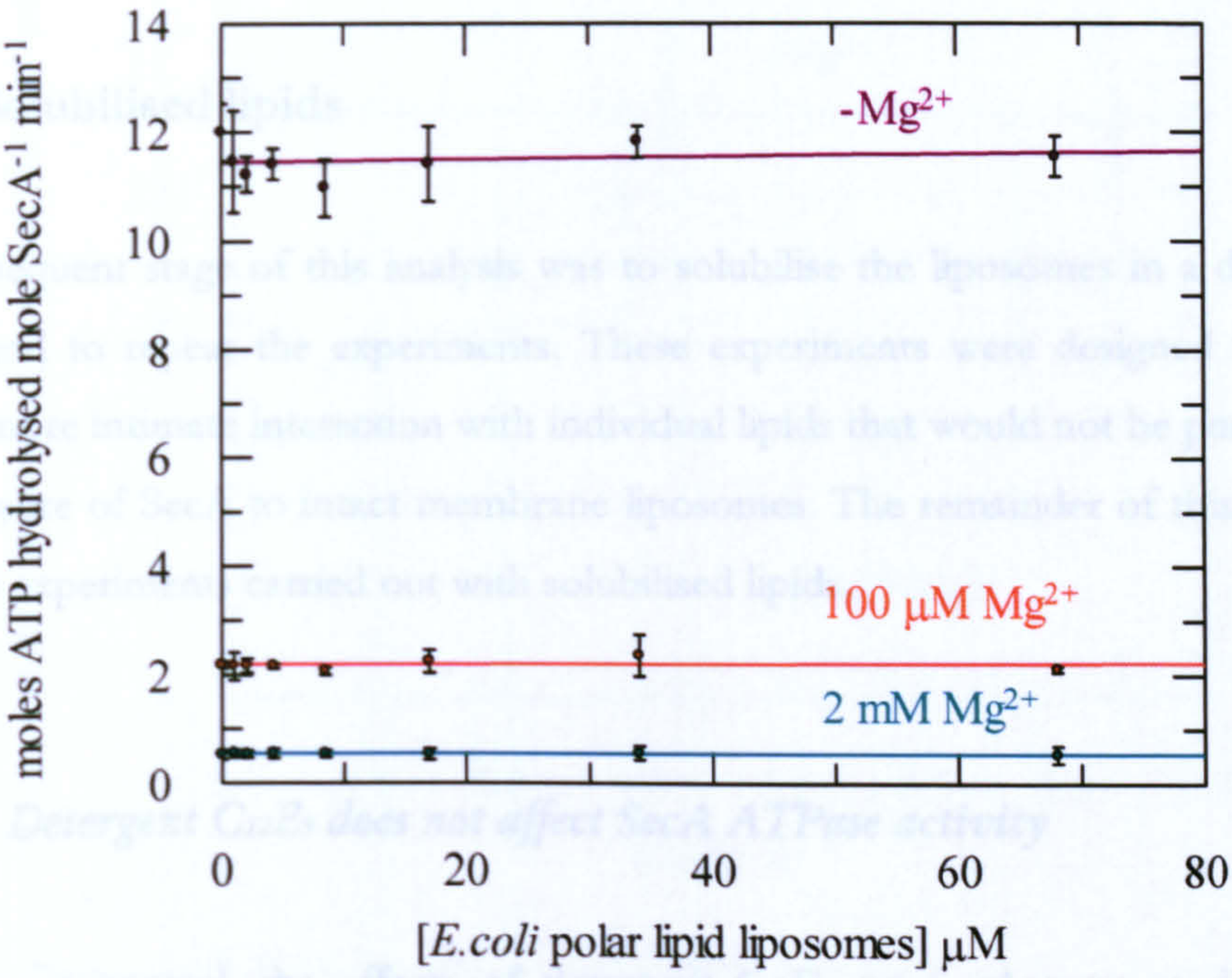

Figure 3-8. Polar lipid liposomes do not affect SecA ATPase activity.

The ATPase activity of SecA (0.3 μM) was measured in the presence of 100 μM ATP in TK buffer with residual Mg^{2+} (purple trace), 100 μM Mg^{2+} (orange trace) or in TKM buffer (2 mM Mg^{2+}; blue trace), with increasing concentrations of total *E. coli* polar lipid liposomes. Error bars represent SD from 3-4 replicates.

3.4.2 Solubilised lipids

The subsequent stage of this analysis was to solubilise the liposomes in a detergent ($C_{12}E_9$) and to repeat the experiments. These experiments were designed to bring about a more intimate interaction with individual lipids that would not be possible by the exposure of SecA to intact membrane liposomes. The remainder of this chapter concerns experiments carried out with solubilised lipids.

3.4.2.1 Detergent $C_{12}E_9$ does not affect SecA ATPase activity

Initially as a control, the effects of detergent $C_{12}E_9$ on SecA were studied. The ATPase activity of SecA was measured in the presence of 100 μM ATP in the presence and absence of Mg^{2+}, with increasing concentrations of $C_{12}E_9$ (Figure 3-9). Under both conditions there was no discernable effect of increasing detergent concentration. Taking this further, the Michaelis-Menten parameters were re-defined under high (0.6%) $C_{12}E_9$ conditions in residual Mg^{2+} (Figure 3-10 and Table 3-4). The detergent, unlike DDM (data not shown) was shown to change neither the affinity of SecA for ATP, nor the turnover rate and thus is an appropriate solubilising agent for use in these experiments.

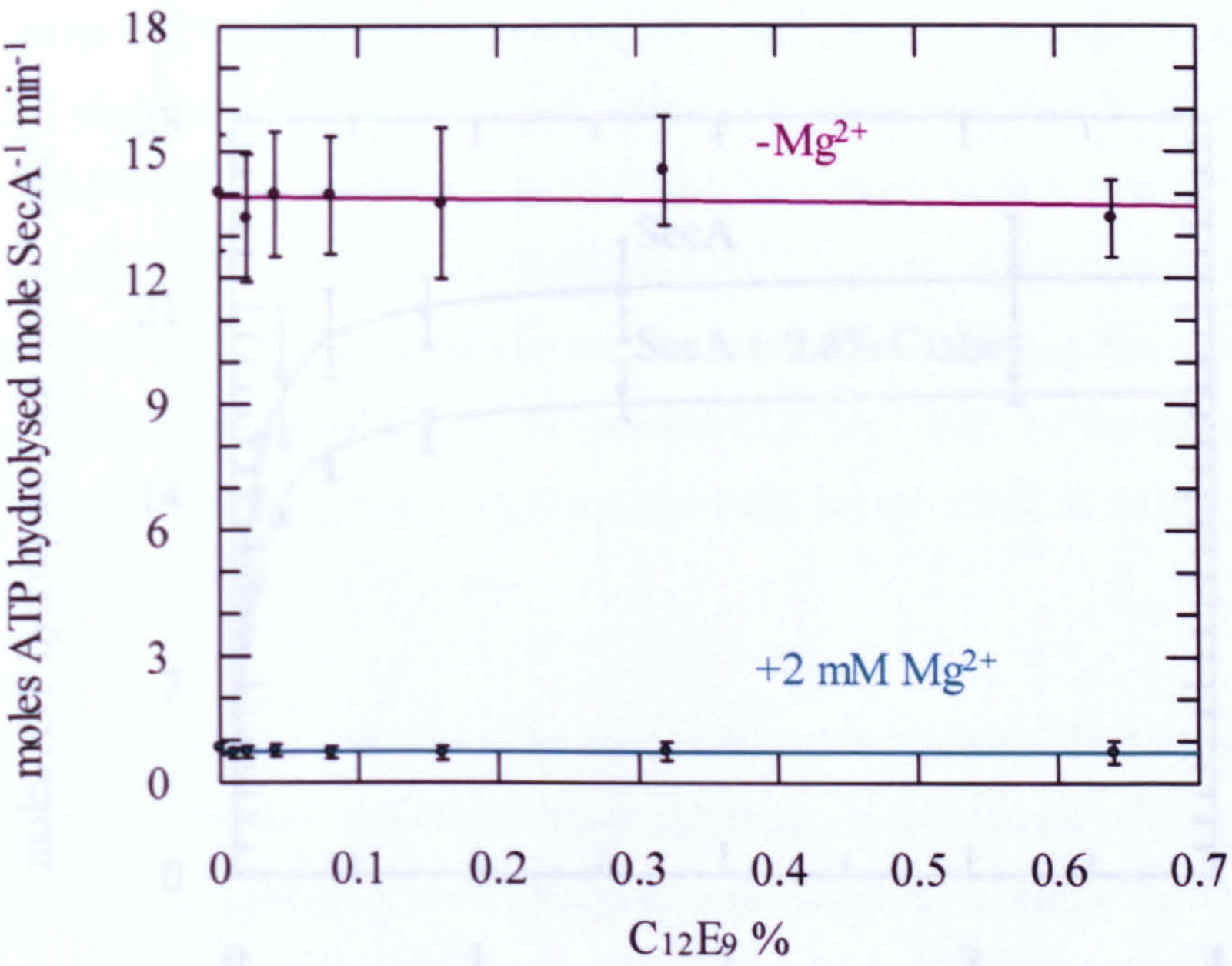

Figure 3-9. Detergent $C_{12}E_9$ has no effect on SecA ATPase activity.

The ATPase activity of SecA (0.3 μM) was measured in the presence of 100 μM ATP in both TK (purple trace) and TKM (blue trace) buffers with increasing concentrations of $C_{12}E_9$. Error bars represent SD from 3 replicates.

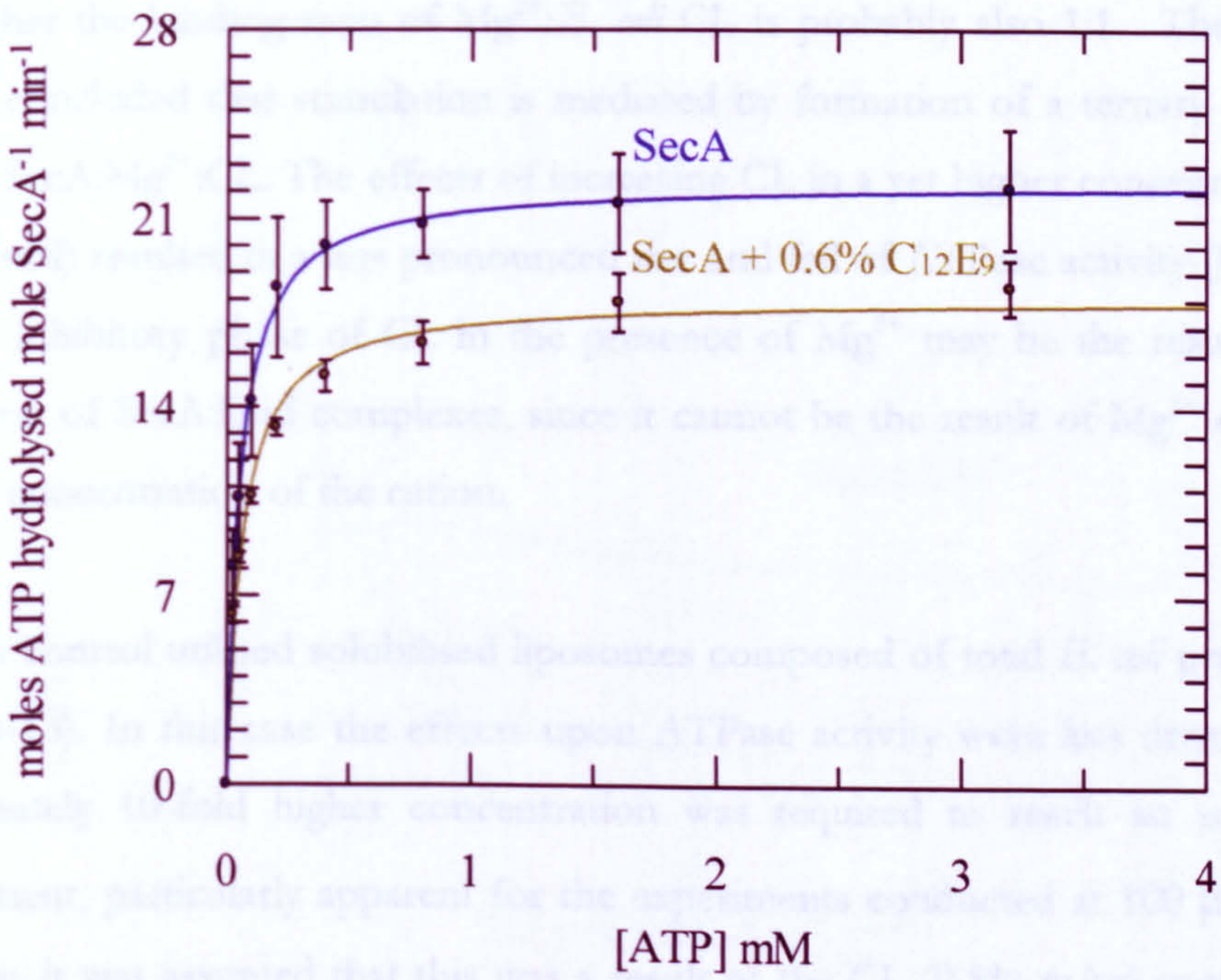

Figure 3-10. Detergent $C_{12}E_9$ does not significantly affect the affinity of SecA for ATP or the turnover rate.

The ATPase activities of SecA (0.3 μM; blue trace, Figure 3-1) and SecA in the presence if 0.6% $C_{12}E_9$ were compared (0.3 μM; olive trace). Both were measured with increasing ATP concentrations in TK buffer, and fitted according to the Michaelis-Menten equation (Equation 2-1, Materials and Methods). Error bars represent SD from 4-6 replicates. The calculated values of $K_{M[ATP]}$ and k_{cat} are shown in Table 3-4.

3.4.2.2 Cardiolipin solubilised in $C_{12}E_9$ counteracts the magnesium mediated inhibiton

Experiments were performed as of the previous ones with intact liposomes. Lipid stock solutions were made at 10 mg/ml (~10 mM), solubilised with 0.1% $C_{12}E_9$ and used as indicated (Figure 3-11). In conditions containing residual Mg^{2+}, CL was found to inhibit the ATPase activity, again presumably due to chelation of the Mg^{2+} required for the hydrolysis of ATP. At higher concentrations of Mg^{2+} (100 μM) there was a striking increase in activity peaking at approximately 2.5 μM CL, followed by a gradual reduction. This indicates that the alleviation of inhibition effect cannot be simply explained by the chelation of Mg^{2+}; it is unlikely that 1 CL molecule could chelate 40 Mg^{2+} ions (Figure 3-12). The ratio of Ca^{2+}: bovine CL was never higher

than 1:1 under any condition (De Kruijff et al., 1982), thus by extrapolation we can assume that the binding ratio of Mg^{2+}:*E. coli* CL is probably also 1:1. Therefore it must be concluded that stimulation is mediated by formation of a ternary complex between SecA:Mg^{2+}:CL. The effects of increasing CL in a yet higher concentration of Mg^{2+} (2 mM) resulted in a less pronounced rise and fall of ATPase activity (Figure 3-11). The inhibitory phase of CL in the presence of Mg^{2+} may be the result of the aggregation of SecA:lipid complexes, since it cannot be the result of Mg^{2+} chelation at such a concentration of the cation.

A further control utilised solubilised liposomes composed of total *E. coli* polar lipids (Figure 3-13). In this case the effects upon ATPase activity were less dramatic. An approximately 10-fold higher concentration was required to reach an equivalent enhancement, particularly apparent for the experiments conducted at 100 μM Mg^{2+}. Therefore, it was assumed that this was a result of the CL (9.8% w/w) contained in the *E. coli* polar lipid stocks. This again reinforces the notion that CL specifically is responsible for the lipid-stimulated effects on SecA ATPase activity.

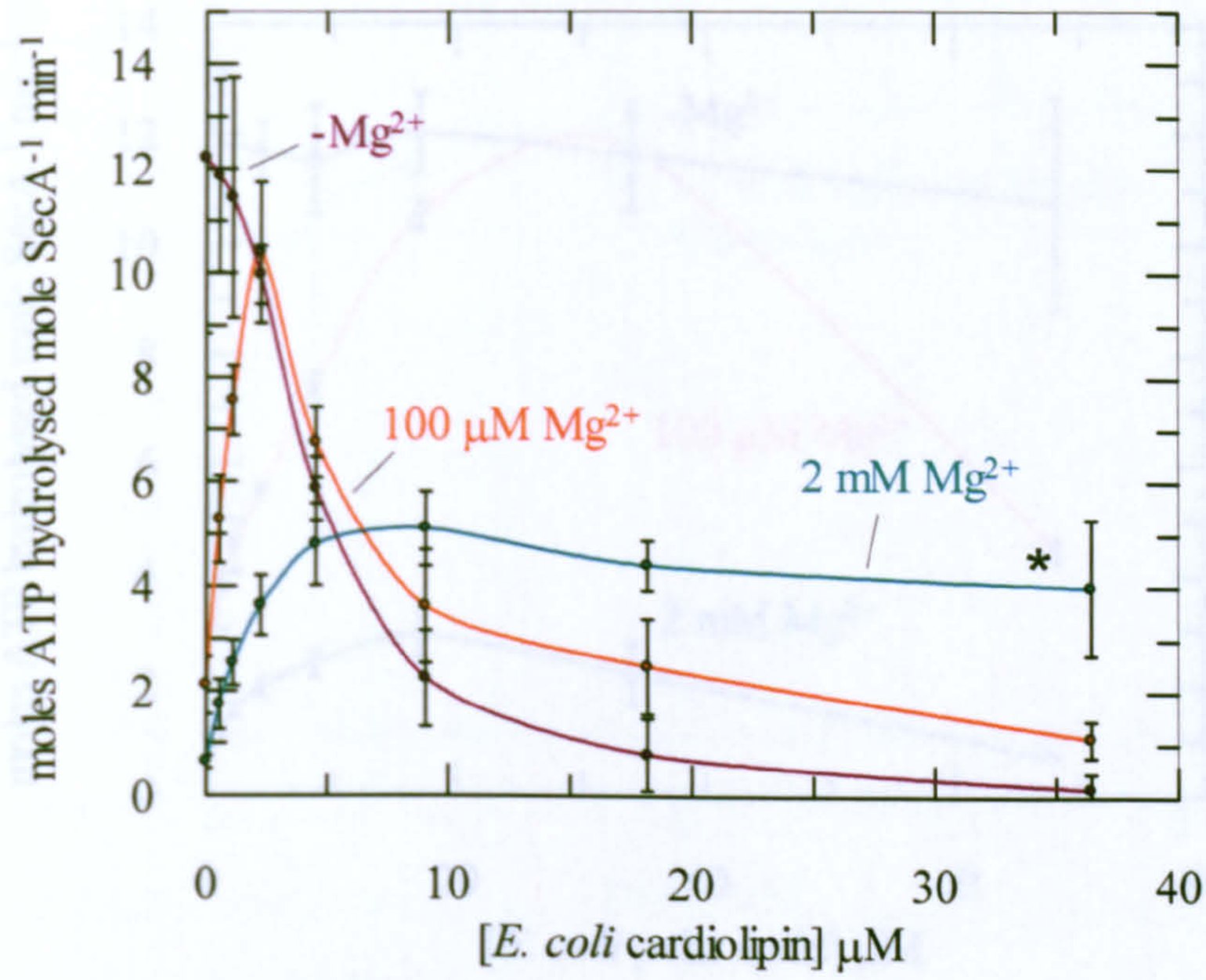

Figure 3-11. Cardiolipin reduces the inhibitory potency magnesium has for the ATPase activity of SecA.

The ATPase activity of SecA (0.3 μM) was measured in the presence of 100 μM ATP in TK buffer with residual Mg^{2+} (purple trace), 100 μM Mg^{2+} (orange trace) or 2 mM Mg^{2+} in TKM buffer (blue trace), with increasing concentrations of CL solubilised in $C_{12}E_9$. Error bars represent SD from 3 replicates. The asterisk denotes conditions used to redefine the Michaelis-Menten parameters (Figure 3-14).

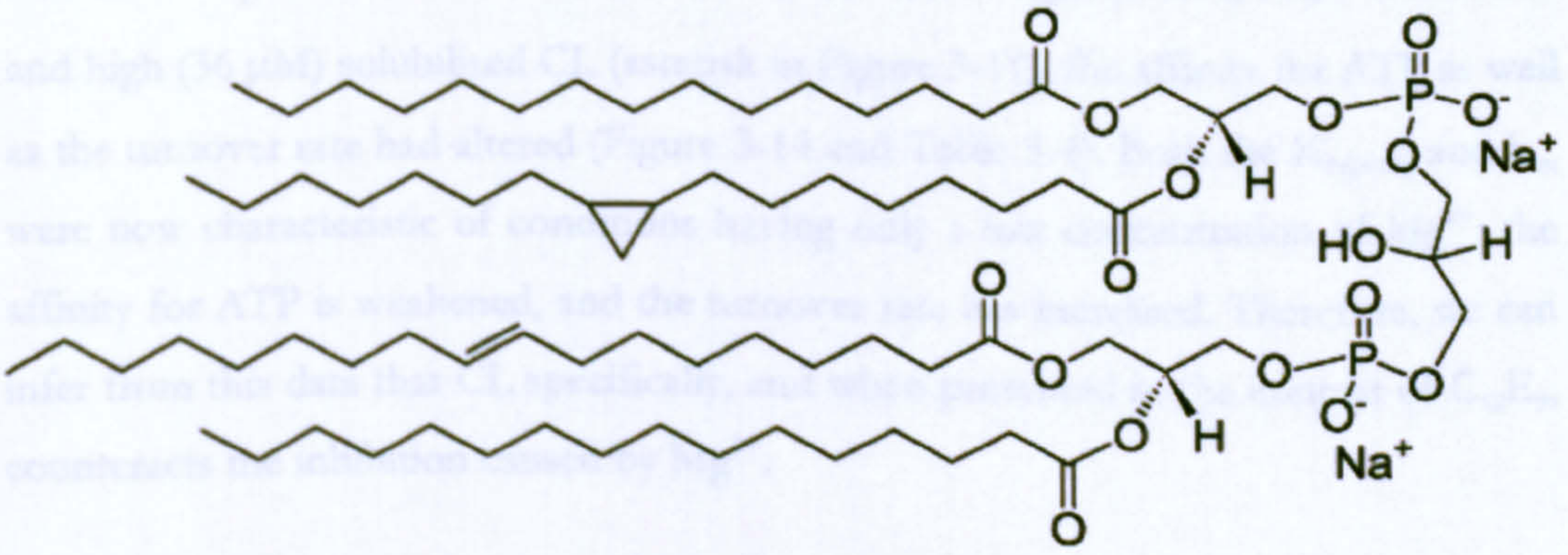

Figure 3-12. Cardiolipin structure.

Divalent cations bind to the polar headgroups of phospholipid molecules, neutralising the charge. The ratio of Mg^{2+}:CL is probably 1:1.

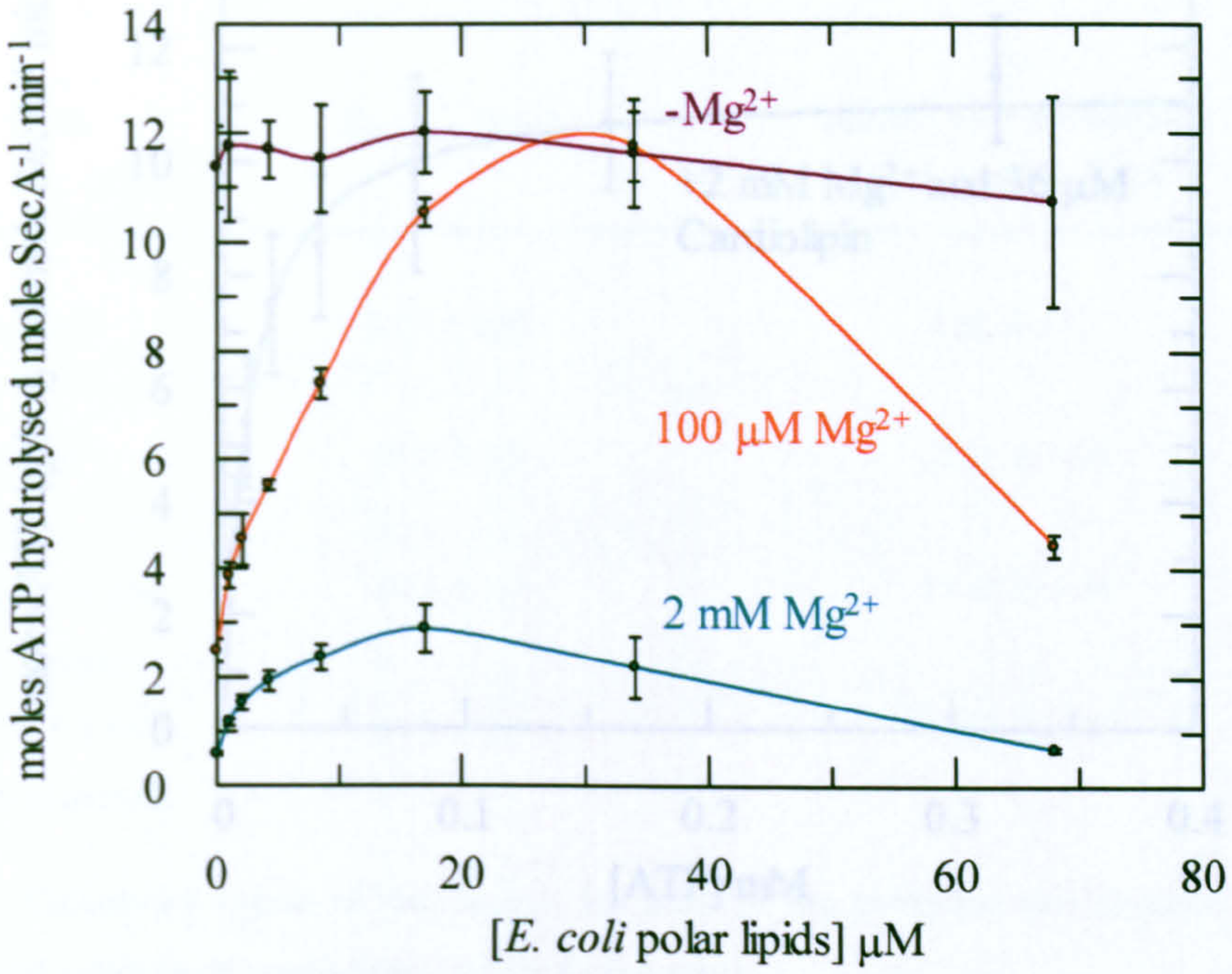

Figure 3-13. The activation of magnesium inhibited SecA requires the addition of a larger quantity of total *E. coli* polar lipids.

The ATPase activity of SecA (0.3 μM) was measured in the presence of 100 μM ATP in TK buffer with residual Mg^{2+} (purple trace), 100 μM Mg^{2+} (orange trace) or 2 mM Mg^{2+} in TKM buffer (blue trace), with increasing concentrations of total polar lipids (which contain 9.8% CL) solubilised in $C_{12}E_9$. Error bars represent SD from 3 replicates.

The next step was to ascertain whether or not under high (2 mM) Mg^{2+} conditions and high (36 μM) solubilised CL (asterisk in Figure 3-11), the affinity for ATP as well as the turnover rate had altered (Figure 3-14 and Table 3-4). Both the $K_{M[ATP]}$ and k_{cat} were now characteristic of conditions having only a low concentration of Mg^{2+}; the affinity for ATP is weakened, and the turnover rate has increased. Therefore, we can infer from this data that CL specifically, and when presented in the context of $C_{12}E_9$, counteracts the inhibition caused by Mg^{2+}.

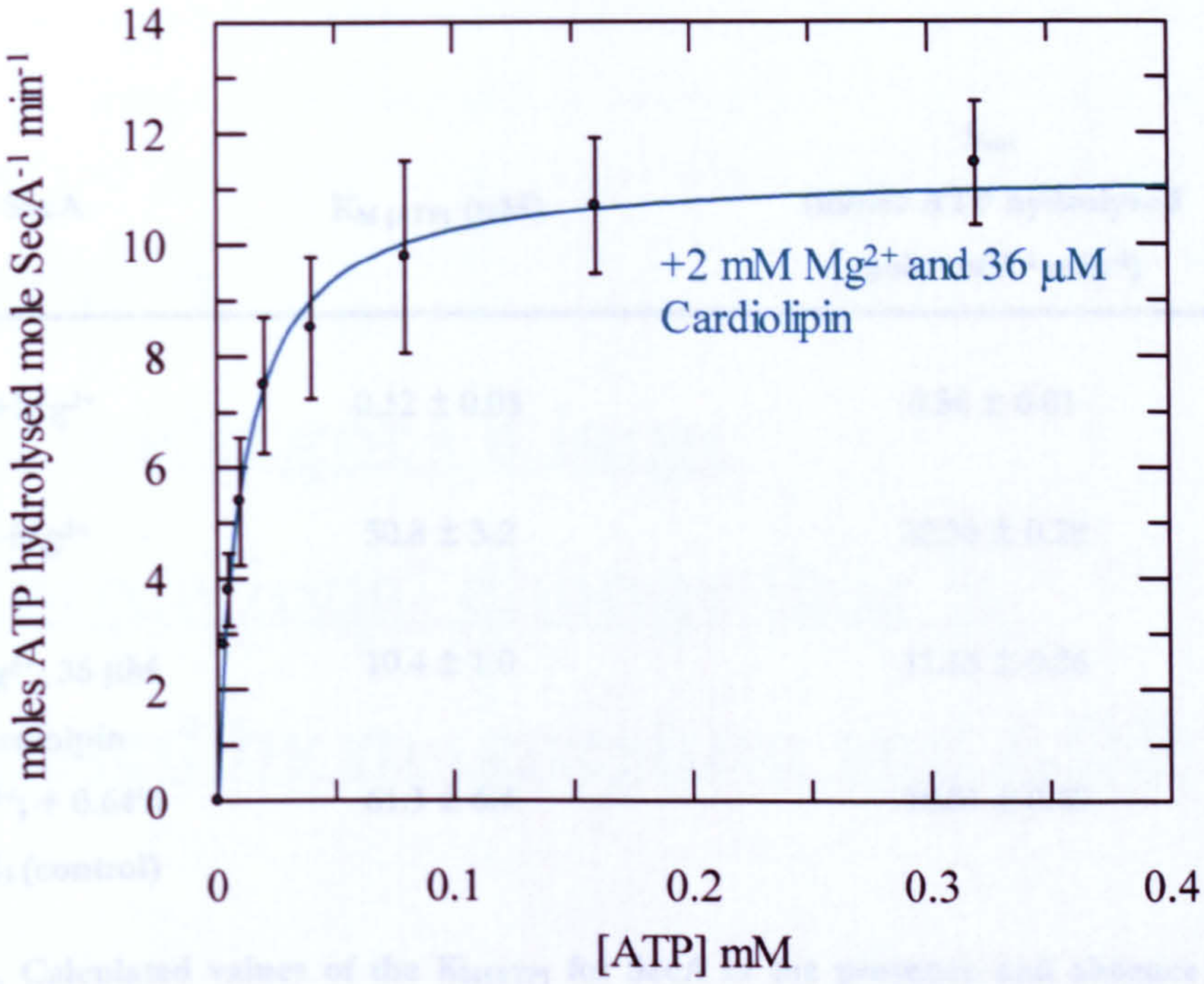

Figure 3-14. Cardiolipin counteracts the decrease in $K_{M[ATP]}$ and k_{cat} caused by magnesium.

The ATPase activity of SecA (0.3 μM) was measured with 36 μM $C_{12}E_9$-solubilised CL in TKM buffer (asterisk in Figure 3-11), over a range of ATP concentrations and fitted according to the Michaelis-Menten equation (Equation 2-1, Materials and Methods). Error bars represent SD from 4-6 replicates. Calculated values of $K_{M[ATP]}$ and k_{cat} are shown in Table 3-4.

SecA	$K_{M\,[ATP]}$ (μM)	k_{cat} (moles ATP hydrolysed mole $secA^{-1}$ min^{-1})
$+Mg^{2+}$	0.32 ± 0.03	0.56 ± 0.01
$-Mg^{2+}$	50.8 ± 3.2	22.36 ± 0.28
$+Mg^{2+}$; 36 μM cardiolpin	10.4 ± 1.0	11.33 ± 0.26
$-Mg^{2+}$; + 0.64% $C_{12}E_9$ (control)	61.3 ± 6.4	18.07 ± 0.40

Table 3-4. Calculated values of the $K_{M[ATP]}$ for SecA in the presence and absence of 2 mM Mg^{2+}, 36 μM solubilised cardiolipin and $C_{12}E_9$ (control).

These values are compared to the values in +/-Mg^{2+} conditions. The data were collected according to Figures 3-1, 3-2, 3-10 and 3-14, and fitted to the Michaelis-Menten equation (Equation 2-1, Materials and Methods). SE from the fitting procedure is shown.

3.5 Chapter Summary

This chapter describes a strong Mg^{2+}-dependent inhibition of SecA, which affects both the wild-type protein and the mutant SecA-Δ11/N95. By a global fit of Mg^{2+} inhibition data at two ATP concentrations, it was determined that this inhibition acts via an allosteric binding site, distinct from that required for hydrolysis of ATP. The Mg^{2+} inhibition can be alleviated by cardiolipin, most effectively when solubilised in detergent solution. Finally, the binding affinity for ADP is also increased by Mg^{2+}, and the product of the ATPase reaction exhibits a competitive inhibition effect.

Chapter 4

SecA undergoes a large conformational change that is regulated by magnesium and ADP

4.1 Gel Filtration Chromatography

4.1.1 A reversible magnesium dependent change in the structure of SecA is apparent during gel filtration chromatography

Experiments were carried out by gel filtration chromatography to explore the effects of Mg^{2+} on the structure of SecA (Section 2.6, Materials and Methods). The method relies on the exclusion of particles within a specific range of sizes and separates molecules on this basis according to their hydrodynamic radius. Thus, gross differences in structure and in oligomeric states can be monitored in a rudimentary manner.

The potent inhibition of the ATPase activity by Mg^{2+} suggests an alteration in the structure of SecA, particularly at the NBF. This could be either by a change in the tertiary structure, quaternary structure or both. Analytical gel filtration experiments were performed with a Superose 6 HR 10/30 column with approximately 10 nmoles SecA or SecA-Δ11/N95 per experiment and the absorbance was measured at 280 nm.

SecA was first applied in buffer containing 20 mM $MgCl_2$ and then 50 mM EDTA. The elution volumes differed dramatically according to the presence of Mg^{2+} (0.35 ml; Figure 4-1). Re-analysis of the samples in a reciprocal fashion, that is, after dialysis of the Mg^{2+} depleted sample in the presence of the cation and vice versa, resulted in a reversal of this effect.

The column was calibrated using Biorad molecular weight standards (data not shown) and the elution volumes were consistent with an object the size of a SecA dimer. However, the associative nature of SecA probably precludes such a simple analysis.

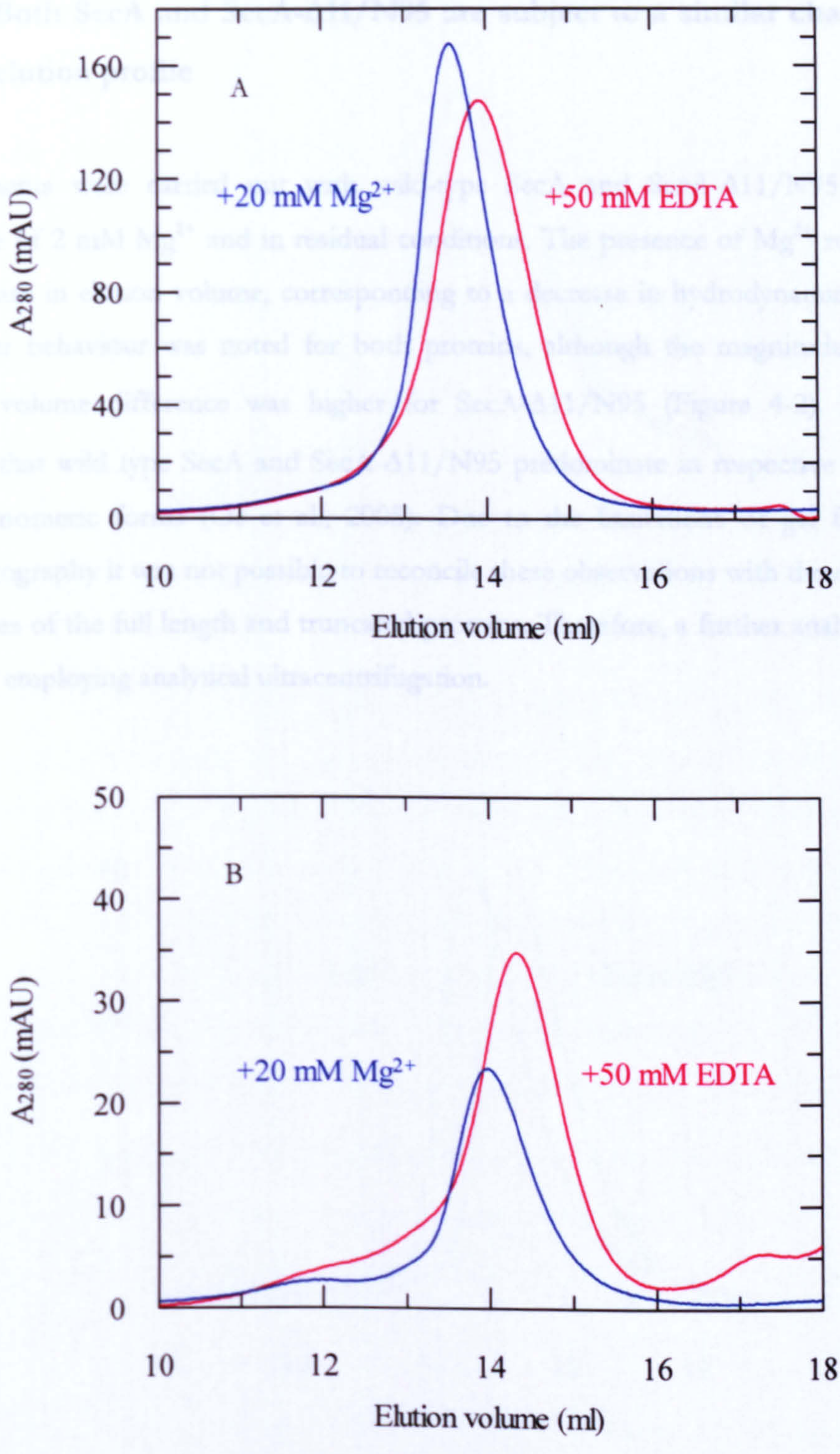

Figure 4-1. The structural change detected by gel filtration chromatography is fully reversible.

(A) 10 nmoles of SecA was separated by gel filtration chromatography in TK buffer plus 20 mM Mg^{2+} (blue trace) or 50 mM EDTA (red trace) using a Superose 6 HR 10/30 column.
(B) Samples from the previous elution were collected, dialysed and re-applied to the column under the reverse condtions to either remove or re-supplement with Mg^{2+}.

4.1.2 Both SecA and SecA-Δ11/N95 are subject to a similar change in elution profile

Experiments were carried out with wild-type SecA and SecA-Δ11/N95 in the presence of 2 mM Mg^{2+} and in residual conditions. The presence of Mg^{2+} results in an increase in elution volume, corresponding to a decrease in hydrodynamic radius. A similar behaviour was noted for both proteins, although the magnitude of the elution volume difference was higher for SecA-Δ11/N95 (Figure 4-2). Reports suggest that wild type SecA and SecA-Δ11/N95 predominate in respective dimeric and monomeric forms (Or et al., 2005). Due to the limitations of gel filtration chromatography it was not possible to reconcile these observations with the reported properties of the full length and truncated proteins. Therefore, a further analysis was pursued employing analytical ultracentrifugation.

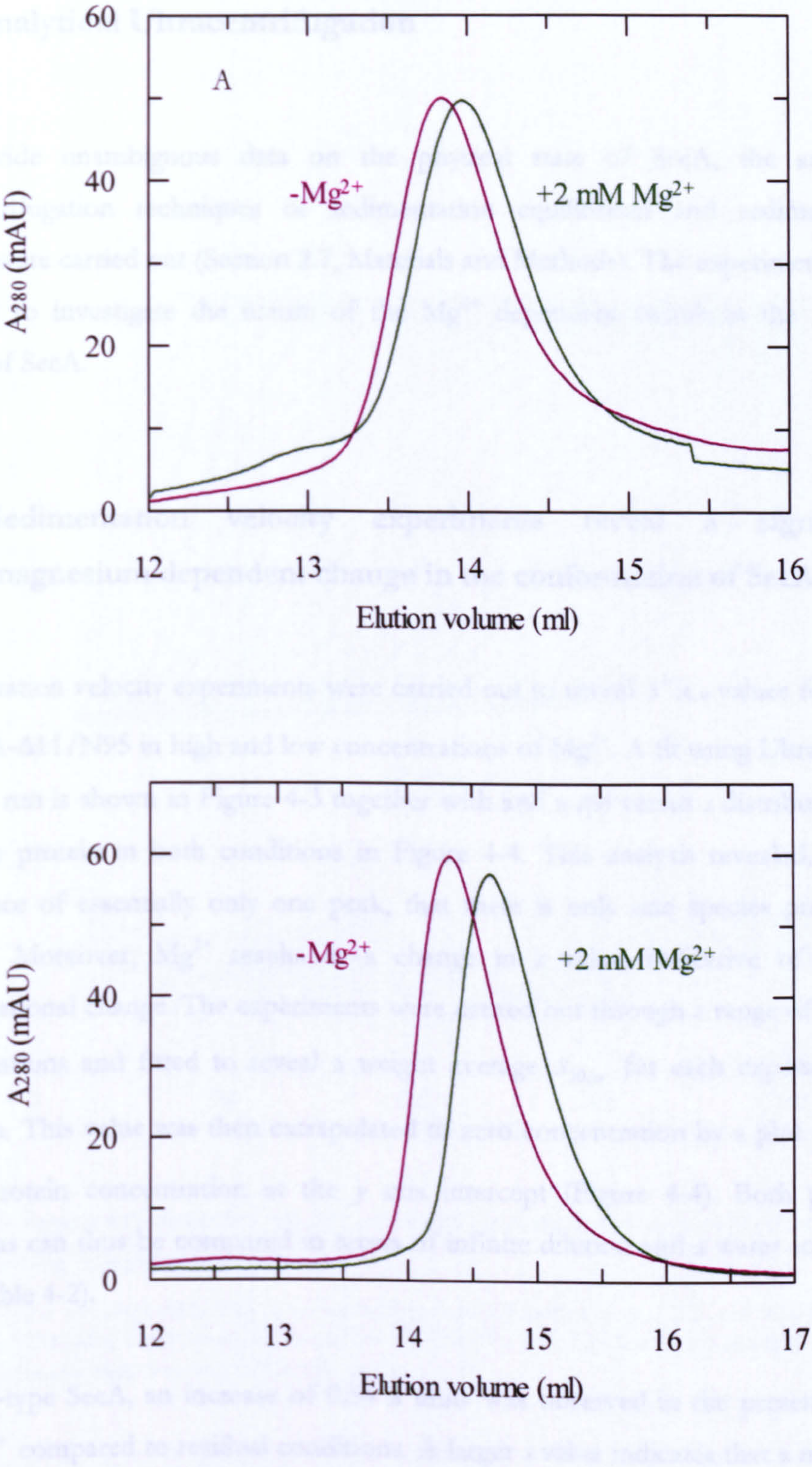

Figure 4-2. Both SecA and SecA-Δ11/N95 undergo a change in structure in the presence of magnesium.

(A) 10 nmoles of SecA was separated by gel filtration chromatography in TK (purple trace) and TKM buffers (green trace) using a Superose 6 HR 10/30 column.
(B) The procedure was repeated with 10 nmoles SecA-Δ11/N95.

4.2 Analytical Ultracentrifugation

To provide unambiguous data on the physical state of SecA, the analytical ultracentrifugation techniques of sedimentation equilibrium and sedimentation velocity were carried out (Section 2.7, Materials and Methods). The experiments were designed to investigate the nature of the Mg^{2+} dependent switch in the ATPase activity of SecA.

4.2.1 Sedimentation velocity experiments reveal a significant magnesium dependent change in the conformation of SecA

Sedimentation velocity experiments were carried out to reveal $s^{o}_{20,w}$ values for SecA and SecA-Δ11/N95 in high and low concentrations of Mg^{2+}. A fit using Ultrascan of a typical run is shown in Figure 4-3 together with and a *c(s)* versus *s* distribution for wild-type protein in both conditions in Figure 4-4. This analysis revealed, by the appearance of essentially only one peak, that there is only one species present in solution. Moreover, Mg^{2+} results in a change in *s* value, indicative of a large conformational change. The experiments were carried out through a range of protein concentrations and fitted to reveal a weight average $s_{20,w}$ for each experiment in Ultrascan. This value was then extrapolated to zero concentration by a plot of $s_{20,w}$ versus protein concentration at the *y* axis intercept (Figure 4-4). Both proteins conditions can thus be compared in terms of infinite dilution and a water solvent at 20°C (Table 4-2).

For wild-type SecA, an increase of 0.54 S units was observed in the presence of 2 mM Mg^{2+} compared to residual conditions. A larger *s* value indicates that a molecule sediments more rapidly, indicating either an increase in mass due to oligomerisation, or a compaction in shape leading to decreased friction. A shift of 0.54 S is compatible with the latter possibility and consistent with the gel filtration analysis where Mg^{2+} was found to increase SecA elution volume (corresponding to a decrease in apparent size). It was therefore concluded that Mg^{2+} results in a conformational change within SecA that renders the structure more tightly packed.

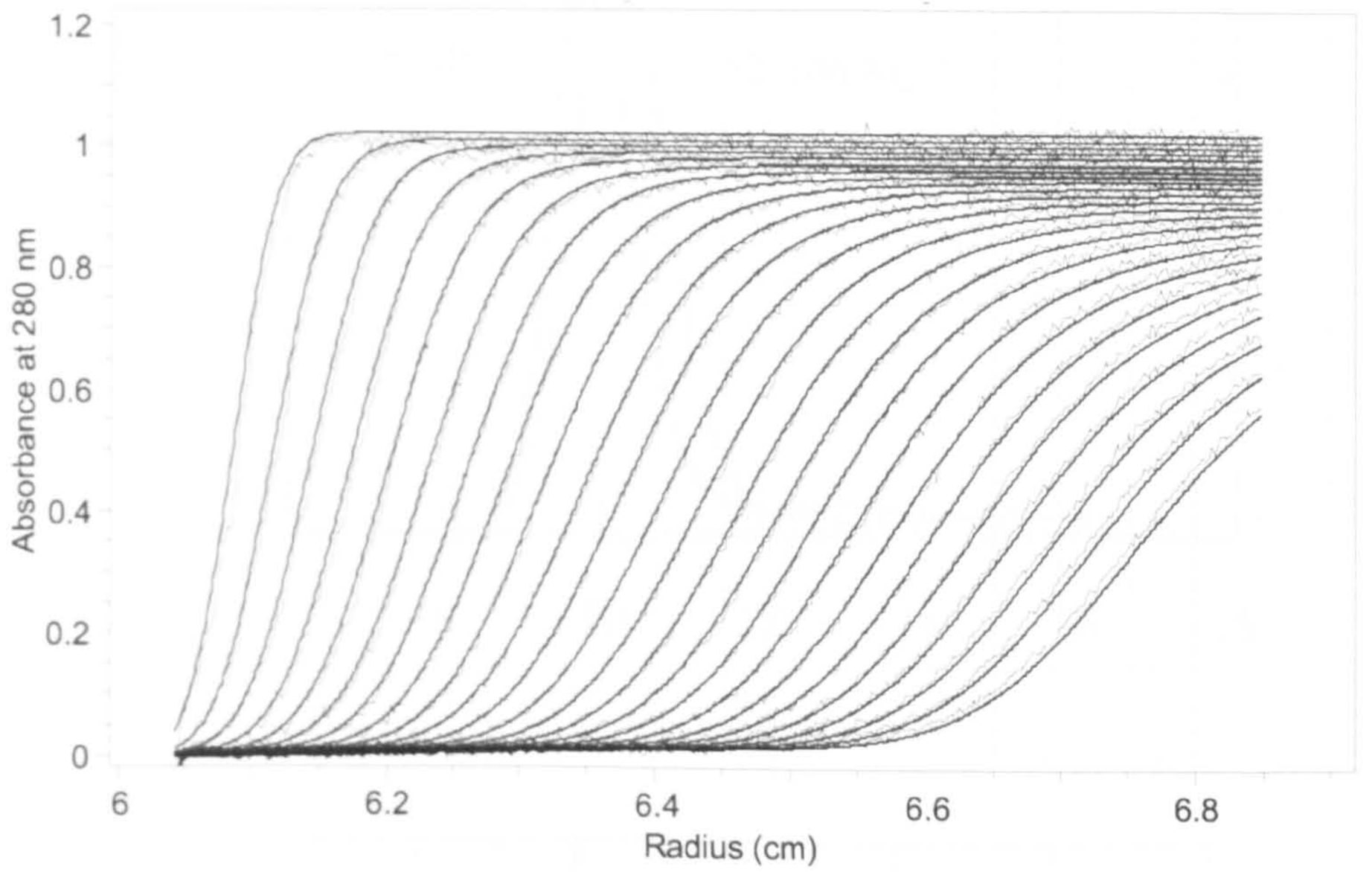

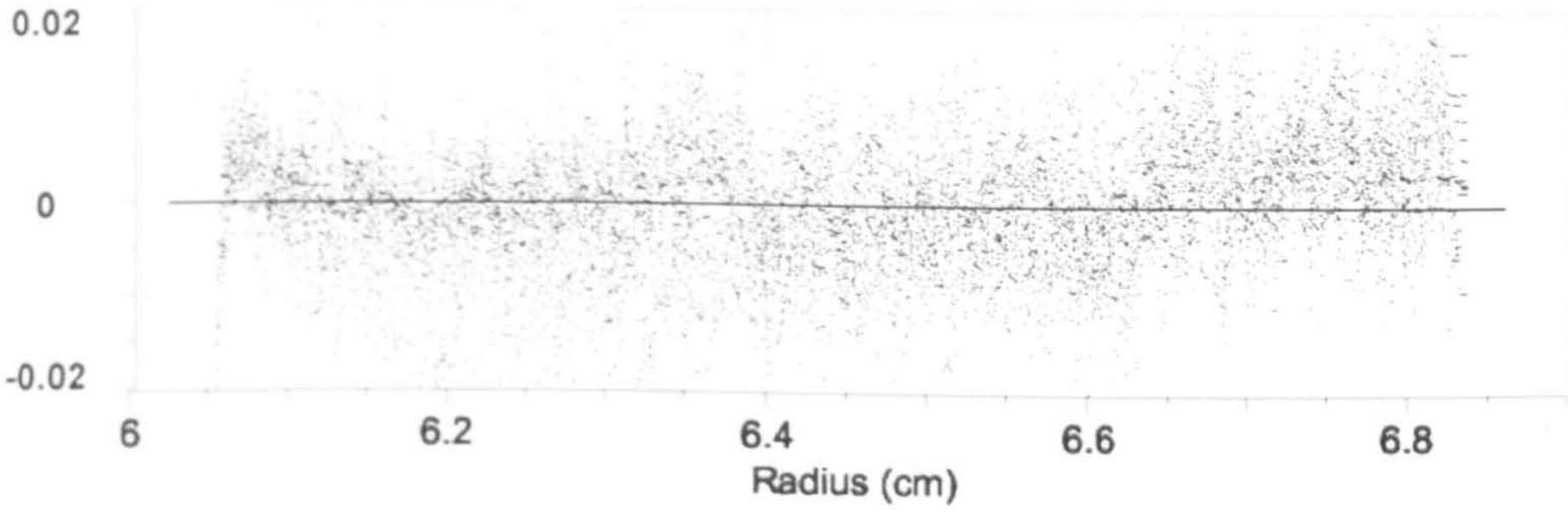

Figure 4-3. Typical sedimentation velocity scans and the corresponding fit (with residual values) for SecA in residual magnesium.

1-13 μM SecA or SecA-Δ11/N95 were centrifuged at 130,000 x *g* at 25°C and analysed by a continuous *c(s)* model, fitted using Ultrascan (Demeler, 2005). The data shown are example scans and a corresponding fit from 10 μM SecA in TK buffer.

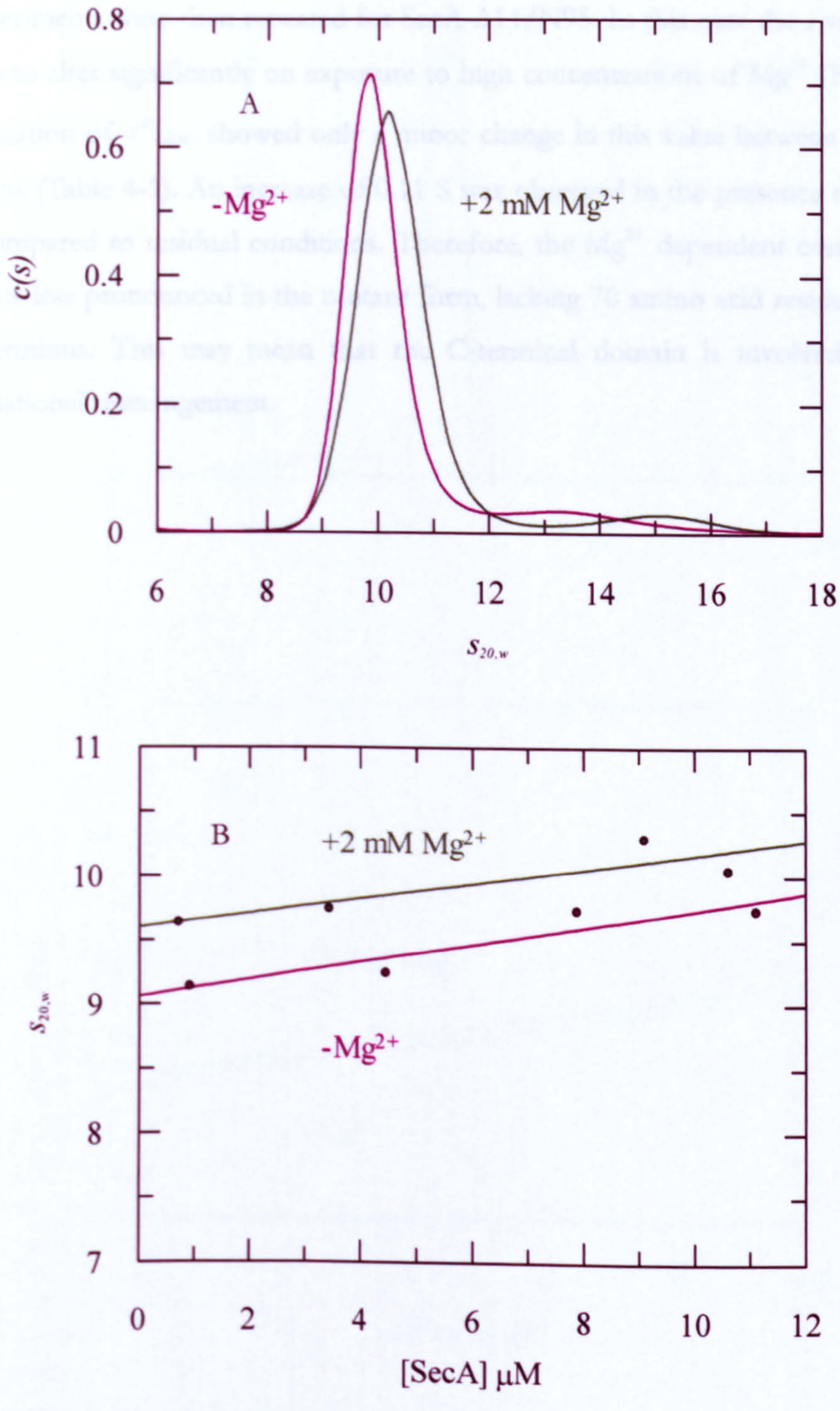

Figure 4-4. Sedimentation velocity reveals a large magnesium dependent conformational change in SecA.

(A) Scans were fitted to a continuous *c(s)* model using Ultrascan to yield values for $s_{20,w}$ under a range of concentrations and corrected for TK (purple trace) and TKM (green trace) buffer conditions. The data shown are an example distribution of 4 μM SecA.

(B) These values were plotted versus SecA concentration to reveal $s^{o}_{20,w}$ under TK (purple trace) and TKM (green trace) buffer conditions (Table 4-1).

The experiments were then repeated for SecA-Δ11/N95. In this case the *s* value was not seen to alter significantly on exposure to high concentrations of Mg^{2+} (Figure 4-5). Calculation of $s^{o}_{20,w}$ showed only a minor change in this value between the two conditions (Table 4-1). An increase of 0.11 S was observed in the presence of 2 mM Mg^{2+}, compared to residual conditions. Therefore, the Mg^{2+} dependent compaction of SecA is less pronounced in the mutant form, lacking 70 amino acid residues from the C-terminus. This may mean that the C-terminal domain is involved in this conformational rearrangement.

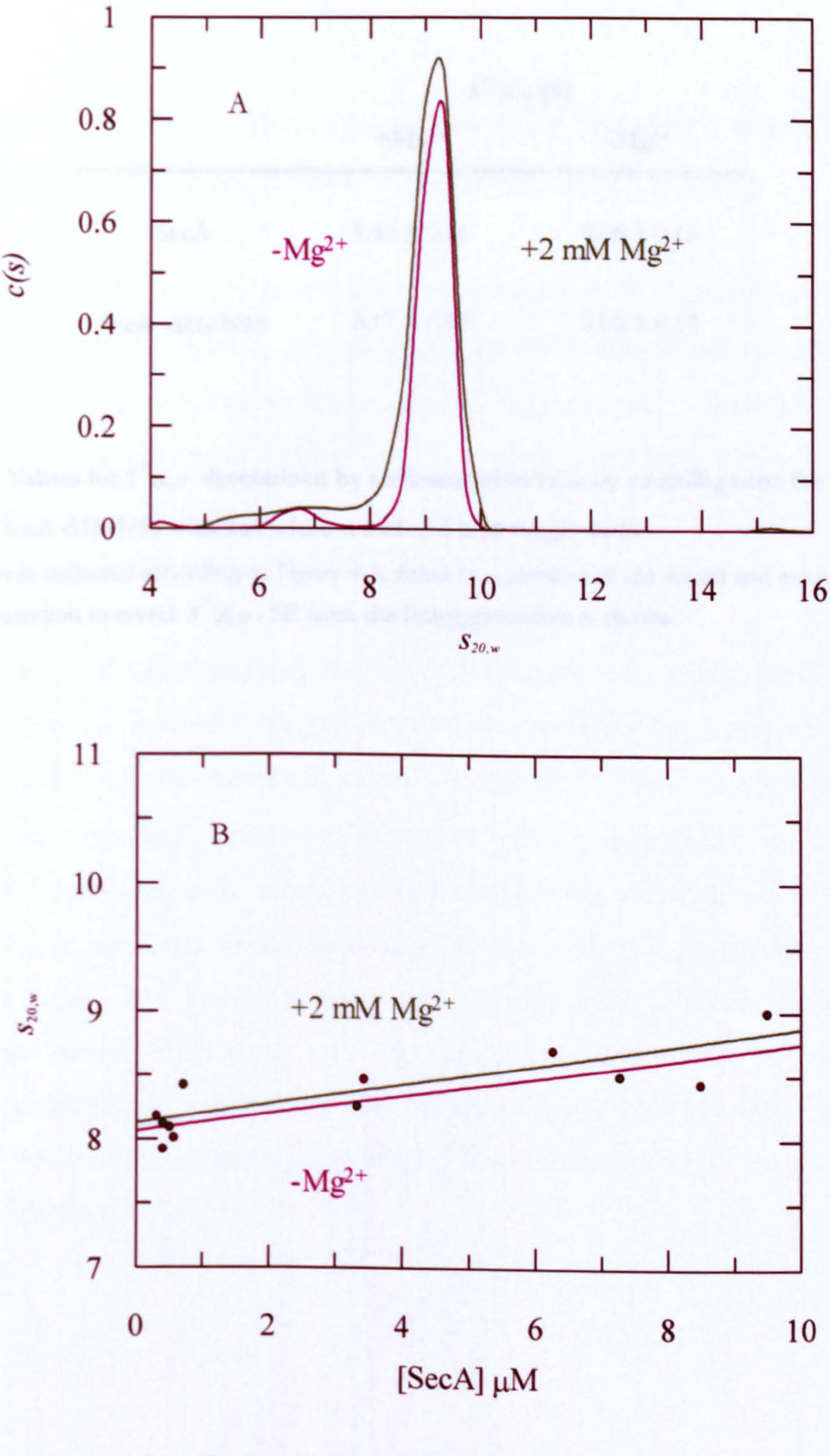

Figure 4-5. Sedimentation velocity reveals a small magnesium dependent conformational change in SecA-Δ11/N95.

(A) Scans were fitted to a continuous *c(s)* model using Ultrascan to yield values for $s_{20,w}$ under a range of concentrations and corrected for TK (purple trace) and TKM (green trace) buffer conditions. The data shown are an example distribution of 4 μM SecA-Δ11/N95.

(B) These values were plotted versus SecA concentration to reveal $s^{o}_{20,w}$ under TK (purple trace) and TKM (green trace) buffer conditions (Table 4-1).

	$S^{o}_{20,w}$ (S)	
	+Mg^{2+}	**-Mg^{2+}**
SecA	9.60 ± 0.16	9.06 ± 0.13
SecA-Δ11/N95	8.17 ± 0.10	8.06 ± 0.12

Table 4-1. Values for $S^{o}_{20,w}$ determined by sedimentation velocity centrifugation for wild-type SecA and SecA-Δ11/N95 with and without added 2 mM magnesium.

The data were collected according to Figure 4-3, fitted to a continuous *c(s)* model and extrapolated to zero concentration to reveal $S^{o}_{20,w}$. SE from the fitting procedure is shown.

4.2.2 Sedimentation equilibrium experiments determine that SecA is a stable dimer in the presence or absence of magnesium

Sedimentation equilibrium experiments were carried out in a range of SecA and SecA-Δ11/N95 concentrations (0.4-13 μM) with and without added Mg^{2+}. These were analysed with Ultrascan to yield molecular weight values. A typical fit from an experiment containing SecA without Mg^{2+} at various centrifugal forces determines the corresponding residuals (Figure 4-6). A global fit of the data reveals a single molecular weight value for the proteins in both conditions.

This data revealed unambiguously that SecA is a dimer in the presence and absence of magnesium, the molecular weights determined were 200.1 ± 7.1 kDa and 201.6 ± 6.4 kDa respectively (the calculated weight of a monomer based on sequence is 102 kDa). Rather surprisingly, SecA-Δ11/N95, previously reported to be a monomer (Or et al., 2005), was found to be a dimer as well, with a molecular weight of 184.6 ± 7.1 kDa in the presence of magnesium, and 181.5 ± 8.3 kDa in the absence (the calculated weight of a monomer based on sequence is 94 kDa). In all cases, the monomers were in such rarity that they could not be detected with sufficient accuracy to determine a dissociation constant, an indication that this value must therefore be in the low nanomolar range. The molecular weight in this case is therefore the weight average.

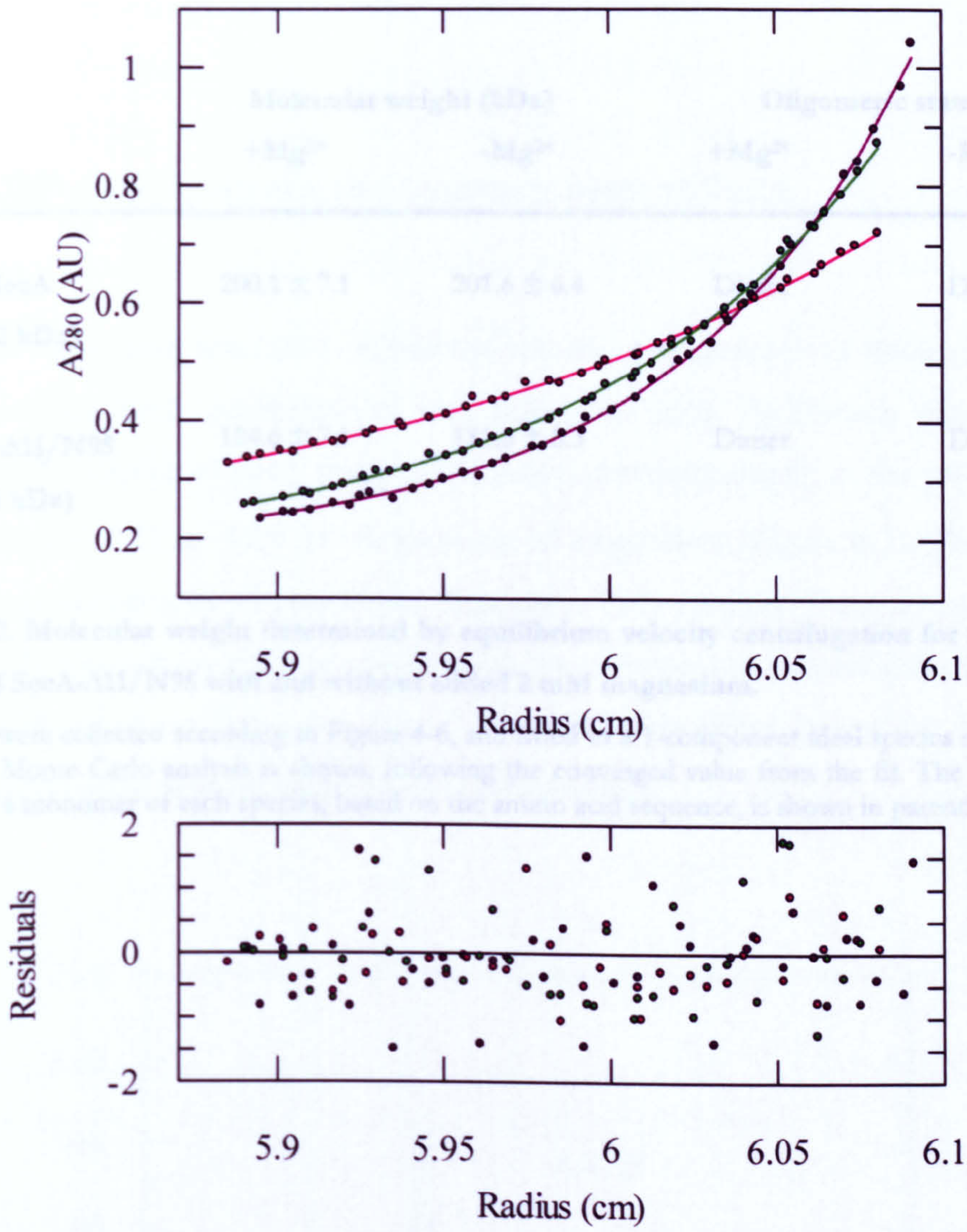

Figure 4-6. Typical sedimentation equilibrium scans and the corresponding fit (with residual values) for SecA in residual concentrations of magnesium.

1-13 μM SecA or SecA-Δ11/N95 were centrifuged at three speeds at 25°C in either TK or TKM buffers. Equilibrium scans were taken at 16 and 20 hours, and the data analysed using a 1-component ideal species model in Ultrascan (Demeler, 2005). The data shown are example scans and a corresponding fit from an experiment containing 1.5 μM SecA in TK buffer at 3,000 x *g* (pink trace), 5,800 x *g* (green trace) and 8,000 x *g* (purple trace). A global fit of all data reveals a weight average molecular weight, shown in Table 4-2.

	Molecular weight (kDa)		Oligomeric state	
	$+Mg^{2+}$	$-Mg^{2+}$	$+Mg^{2+}$	$-Mg^{2+}$
SecA (102 kDa)	200.1 ± 7.1	201.6 ± 6.4	Dimer	Dimer
SecA–Δ11/N95 (94 kDa)	184.6 ± 7.1	181.5 ± 8.3	Dimer	Dimer

Table 4-2. Molecular weight determined by equilibrium velocity centrifugation for wild type SecA and SecA-Δ11/N95 with and without added 2 mM magnesium.

The data were collected according to Figure 4-6, and fitted to a 1-component ideal species model. SD from the Monte Carlo analysis is shown, following the converged value from the fit. The molecular weight of a monomer of each species, based on the amino acid sequence, is shown in parenthesis.

4.3 ADP also promotes the compact form of SecA

It was of subsequent interest to determine whether the presence of nucleotides had any effects on SecA conformation and oligomeric state. Preliminary experiments separated 10 nmoles of SecA using gel filtration chromatography in the presence of either 100 μM ATP or ADP in the presence of magnesium (Figure 4-7). The elution profile was the same in all conditions, thus most likely resulting from dimeric forms of SecA. It was not possible to confirm this by sedimentation equilibrium analytical ultracentrifugation, as SecA was found to be unstable when bound by ADP and formed aggregates over the required long time periods.

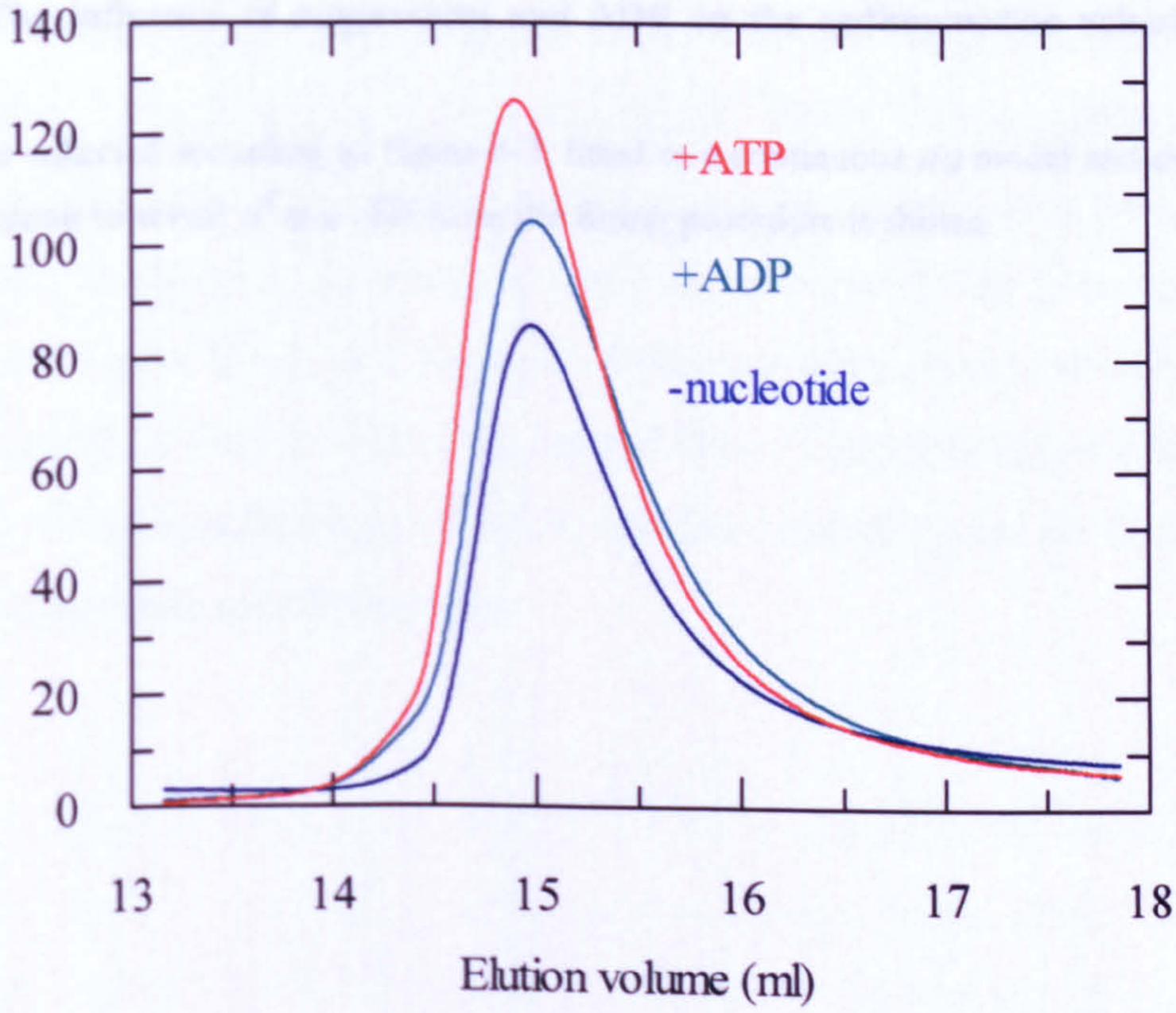

Figure 4-7. Analytical gel filtration chromatography shows a similar species of SecA in the apo state, and in the presence of ADP and ATP.

10 nmoles of SecA was separated by gel filtration chromatography in TKM buffer (dark blue trace), plus 100 μM ADP (pale blue trace) and plus 100 μM ATP (orange trace) using a Superose 6 HR 10/30 column.

Sedimentation velocity experiments require considerably less time and could be carried out in spite of the aggregation tendency. Inclusion of ATP was not considered as the time course of the experiment would lead to hydrolysis and production of ADP. The data were again fitted to a continuous *c(s)* model using Ultrascan, an extrapolated to yield values for $s^{o}_{20,w}$ through a range of SecA concentrations with and without added Mg^{2+}, and 100 μM ADP (Table 4-3). The presence of ADP bound to SecA results in the compact conformation, even in residual Mg^{2+} conditions.

	$s^{*}_{20,w}$ (S)			
Mg^{2+}	+	+	-	-
ADP	-	+	-	+
SecA	9.60 ± 0.16	9.60 ± 0.11	9.06 ± 0.13	9.56 ± 0.05

Table 4-3. The influence of magnesium and ADP on the sedimentation velocity profile of SecA.

The data were collected according to Figure 4-3, fitted to a continuous *c(s)* model and extrapolated to zero concentration to reveal $s^{o}_{20,w}$. SE from the fitting procedure is shown.

4.4 SecA undergoes a large conformational change upon binding to the cytosolic face of SecYEG

To probe for possible conformational changes induced by the interaction of SecA with SecYEG, limited proteolysis was performed on the individual partners and a complex of a dimer of SecYEG, stabilised by a monoclonal antibody (Tziatzios et al., 2004), bound to two SecA protomers ($SecYEG_2.SecA_2.10A4$; Section 2.8, Materials and Methods).

SecA alone is relatively resistant to proteolysis by trypsin, and largely remained intact in the conditions employed (Figure 4-8). In contrast, SecY (with and without the antibody) is rapidly cleaved, resulting in the appearance of a band between SecY and SecE, due to cleavage at residue R255 located in the cytoplasmic loop between transmembrane helicies 6 and 7 (Brundage et al., 1990). The complex of SecYEG and SecA stabilised by monoclonal antibody showed that SecA became considerably more sensitive to degradation, where as SecY was protected. The protection of SecY was dependent upon SecA, and was not elicited by the presence of antibody alone (compare $SecYEG_2.10A4$ to $SecYEG_2.SecA_2.10A4$). This association must therefore occlude the 6-7 cytoplasmic loop of SecY, and SecA reconfigures SecA into an open, proteolytically sensitive conformation.

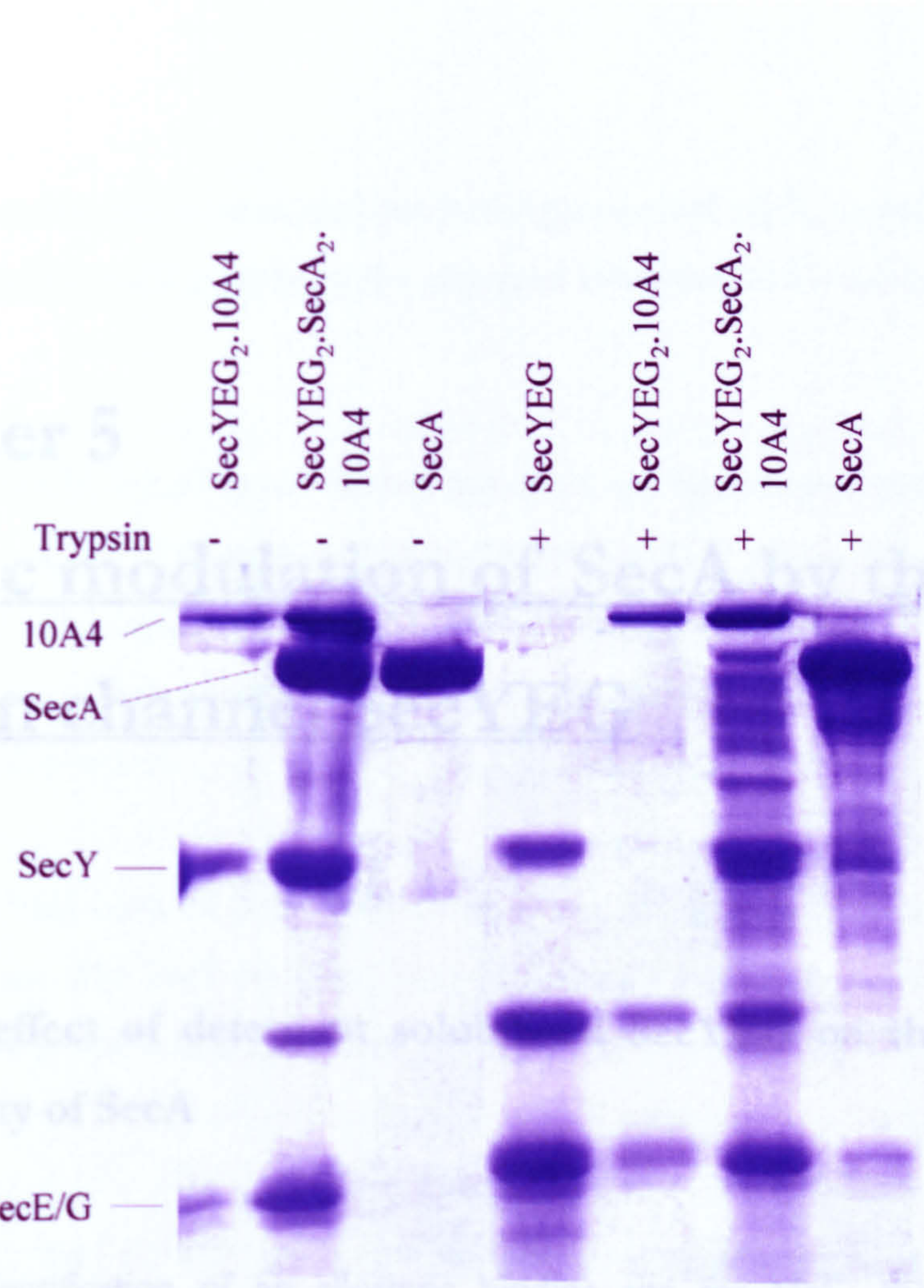

Figure 4-8. SecA interaction with SecYEG results in a protection of the channel complex, and an increased susceptibility of the motor protein.

SecYEG, SecA, SecYEG$_2$.10A4 and SecYEG$_2$.SecA$_2$.10A4 were subjected to proteolysis by trypsin. Protein fragments were subsequently resolved by SDS-PAGE and stained with Coomassie blue. Positions of the different proteins are indicated.

4.5 Chapter Summary

It can be concluded from the analytical gel filtration and ultracentrifugation data that Mg^{2+} binding results in a large conformational change within SecA, and that the dimeric state is retained. Also, in contrast to previous work (Or et al., 2005), SecA-Δ11/N95 is a dimer and is subjected to a similar change, albeit to a less significant degree. ADP bound to SecA reveals $s^{o}_{20,w}$ values similar to that in the presence of Mg^{2+}, suggesting a compaction of the structure. A more open conformation of SecA is demonstrated by an increased sensitivity to trypsin upon binding to the SecYEG complex.

Chapter 5

Kinetic modulation of SecA by the protein channel SecYEG

5.1 The effect of detergent solubilised SecYEG on the ATPase activity of SecA

After the identification of an allosteric binding site for Mg^{2+}, the subsequent experiments were aimed towards elucidating the effects of the SecYEG channel in this respect. It is known that the catalytic activity of SecA is stimulated by the presence of lipid membranes containing SecYEG (Lill et al., 1990). Experiments in detergent solution were conducted in order to dissect the contribution that the protein SecYEG, and lipid components have in this augmentation.

5.1.1 SecYEG strongly stimulates the ATPase activity of SecA via a weak interaction of the two

Increasing concentrations of a SecYEG preparation dissolved in 0.1% $C_{12}E_9$ were titrated into a standard kinetic assay reaction, with a constant background of 0.1% $C_{12}E_9$ (surfactant conditions were shown not to influence the ATPase activity of SecA). It is known that protein translocation has a requirement for high concentrations (2 mM) of Mg^{2+} (A. Robson and I. Collinson, unpublished results).

Therefore, experiments were carried out in the presence of Mg^{2+}, to determine if the SecYEG complex could counteract the observed inhibition and activate the ATPase activity.

The reaction could indeed by stimulated, but could not be saturated with the highest concentration of SecYEG employed (8.4 μM) (Figure 5-1). An excess of nearly 30-fold SecYEG over SecA indicates that the interaction between the two proteins under these steady-state conditions is a weak one. However the stimulation is very high (a 14-fold increase).

BSA and SecYEβ from *M. jannaschii* had no effect on ATPase activation under the same conditions. The SecY complex from *M. jannaschii* serves as a useful control, as archaea do not posess a SecA protein.

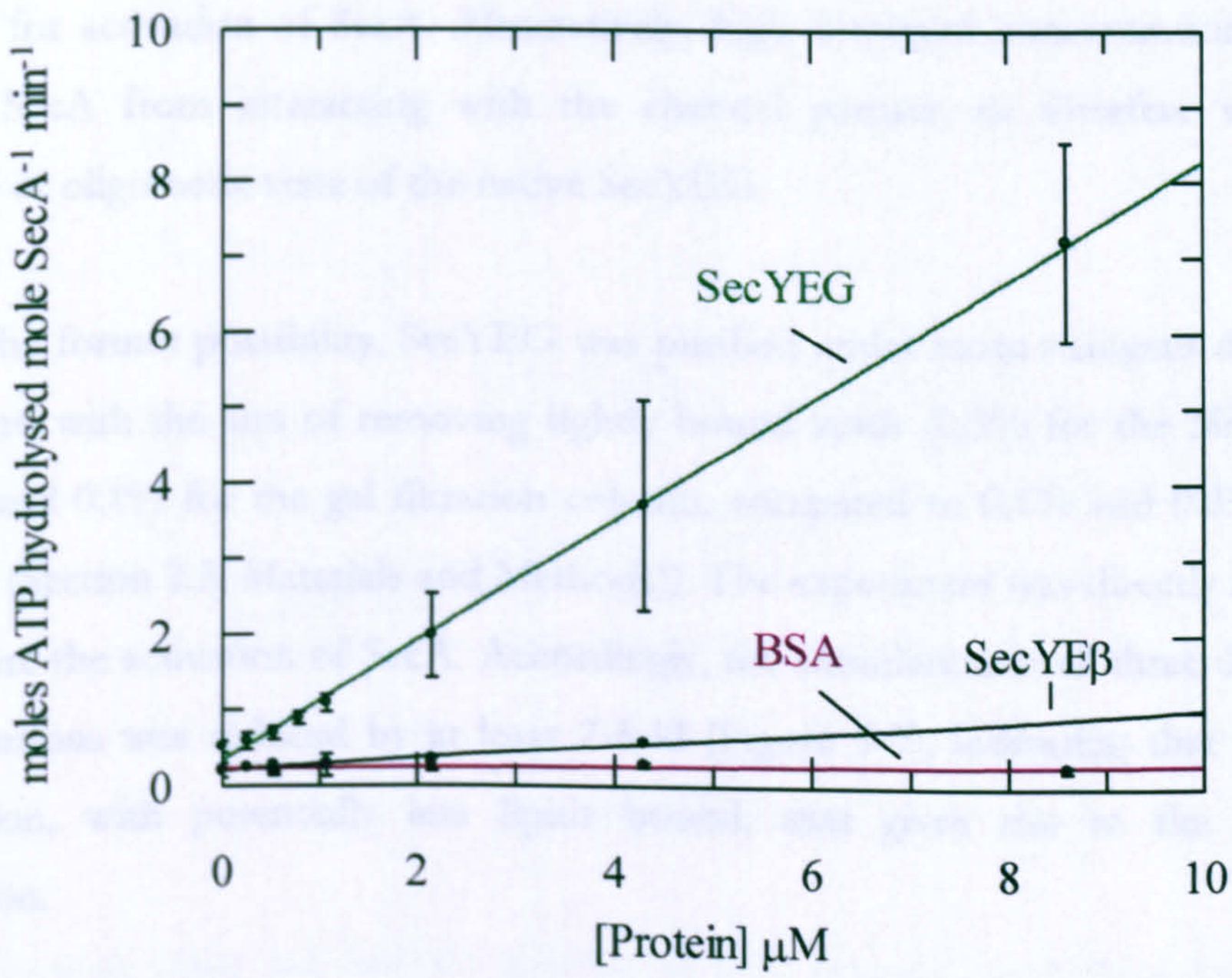

Figure 5-1. Solubilised SecYEG results in a strong stimulation of SecA ATPase activity, via a weak interaction.

The ATPase activity of SecA (0.3 μM) was measured in the presence of 1 mM ATP in TKM buffer with 0.1% $C_{12}E_9$ and increasing concentrations of solubilised SecYEG (green trace). A titration of BSA (purple trace) and *M. jannaschii* SecYEβ (black trace) is shown as a control. Error bars represent SD from 3 replicates.

5.1.2 The stimulatory effect of SecYEG on SecA is diminished by increasing concentrations of $C_{12}E_9$

The assay was then repeated, with different background concentrations of $C_{12}E_9$; 0.03% and 0.5% (Figure 5-2). It is thought that the SecYEG complex has lipid molecules specifically and permanently bound, even when solubilised in detergent (F. Duong and I. Collinson, unpublished results). These studies were also inspired by our observations in relation to the activation of the ATPase activity of SecA by CL in solution (Section 3.4.2.2). Thus, it was predicted that increasing concentrations of detergent would extract more of these bound lipids, and this effect could be rationalised with respect to the ATPase activity.

Clearly, higher concentrations of $C_{12}E_9$ reduce the magnitude of the activation by SecYEG. There are several explanations for this observation. Higher detergent concentrations might displace specific lipids from the SecYEG complex that are required for activation of SecA. Alternatively, high detergent concentrations could prevent SecA from interacting with the channel partner, or interfere with the structure or oligomeric state of the native SecYEG.

To test the former possibility, SecYEG was purified under more stringent detergent conditions, with the aim of removing tightly bound lipids (0.5% for the Ni^{2+}-affiity column and 0.1% for the gel filtration column, compared to 0.1% and 0.05% used formerly (Section 2.3, Materials and Methods)). The experiment was directly repeated to measure the activation of SecA. Accordingly, the stimulation at all three detergent concentrations was reduced by at least 2-fold (Figure 5-2), indicating that the new preparation, with potentially less lipids bound, that gives rise to the reduced stimulation.

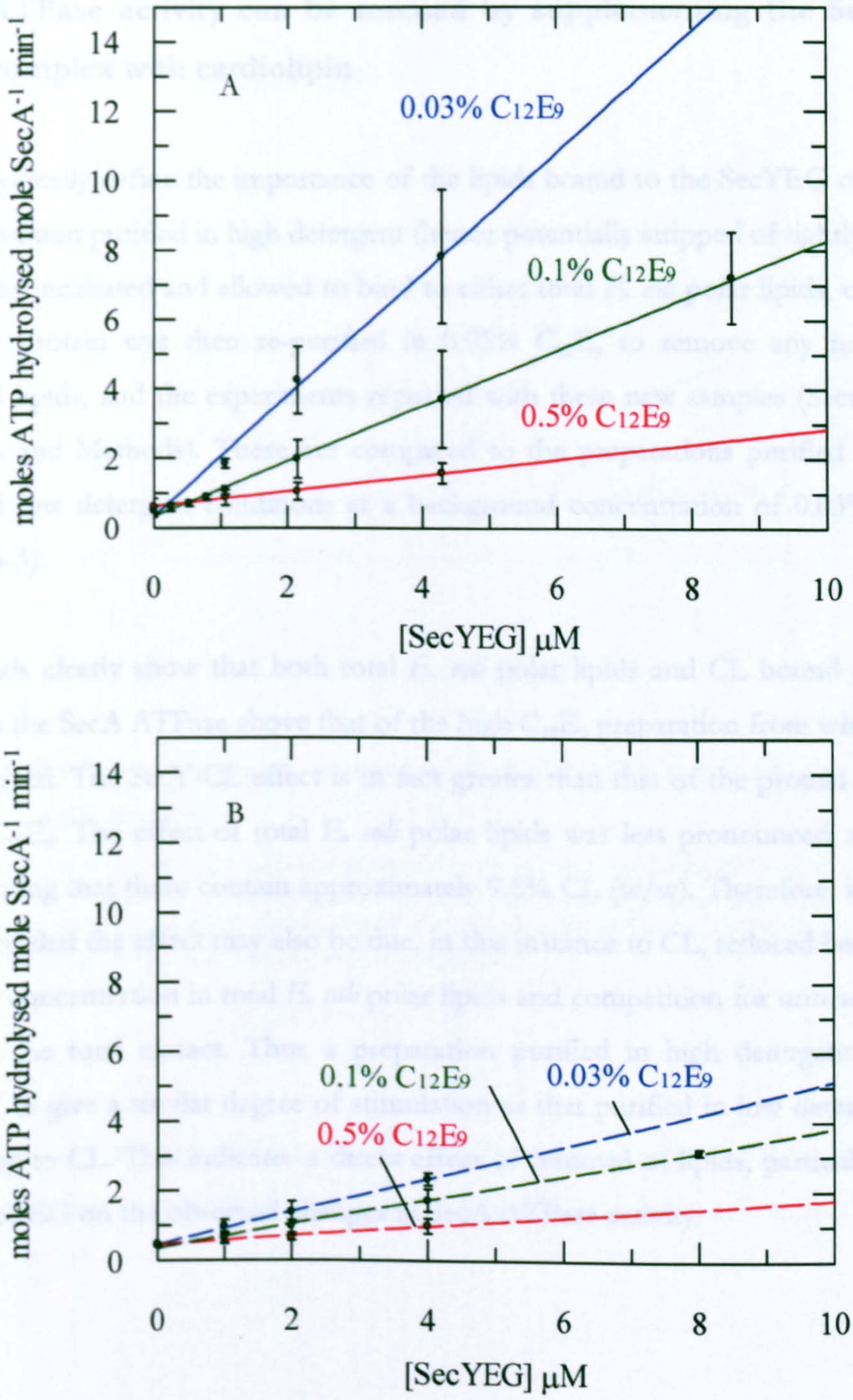

Figure 5-2. Both $C_{12}E_9$ and SecYEG purified in high detergent conditions reduces the activation of SecA

(A) The ATPase activity of SecA (0.3 μM) was measured in the presence of 1 mM ATP in TKM buffer with increasing concentrations of solubilised SecYEG purified in low (0.05%) detergent, at 0.03% $C_{12}E_9$ (blue trace) and 0.5% $C_{12}E_9$ (red trace). This is compared to previous data at 0.1% $C_{12}E_9$ (green trace). Error bars represent SD from 2-3 replicates.

(B) The experiment was repeated with SecYEG purified in high (0.1%) detergent. Error bars represent SD from 2 replicates.

5.1.3 ATPase activity can be rescued by supplementing the SecYEG complex with cardiolipin

To categorically define the importance of the lipids bound to the SecYEG complex, the preparation purified in high detergent (hence potentially stripped of tightly bound lipids) was incubated and allowed to bind to either total *E. coli* polar lipids, or *E. coli* CL. The protein was then re-purified in 0.05% $C_{12}E_9$ to remove any remaining unbound lipids, and the experiments repeated with these new samples (Section 2.3, Materials and Methods). These are compared to the preparations purified in both high and low detergent conditions at a background concentration of 0.03% $C_{12}E_9$ (Figure 5-3).

The trends clearly show that both total *E. coli* polar lipids and CL bound to SecY increases the SecA ATPase above that of the high $C_{12}E_9$ preparation from which they were derived. The SecY-CL effect is in fact greater than that of the protein purified in low $C_{12}E_9$. The effect of total *E. coli* polar lipids was less pronounced, and it is worth noting that these contain approximately 9.8% CL (w/w). Therefore, it can be concluded that the effect may also be due, in this instance to CL, reduced because of its lower concentration in total *E. coli* polar lipids and competition for non-activating lipids in the total extract. Thus a preparation purified in high detergent can be 'rescued' to give a similar degree of stimulation as that purified in low detergent, by re-binding to CL. This indicates a direct effect of removal of lipids, particularly CL, from SecYEG on the observed changes in SecA ATPase activity.

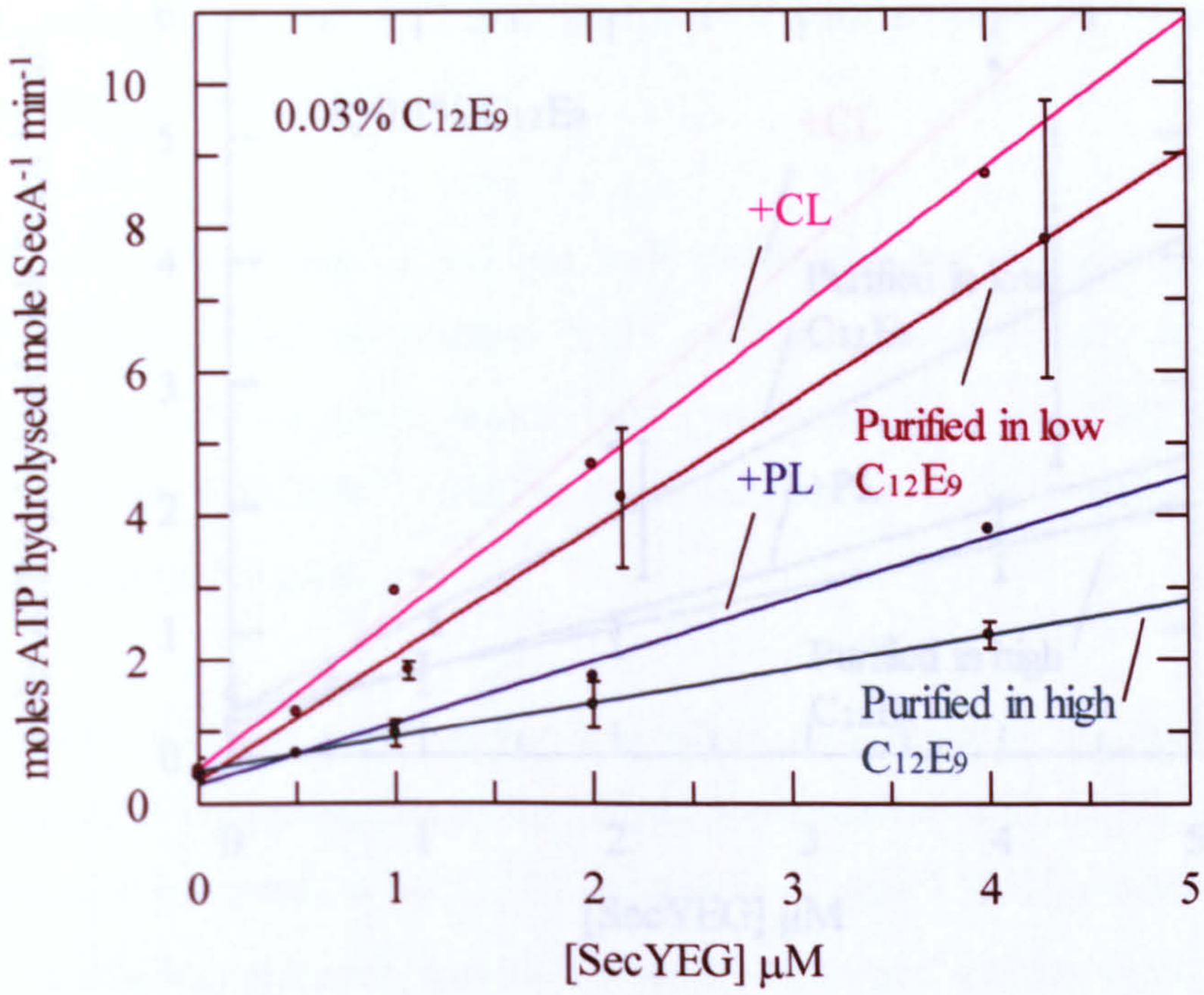

Figure 5-3. Cardiolipin rescues the stimulatory effect of SecYEG that has been previously depleted of tightly bound lipids.

The ATPase activity of SecA (0.3 μM) was measured in the presence of 1 mM ATP in TKM buffer at 0.03% $C_{12}E_9$ with increasing concentrations of SecYEG purified in high $C_{12}E_9$ (teal trace), low $C_{12}E_9$ (maroon trace) and high $C_{12}E_9$ re-supplemented with *E. coli* polar lipids (PL) (navy trace) and *E. coli* CL (pink trace). Error bars represent SD from 2-3 replicates.

The experiment was then repeated in the presence of 0.1% and 0.5% $C_{12}E_9$, and as expected the degree of activation was reduced at higher concentrations of detergent (Figure 5-4).

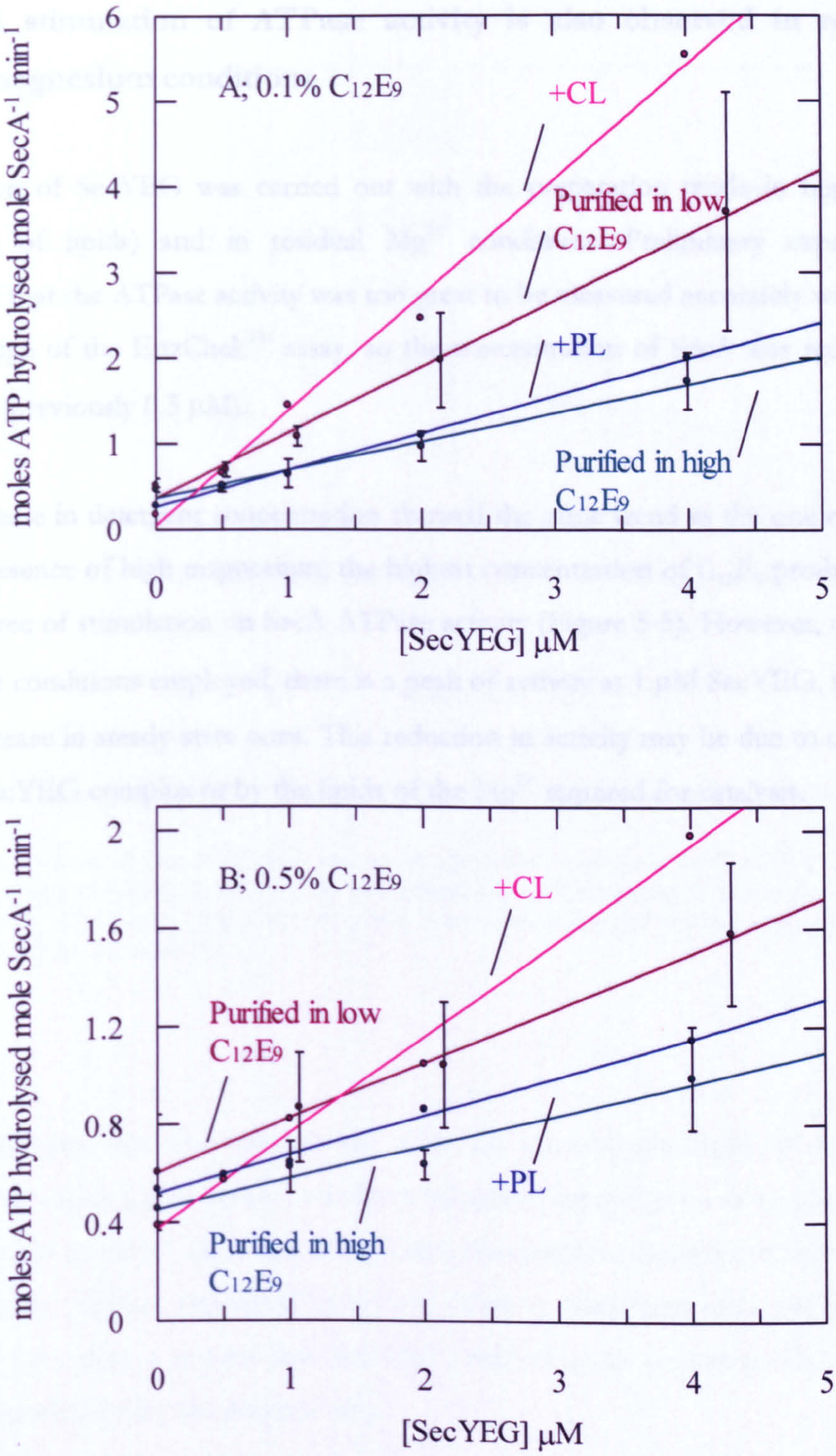

Figure 5-4. The stimulation of the ATPase activity at high and low concentrations of $C_{12}E_9$.

(A) The ATPase activity of SecA (0.3 μM) was measured in the presence of 1 mM ATP in TKM buffer at 0.1% $C_{12}E_9$ with increasing concentrations of SecYEG, purified in high (0.1%) $C_{12}E_9$ (teal trace), low (0.05%) $C_{12}E_9$ (maroon trace) and high $C_{12}E_9$ re-supplemented with *E. coli* polar lipids (PL) (navy trace) and *E. coli* CL (pink trace). Error bars represent SD from 2-3 replicates.
(B) The experiment was repeated at 0.5% $C_{12}E_9$.

5.1.4 A stimulation of ATPase activity is also observed in residual magnesium conditions

A titration of SecYEG was carried out with the preparation made in high $C_{12}E_9$ (stripped of lipids) and in residual Mg^{2+} conditions. Preliminary experiments indicated that the ATPase activity was too great to be measured accurately within the linear range of the EnzChek™ assay, so the concentration of SecA was reduced to 0.05 μM (previously 0.3 μM).

The increase in detergent concentration showed the same trend as the one observed in the presence of high magnesium; the highest concentration of $C_{12}E_9$ produced the least degree of stimulation on SecA ATPase activity (Figure 5-5). However, under all detergent conditions employed, there is a peak of activity at 1 μM SecYEG, followed by a decrease in steady-state rates. This reduction in activity may be due to chelation by the SecYEG complex or by the lipids of the Mg^{2+} required for catalysis.

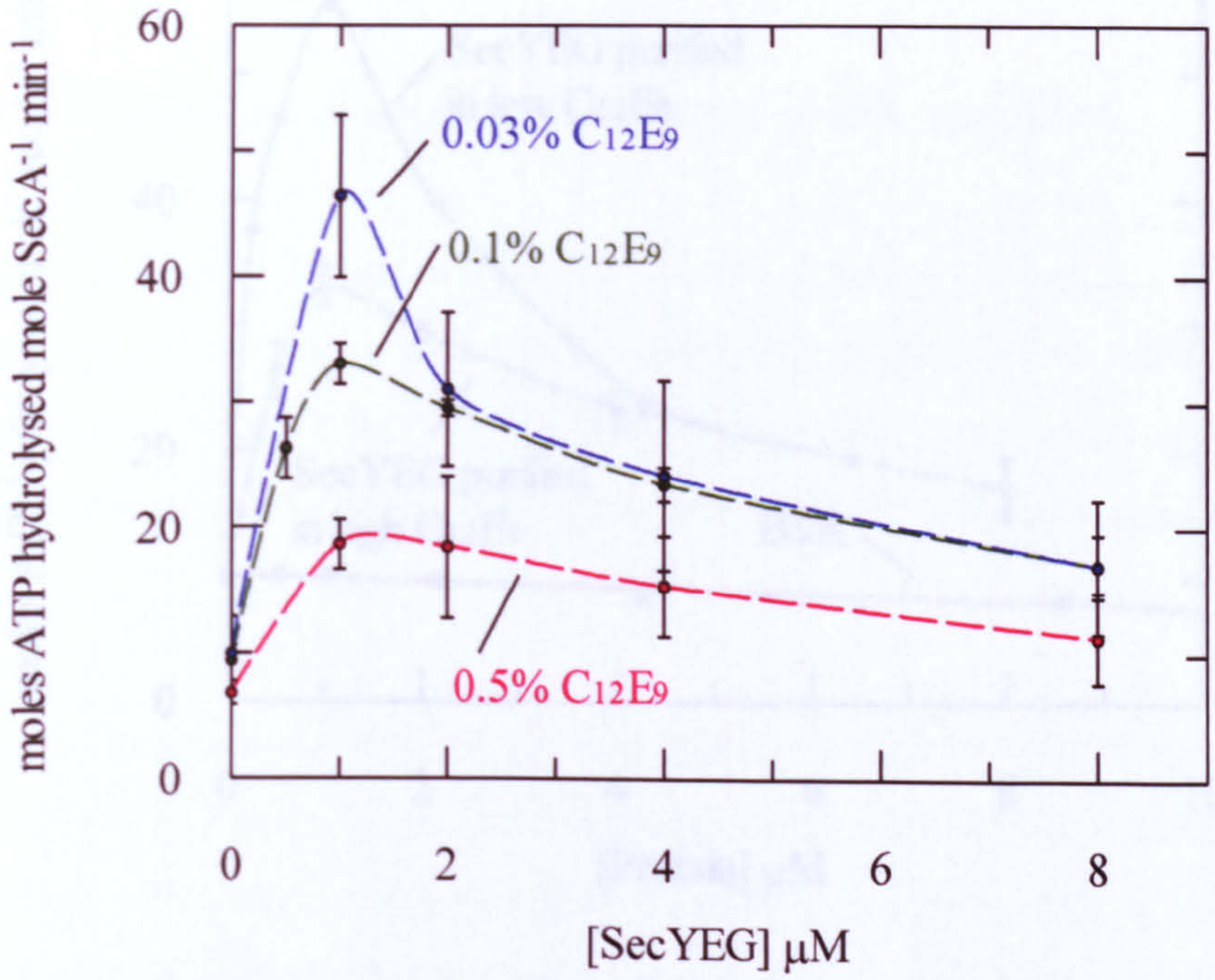

Figure 5-5. $C_{12}E_9$ reduces the activation of SecA by SecYEG in residual concentrations of magnesium.

The ATPase activity of SecA (0.05 μM) was measured in the presence of 1 mM ATP in TK buffer with increasing concentrations of SecYEG purified in high (0.1%) detergent, at 0.03% $C_{12}E_9$ (blue dashed trace), 0.1% $C_{12}E_9$ (green dashed trace) and 0.5% $C_{12}E_9$ (red dashed trace). Error bars represent SD from 2-3 replicates.

An experiment was also carried out with the preparation made in low $C_{12}E_9$ conditions, which again showed an increased effect compared to that made in high detergent. As a control, BSA was titrated into the reaction and also showed a gradual reduction in ATPase activity (Figure 5-6). This is consistent with the idea that proteins can act as a general sink for Mg^{2+}, depleting the concentration such that there is insufficient for the catalytic site.

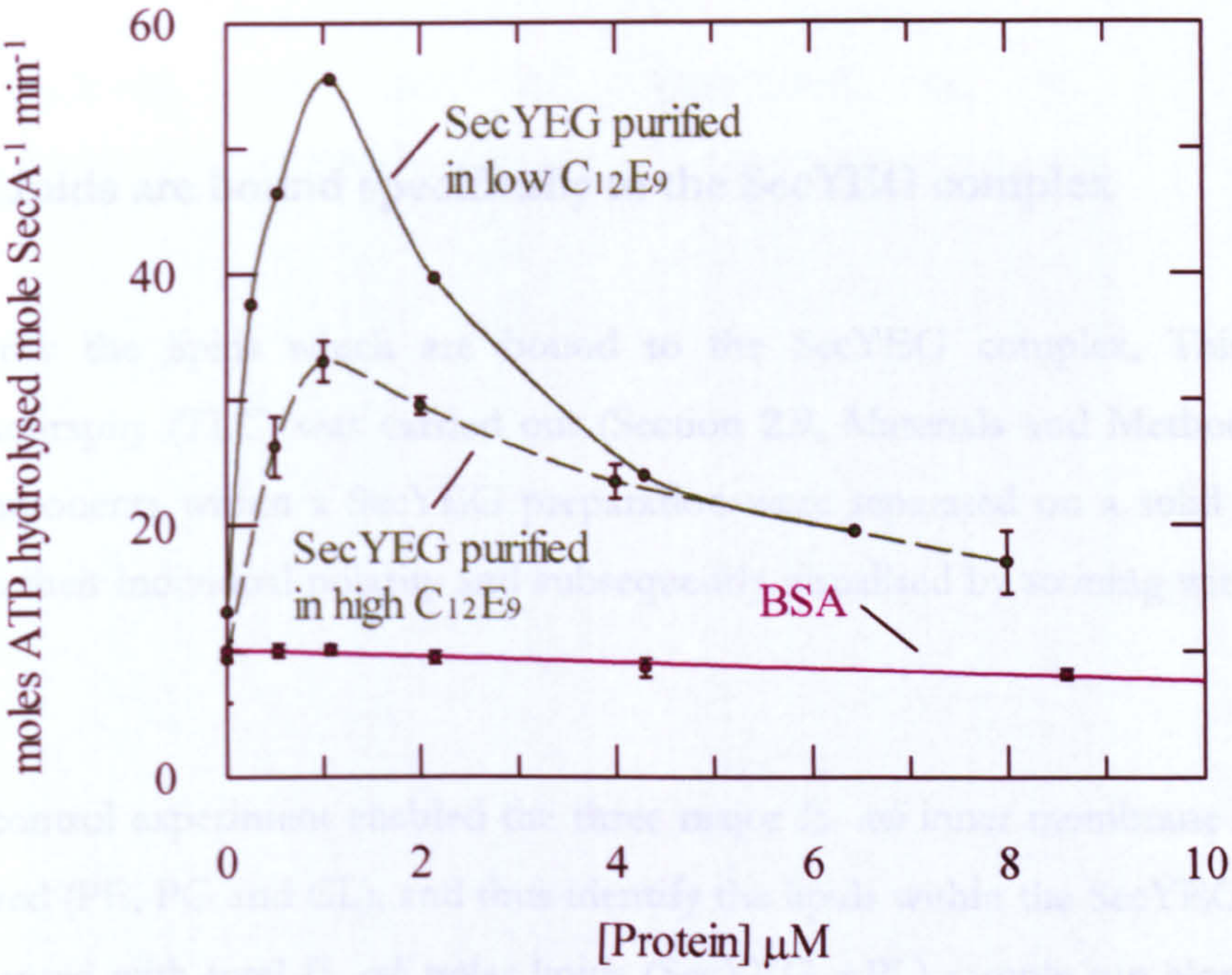

Figure 5-6. SecYEG purified in high detergent conditions reduces the activation of SecA in residual concentrations of magnesium.

The ATPase activity of SecA (0.05 μM) was measured in the presence of 1 mM ATP in TK buffer with 0.1% $C_{12}E_9$ and increasing concentrations of SecYEG purified in high (0.1%) detergent (green dashed trace) and low (0.05%) detergent (green solid trace). A titration of BSA under the same conditions is shown as a control. Error bars represent SD from 2-3 replicates.

5.1.5 Lipids are bound specifically to the SecYEG complex

To identify the lipids which are bound to the SecYEG complex, Thin Layer Chromatography (TLC) was carried out (Section 2.9, Materials and Methods). The lipid components within a SecYEG preparation were separated on a solid support based on their individual polarity and subsequently visualised by staining with iodine vapour.

First, a control experiment enabled the three major *E. coli* inner membrane lipids to be resolved (PE, PG and CL), and thus identify the lipids within the SecYEG sample supplemented with total *E. coli* polar lipids (SecYEG +PL) sample run alongside it. This could then be used to distinguish the lipids within the other samples of SecYEG that had been either supplemented or depleted of lipids.

The sample supplemented with total *E. coli* phospholipids (SecYEG +PL) contained mostly PE and CL, with little or no PG visible at this concentration (Figure 5-8; left panel). Polar lipids contain 58% PE, 15% PG and 10% CL, indicating a preference of SecYEG for the latter. Comparing the SecYEG preparation depleted in lipids (High $C_{12}E_9$; right panel) and the one supplemented with CL indicates that this lipid has bound to the SecYEG complex. It also shows that the preparation washed in high detergent retains a fraction of the tightly bound lipids. The sample supplemented with total *E. coli* phospholipids has been enriched by CL and PE, indicating that PE can bind to the complex at the expense of CL (present in approximately 7-fold excess over the latter).

These findings help to explain the steady-state kinetics studies carried out with these supplemented preparations. Adding CL back to SecYEG results in the lipid binding to the protein, which now has a stronger stimulation on the SecA ATPase activity. Addition of total *E. coli* polar lipids to SecYEG has a lesser degree of stimulation because some of the lipid binding sites are occupied by PE, which do not confer the activation properties to SecYEG.

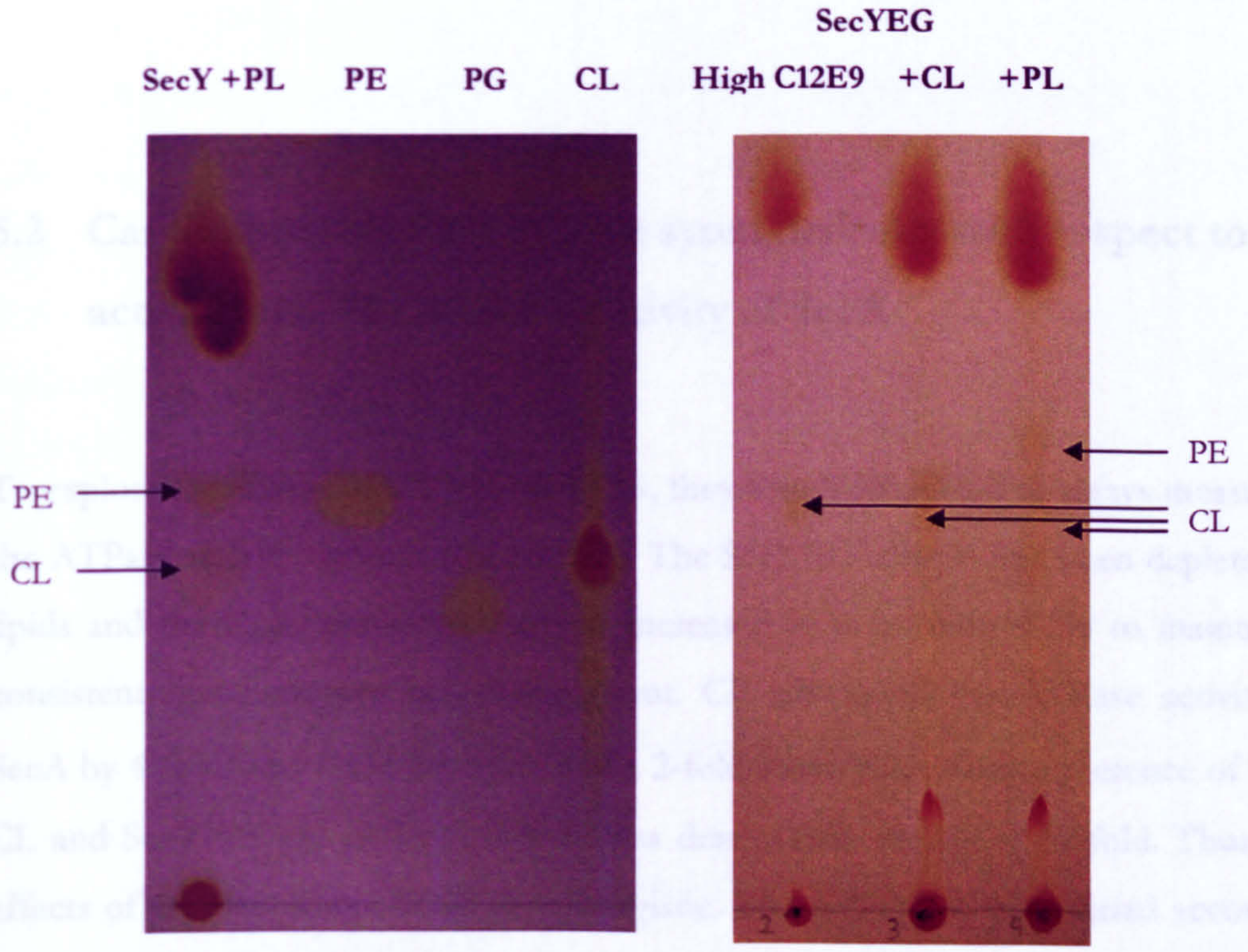

Figure 5-7. Thin Layer Chromatography reveals the lipid composition of various SecYEG preparations.

Left panel; 20 mg of *E. coli* PE, PG and CL were spotted onto the TLC plate, with a mobile phase composed of 70% (v/v) chloroform and 25% (v/v) methanol. The solvent was allowed to rise up the plate by capillary action in a chamber with a saturated solvent atmosphere, and was subsequently dried and stained with iodine vapour. This was compared to 40 μg SecYEG supplemented with total *E. coli* polar lipids (SecYEG +PL).

Right panel; SecYEG preparations (40 μg) purified in high concentrations of $C_{12}E_9$, and supplemented with CL (+CL) and total *E. coli* polar lipids (+PL) were separated in the same manner.

5.2 Cardiolipin and SecYEG act synergistically with respect to the activation of the ATPase activity of SecA

To explore the effects of CL and SecYEG, they were both added to assays measuring the ATPase activity of SecA (Figure 5-8). The SecYEG sample had been depleted of lipids and the $C_{12}E_9$ concentration was increased to a constant 0.1% to maintain a consistent lipid:detergent ratio throughout. CL stimulated the ATPase activity of SecA by 4-fold, and 1 μM SecYEG had a 2-fold stimulation. In the presence of both CL and SecYEG, the ATPase activity was dramatically increased 19-fold. Thus, the effects of the two components are synergistic. These data sets were fitted according to a ligand binding equation (Equation 2-6, Materials and Methods) to reveal $K_{d[SecA-CL]}$ and $K_{d[SecA-CL-SecYEG]}$ (Table 5-1). The K_d values are similar in the presence and absence of SecYEG, indicating that CL binds to SecA in the same manner and SecYEG is required to fully confer its stimulatory effect.

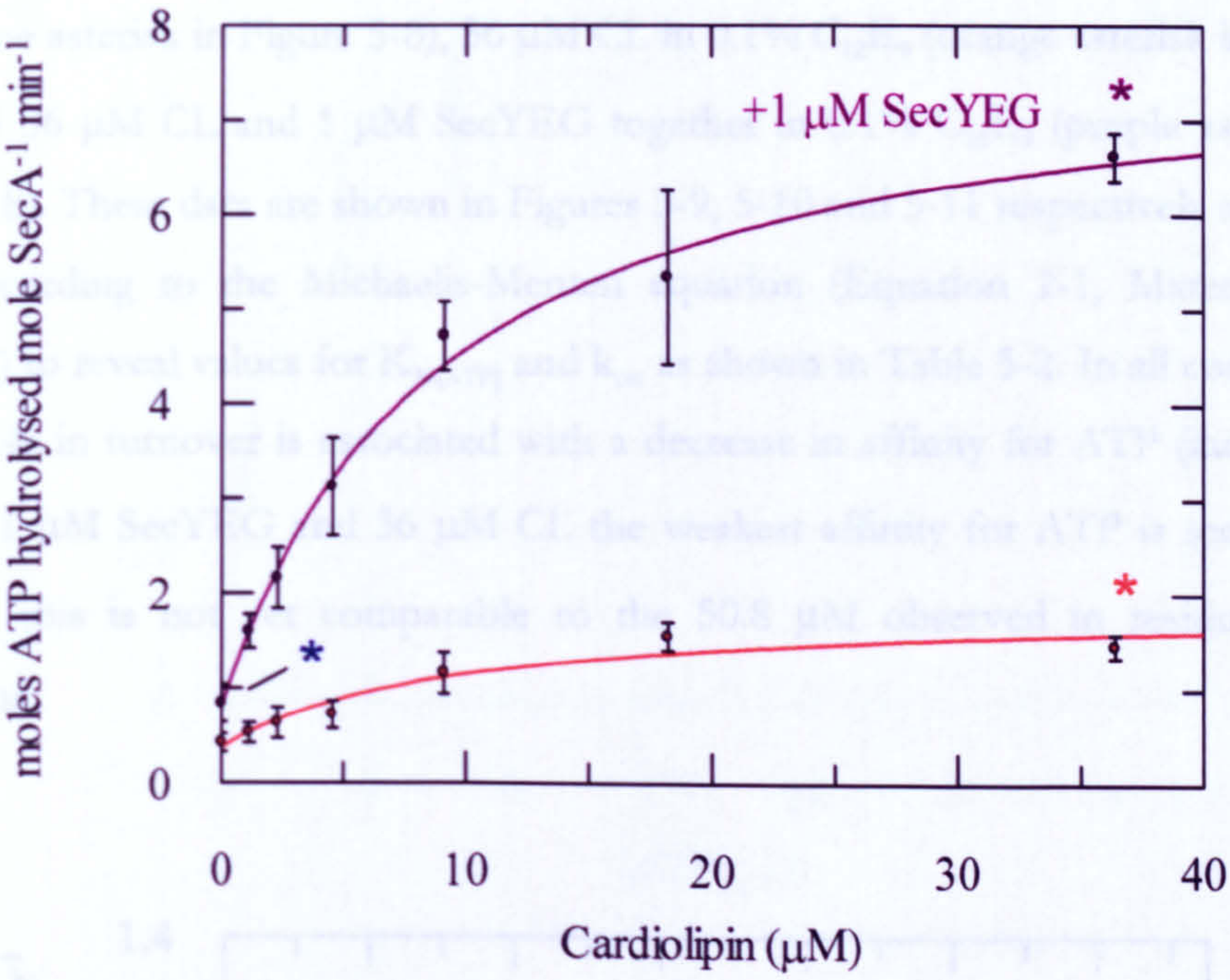

Figure 5-8. The effects of cardiolipin and SecYEG are synergistic with regard to the activation of the ATPase activity of SecA.

The ATPase activity of SecA (0.3 μM) was measured in the presence of 1 mM ATP in TKM buffer with 0.1% $C_{12}E_9$ and increasing concentrations of CL (orange trace), and in the same conditions plus 1 μM SecYEG (purple trace). These data sets were fitted according to a ligand binding equation (Equation 2-6, Materials and Methods) and calculated K_d values are shown in Table 5-1. Error bars represent SD from 3-4 replicates. The asterisks denote conditions used to redefine the Michaelis-Menten parameters (Figures 5-9, 5-10 and 5-11).

SecA	$K_{d\ [CL]}$ (μM)	k_{cat} (moles ATP mole $SecA^{-1}$ min^{-1})
+Mg^{2+}; in 0.1% $C_{12}E_9$	9.7 ± 5.7	1.53 ± 0.27
+Mg^{2+}; + 1μM SecYEG in 0.1% $C_{12}E_9$	9.0 ± 1.7	7.16 ± 0.39

Table 5-1. Calculated K_d values for cardiolipin to SecA in the presence of 2 mM magnesium, with and without SecYEG.

The data were collected according to Figure 5-8, and fitted to a ligand binding equation (Equation 2-6, Materials and Methods). SE from the fitting procedure is shown.

The Michaelis-Menten parameters were now redefined, at 1 μM SecYEG in 0.1% $C_{12}E_9$ (blue asterisk in Figure 5-8), 36 μM CL in 0.1% $C_{12}E_9$ (orange asterisk in Figure 5-8), and 36 μM CL and 1 μM SecYEG together in 0.1% $C_{12}E_9$ (purple asterisk in Figure 5-8). These data are shown in Figures 5-9, 5-10 and 5-11 respectively and were fitted according to the Michaelis-Menten equation (Equation 2-1, Materials and Methods) to reveal values for $K_{M[ATP]}$ and k_{cat} as shown in Table 5-2. In all conditions, an increase in turnover is associated with a decrease in affinity for ATP (increase in K_M). At 1 μM SecYEG and 36 μM CL the weakest affinity for ATP is seen at 3.9 μM, but this is not yet comparable to the 50.8 μM observed in residual Mg^{2+} conditions.

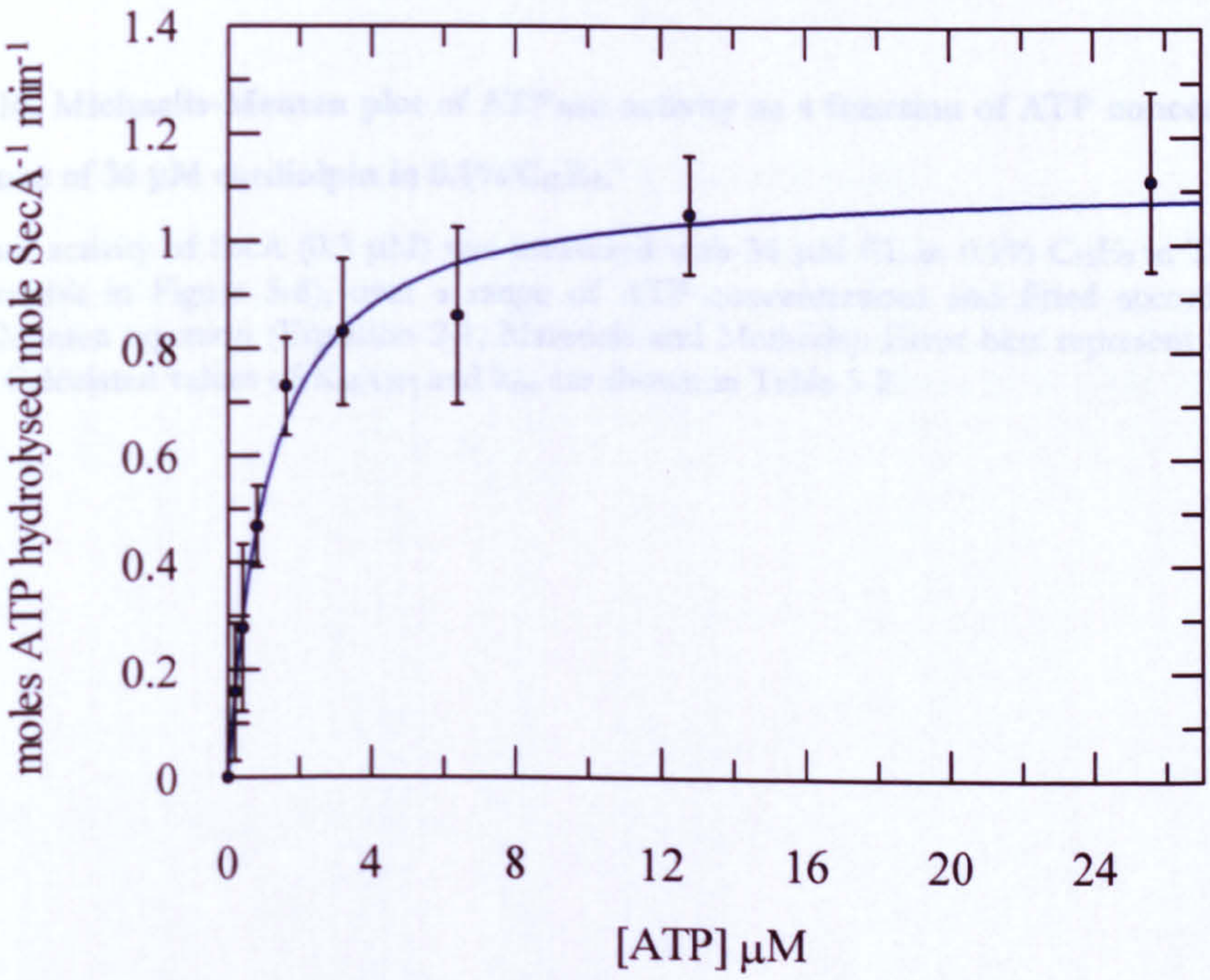

Figure 5-9. Michaelis-Menten plot of ATPase activity as a function of ATP concentration in the presence of 1 μM SecYEG in 0.1% $C_{12}E_9$.

The ATPase activity of SecA (0.3 μM) was measured with 1 μM SecYEG in 0.1% $C_{12}E_9$ in TKM buffer (blue asterisk in Figure 5-8), over a range of ATP concentrations and fitted according to the Michaelis-Menten equation (Equation 2-1, Materials and Methods). Error bars represent SD from 4 replicates. Calculated values of $K_{M[ATP]}$ and k_{cat} are shown in Table 5-2.

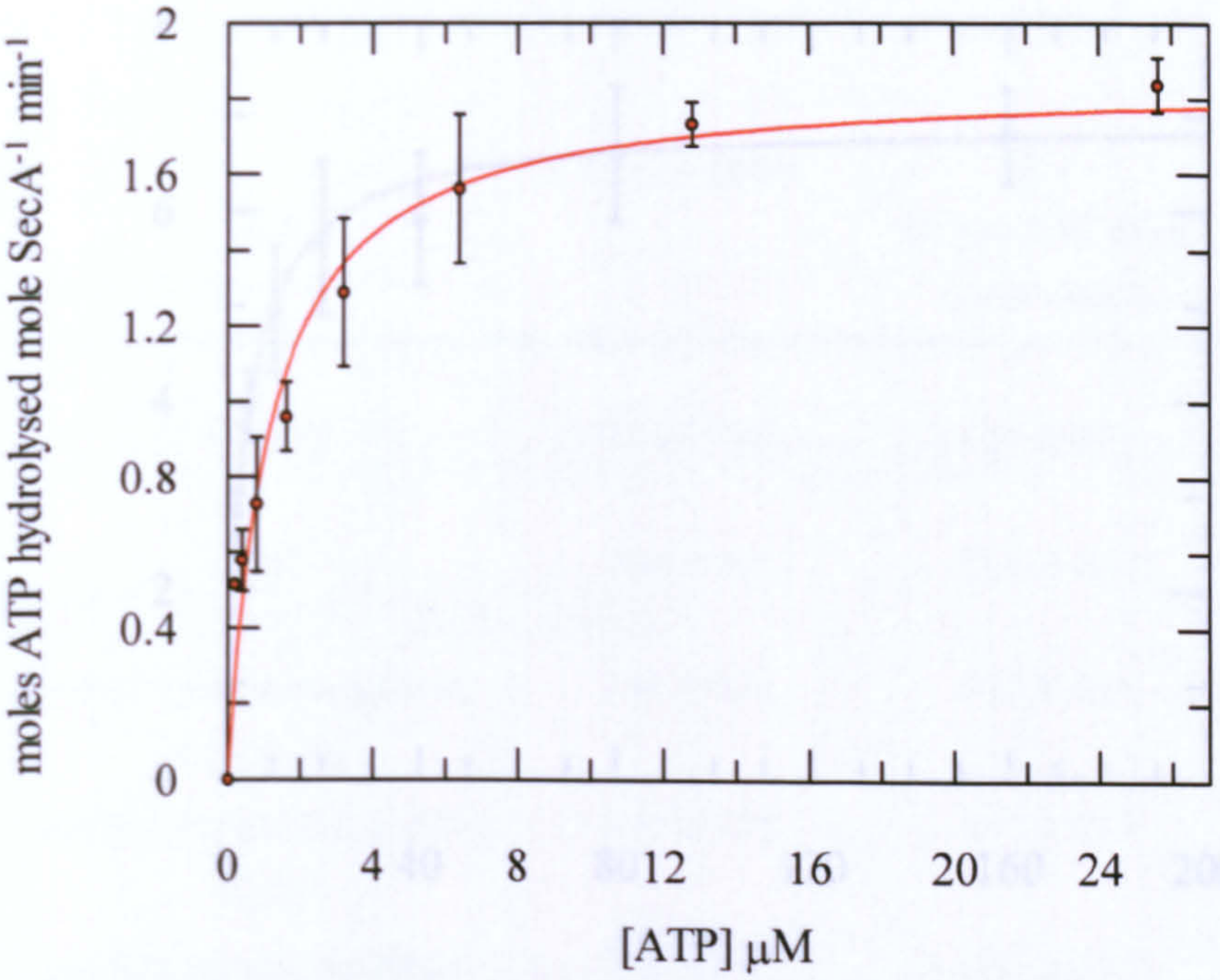

Figure 5-10. Michaelis-Menten plot of ATPase activity as a function of ATP concentration in the presence of 36 μM cardiolpin in 0.1% $C_{12}E_9$.

The ATPase activity of SecA (0.3 μM) was measured with 36 μM CL in 0.1% $C_{12}E_9$ in TKM buffer (orange asterisk in Figure 5-8), over a range of ATP concentrations and fitted according to the Michaelis-Menten equation (Equation 2-1, Materials and Methods). Error bars represent SD from 3 replicates. Calculated values of $K_{M[ATP]}$ and k_{cat} are shown in Table 5-2.

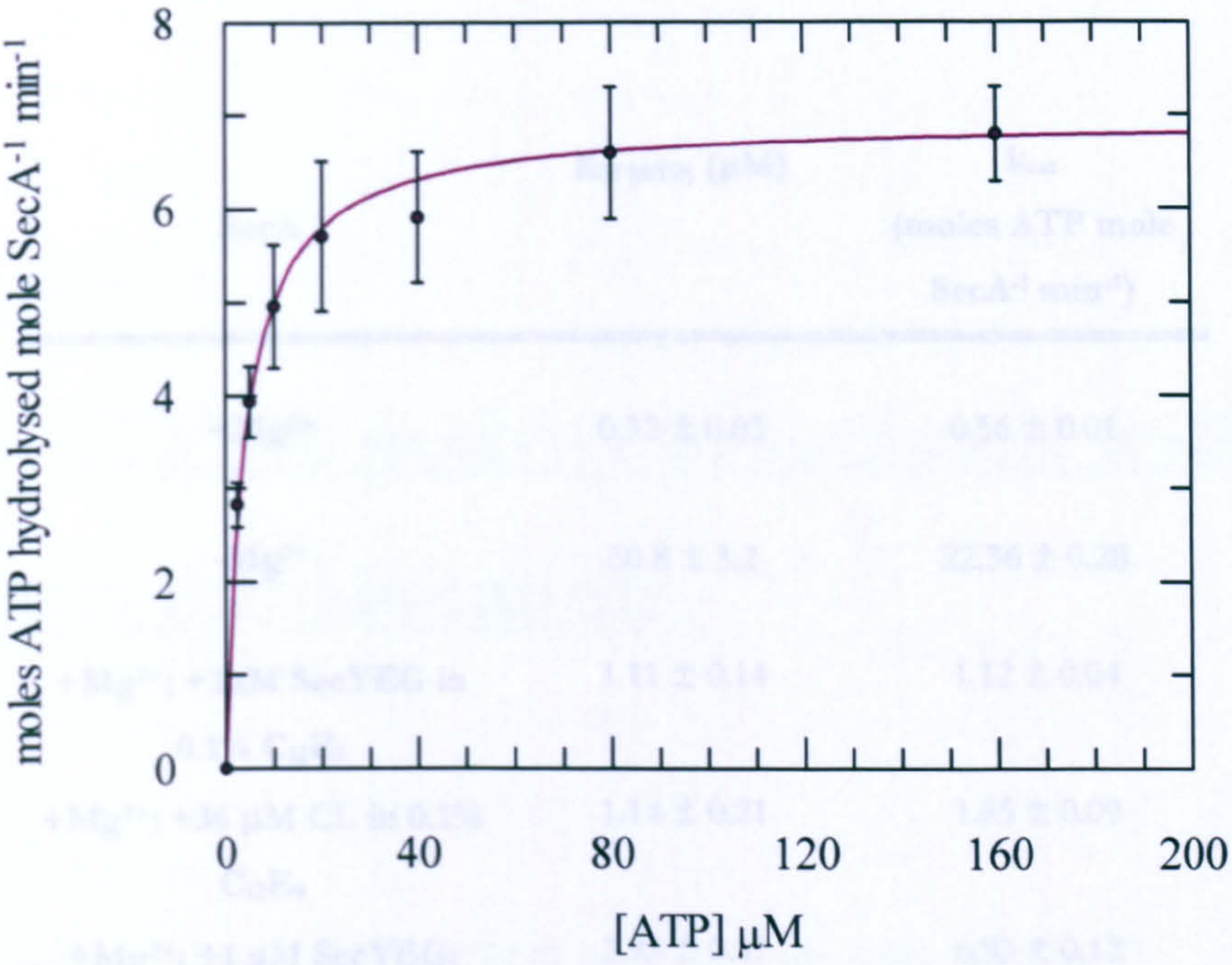

Figure 5-11. Michaelis-Menten plot of ATPase activity as a function of ATP concentration in the presence of 36 μM cardiolpin and 1 μM SecYEG in 0.1% $C_{12}E_9$.

The ATPase activity of SecA (0.3 μM) was measured with 36 μM CL and 1 μM SecYEG in 0.1% $C_{12}E_9$ in TKM buffer (purple asterisk in Figure 5-8), over a range of ATP concentrations and fitted according to the Michaelis-Menten equation (Equation 2-1, Materials and Methods). Error bars represent SD from 4 replicates. Calculated values of $K_{M[ATP]}$ and k_{cat} are shown in Table 5-2.

SecA	$K_{M\ [ATP]}$ (μM)	k_{cat} (moles ATP mole SecA^{-1} min^{-1})
$+Mg^{2+}$	0.32 ± 0.03	0.56 ± 0.01
$-Mg^{2+}$	50.8 ± 3.2	22.36 ± 0.28
$+Mg^{2+}$; +1μM SecYEG in 0.1% $C_{12}E_9$	1.11 ± 0.14	1.12 ± 0.04
$+Mg^{2+}$; +36 μM CL in 0.1% $C_{12}E_9$	1.14 ± 0.21	1.85 ± 0.09
$+Mg^{2+}$; +1 μM SecYEG; + 36 μM CL in 0.1% $C_{12}E_9$	3.93 ± 0.37	6.93 ± 0.12

Table 5-2. Calculated values of the $K_{M[ATP]}$ for SecA in the presence of 1 μM SecYEG, 36 μM cardiolipin and both 1 μM SecYEG and 36 μM cardiolipin together, all in 0.1% $C_{12}E_9$.
These values are compared to the values in +/-Mg^{2+} conditions. The data were collected according to Figures 3-1, 3-2, 5-9, 5-10 and 5-11, and fitted to the Michaelis-Menten equation (Equation 2-1, Materials and Methods). SE from the fitting procedure is shown.

5.3 Chapter Summary

This chapter describes the stimulatory effects of the SecYEG complex on the SecA ATPase activity when solubilised in detergent $C_{12}E_9$, and demonstrates how this is related to the lipids bound. Thin layer chromatography showed that lipids are still bound to SecYEG even when washed in high detergent, and that incubation with lipids results in an association with the complex with an corresponding increased stimulatory effect upon SecA. The stimulation mediated by cardiolipin was investigated further by steady-state assays, and in conjunction with SecYEG is shown to propagate a synergistic stimulation of ATPase activity.

Chapter 6

The ATPase activity associated with protein translocation

6.1 Reconstitution of SecYEG into *E. coli* polar lipids

SecYEG was reconstituted into phospholipid liposomes containing total *E. coli* polar lipids (Section 2.4, Materials and Methods). The same protocol was also carried out in the absence of protein, to create empty liposomes for use as a negative control. All of these experiments were performed in the presence of 2 mM Mg^{2+}, to mimic physiological conditions.

6.1.1 SecYEG proteoliposomes completely counteract magnesium inhibition of the ATPase activity of SecA

Increasing concentrations of total *E. coli* liposomes with and without SecYEG were titrated into a standard kinetic assay (Figure 6-1). The latter shows an increase in ATPase activity up to 1.2 mM polar lipids, but this is enhanced by a factor of 5 in the presence of 1 μM SecYEG. The data were fitted to a ligand-binding equation (Equation 2-6, Materials and Methods) to reveal K_d values for SecA binding to liposomes in the presence and absence of SecYEG. The k_{cat} in the presence of SecYEG proteoliposomes is comparable to that found in residual Mg^{2+} conditions (Table 6-1).

The data show that SecA binds to the empty liposomes 2-fold weaker than in the presence of SecYEG, the latter which results in a 50-fold stimulation (compared to SecA alone with 2 mM Mg^{2+}). This indicates a specific effect of SecYEG on promoting increased ATP turnover by SecA, which is able to saturate the reaction. This could be related to the way in which both the lipids and SecYEG are presented to SecA, that is, in the native-like state of the membrane bilayer.

Assuming that the SecYEG complex inserts equally into the membrane in both orientations, only half of it will be orientated with the cytoplasmic face presenting outwards and thus be available to interact with SecA. Therefore, the maximum concentration of active SecYEG is probably 0.5 μM.

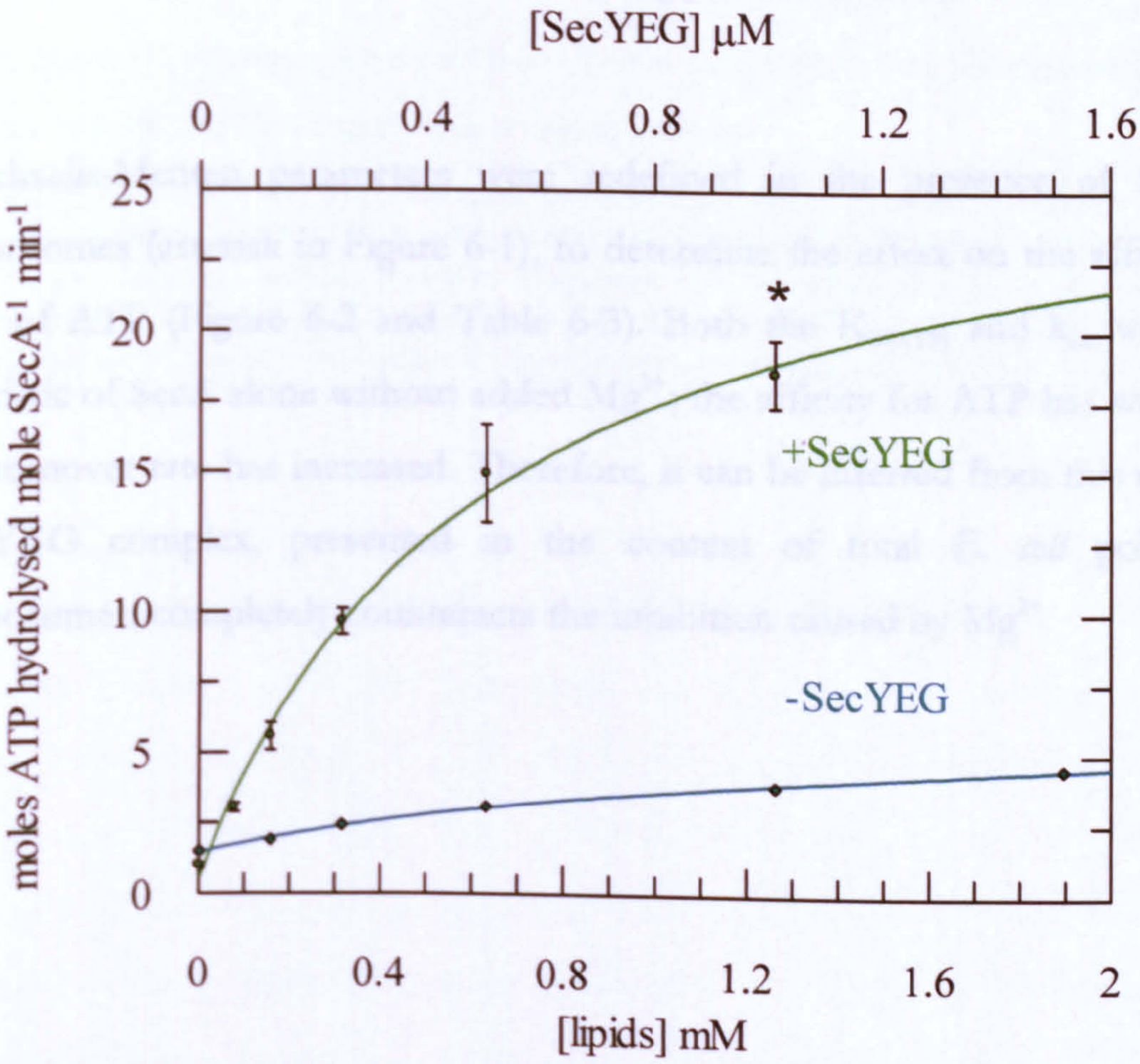

Figure 6-1. SecYEG reconstituted into liposomes has a pronounced stimulatory effect on the ATPase activity of SecA.

The ATPase activity of SecA (0.3 μM) was measured in the presence of 1 mM ATP in TKM buffer with increasing concentrations of SecYEG reconstituted into liposomes (green trace) and empty liposomes (blue trace). The concentration of active SecYEG orientated correctly is approximately half of that shown on the upper *x* axis. The data were fitted according to a ligand binding equation (Equation 2-6, Materials and Methods) and calculated K_d values are shown in Table 6-1. Error bars represent SD from 3 replicates. The asterisk denotes conditions used to redefine the Michaelis-Menten parameters (Figure 6-2).

SecA	$K_{d[liposomes]}$ (mM)	k_{cat} (moles ATP mole SecA^{-1} min^{-1})
+Mg^{2+}; empty total *E. coli* polar lipid liposomes	1.57 ± 0.29	5.47 ± 0.47
+Mg^{2+}; SecYEG in total *E. coli* polar lipid proteoliposomes	0.65 ± 0.14	27.85 ± 2.38

Table 6-1. Calculated K_d values for SecA to empty liposomes, and to proteoliposomes containing reconstituted SecYEG.

The data were collected according to Figures 6-1 and 6-2, and fitted to a ligand binding equation (Equation 2-6, Materials and Methods). SE from the fitting procedure is shown.

The Michaelis-Menten parameters were redefined in the presence of SecYEG proteoliposomes (asterisk in Figure 6-1), to determine the effect on the affinity and turnover of ATP (Figure 6-2 and Table 6-3). Both the $K_{M[ATP]}$ and k_{cat} were now characteristic of SecA alone without added Mg^{2+}; the affinity for ATP has weakened, and the turnover rate has increased. Therefore, it can be inferred from this data that the SecYEG complex, presented in the context of total *E. coli* polar lipid proteoliposomes, completely counteracts the inhibition caused by Mg^{2+}.

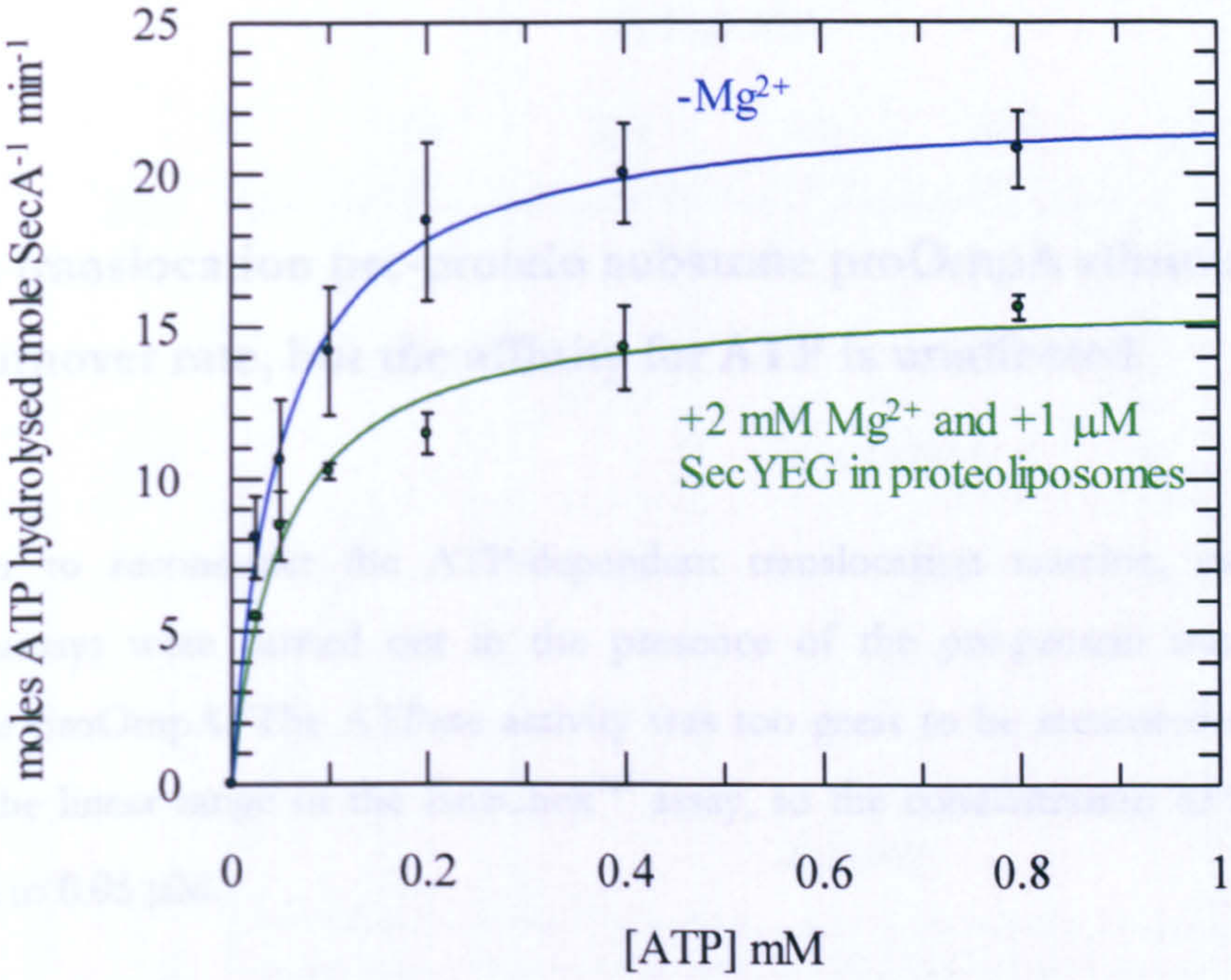

Figure 6-2. Michaelis-Menten plot of ATPase activity as a function of ATP concentration in the presence of 1 μM SecYEG reconstituted into liposomes.

The ATPase activity of SecA (0.3 μM) was measured with 1 μM SecYEG reconstituted into liposomes in TKM buffer (asterisk in Figure 6-1), over a range of ATP concentrations (green trace) and fitted according to the Michaelis-Menten equation (Equation 2-1, Materials and Methods). Error bars represent SD from 3 replicates. This is compared to the data obtained for SecA alone in residual Mg^{2+} conditions (blue trace) (Figure 3-2). Calculated values of $K_{M[ATP]}$ and k_{cat} are shown in Table 6-3.

6.2 A translocation pre-protein substrate proOmpA stimulates the turnover rate, but the affinity for ATP is unaffected

In order to reconstruct the ATP-dependent translocation reaction, steady-state kinetic assays were carried out in the presence of the pre-protein translocation substrate proOmpA. The ATPase activity was too great to be measured accurately within the linear range of the EnzChek™ assay, so the concentration of SecA was reduced to 0.05 μM.

ProOmpA is the classical SecA-dependent substrate used in most of the functional studies in the literature. The construct used in these experiments is 235 amino acid residues in length, and has been shown to be successfully translocated *in vitro* (Osborne and Rapoport, 2007). In order for translocation to occur, the pre-protein must be presented in an unfolded state, maintained by either a chaperone (SecB), or a denaturant (urea) to maintain a translocation competent conformation (Lecker et al., 1990).

Increasing concentrations of proOmpA (unfolded in 6 M urea) were titrated into the assay in the presence of 1 μM (effectively 0.5 μM) SecYEG reconstituted into liposomes (asterisk in Figure 6-1; shown in Figure 6-3). This shows a dramatic stimulation of ATPase activity, the turnover rate is now 1000-fold faster than observed for SecA alone in the presence of 2 mM Mg^{2+}. The data were fitted according to a ligand binding equation (Equation 2-7, Materials and Methods) and the calculated $K_{d[SecA\text{-}proOmpA;\ E.\ coli\ polar\ lipid\ proteoliposomes]}$ is shown in Table 6-2. This indicates a very tight binding of SecA to proOmpA in these conditions, in the low nanomolar range. Importantly, urea did not effect the stimulation of ATPase activity in the conditions employed (up to 250 mM).

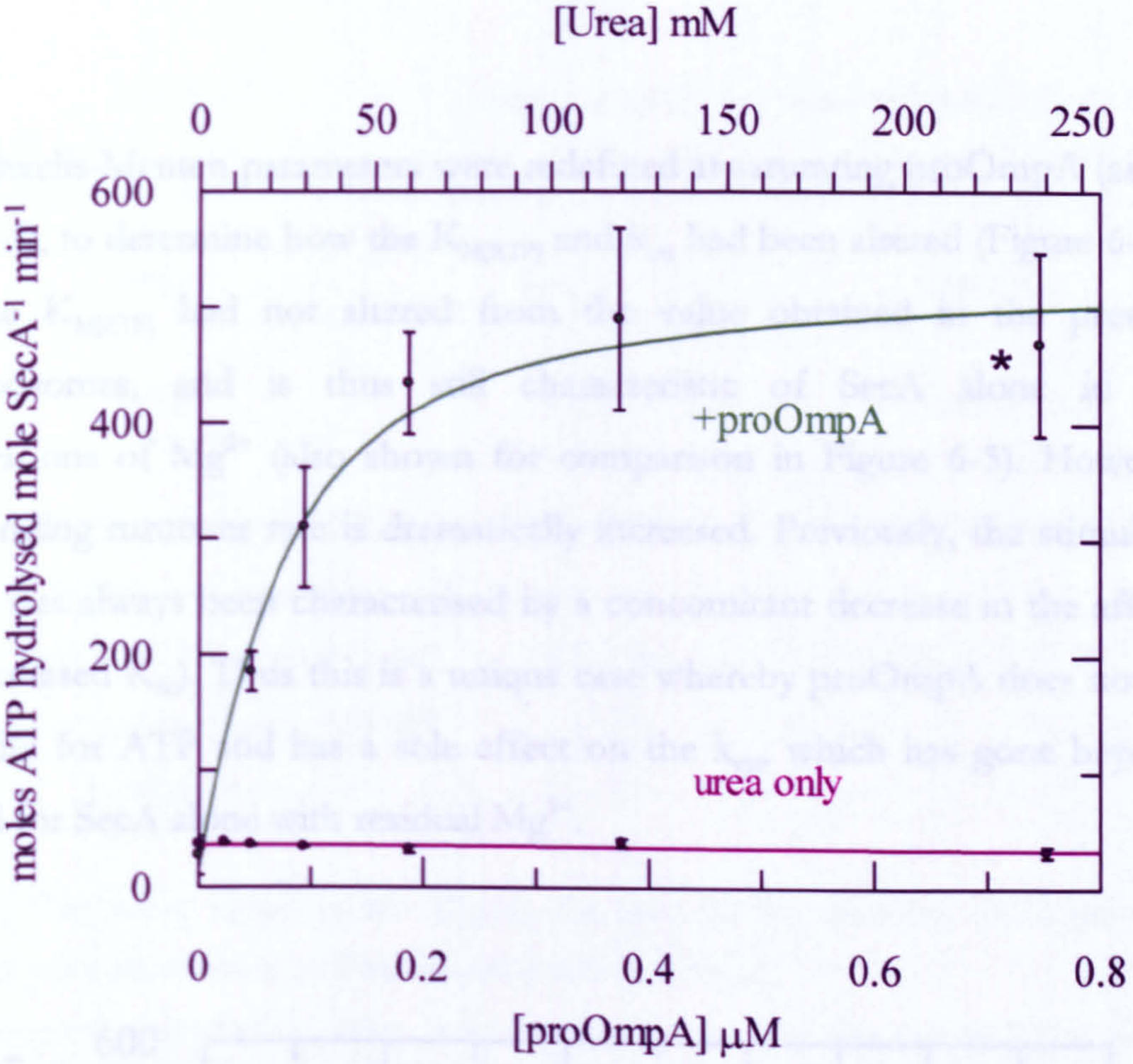

Figure 6-3. proOmpA stimulates the ATPase activity of SecA in the context of membrane bound SecYEG.

The ATPase activity of SecA (0.05 μM) was measured in the presence of 1 mM ATP in TKM buffer with 1 μM SecYEG reconstituted into liposomes, and increasing concentrations of proOmpA (green trace). This is compared to a control experiment in the same conditions where urea was titrated into the reaction, in the absence of proOmpA (purple trace). The proOmpA data sets were fitted according to a ligand binding equation (Equation 2-7, Materials and Methods) and the calculated K_d value is shown in Table 6-2. Error bars represent SD from 2-6 replicates. The asterisk denotes conditions used to redefine the Michaelis-Menten parameters (Figure 6-4).

SecA	$K_{d\ [proOmpA]}$ (μM)	k_{cat} (moles ATP hydrolysed mole $SecA^{-1}$ min^{-1})
+Mg^{2+}; 1 μM SecYEG in total *E. coli* polar lipid proteoliposomes	0.047 ± 0.017	514.28 ± 41.18

Table 6-2. Calculated K_d value for SecA to proOmpA in the presence of SecYEG reconstituted into *E. coli* polar lipid liposomes.

The data were collected according to Figure 6-4, and fitted to a ligand binding equation (Equation 2-7, Materials and Methods). SE from the fitting procedure is shown.

The Michaelis-Menten parameters were redefined at saturating proOmpA (asterisk in Figure 6-4), to determine how the $K_{M[ATP]}$ and k_{cat} had been altered (Figure 6-5; Table 6-3). The $K_{M[ATP]}$ had not altered from the value obtained in the presence of proteoliposomes, and is thus still characteristic of SecA alone in residual concentrations of Mg^{2+} (also shown for comparison in Figure 6-5). However, the corresponding turnover rate is dramatically increased. Previously, the stimulation of turnover has always been characterised by a concomitant decrease in the affinity for ATP (increased K_M). Thus this is a unique case whereby proOmpA does not change the affinity for ATP and has a sole effect on the k_{cat}, which has gone beyond that observed for SecA alone with residual Mg^{2+}.

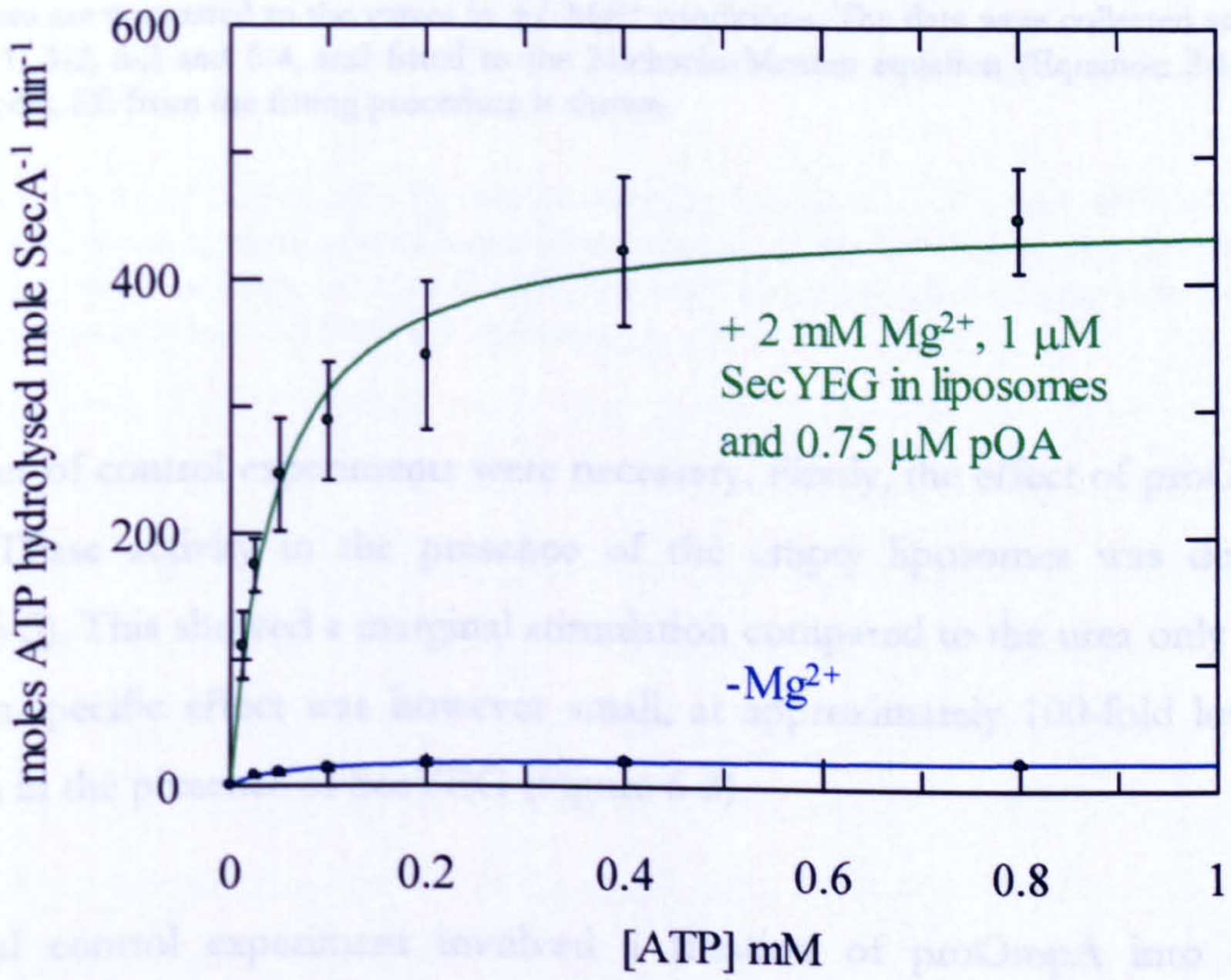

Figure 6-4. Michaelis-Menten plot of ATPase activity as a function of ATP concentration in the presence of SecYEG reconstituted in liposomes and proOmpA.

The ATPase activity of SecA (0.05 μM) was measured with 1 μM SecYEG reconstituted into liposomes and 0.75 μM proOmpA in TKM buffer (asterisk in Figure 6-3), over a range of ATP concentrations (green trace) and fitted according to the Michaelis-Menten equation (Equation 2-1, Materials and Methods). Error bars represent SD from 3 replicates. This is compared to the data obtained in residual Mg^{2+} conditions (blue trace) (Figure 3-2). Calculated values of $K_{M[ATP]}$ and k_{cat} are shown in Table 6-3.

SecA	$K_{M\,[ATP]}$ (μM)	k_{cat} (moles ATP hydrolysed mole $secA^{-1}$ min^{-1})
$+Mg^{2+}$	0.32 ± 0.03	0.56 ± 0.01
$-Mg^{2+}$	50.8 ± 3.2	22.36 ± 0.28
$+Mg^{2+}$; 1 μM SecYEG in total *E. coli* polar lipid proteoliposomes	51.1 ± 7.8	15.92 ± 0.62
$+Mg^{2+}$; 1 μM SecYEG in total *E. coli* polar lipid proteoliposomes; 0.75 μM proOmpA	46.1 ± 6.6	456.27 ± 17.21

Table 6-3. Calculated values of the $K_{M[ATP]}$ for SecA in the presence of magnesium and SecYEG in proteoliposomes, and additionally with proOmpA.

These values are compared to the values in +/-Mg^{2+} conditions. The data were collected according to Figures 3-1, 3-2, 6-2 and 6-4, and fitted to the Michaelis-Menten equation (Equation 2-1, Materials and Methods). SE from the fitting procedure is shown.

A number of control experiments were necessary. Firstly, the effect of proOmpA on SecA ATPase activity in the presence of the empty liposomes was determined (Figure 6-5). This showed a marginal stimulation compared to the urea only titration. This non-specific effect was however small, at approximately 100-fold lower than that seen in the presence of SecYEG (Figure 6-3).

The final control experiment involved a titration of proOmpA into an assay containing only SecA in the absence of any liposomes (Figure 6-5). This showed absolutely no effect of pre-protein on ATPase activity. Therefore it can be concluded that proOmpA specifically stimulates the ATPase activity of SecA in the presence of membrane bound SecYEG.

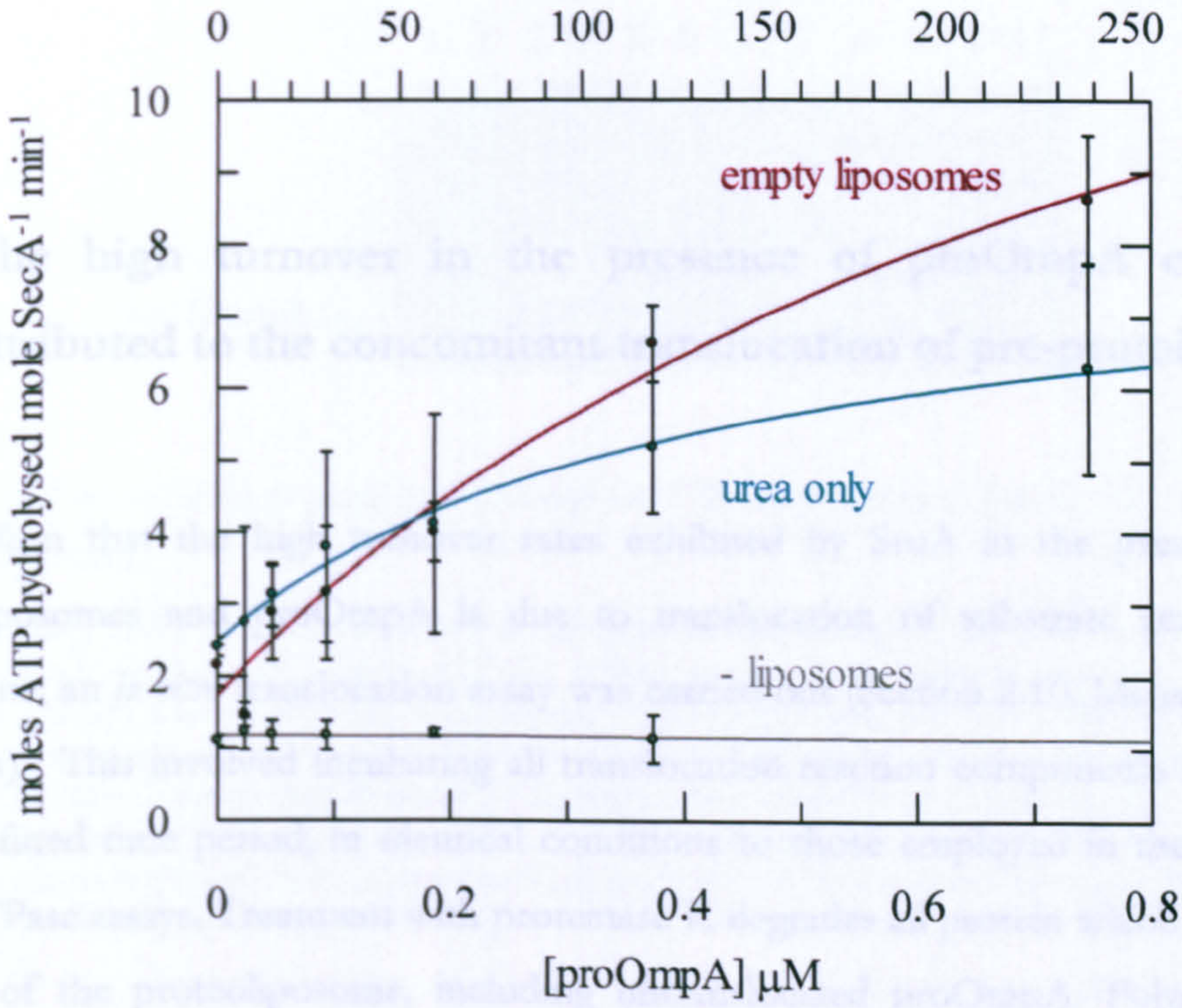

Figure 6-5. The stimulation of the ATPase activity of SecA by proOmpA requires lipids and SecYEG.

The ATPase activity of SecA (0.05 μM) was measured in the presence of 1 mM ATP in TKM buffer with increasing concentrations of proOmpA in the absence of any lipids (grey trace), in the presence of empty liposomes (maroon trace), and with urea only in the presence of empty liposomes (blue trace). Error bars represent SD from 2-3 replicates.

6.3 The high turnover in the presence of proOmpA can be attributed to the concomitant translocation of pre-protein

To confirm that the high turnover rates exhibited by SecA in the presence of proteoliposomes and proOmpA is due to translocation of substrate across the membrane, an *in vitro* translocation assay was carried out (Section 2.10, Materials and Methods). This involved incubating all translocation reaction components together for a defined time period, in identical conditions to those employed in the steady-state ATPase assays. Treatment with proteinase K degrades all protein which remains outside of the proteoliposome, including untranslocated proOmpA. Polypeptides were then separated by SDS-PAGE, and the protease protected protein identified by Western blot and chemiluminescence.

A time course was carried out up to 120 minutes (Figure 6-6, lanes 2-7), however it was seen that import reached a maximum after 30 minutes. Lanes 8-12 are the negative controls which did not show any translocation activity up to 120 minutes, with the exception of lane 11, which was carried out under residual Mg^{2+} conditions. Lane 1 shows a sample which has not been protease treated and was loaded as a measure of 10% of the total proOmpA used in each reaction. Comparing this lane to the imported protein samples indicates that the total proOmpA imported into the proteoliposomes barely reached about 5% of the total protein available. This is probably because the protein forms aggregates after a short time due to dilution of the urea, and is thus unavailable for translocation (Crooke et al., 1988) (A. Robson, M. Sun and I. Collinson, unpublished results). Some protein is imported in residual Mg^{2+} conditions, but a comparison of lanes 6 and 11 (depicting experiments carried out for the same time under the two buffer conditions) shows that it is severely impaired. Thus, Mg^{2+} is required for translocation.

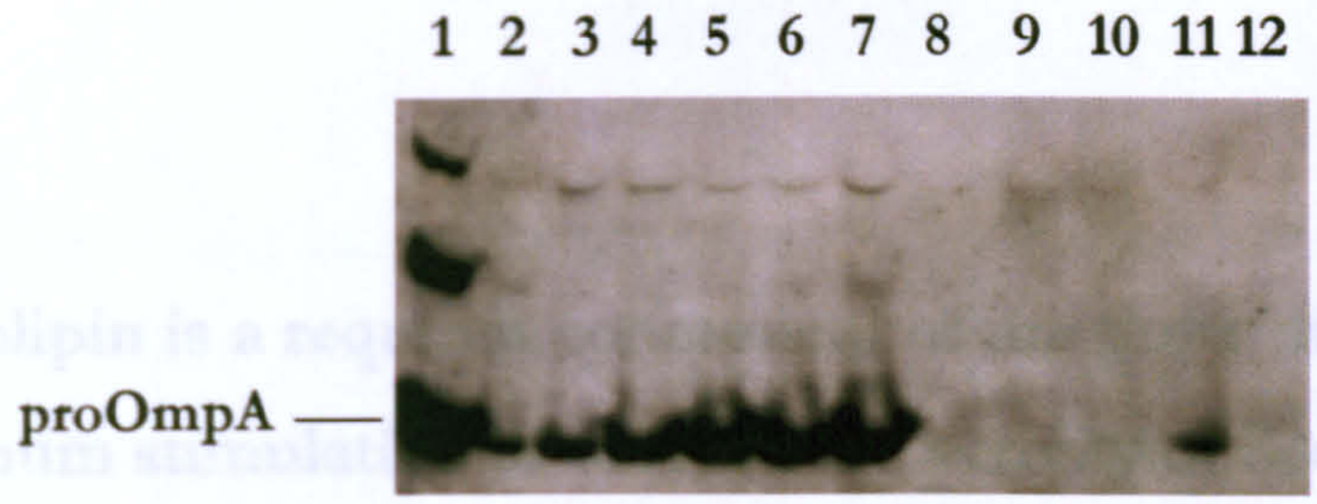

Figure 6-6. Translocation of proOmpA through SecYEG reconstituted into *E. coli* liposomes by wild-type SecA.

SecA (0.05 μM), SecYEG (1 μM) reconstituted into total *E. coli* polar lipids and proOmpA (0.75 μM) were incubated together with 1 mM ATP for a time course. Successfully translocated (protease-protected) proOmpA was detected by Western blot and chemiluminescence. The sample in lane 1 had not been protease treated and was loaded as a measure of 10 % of the total proOmpA used in each reaction. The other lanes are as follows: 2-7 – increasing time course for proOmpA translocated into *E. coli* total polar lipid proteoliposomes at 1, 5, 10, 30, 60 and 120 minutes respectively, 8-12 – negative controls incubated for 90 minutes in the absence of SecYEG (empty liposomes), SecA, ATP, Mg^{2+} and proOmpA respectively.

6.4 Cardiolipin is a required component of the proteoliposome for maximum stimulation of the ATPase activity of SecA

To distinguish the effect of CL from the two other major *E. coli* polar lipids that constitute the bilayer (PE and PG), SecYEG was reconstituted into liposomes composed of the synthetic lipids DOPE and DOPG, in the presence and absence of *E. coli* CL. The synthetic lipids differ from the natural *E. coli* forms by having a fixed chain length of 18 carbon atoms. The ratio of lipids mixed together approximated that of the natural *E. coli* polar lipid composition.

Increasing concentrations of the synthetic lipid proteoliposomes (reconstituted with SecYEG) were titrated into the standard kinetic assay reaction (Figure 6-7). These data are compared to that of the natural *E. coli* polar lipid proteoliposomes (Figure 6-1). The synthetic lipid proteoliposomes also stimulate the ATPase activity in all conditions. The stimulation observed in the presence of DOPE, DOPG and CL was similar to that engendered by natural *E. coli* polar lipids. Therefore, in respect of ATPase stimulation, the synthetic lipids DOPE and DOPG are able to substitute for natural *E. coli* lipids. However, in the absence of CL, the maximum stimulation capacity was reduced by approximately 2-fold compared to in the presence of this lipid. This demonstrates that the membrane bound SecYEG complex promotes an increased catalytic activity more efficiently in the presence of CL.

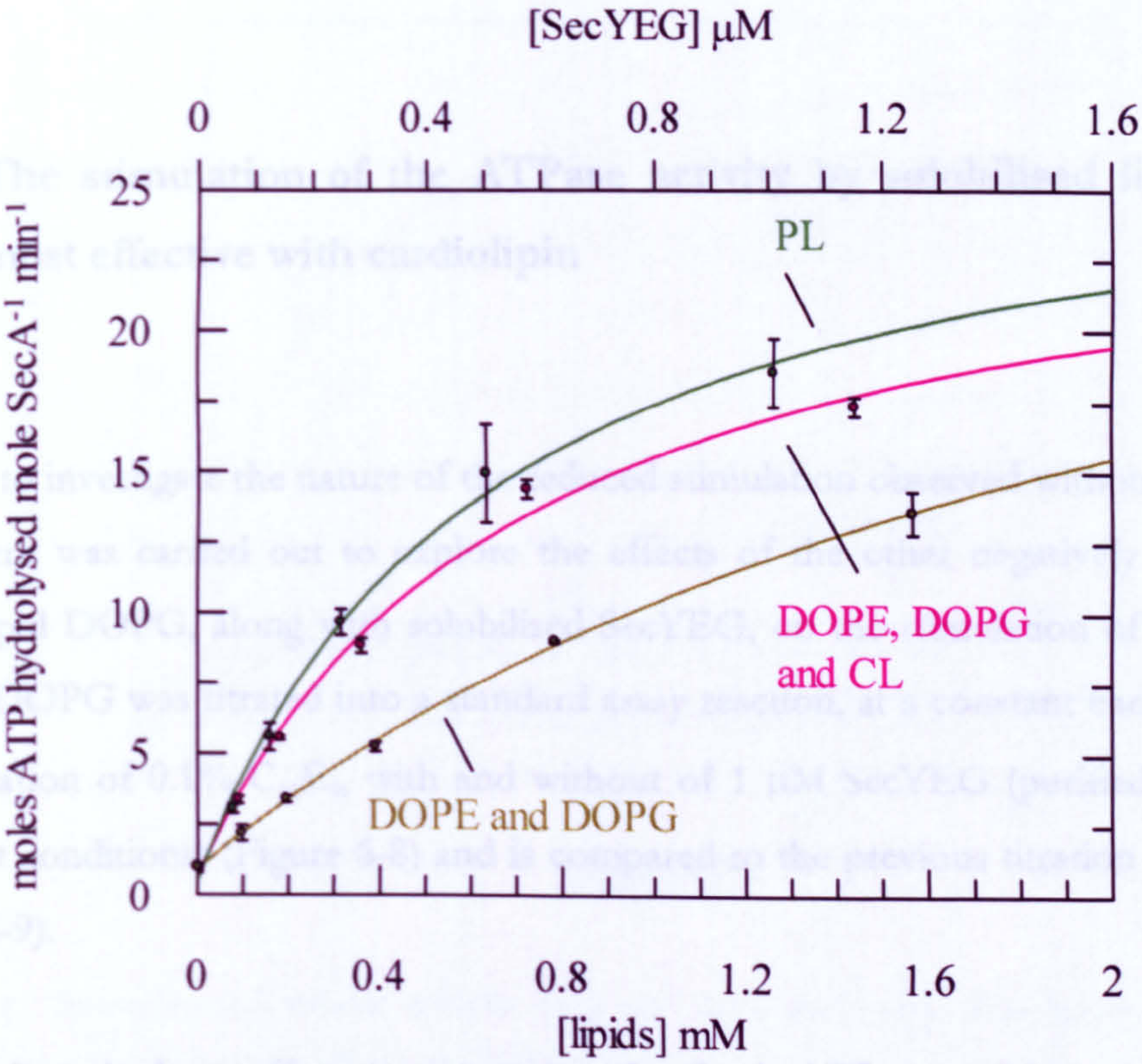

Figure 6-7. SecYEG reconstituted into liposomes without cardiolipin are not as effective with respect to the stimulation of the ATPase activity of SecA.

The ATPase activity of SecA (0.3 μM) was measured in the presence of 1 mM ATP in TKM buffer with increasing concentrations of SecYEG reconstituted into liposomes consisting of total *E. coli* polar lipids (PL; green trace), of DOPE, DOPG and CL (pink trace) and of DOPE and DOPG only (olive trace). The concentration of active SecYEG orientated correctly is approximately half of that shown on the upper *x* axis. Error bars represent SD from 2-3 replicates.

6.4.1 The stimulation of the ATPase activity by solubilised lipids is most effective with cardiolipin

In order to investigate the nature of the reduced stimulation observed without CL, an experiment was carried out to explore the effects of the other negatively charged bilayer lipid DOPG, along with solubilised SecYEG, on the stimulation of ATPase activity. DOPG was titrated into a standard assay reaction, at a constant background concentration of 0.1% $C_{12}E_9$, with and without of 1 μM SecYEG (purified in high detergent conditions) (Figure 6-8) and is compared to the previous titration with CL (Figure 5-9).

DOPG alone had no effect on increasing the SecA ATPase activity, and only a marginal one in the presence of 1 μM SecYEG. Therefore, the stimulation of ATPase activity by DOPG in the presence of SecYEG is more potent in the membrane bound state, compared to the detergent solubilised form. DOPG does not therefore behave comparably to CL.

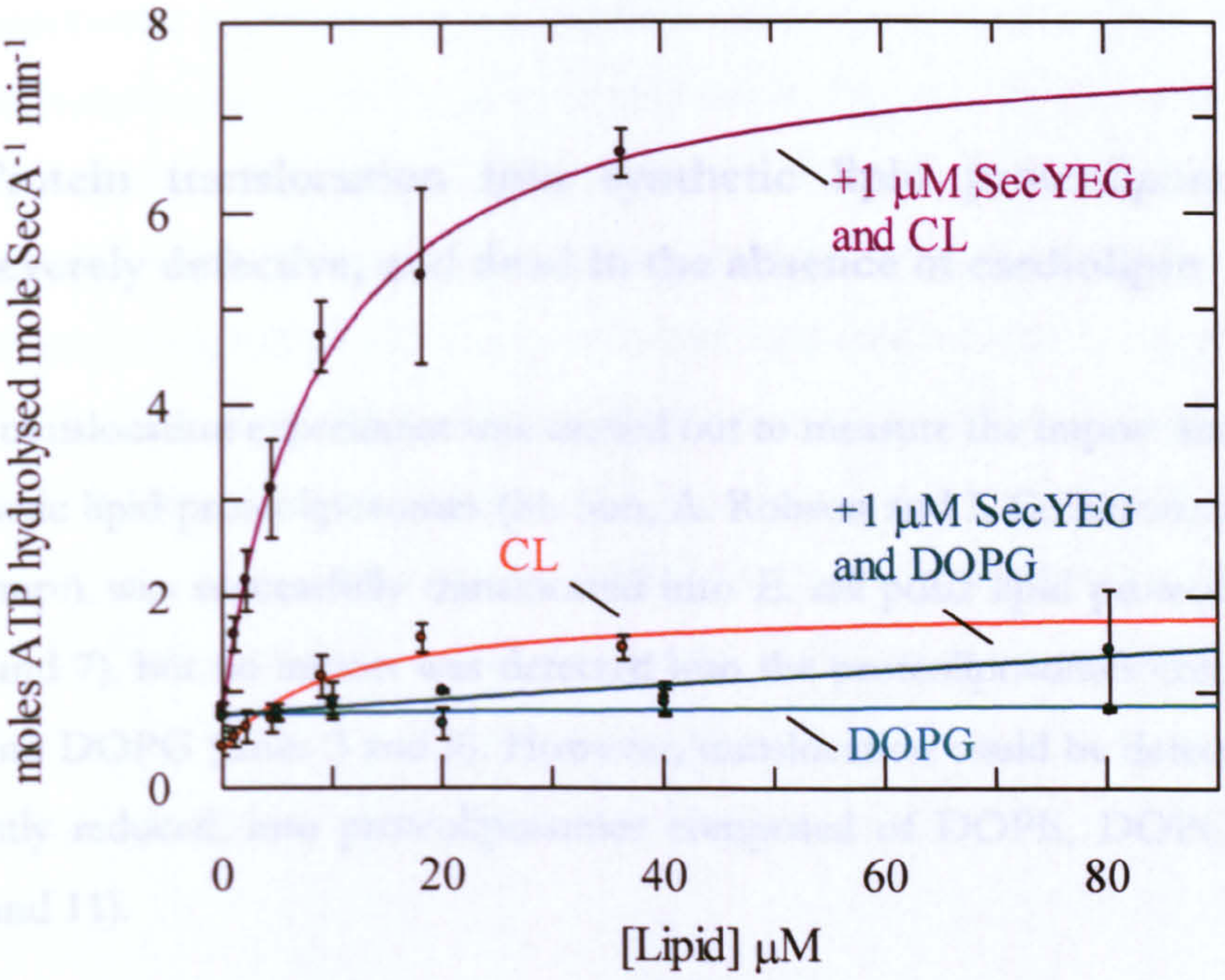

Figure 6-8. Detergent solubilised DOPG does not have the same stimulatory effect as cardiolipin on stimulating the ATPase activity of SecA.

The ATPase activity of SecA (0.3 μM) was measured in the presence of 1 mM ATP in TKM buffer with 0.1% $C_{12}E_9$ and increasing concentrations of DOPG (blue trace), and in the same conditions plus 1 μM SecYEG (teal trace). These data sets are compared to the same experiment using CL (Figure 5-9).

6.4.2 Protein translocation into synthetic lipid proteoliposomes is severely defective, and dead in the absence of cardiolipin

Another translocation experiment was carried out to measure the import kinetics into the synthetic lipid proteoliposomes (M. Sun, A. Robson and I. Collinson) (Figure 6-9). proOmpA was successfully translocated into *E. coli* polar lipid proteoliposomes (lanes 1 and 7), but no import was detected into the proteoliposomes composed of DOPE and DOPG (lanes 3 and 9). However, translocation could be detected, albeit significantly reduced, into proteoliposomes composed of DOPE, DOPG and CL (lanes 5 and 11).

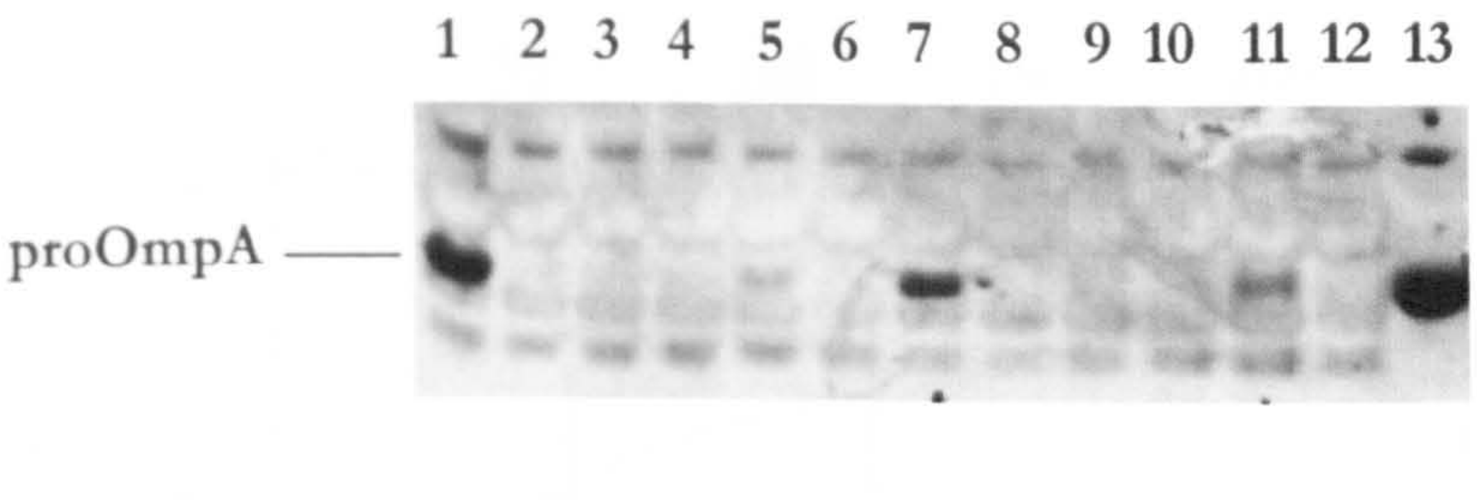

Figure 6-9. Protein translocation is severely defective into proteoliposomes composed of synthetic lipids, and dead in the absence of cardiolipin.

SecA (0.05 μM), SecYEG (1 μM) reconstituted into varying composition liposomes and proOmpA (0.75 μM) were incubated together with 1 mM ATP for a time course. Successfully translocated (protease-protected) proOmpA was detected by Western blot and chemiluminescence. The sample in lane 13 had not been protease treated and was loaded as a measure of 10 % of the total proOmpA used in each reaction. The other lanes are derived from the following conditions (even numbers were carried out in the absence of ATP as negative controls): 1-2 and 7-8 – SecYEG reconstituted into total *E. coli* polar lipids, 3-4 and 9-10 - SecYEG reconstituted into liposomes consisting of DOPE and DOPG, 5-6 and 11-12 - SecYEG reconstituted into liposomes consisting of DOPE, DOPG and CL.

These experiments indicated that the synthetic lipids are competent with respect to ATPase stimulation via SecYEG (without proOmpA; Figure 6-7), but not in terms of translocation activity (Figure 6-9). To explore this further, the steady-state kinetics were examined in the presence of synthetic lipid proteoliposomes, together with proOmpA and compared to the results obtained with total natural *E. coli* polar lipids (Figure 6-10). The data obtained in the presence of synthetic lipids were fitted according to a ligand binding equation (Equation 2-7, Materials and Methods) to reveal the $K_{d[SecA\text{-}proOmpA]}$ under these conditions. It is apparent that the binding affinity of proOmpA to SecA is extremely tight in the presence of synthetic lipids, but the ATPase activity is not stimulated to such a degree. This reflects their inability to promote a high level of translocation activity (Figure 6-9).

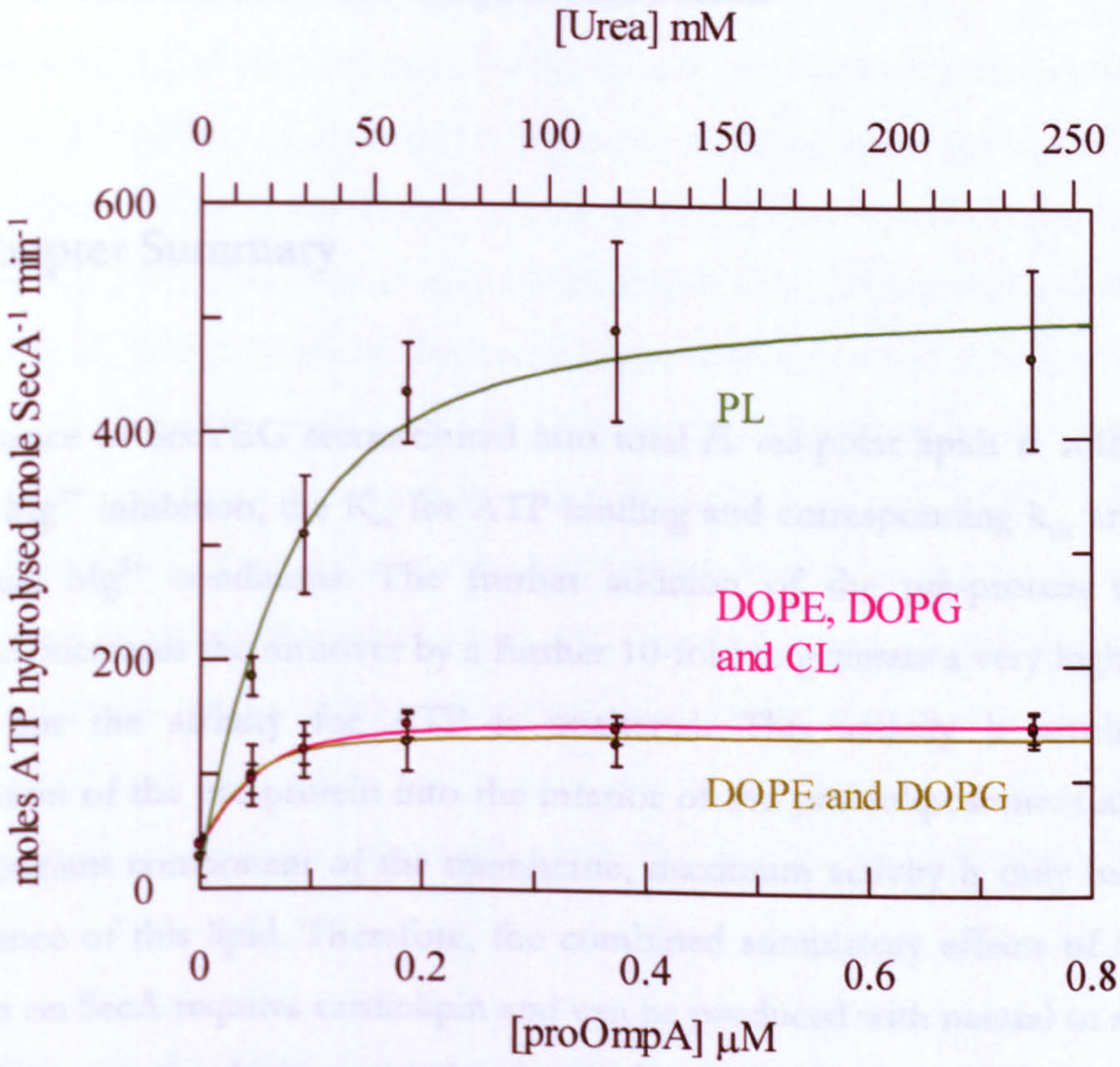

Figure 6-10. Proteoliposomes composed of the synthetic lipids are defective in proOmpA mediated stimulation of SecA ATPase activity.

The ATPase activity of SecA (0.05 μM) was measured in the presence of 1 mM ATP in TKM buffer with 1 μM SecYEG reconstituted into liposomes consisting of DOPE, DOPG and CL (pink trace) and liposomes composed of DOPE and DOPG only (olive trace), and increasing concentrations of proOmpA. This is compared to SecYEG reconstituted into total *E. coli* proteoliposomes (PL, green trace, Figure 6-3). The data sets were fitted according to a tight ligand binding equation (Equation 2-7, Materials and Methods) and the calculated K_d values are shown in Table 6-4. Error bars represent SD from 2-6 replicates.

SecA	$K_{d\ [proOmpA]}$ (μM)	k_{cat} (moles ATP mole SecA^{-1} min^{-1})
+Mg^{2+}; 1 μM SecYEG in total *E. coli* polar lipid proteoliposomes	0.047 ± 0.017	514.28 ± 41.18
+Mg^{2+}; 1 μM SecYEG in DOPE, DOPG and CL proteoliposomes	0.018 ± 0.005	113.23 ± 5.38
+Mg^{2+}; 1 μM SecYEG in DOPE and DOPG proteoliposomes	0.012 ± 0.005	98.42 ± 7.12

Table 6-4. Calculated K_d values for SecA to proOmpA via SecYEG reconstituted into liposomes of differing lipid composition.

The data were collected according to Figure 6-10, and fitted to a ligand binding equation (Equation 2-7, Materials and Methods). SE from the fitting procedure is shown.

6.5 Chapter Summary

The presence of SecYEG reconstituted into total *E. coli* polar lipids is sufficient to alleviate Mg^{2+} inhibition, the K_M for ATP binding and corresponding k_{cat} are similar to residual Mg^{2+} conditions. The further addition of the pre-protein substrate proOmpA increases the turnover by a further 10-fold to generate a very highly active species, but the affinity for ATP is unaltered. This activity is attributed to translocation of the pre-protein into the interior of the proteoliposome. Cardiolipin is an important component of the membrane, maximum activity is only reached in the presence of this lipid. Therefore, the combined stimulatory effects of SecYEG and lipids on SecA requires cardiolipin and can be produced with natural or synthetic lipids. However, the higher stimulated rate in the presence of proOmpA, and concomitant protein translocation, requires that the SecYEG complex is in a natural lipid environment, also with cardiolipin.

Chapter 7

Discussion

7.1 The Objective

Our understanding of the molecular mechanism of Sec-dependent translocation and the specific role of SecA is incomplete. There are six X-ray structures available of the motor protein ATPase, five dimers (Hunt et al., 2002; Papanikolau et al., 2007; Sharma et al., 2003; Vassylyev et al., 2006; Zimmer et al., 2006) and one monomer (Osborne et al., 2004). Much of the perplexity resides in the lack of consensus with respect to the active oligomeric form of the protein and its channel partner SecYEG, the processive nature of the reaction and the stoichiometry of ATP / amino acid translocated. These uncertainties are understandable in view of the fact that there is little data to describe the interactions that occur between SecYEG, SecA and substrate. There is also a paucity of information on the kinetics and the hydrolytic cycle of SecA and the nature and timing of the reactions that bring about the conformational changes that ultimately drive the passage of proteins through the membrane.

The experiments described address a fundamental aspect of the system; the ATP hydrolytic reaction cycle of SecA. This began at the simplest level, with the aim to elucidate the steady-state ATPase mechanism. SecA has been characterised by ATPase assays and the observed kinetics have been related to conformational changes by analytical ultracentrifugation. This was then extended by relating the ATPase activity to the effect of various partner protein interactions, including the SecYEG channel, and a pre-protein substrate proOmpA. In the presence of specific lipid components of the bilayer, pre-protein was found to change the steady-state

complex, and the observations could thus be used to make predictions pertinent to the translocation reaction cycle.

7.2 Magnesium exerts a strong inhibition on ATPase activity

Initial experiments aimed to fully characterise the steady-state ATPase activity of SecA in solution. This was primarily carried out in the presence of 2 mM Mg^{2+}, due to the ubiquitous requirement of this cofactor for ATP hydrolysis. However, when the cation concentration was altered, dramatic changes in ATPase activity were observed, thus an investigation was carried out to define this effect.

Assays carried out in the presence of 2 mM Mg^{2+} revealed an extremely tight binding affinity for ATP and slow rate of turnover. A powerful effect was noted under residual Mg^{2+} conditions, the binding affinity was now weak, and the turnover rate much faster (Table 7-1). The data indicate that the inhibition is by binding of Mg^{2+} to an allosteric site distinct from the nucleotide binding cleft, which leads to an increase in SecA affinity for ATP and a corresponding decrease in the rate of turnover. Other divalent cations also inhibit SecA ATP hydrolysis (not shown), but as free Mg^{2+} is present at the highest cellular concentration, they will almost certainly be outcompeted. The total concentration of SecA in the *E. coli* cell varies between 5-10 μM, (Akita et al., 1991; Or et al., 2002), and the concentration of free Mg^{2+} in bacterial cells is approximately 1 mM (Froschauer et al., 2004). Thus there is an approximate 100-fold excess of Mg^{2+} over SecA, which would be sufficient to completely inhibit the ATPase reaction in the cytosol and prevent futile consumption of ATP.

The mutant protein SecA-Δ11/N95 behaved in essentially the same manner as the wild type, indicating that the two proteins are both subjected to the same regulation. Therefore the 11 N-terminal and 70 C-terminal residues do not contribute to this effect. It has been proposed that Zn^{2+} binds to the C-terminal 22 residues of SecA (Fekkes et al., 1999) to stabilise the interaction with the molecular chaperone SecB

(Fekkes et al., 1997). The divalent cation-binding site determined in this study cannot be the same one that co-ordinates Zn^{2+}, as that is confined to the 70 amino acids that were truncated from the C-terminus of SecA-Δ11/N95 (Or et al., 2005). In addition, a wild type SecA protein lacking a hexahistidine tag was expressed, and the inhibitory effect of Mg^{2+} was shown not to be attributable to the C-terminal modification (data not shown).

The fact that Mg^{2+} is both an inhibitor and an essential cofactor to the enzyme has meant that many of the previous results on the activity of SecA have been difficult to interpret. Moreover, the inevitable variation of the cation concentration due to the chelating properties of ATP will have added further confusion. There are anomalies in the literature with regard to SecA behaviour and Mg^{2+} concentration, which have largely been ignored (Section 1.6.5.3). The characterisation of the allosteric site can now explain some of the contradictory data. For example, SecA has been reported to contain two binding sites for nucleotide of different affinities within a single protomer (Mitchell and Oliver, 1993). This was by observation of a point of inflection in ATP binding affinity across a concentration gradient. By close inspection, it can be seen that the binding affinity is weakened when the ATP concentration was raised above the Mg^{2+} concentration, probably due to chelation of the cation away from the allosteric site.

7.3 Magnesium inhibition of ATPase activity is accompanied by a compaction of the SecA dimer

The observed change in affinity for ATP caused by Mg^{2+} indicates that a conformational change occurs upon binding. The nature of this conformational change was characterised by gel filtration chromatography, analytical ultracentrifugation and by exposure of translocation complexes to protease.

Gel filtration studies carried out on wild-type SecA indicated a reversible Mg^{2+}-dependent change in structure, and a decrease in hydrodynamic radius in the

presence of the cation. A similar shift was seen for the terminally truncated mutant SecA-Δ11/N95. Sedimentation equilibrium analysis determined that the molecular mass of both proteins were unchanged by Mg^{2+}, being consistent with a dimeric structure in both cases. Thus the decrease in hydrodynamic radius must be due to a conformational change within the dimer species.

The results of sedimentation velocity experiments reveal that structural rearrangements of the dimer are quite large, with the Mg^{2+}-bound form of the protein having a significantly larger (approximately 6%) Svedberg constant. Interpreted empirically, this is equivalent to the difference in sedimentation behaviour between bovine carboxypeptidase A and bovine superoxide dismutase (Squire and Himmel, 1979). These proteins have the same molecular mass and partial specific volumes but the latter is 40% longer in its longest axis (from 50Å to 72Å). Hence, the change in sedimentation coefficient observed in SecA could represent a considerable compaction of the dimeric structure, that is associated with a dramatically reduced catalytic activity.

A slightly surprising aspect of this analysis was the indication that the predicted monomeric mutant SecA-Δ11/N95 is actually a dimer, in contrast to previous findings (Or et al., 2005). However, this protein does not undergo such a large conformational change upon Mg^{2+} binding; probably due in part to its smaller size, and possibly also to the truncation of the C-terminus. Thus, it might be that the C-terminal domain is involved in this conformational change. Independent studies employing Nuclear Magnetic Resonance (NMR) have also implicated the C-terminus of SecA as a highly flexible part of the structure (Chou et al., 2002; Gelis et al., 2007).

In support of these observations, a similar mutant to SecA-Δ11/N95, SecA9-861 (the N-terminal nonapeptide and C-terminal 40 residues are removed), could also maintain a dimeric structure and support protein translocation (Karamanou et al., 2005). However, this is not to say that a monomeric form of SecA does not play a part at some stage of the transport process.

7.4 ADP competitively inhibits the ATPase activity, and also promotes a compaction of SecA

The effects of ADP on the steady-state kinetics and structure of SecA were also investigated. In the presence of Mg^{2+}, the affinity for ADP was found to be increased by approximately 200 fold, very similar to the effect on the ATP affinity (150 fold increase). This indicates that the binding of ADP is similarly sensitive to the change induced by Mg^{2+} binding. The results presented here and elsewhere show that neither ADP or ATP affect the dimeric conformation of SecA in solution (Akita et al., 1991; Driessen, 1993; Or et al., 2002; Shilton et al., 1998; Woodbury et al., 2002). However, the presence of ADP in residual Mg^{2+} conditions promotes the compact form of SecA observed in the presence of high concentrations of Mg^{2+}. A similar effect of ADP has been reported, employing steady-state tryptophan fluorescence anisotropy (Fak et al., 2004).

Corresponding to the ADP-induced compaction of the structure is a competitive inhibition of ATPase activity. This is consistent with the observation that the steady-state cycle is limited by the release of ADP (Zito et al., 2005) (A. Robson, A. R. Clarke and I. Collinson, unpublished results). Interestingly, quench flow experiments that measure pre-steady-state activity determine that Mg^{2+} does not affect the rate of ATP hydrolysis, but the release of ADP (A. Robson, A. R. Clarke and I. Collinson, unpublished results). Therefore, all the data suggest that Mg^{2+} exerts its effect not on the rate of phosphodiester bond cleavage, but by stabilising the SecA-ADP steady-state complex.

7.5 Cardiolipin activates the ATPase activity of SecA

SecA is water-soluble, but due to the nature of its role in translocation has an intimate association with the lipid bilayer. It has been reported that acidic phospholipids increase SecA ATPase activity (Ahn and Kim, 1998; Lill et al., 1990). Moreover, reports show that acidic phospholipids are required for protein translocation (Alami et al., 2007; de Vrije et al., 1988; Hendrick and Wickner, 1991; Kusters et al., 1991; Suzuki et al., 1999; van der Does et al., 2000). There have also been accounts of lipid binding sites on SecA (Breukink et al., 1993; Breukink et al., 1995). The ability of lipids such as CL to chelate divalent cations (Brenza et al., 1985) might indicate that the observed activation in ATPase activity is not a direct effect of the lipid, but is manifested by its ability to extract Mg^{2+} from its inhibitory binding site.

In the presence of residual concentrations of Mg^{2+}, CL is inhibitory to the SecA ATPase activity, probably due to chelation of the cation. In the presence of Mg^{2+}, CL solubilised in $C_{12}E_9$ alleviates the inhibition and increases the K_M for ATP towards the one observed for SecA alone with residual Mg^{2+} (Table 7-1). Total *E. coli* polar lipids have a 10-fold reduced effect, probably due to the 9.8% total CL content. This alleviation effect was not a simple bulk chelation of Mg^{2+}, as the activation is observed with only 2.4 μM CL in the presence of 100 μM Mg^{2+}. Instead, the effect is specific to SecA and is likely to occur upon the formation of a SecA:Mg^{2+}:CL ternary complex. In this way, the Mg^{2+} may be shifted from the allosteric site by local interaction with the CL. This raises the possibility that this activation could be promoted by a specific CL molecule encountered only during the initiation of protein translocation, which could be important in the activation of the enzyme as it delivers substrate protein in the vicinity of the membrane and the Sec complex. Interestingly, CL has also been shown to stabilise the dimeric and active form of the SecYEG complex in *E. coli* (F. Duong and I. Collinson, unpublished results).

Both CL and total *E. coli* polar lipid liposomes have different effects on SecA ATPase activity compared to their soluble form in the detergent $C_{12}E_9$. The soluble forms are much more effective in this respect, which may mean that it is manifested via an intimate association with the lipid, rather than by an effect of the bulk membrane.

7.6 SecYEG acts synergistically with cardiolipin

Addition of CL to steady-state ATPase assays brings about a weakening of the ATP binding affinity that is closer to the residual Mg^{2+} conditions. However, the protein is not fully active in terms of potential catalytic turnover, thus the effects of the SecYEG channel were also investigated.

The ATPase activity was indeed activated by soluble SecYEG, but the effects were dependent upon the $C_{12}E_9$ concentration. This detergent itself does not affect SecA directly, thus this must be an indirect effect mediated via the SecYEG complex. This was shown by TLC to be as a result of the lipids bound; at higher detergent concentrations more of the lipids are removed, resulting in a preparation that was less potent with respect to the stimulation. Re-supplementing the depleted complex with CL rescues the activity back to that of a preparation purified in low detergent, that had not been depleted of lipids.

SecYEG increases the rate of reaction, and therefore must promote product release, as the steady-state SecA complex is SecA-ADP (Zito et al., 2005) (A. Robson, A. R. Clarke and I. Collinson, unpublished results). The binding affinity for SecA to SecYEG in detergent solution, in the presence of Mg^{2+} and the non-hydrolysable ATP analogue AMP-PNP, was determined to be tight, (~0.1 μM) (Robson et al., 2007). In the steady-state conditions employed in this study, the interaction of SecA with soluble SecYEG in the presence of Mg^{2+} and ATP is weak, exemplified by the inability to saturate 0.05 μM SecA up to 8.4 μM SecYEG. Assuming that AMP-PNP is an appropriate substitute for ATP, the steady-state complex SecA-ADP must

therefore have a low affinity interaction with SecYEG. Elsewhere, ADP release from SecA has been shown to accelerate 4-fold when bound to the SecYEG complex (Natale et al., 2004). This supports the notion that after ATP hydrolysis, SecA retracts from SecYEG and the membrane (den Blaauwen et al., 1996; Fak et al., 2004; Hunt et al., 2002; Shilton et al., 1998; Ulbrandt et al., 1992).

CL and SecYEG both activate the ATPase activity, but together their effects are synergistic. CL when solubilised in $C_{12}E_9$ does stimulate the ATPase activity, however the presence of the channel partner weakens the $K_{M[ATP]}$ and increases the turnover closer to residual Mg^{2+} conditions (Table 7-1). In a biological context, this would ensure that SecA is only activated *in situ*, that is in the presence of both CL and SecYEG.

7.7 SecYEG presented in the context of cardiolipin containing liposomes completely alleviates the inhibition by magnesium

SecA can be saturated at much lower concentrations of SecYEG when the protein is presented in context of a lipid bilayer. The steady-state complex of SecA binds to the empty vesicles 2-fold weaker than to SecYEG-containing proteoliposomes, ensuring that full activation only occurs when bound to the complex. Under these conditions the Mg^{2+} inhibition is completely alleviated; both the $K_{M[ATP]}$ and k_{cat} are now characteristic of residual concentrations of Mg^{2+}. This indicates that SecYEG reconstituted into total *E. coli* polar lipids is sufficient to completely overcome the Mg^{2+} inhibition of the ATPase (Table 7-1).

7.7.1 proOmpA further stimulates the ATPase activity, but does not change the affinity for ATP

In order to reassemble the entire translocation reaction and analyse the consequence to the steady-state ATPase reaction, the effects of unfolded pre-protein were assessed. proOmpA in the presence of Mg^{2+} and total *E. coli* proteoliposomes promotes a highly active species of SecA (1000-fold more active than SecA alone in the presence Mg^{2+}). This occurs by virtue of a tight binding of pre-protein to SecA (K_d = 79 nM), in a state that promotes its translocation. This value is comparable to one obtained for translocation of proOmpA into IMVs bearing overexpressed SecYEG ($K_{M[proOmpA]}$ = 180 nM) (de Keyzer et al., 2002). Notably, the $K_{M[ATP]}$ is unaffected by translocation of proOmpA, (Table 7-1), indicating that there has been a change in the steady-state complex.

These observations have been reconciled and used to propose a kinetic model for pre-protein translocation involving the inter-conversion between two steady-state complexes, coupling the ATP hydrolysis cycle to substrate binding and translocation. The SecA steady-state equation was derived (Equation 2-8, Materials and Methods), which enabled the $K_{M[ATP]}$ to be defined within the two model systems (system I, in the presence of SecYEG proteoliposomes without proOmpA; and system II, in the presence of both SecYEG proteoliposomes and proOmpA). In system II, k_{cat} has increased approximately 30-fold in comparison to system I, without affecting the binding affinity (K_M) for ATP (Table 7-1). In system II $K_{M[ATP]} = K_{d[ATP]}$, where as in system I, $K_{M[ATP]} = 0.04K_{d[ATP]}$ (Section 2.5.2.6). Therefore, during the proOmpA induced conversion of the steady-state complex (I $\longrightarrow$ II), the $K_{d[ATP]}$ must have decreased in compensation (as $K_{M[ATP]}$ is unchanged). The rate limiting step is now k_2 (Figure 7-1), thus the steady-state complex in the presence of proOmpA is SecA-ATP. This could be explained by proOmpA having a low affinity for SecA-ADP, and high affinity for SecA-ATP. Thus, translocation of pre-protein may proceed by substrate stabilisation of the ATP bound form of SecA. A further consequence of the model is the subsequent hydrolysis of ATP to ADP, and a concomitant destabilisation of this complex. In this case where ADP release no longer acts as rate limiting, k_{cat} is limited by the rate of ATP bond cleavage.

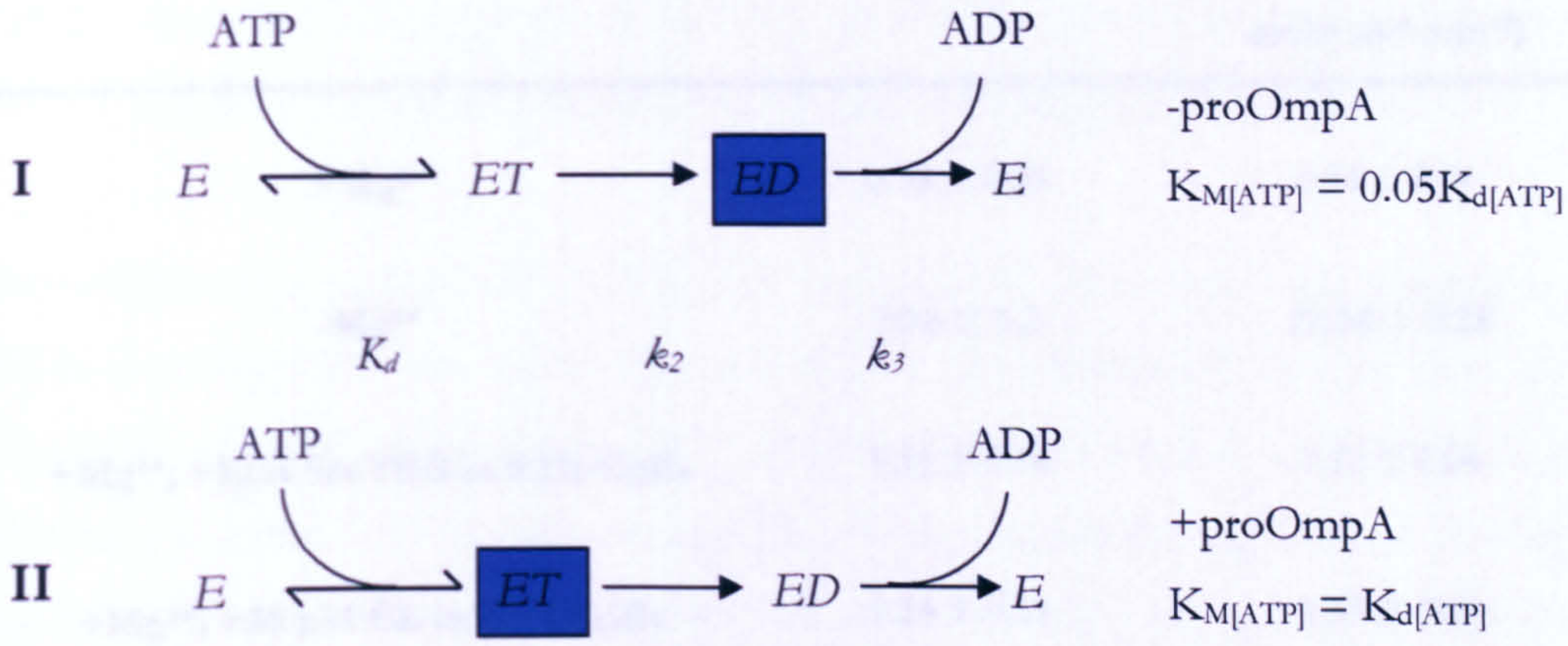

Figure 7-1. Two state model of the hydrolytic cycle of SecA.

Schematic overview depicting a change in the steady-state complex, mediated by proOmpA. E = apo enzyme, ET = enzyme-ATP complex and ED = enzyme-ADP complex. System I is defined by the presence of SecYEG proteoliposomes and the absence of proOmpA; and system II is defined by the presence of both SecYEG proteoliposomes and proOmpA. The steady-state complex is shown by a blue box in each case.

SecA	$K_{M\ [ATP]}$ (μM)	k_{cat} (moles ATP hydrolysed mole sA^{-1} min^{-1})
$+Mg^{2+}$	0.32 ± 0.03	0.56 ± 0.01
$-Mg^{2+}$	50.8 ± 3.2	22.36 ± 0.28
$+Mg^{2+}$; +1μM SecYEG in 0.1% $C_{12}E_9$	1.11 ± 0.14	1.12 ± 0.04
$+Mg^{2+}$; +36 μM CL in 0.1% $C_{12}E_9$	1.14 ± 0.21	1.85 ± 0.09
$+Mg^{2+}$; +1 μM SecYEG; + 36 μM CL in 0.1% $C_{12}E_9$	3.92 ± 0.37	6.93 ± 0.12
$+Mg^{2+}$; 1 μM SecYEG in total *E. coli* polar lipid proteoliposomes	51.1 ± 7.8	15.92 ± 0.62
$+Mg^{2+}$; 1 μM SecYEG in total *E. coli* polar lipid proteoliposomes; 0.75 μM proOmpA	46.1 ± 6.6	456.27 ± 17.21
SecA–Δ11/N95; $+Mg^{2+}$	0.40 ± 0.03	0.96 + 0.02
SecA–Δ11/N95; $-Mg^{2+}$	47.7 ± 3.7	30.16 ± 0.47

Table 7-1. SecA kinetic parameters.

7.7.2 The lipid composition of the proteoliposome is important to the activated kinetic properties of SecA during translocation

Proteoliposomes composed of DOPE and DOPG (but not CL) stimulate the ATPase activity, but not to its full potential. It was postulated that another *E. coli* negatively charged bilayer lipid, PG, could perform a similar role to CL (a CL molecule is formed by two PG molecules linked together by a glycerol). It is highly unlikely that this effect could be attributed to PE, as it is not a potential chelator of Mg^{2+}. Moreover, it has not been implicated as an important lipid with respect to the translocation reaction (Ahn and Kim, 1998; Alami et al., 2007; de Vrije et al., 1989; Kusters et al., 1991; Lill et al., 1990; Suzuki et al., 1999; van der Does et al., 2000). In contrast to the observations in proteoliposomes, DOPG had only minor effects in solution on stimulation of the ATPase activity of SecA. Thus the increase in activity seen in proteoliposomes must be attributed to the manner and conformation in which SecYEG is presented to SecA, in the context of a lipid membrane.

In the presence of CL, the synthetic lipids DOPE and DOPG can substitute for natural *E. coli* PE and PG in terms of proteoliposome stimulation on SecA, but are severely compromised with respect to the proOmpA-mediated ATPase activity (5-fold reduced) and protein translocation *in vitro*. In these conditions, SecA still binds to proOmpA equally tightly, comparable to conditions employing total *E. coli* polar lipids (the K_d values are all in the nanomolar range). Thus the synthetic proteoliposomes are defective in an advanced stage of pre-protein translocation through the membrane. This is probably due to the reduced flexibility of the membrane, or induction of an inactive conformation of SecYEG, perhaps due to a fixed carbon chain length of 18 carbon atoms (*E. coli* phospholipid chain lengths are mostly 16). A similar effect has been noted with the Ca^{2+}-ATPase pump, where aspects of the activity are exquisitely dependent upon the membrane phospholipid chain length (Lee, 2003). The stimulation of ATPase activity associated with the reconstituted SecYEG alone (without proOmpA) is not sensitive to the source of the lipids used (synthetic or natural), possibly because this effect is mediated by the polar

headgroups which remain unchanged. However, when proOmpA was included in the study, the sensitivity in this respect became apparent.

A polypeptide unfolded in urea and subsequently diluted out in buffer assumes a secondary structure in a time frame of milliseconds (Kim and Baldwin, 1982). Hence, the reduction in both ATPase and subsequent translocation activities indicates that more of the proOmpA will form aggregates and be unavailable for translocation (Crooke et al., 1988) (M. Sun, unpublished results). This explains why import is so low, even over a long time frame. Translocation does not occur at all in the proteoliposomes containing only DOPE and DOPG, therefore it appears as though CL is important in the coupling of ATPase activity to translocation.

A dependence upon phospholipids (particularly CL) is seen in the case of the F_1F_0-ATPase, whereby the acidic phospholipids of the mitochondrial inner membrane were shown to enable a Mg^{2+} mediated activation of activity (Ye and Lin, 1990). CL is also found specifically bound to the cytochrome bc1 complex (Hayer-Hartl et al., 1992; Lange et al., 2001), the removal of which renders the complex inactive for electron transport (Gomez and Robinson, 1999). This suggests an important role for CL in multiple energy transducing systems.

7.8 The C-terminus of SecA is implicated as a conformational switch in the reaction mechanism

The association of SecYEG with SecA results in the detachment of the C-terminus from the NBF of the latter (Karamanou et al., 1999). SecA may only interact with proOmpA in the presence of SecYEG proteoliposomes; an observation supported elsewhere by the demonstration that a detachment of the C-terminus is a requirement for signal-peptide binding (Gelis et al., 2007). An extended structure of SecA is demonstrated by analytical ultracentrifugation under residual Mg^{2+} conditions, and by the increased sensitivity to trypsin on binding to the SecYEG complex, both corresponding to an elevated ATPase activity. This raises the possibility that the activation and conformational changes within the C-terminus are induced by removal of Mg^{2+} at the membrane.

Binding of SecA to SecYEG has been shown to abrogate the Mg^{2+} inhibition (Robson et al., 2007), thus it could be predicted that this is due to an opening of the SecA structure, and detachment of the C-terminus from the NBFs, enabling increased turnover. Disruption of a large region (292 residues) of the C-terminal domain, and also specific residues 783-795 (ΔIRA1) leads to an increase in ATPase activity (Karamanou et al., 1999; Triplett et al., 2001). In contrast to the wild type protein, this activity is not further stimulated by the presence of lipids; therefore, perhaps this is because the ΔIRA1 mutants have lost the ability to become the subject of Mg^{2+} inhibition.

7.9 Conclusions

The results presented here describe a comprehensive analysis of the steady-state kinetics of the isolated motor domain of the major bacterial protein translocation apparatus. A conformational change in the dimer regulated by Mg^{2+} brings about a large shift in the properties of the nucleotide binding affinity and turnover of the enzyme. Interaction with SecYEG and CL together alleviate Mg^{2+} inhibition, and this is fully achieved in proteoliposomes composed of total *E. coli* polar lipids. CL is bound specifically to the SecYEG complex, ensuring that full activation only occurs *in situ*, on correct targeting to the channel (Figure 7-2).

The following model presented fits the data and describes the productive association of proOmpA to SecA and SecYEG (Figure 7-3). SecA binds tightly and translocates pre-protein proOmpA only in the presence of SecYEG proteoliposomes containing CL. Translocation of pre-protein proceeds by the binding of proOmpA to the ATP-bound form of the enzyme. Associated with hydrolysis is likely to be a conformational change within SecA which pushes pre-protein across the membrane, and proOmpA is released by SecA-ADP. SecYEG also has a low affinity interaction with ADP-bound form, suggesting a retraction (although not necessarily a dissociation) from the channel concomitant with hydrolysis.

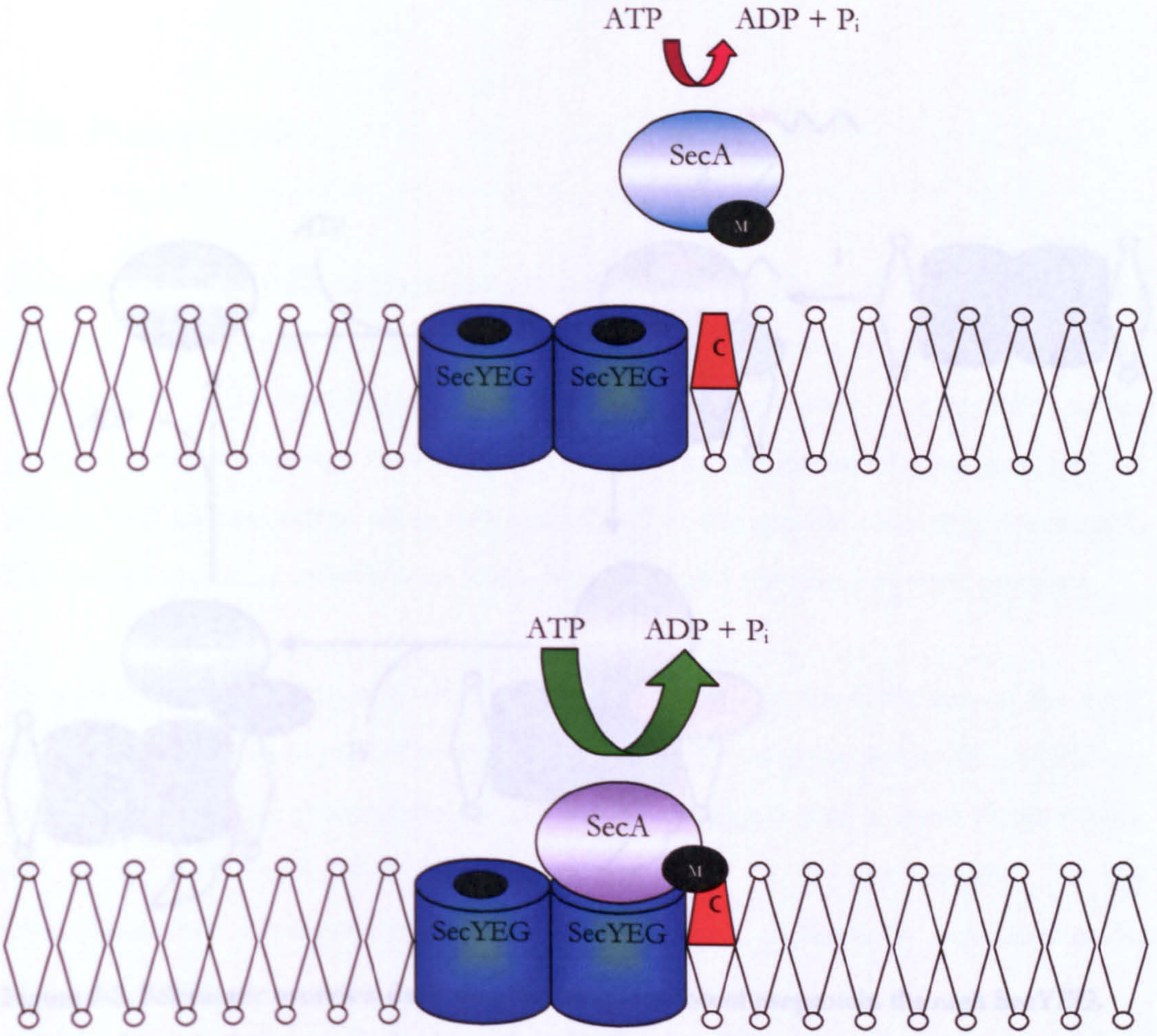

Figure 7-2. Schematic overview depicting alleviation of magnesium-induced inhibition, mediated by cardiolipin.

A dimer of SecA is shown as a single object. SecA with Mg^{2+} (black; M) bound to an allosteric binding site stabilises SecA-ADP and therefore has low catalytic activity, denoted by the smaller red arrow. When SecA is targeted to the membrane, cardiolipin (orange; C), bound to SecYEG, can alleviate this inhibition, probably by formation of a SecA-Mg^{2+}-cardiolipin complex. In this ternary complex the cardiolipin shifts the Mg^{2+} from the inhibitory site, the resulting species having a lower affinity for nucleotide and an increase in catalytic activity, denoted by the larger green arrow.

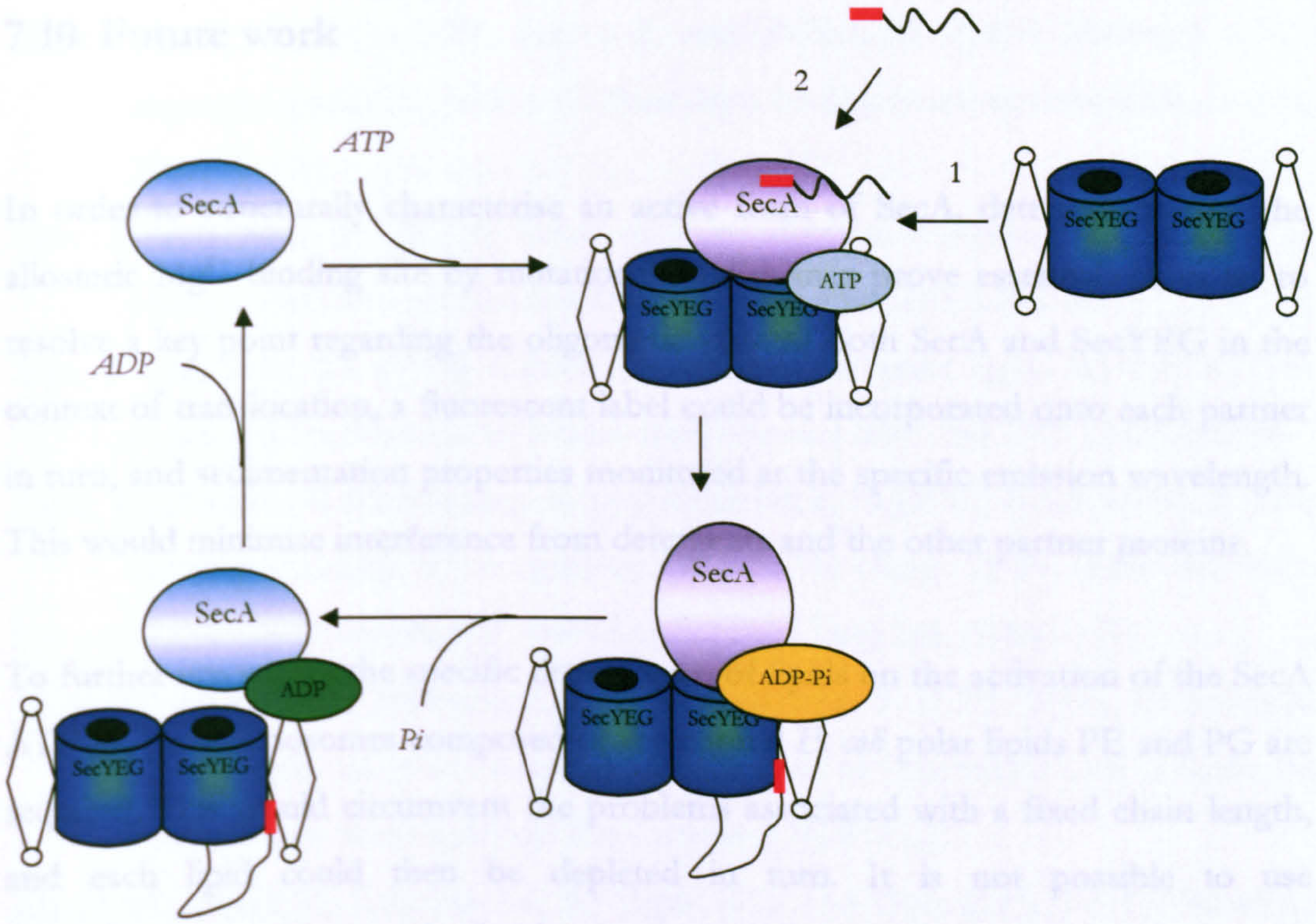

Figure 7-3. Schematic overview depicting the translocation of preprotein through SecYEG.

A dimer of SecA is shown as a single object. SecA binds to membrane bound SecYEG and cardiolipin prior to binding pre-protein. SecA-ATP has a high affinity for preprotein and the complex is stabilised in this form. It is likely that on ATP hydrolysis a conformational change occurs, resulting in translocation of pre-protein across the membrane. SecA-ADP has a weak association for both SecYEG and pre-protein, suggesting a retraction, although not necessarily a dissociation from the membrane. This model does not rule out a dissociation of the SecA dimer at some point of the reaction cycle.

7.10 Future work

In order to structurally characterise an active form of SecA, determination of the allosteric Mg^{2+} binding site by mutational studies may prove essential. In order to resolve a key point regarding the oligomeric state of both SecA and SecYEG in the context of translocation, a fluorescent label could be incorporated onto each partner in turn, and sedimentation properties monitored at the specific emission wavelength. This would minimise interference from detergents and the other partner proteins.

To further investigate the specific dependence of lipids on the activation of the SecA ATPase, proteoliposomes composed of the natural *E. coli* polar lipids PE and PG are required. This would circumvent the problems associated with a fixed chain length, and each lipid could then be depleted in turn. It is not possible to use proteoliposomes composed of only one type of lipid, as these do not form stable vesicle structures.

Paramount to understanding the translocation reaction cycle is elucidation of the mechanism of pre-protein transport across the membrane. Translocation may proceed by an inchworm stepping mechanism, common to the helicase PcrA, whereby one base pair is translocated per hydrolysis of one molecule of ATP (Dillingham et al., 2000). Alternatively, a Brownian ratchet mechanism analagous to that used by the ER motor BiP could be involved, whereby the hydrolysis cycle involves an interconversion of two distinct conformational states with a concomitant power stroke, resulting in translocation of large sections of substrate per single turnover of nucleotide (Matlack et al., 1999). Clearly a combination of both single and population molecule studies are required to resolve this question.

References

Abrahams, J.P., Leslie, A.G.W., Lutter, R. and Walker, J.E. (1994) Structure at 2.8 angstrom resolution of F-1-ATPase from bovine heart mitochondria. *Nature*, **370**, 621-628.

Ahn, T. and Kim, H. (1994) SecA of *Escherichia coli* traverses lipid bilayer of phospholipid vesicles. *Biochem Biophys Res Commun*, **203**, 326-330.

Ahn, T. and Kim, H. (1998) Effects of nonlamellar-prone lipids on the ATPase activity of SecA bound to model membranes. *J Biol Chem*, **273**, 21692-21698.

Akita, M., Sasaki, S., Matsuyama, S. and Mizushima, S. (1990) SecA interacts with secretory proteins by recognizing the positive charge at the amino terminus of the signal peptide in *Escherichia coli*. *J Biol Chem*, **265**, 8164-8169.

Akita, M., Shinkai, A., Matsuyama, S. and Mizushima, S. (1991) SecA, an Essential Component of the Secretory Machinery of *Escherichia coli*, Exists As Homodimer. *Biochem Biophys Res Commun*, **174**, 211-216.

Alami, M., Dalal, K., Lelj-Garolla, B., Sligar, S.G. and Duong, F. (2007) Nanodiscs unravel the interaction between the SecYEG channel and its cytosolic partner SecA. *Embo J*, **26**, 1995-2004.

Alder, N.N., Shen, Y., Brodsky, J.L., Hendershot, L.M. and Johnson, A.E. (2005) The molecular mechanisms underlying BiP-mediated gating of the Sec61 translocon of the endoplasmic reticulum. *J Cell Biol*, **168**, 389-399.

Arkowitz, R.A., Joly, J.C. and Wickner, W. (1993) Translocation Can Drive the Unfolding of a Preprotein Domain. *Embo J*, **12**, 243-253.

Arkowitz, R.A. and Wickner, W. (1994) SecD and SecF are required for the proton electrochemical gradient stimulation of preprotein translocation. *Embo J*, **13**, 954-963.

Baud, C., Karamanou, S., Sianidis, G., Vrontou, E., Politou, A.S. and Economou, A. (2002) Allosteric communication between signal peptides and the SecA protein DEAD motor ATPase domain. *J Biol Chem*, **277**, 13724-13731.

Beck, K., Eisner, G., Trescher, D., Dalbey, R.E., Brunner, J. and Muller, M. (2001) YidC, an assembly site for polytopic *Escherichia coli* membrane proteins located in immediate proximity to the SecYE translocon and lipids. *Embo Rep*, **2**, 709-714.

Beck, K., Wu, L.F., Brunner, J. and Muller, M. (2000) Discrimination between SRP- and SecA/SecB-dependent substrates involves selective recognition of nascent chains by SRP and trigger factor. *Embo J*, **19**, 134-143.

Beckmann, R., Bubeck, D., Grassucci, R., Penczek, P., Verschoor, A., Blobel, G. and Frank, J. (1997) Alignment of conduits for the nascent polypeptide chain in the ribosome-Sec61 complex. *Science*, **278**, 2123-2126.

Beckmann, R., Spahn, C.M., Eswar, N., Helmers, J., Penczek, P.A., Sali, A., Frank, J. and Blobel, G. (2001) Architecture of the protein-conducting channel associated with the translating 80S ribosome. *Cell*, **107**, 361-372.

Bellafiore, S., Ferris, P., Naver, H., Gohre, V. and Rochaix, J.D. (2002) Loss of Albino3 leads to the specific depletion of the light-harvesting system. *Plant Cell*, **14**, 2303-2314.

Benach, J., Chou, Y.T., Fak, J.J., Itkin, A., Nicolae, D.D., Smith, P.C., Wittrock, G., Floyd, D.L., Golsaz, C.M., Gierasch, L.M. and Hunt, J.F. (2003) Phospholipid-induced monomerization and signal-peptide-induced oligomerization of SecA. *J Biol Chem*, **278**, 3628-3638.

Berks, B.C. (1996) A common export pathway for proteins binding complex redox cofactors? *Mol Microbiol*, **22**, 393-404.

Bessonneau, P., Besson, V., Collinson, I. and Duong, F. (2002) The SecYEG preprotein translocation channel is a conformationally dynamic and dimeric structure. *Embo J*, **21**, 995-1003.

Bieker, K.L., Phillips, G.J. and Silhavy, T.J. (1990) The sec and prl genes of *Escherichia coli*. *J Bioenerg Biomembr*, **22**, 291-310.

Bieker, K.L. and Silhavy, T.J. (1990) PrlA (SecY) and PrlG (SecE) Interact Directly and Function Sequentially During Protein Translocation in *E. coli*. *Cell*, **61**, 833-842.

Blobel, G. and Dobberstein, B. (1975) Transfer to proteins across membranes. II. Reconstitution of functional rough microsomes from heterologous components. *J Cell Biol*, **67**, 852-862.

Blobel, G. and Sabatini, D.D. (1971) Ribosome-membrane interaction in eukaryotic cells. *Biomembranes*, **2**, 193-195.

Bonnefoy, N., Kermorgant, M., Groudinsky, O., Minet, M., Slonimski, P.P. and Dujardin, G. (1994) Cloning of a human gene involved in cytochrome

oxidase assembly by functional complementation of an oxa1- mutation in Saccharomyces cerevisiae. *Proc Natl Acad Sci USA*, **91**, 11978-11982.

Bostina, M., Mohsin, B., Kuhlbrandt, W. and Collinson, I. (2005) Atomic model of the *E. coli* membrane-bound protein translocation complex SecYEG. *J Mol Biol*, **352**, 1035-1043.

Boyer, P.D. (1993) The binding change mechanism for ATP synthase-some probabilities and possibilities. *Biochim Biophys Acta*, **1140**, 215-250.

Brenza, J.M., Neagle, C.E. and Sokolove, P.M. (1985) Interaction of Ca^{2+} with cardiolipin-containing liposomes and its inhibition by adriamycin. *Biochem Pharmacol*, **34**, 4291-4298.

Breukink, E., Demel, R.A., de Korte-Kool, G. and de Kruijff, B. (1992) SecA insertion into phospholipids is stimulated by negatively charged lipids and inhibited by ATP: a monolayer study. *Biochemistry*, **31**, 1119-1124.

Breukink, E., Keller, R.C.A. and de Kruijff, B. (1993) Nucleotide and negatively charged lipid-dependent vesicle aggregation caused by SecA. Evidence that SecA contains two lipid-binding sites. *FEBS Lett*, **331**, 19-24.

Breukink, E., Nouwen, N., van Raalte, A., Mizushima, S., Tommassen, J. and de Kruijff, B. (1995) The C terminus of SecA is involved in both lipid binding and SecB binding. *J Biol Chem*, **270**, 7902-7907.

Breyton, C., Haase, W., Rapoport, T.A., Kühlbrandt, W. and Collinson, I. (2002) Three-dimensional structure of the bacterial protein-translocation complex SecYEG. *Nature*, **418**, 662-665.

Brickman, E., Oliver, D., Garwin, J., Kumamoto, C. and Beckwith, J. (1984) The use of extragenic suppressors to define genes involved in protein export in *Escherichia coli*. *Mol Gen Genet*, **196**, 24-27.

Brodsky, J.L. and Schekman, R. (1993) A sec63p-BiP Complex from Yeast Is Required for Protein Translocation in a Reconstituted Proteoliposome. *J Cell Biol*, **123**, 1355-1363.

Brundage, L., Hendrick, J.P., Schiebel, E., Driessen, A.J. and Wickner, W. (1990) The purified *E. coli* integral membrane protein SecY/E is sufficient for reconstitution of SecA-dependent precursor protein translocation. *Cell*, **62**, 649-657.

Bu, Z., Wang, L. and Kendall, D.A. (2003) Nucleotide binding induces changes in the oligomeric state and conformation of Sec A in a lipid environment: a small-angle neutron-scattering study. *J Mol Biol*, **332**, 23-30.

Cannon, K.S., Or, E., Clemons, W.M., Jr., Shibata, Y. and Rapoport, T.A. (2005) Disulfide bridge formation between SecY and a translocating polypeptide localizes the translocation pore to the center of SecY. *J Cell Biol*, **169**, 219-225.

Chen, L. and Tai, P.C. (1985) ATP is essential for protein translocation into *Escherichia coli* membrane vesicles. *Proc Natl Acad Sci USA*, **82**, 4384-4388.

Chen, X., Xu, H. and Tai, P.C. (1996) A significant fraction of functional SecA is permanently embedded in the membrane. SecA cycling on and off the membrane is not essential during protein translocation. *J Biol Chem*, **271**, 29698-29706.

Chou, Y.T., Swain, J.F. and Gierasch, L.M. (2002) Functionally significant mobile regions of *Escherichia coli* SecA ATPase identified by NMR. *J Biol Chem*, **277**, 50985-50990.

Christensen, H., Martin, M.T. and Waley, S.G. (1990) Beta-lactamases as fully efficient enzymes. Determination of all the rate constants in the acyl-enzyme mechanism. *Biochem J*, **266**, 853-861.

Chua, N.H. and Schmidt, G.W. (1978) Post-translational transport into intact chloroplasts of a precursor to the small subunit of ribulose-1,5-bisphosphate carboxylase. *Proc Natl Acad Sci USA*, **75**, 6110-6114.

Clark, S.A. and Theg, S.M. (1997) A folded protein can be transported across the chloroplast envelope and thylakoid membranes. *Mol Biol Cell*, **8**, 923-934.

Collinson, I., Breyton, C., Duong, F., Tziatzios, C., Schubert, D., Or, E., Rapoport, T.A. and Kühlbrandt, W. (2001) Projection structure and oligomeric properties of a bacterial core protein translocase. *Embo J*, **20**, 2462-2471.

Connolly, T., Rapiejko, P.J. and Gilmore, R. (1991) Requirement of GTP Hydrolysis for Dissociation of the Signal Recognition Particle from Its Receptor. *Science*, **252**, 1171-1173.

Crooke, E., Brundage, L., Rice, M. and Wickner, W. (1988) ProOmpA spontaneously folds in a membrane assembly competent state which trigger factor stabilizes. *Embo J*, **7**, 1831-1835.

Cornelis, G.R. (2006) The type III secretion injectisome. *Nat Rev Microbiol*, **4**, 811-825.

Crowley, K., Liao, S., Worrell, V., Reinhart, G. and Johnson, A. (1994a) Secretory proteins move through the endoplasmic reticulum membrane via an aqueous, gated pore. *Cell*, **78**, 461-471.

Crowley, K.S., Liao, S.R., Worrell, V.E., Reinhart, G.D. and Johnson, A.E. (1994b) Secretory proteins move through the endoplasmic reticulum membrane via an aqueous, gated pore. *Cell*, **78**, 461-471.

Crowther, R., Henderson, R. and Smith, J. (1996) MRC image processing programs. *J Struct Biol*, **116**, 9-16.

Cunningham, K. and Wickner, W. (1989) Specific recognition of the leader region of precursor proteins is required for the activation of translocation ATPase of *Escherichia coli*. *Proc Natl Acad Sci USA*, **86**, 8630-8634.

Dalbey, R.E., Kuhn, A. and von Heijne, G. (1995) Directionality in protein translocation across membranes: the N-tail phenomenon. *Trends Cell Biol*, **5**, 380-383.

Demeler, B. and Saber, H. (1998) Determination of molecular parameters by fitting sedimentation data to finite-element solutions of the Lamm equation. *Biophys J*, **74**, 444-454.

Demeler, B., Scott, D. J., Harding, S.E. and Rowe, A.J. (2005) *A Comprehensive Data Analysis Software Package for Analytical Ultracentrifugation Experiments. Modern Analytical Ultracentrifugation: Techniques and Methods.*

de Keyzer, J., Van der Does, C. and Driessen, A.J. (2002) Kinetic analysis of the translocation of fluorescent precursor proteins into *Escherichia coli* membrane vesicles. *J Biol Chem*, **277**, 46059-46065.

de Keyzer, J., van der Does, C., Kloosterman, T.G. and Driessen, A.J.M. (2003) Direct Demonstration of ATP-dependent Release of SecA from a Translocating Preprotein by Surface Plasmon Resonance. *J Biol Chem*, **278**, 29581-29586.

de Keyzer, J., van der Sluis, E.O., Spelbrink, R.E., Nijstad, N., de Kruijff, B., Nouwen, N., van der Does, C. and Driessen, A.J. (2005) Covalently dimerized SecA is functional in protein translocation. *J Biol Chem*, **280**, 35255-35260.

de Kruijff, B., Verkleij, A.J., Leunissen-Bijvelt, J., Van Echteld, C.J., Hille, J. and Rijnbout, H. (1982) Further aspects of the Ca^{2+}-dependent polymorphism of bovine heart cardiolipin. *Biochim Biophys Acta*, **693**, 1-12.

de Vrije, T., Batenburg, A.M., Jordi, W. and de Kruijff, B. (1989) Inhibition of PhoE translocation across *Escherichia coli* inner-membrane vesicles by synthetic signal peptides suggests an important role of acidic phospholipids in protein translocation. *Eur J Biochem*, 180, 385-392.

de Vrije, T., de Swart, R., Dowhan, W., Tommassen, J. and de Kruijff, B. (1988) Phosphatidylglycerol is involved in protein translocation across *Escherichia coli* inner membranes. *Nature*, 334, 173-175.

den Blaauwen, T., Fekkes, P., de Wit, J.G., Kuiper, W. and Driessen, A.J. (1996) Domain interactions of the peripheral preprotein Translocase subunit SecA. *Biochemistry*, 35, 11994-12004.

den Blaauwen, T., Terpetschnig, E., Lakowicz, J.R. and Driessen, A.J. (1997) Interaction of SecB with soluble SecA. *FEBS Lett*, 416, 35-38.

den Blaauwen, T., van der Wolk, J.P., van der Does, C., van Wely, K.H. and Driessen, A.J. (1999) Thermodynamics of nucleotide binding to NBS-I of the *Bacillus subtilis* preprotein translocase subunit SecA. *FEBS Lett*, 458, 145-150.

Derman, A., Puziss, J., Bassford, P.J. and Beckwith, J. (1993) A signal sequence is not required for protein export in prlA mutants of *Escherichia coli*. *Embo J*, 12, 879-888.

Dillingham, M.S., Wigley, D.B. and Webb, M.R. (2000) Demonstration of unidirectional single-stranded DNA translocation by PcrA helicase: measurement of step size and translocation speed. *Biochemistry*, 39, 205-212.

Ding, H., Hunt, J.F., Mukerji, I. and Oliver, D. (2003) *Bacillus subtilis* SecA ATPase Exists as an Antiparallel Dimer in Solution. *Biochemistry*, 42, 8729-8738.

Doud, S.K., Chou, M.M. and Kendall, D.A. (1993) Titration of Protein Transport Activity by Incremental Changes in Signal Peptide Hydrophobicity. *Biochemistry*, 32, 1251-1256.

Driessen, A. (1993) SecA, the peripheral subunit of the *Escherichia coli* precursor protein translocase, is functional as a dimer. *Biochemistry*, 32, 13190-13197.

Driessen, A., Manting, E. and van, d.D.C. (2001) The structural basis of protein targeting and translocation in bacteria. *Nat Struct Biol*, 8, 492-498.

Driessen, A.J. (2001) SecB, a molecular chaperone with two faces. *Trends Microbiol*, 9, 193-196.

Duong, F. (2003) Binding, activation and dissociation of the dimeric SecA ATPase at the dimeric SecYEG translocase. *Embo J*, 22, 4375-4384.

Duong, F. and Wickner, W. (1997a) Distinct catalytic roles of the SecYE, SecG and SecDFyajC subunits of preprotein translocase holoenzyme. *Embo J*, **16**, 2756-2768.

Duong, F. and Wickner, W. (1997b) The SecDFyajC domain of preprotein translocase controls preprotein movement by regulating SecA membrane cycling. *Embo J*, **16**, 4871-4879.

Duong, F. and Wickner, W. (1999) The PrlA and PrlG phenotypes are caused by a loosened association among the translocase SecYEG subunits. *Embo J*, **18**, 3263-3270.

Dworetzky, S.I. and Feldherr, C.M. (1988) Translocation of RNA-coated gold particles through the nuclear pores of oocytes. *J Cell Biol*, **106**, 575-584.

Economou, A., Pogliano, J., Beckwith, J., Oliver, D. and Wickner, W. (1995) SecA membrane cycling at SecYEG is driven by distinct ATP binding and hydrolysis events and is regulated by SecD and SecF. *Cell*, **83**, 1171-1181.

Economou, A. and Wickner, W. (1994) SecA promotes preprotein translocation by undergoing ATP-driven cycles of membrane insertion and deinsertion. *Cell*, **78**, 835-843.

Egea, P.F., Shan, S.O., Napetschnig, J., Savage, D.F., Walter, P. and Stroud, R.M. (2004) Substrate twinning activates the signal recognition particle and its receptor. *Nature*, **427**, 215-221.

Eichler, J., Brunner, J. and Wickner, W. (1997) The protease-protected 30 kDa domain of SecA is largely inaccessible to the membrane lipid phase. *Embo J*, **16**, 2188-2196.

Eichler, J. and Wickner, W. (1997) Both an N-terminal 65-kDa domain and a C-terminal 30-kDa domain of SecA cycle into the membrane at SecYEG during translocation. *Proc Natl Acad Sci USA*, **94**, 5574-5581.

Elston, T., Wang, H. and Oster, G. (1998) Energy transduction in ATP synthase. *Nature*, **391**, 510-513.

Emr, S.D., Hanley-Way, S. and Silhavy, T. (1981) Suppressor mutations that restore export of a protein with a defective signal sequence. *Cell*, **23**, 79-88.

Emi, B., Trachsel, H., Postma, P.W. and Rosenbusch, J.P. (1982) Bacterial phosphotransferase system. Solubilization and purification of the glucose-specific enzyme II from membranes of Salmonella typhimurium. *J Biol Chem*, **257**, 13726-13730.

Facey, S.J., Neugebauer, S.A., Krauss, S. and Kuhn, A. (2007) The mechanosensitive channel protein MscL is targeted by the SRP to the novel YidC membrane insertion pathway of *Escherichia coli*. *J Mol Biol*, **365**, 995-1004.

Fak, J.J., Itkin, A., Ciobanu, D.D., Lin, E.C., Song, X.J., Chou, Y.T., Gierasch, L.M. and Hunt, J.F. (2004) Nucleotide exchange from the high-affinity ATP-binding site in SecA is the rate-limiting step in the ATPase cycle of the soluble enzyme and occurs through a specialized conformational state. *Biochemistry*, **43**, 7307-7327.

Fekkes, P., de, W.J., Boorsma, A., Friesen, R. and Driessen, A. (1999) Zinc stabilizes the SecB binding site of SecA. *Biochemistry*, **38**, 5111-5116.

Fekkes, P., van der Does, C. and Driessen, A.J. (1997) The molecular chaperone SecB is released from the carboxy-terminus of SecA during initiation of precursor protein translocation. *Embo J*, **16**, 6105-6113.

Feldherr, C.M., Kallenbach, E. and Schultz, N. (1984) Movement of a karyophilic protein through the nuclear pores of oocytes. *J Cell Biol*, **99**, 2216-2222.

Flower, A., Osborne, R. and Silhavy, T. (1995) The allele-specific synthetic lethality of prlA-prlG double mutants predicts interactive domains of SecY and SecE. *Embo J*, **14**, 884-893.

Focia, P.J., Shepotinovskaya, I.V., Seidler, J.A. and Freymann, D.M. (2004) Heterodimeric GTPase core of the SRP targeting complex. *Science*, **303**, 373-377.

Froderberg, L., Houben, E.N., Baars, L., Luirink, J. and de Gier, J.W. (2004) Targeting and translocation of two lipoproteins in *Escherichia coli* via the SRP/Sec/YidC pathway. *J Biol Chem*, **279**, 31026-31032.

Froschauer, E.M., Kolisek, M., Dieterich, F., Schweigel, M. and Schweyen, R.J. (2004) Fluorescence measurements of free [Mg^{2+}] by use of mag-fura 2 in Salmonella enterica. *FEMS Microbiol Lett*, **237**, 49-55.

Funes, S., Nargang, F.E., Neupert, W. and Herrmann, J.M. (2004) The Oxa2 protein of Neurospora crassa plays a critical role in the biogenesis of cytochrome oxidase and defines a ubiquitous subbranch of the Oxa1/YidC/Alb3 protein family. *Mol Biol Cell*, **15**, 1853-1861.

Gardel, C., Benson, S., Hunt, J., Michaelis, S. and Beckwith, J. (1987) secD, a new gene involved in protein export in *Escherichia coli*. *J Bacteriol*, **169**, 1286-1290.

Gardel, C., Johnson, K., Jacq, A. and Beckwith, J. (1990) The SecD Locus of *E. coli* Codes for 2 Membrane Proteins Required for Protein Export. *Embo J*, **9**, 3209-3216.

Gelis, I., Bonvin, A.M., Keramisanou, D., Koukaki, M., Gouridis, G., Karamanou, S., Economou, A. and Kalodimos, C.G. (2007) Structural Basis for Signal-Sequence Recognition by the Translocase Motor SecA as Determined by NMR. *Cell*, **131**, 756-769.

Gilmore, R. and Blobel, G. (1983) Transient involvement of signal recognition particle and its receptor in the microsomal membrane prior to protein translocation. *Cell*, **35**, 677-685.

Gilmore, R., Walter, P. and Blobel, G. (1982) Protein translocation across the endoplasmic reticulum. II. Isolation and characterization of the signal recognition particle receptor. *J Cell Biol*, **95**, 470-477.

Gomez, B., Jr. and Robinson, N.C. (1999) Phospholipase digestion of bound cardiolipin reversibly inactivates bovine cytochrome bc1. *Biochemistry*, **38**, 9031-9038.

Görlich, D., Prehn, S., Hartmann, E., Kalies, K. and Rapoport, T. (1992) A mammalian homolog of SEC61p and SECYp is associated with ribosomes and nascent polypeptides during translocation. *Cell*, **71**, 489-503.

Görlich, D. and Rapoport, T.A. (1993) Protein Translocation into Proteoliposomes Reconstituted from Purified Components of the Endoplasmic Reticulum Membrane. *Cell*, **75**, 615-630.

Gorter, E., Grendel, F. and (1925) On bimolecular layers of lipids on the chromocytes of the blood. *J Exp Med*, **41**, 439-443.

Gumbart, J. and Schulten, K. (2006) Molecular dynamics studies of the archaeal translocon. *Biophys J*, **90**, 2356-2367.

Guzman, L.M., Belin, D., Carson, M.J. and Beckwith, J. (1995) Tight regulation, modulation, and high-level expression by vectors containing the arabinose PBAD promoter. *J Bacteriol*, **177**, 4121-4130.

Haigh, N.G. and Johnson, A.E. (2002) A new role for BiP: closing the aqueous translocon pore during protein integration into the ER membrane. *J Cell Biol*, **156**, 261-270.

Halic, M., Becker, T., Pool, M.R., Spahn, C.M., Grassucci, R.A., Frank, J. and Beckmann, R. (2004) Structure of the signal recognition particle interacting with the elongation-arrested ribosome. *Nature*, **427**, 808-814.

Hamman, B., Chen, J., Johnson, E. and Johnson, A. (1997) The aqueous pore through the translocon has a diameter of 40-60 A during cotranslational protein translocation at the ER membrane. *Cell*, **89**, 535-544.

Hamman, B.D., Hendershot, L.M. and Johnson, A.E. (1998) BiP maintains the permeability barrier of the ER membrane by sealing the lumenal end of the translocon pore before and early in translocation. *Cell*, **92**, 747-758.

Hanada, M., Nishiyama, K., Mizushima, S. and Tokuda, H. (1994) Reconstitution of an efficient protein translocation machinery comprising SecA and the three membrane proteins, SecY, SecE, and SecG (p12). *J Biol Chem*, **269**, 23625-23631.

Hanein, D., Matlack, K., Jungnickel, B., Plath, K., Kalies, K., Miller, K., Rapoport, T. and Akey, C. (1996) Oligomeric rings of the Sec61p complex induced by ligands required for protein translocation. *Cell*, **87**, 721-732.

Harris, C.R. and Silhavy, T.J. (1999) Mapping an interface of SecY (PrlA) and SecE (PrlG) by using synthetic phenotypes and in vivo cross-linking. *J Bacteriol*, **181**, 3438-3444.

Hartl, F., Lecker, S., Schiebel, E., Hendrick, J. and Wickner, W. (1990) The binding cascade of SecB to SecA to SecY/E mediates preprotein targeting to the *E. coli* plasma membrane. *Cell*, **63**, 269-279.

Hayer-Hartl, M., Schagger, H., von Jagow, G. and Beyer, K. (1992) Interactions of phospholipids with the mitochondrial cytochrome-c reductase studied by spin-label ESR and NMR spectroscopy. *Eur J Biochem*, **209**, 423-430.

Hell, K., Neupert, W. and Stuart, R.A. (2001) Oxa1p acts as a general membrane insertion machinery for proteins encoded by mitochondrial DNA. *Embo J*, **20**, 1281-1288.

Hendrick, J.P. and Wickner, W. (1991) SecA Protein Needs Both Acidic Phospholipids and SecY/E Protein for Functional High-Affinity Binding to the *Escherichia coli* Plasma Membrane. *J Biol Chem*, **266**, 24596-24600.

Hoffmann, B., Stockl, A., Schlame, M., Beyer, K. and Klingenberg, M. (1994) The reconstituted ADP/ATP carrier activity has an absolute requirement for cardiolipin as shown in cysteine mutants. *J Biol Chem*, **269**, 1940-1944.

Houben, E.N., Ten Hagen-Jongman, C.M., Brunner, J., Oudega, B. and Luirink, J. (2004) The two membrane segments of leader peptidase partition one by one into the lipid bilayer via a Sec/YidC interface. *Embo Rep*, **5**, 970-975.

Huber, D., Boyd, D., Xia, Y., Olma, M.H., Gerstein, M. and Beckwith, J. (2005) Use of thioredoxin as a reporter to identify a subset of *Escherichia coli* signal sequences that promote signal recognition particle-dependent translocation. *J Bacteriol*, **187**, 2983-2991.

Hunt, J.F., Weinkauf, S., Henry, L., Fak, J.J., McNicholas, P., Oliver, D.B. and Deisenhofer, J. (2002) Nucleotide Control of Interdomain Interactions in the Conformational Reaction Cycle of SecA. *Science*, **297**, 2018-2026.

Jilaveanu, L.B. and Oliver, D. (2006) SecA dimer cross-linked at its subunit interface is functional for protein translocation. *J Bacteriol*, **188**, 335-338.

Jilaveanu, L.B. and Oliver, D.B. (2007) In vivo membrane topology of *Escherichia coli* SecA ATPase reveals extensive periplasmic exposure of multiple functionally important domains clustering on one face of SecA. *J Biol Chem*, **282**, 4661-4668.

Jilaveanu, L.B., Zito, C.R. and Oliver, D. (2005) Dimeric SecA is essential for protein translocation. *Proc Natl Acad Sci USA*, **102**, 7511-7516.

Karamanou, S., Sianidis, G., Gouridis, G., Pozidis, C., Papanikolau, Y., Papanikou, E. and Economou, A. (2005) *Escherichia coli* SecA truncated at its termini is functional and dimeric. *FEBS Lett*, **579**, 1267-1271.

Karamanou, S., Vrontou, E., Sianidis, G., Baud, C., Roos, T., Kuhn, A., Politou, A.S. and Economou, A. (1999) A molecular switch in SecA protein couples ATP hydrolysis to protein translocation. *Mol Microbiol*, **34**, 1133-1145.

Karamyshev, A.L. and Johnson, A.E. (2005) Selective SecA association with signal sequences in ribosome-bound nascent chains: a potential role for SecA in ribosome targeting to the bacterial membrane. *J Biol Chem*, **280**, 37930-37940.

Kaufmann, A., Manting, E.H., Veenendaal, A.K., Driessen, A.J. and van_der_Does, C. (1999) Cysteine-directed cross-linking demonstrates that helix 3 of SecE is close to helix 2 of SecY and helix 3 of a neighboring SecE. *Biochemistry*, **38**, 9115-9125.

Kebir, M.O. and Kendall, D.A. (2002) SecA specificity for different signal peptides. *Biochemistry*, **41**, 5573-5580.

Keramisanou, D., Biris, N., Gelis, I., Sianidis, G., Karamanou, S., Economou, A. and Kalodimos, C.G. (2006) Disorder-order folding transitions underlie catalysis in the helicase motor of SecA. *Nat Struct Mol Biol*, **13**, 594-602.

Kim, J., Ahn, T., Ko, J., Park, C. and Kim, H. (2001a) Effect of divalent cations on the ATPase activity of *Escherichia coli* SecA. *FEBS Lett*, **493**, 12-16.

Kim, J., Miller, A., Wang, L., Muller, J.P. and Kendall, D.A. (2001b) Evidence that SecB enhances the activity of SecA. *Biochemistry*, **40**, 3674-3680.

Kim, P.S. and Baldwin, R.L. (1982) Specific intermediates in the folding reactions of small proteins and the mechanism of protein folding. *Annu Rev Biochem*, **51**, 459-489.

Kim, Y.J., Rajapandi, T. and Oliver, D. (1994) SecA protein is exposed to the periplasmic surface of the *E. coli* inner membrane in its active state. *Cell*, **78**, 845-853.

Kimura, E., Akita, M., Matsuyama, S. and Mizushima, S. (1991) Determination of a Region in secA That Interacts with Presecretory Proteins in *Escherichia coli*. *J Biol Chem*, **266**, 6600-6606.

Koonin, E.V. and Gorbalenya, A.E. (1992) Autogenous translation regulation by *Escherichia coli* ATPase SecA may be mediated by an intrinsic RNA helicase activity of this protein. *FEBS Lett*, **298**, 6-8.

Kourtz, L. and Oliver, D. (2000) Tyr-326 plays a critical role in controlling SecA-preprotein interaction. *Mol Microbiol*, **37**, 1342-1356.

Kumamoto, C.A. and Beckwith, J. (1983) Mutations in a new gene, secB, cause defective protein localization in *Escherichia coli*. *J Bacteriol*, **154**, 253-260.

Kusters, R., de Vrije, T., Breukink, E. and de Kruijff, B. (1989) SecB Protein Stabilizes a Translocation-Competent State of Purified PrePhoe Protein. *J Biol Chem*, **264**, 20827-20830.

Kusters, R., Dowhan, W. and de Kruijff, B. (1991) Negatively charged phospholipids restore prePhoE translocation across phosphatidylglycerol-depleted *Escherichia coli* inner membranes. *J Biol Chem*, **266**, 8659-8662.

Lamm, O. (1929) Die Differentialgleichung der Ultrazentrifugierung. *Ark. Mat. Astron. Fys.*, **21B**, 1-4.

Lange, C., Nett, J.H., Trumpower, B.L. and Hunte, C. (2001) Specific roles of protein-phospholipid interactions in the yeast cytochrome bc1 complex structure. *Embo J*, **20**, 6591-6600.

Langmuir, I. (1917) The constitution and fundamental properties of solids and liquids. II. Liquids. *J Am Chem Soc*, **39**, 1848-1906.

Lecker, S.H., Driessen, A.J.M. and Wickner, W. (1990) Proompa Contains Secondary and Tertiary Structure Prior to Translocation and Is Shielded from Aggregation by Association with Secb Protein. *Embo J*, **9**, 2309-2314.

Lee, H.C. and Bernstein, H.D. (2001) The targeting pathway of *Escherichia coli* presecretory and integral membrane proteins is specified by the hydrophobicity of the targeting signal. *Proc Natl Acad Sci USA*, **98**, 3471-3476.

Lee, A.G. (2003) Lipid-protein interactions in biological membranes: a structural perspective. *Biochim Biophys Acta*, **1612**, 1-40.

Li, W., Schulman, S., Boyd, D., Erlandson, K., Beckwith, J. and Rapoport, T.A. (2007) The plug domain of the SecY protein stabilizes the closed state of the translocation channel and maintains a membrane seal. *Mol Cell*, **26**, 511-521.

Lill, R., Cunningham, K., Brundage, L., Ito, K., Oliver, D. and Wickner, W. (1989) SecA protein hydrolyzes ATP and is an essential component of the protein translocation ATPase of *Escherichia coli*. *Embo J*, **8**, 961-966.

Lill, R., Dowhan, W. and Wickner, W. (1990) The ATPase activity of SecA is regulated by acidic phospholipids, SecY, and the leader and mature domains of precursor proteins. *Cell*, **60**, 271-280.

Luirink, J., ten Hagen-Jongman, C.M., van der Weijden, C.C., Oudega, B., High, S., Dobberstein, B. and Kusters, R. (1994) An alternative targeting pathway in *Escherichia coli*: studies on the role of FtsY. *Embo J*, **13**, 2289-2296.

Lutter, R., Abrahams, J.P., van Raaij, M.J., Todd, R.J., Lundqvist, T., Buchanan, S.K., Leslie, A.G. and Walker, J.E. (1993) Crystallization of F1-ATPase from bovine heart mitochondria. *J Mol Biol*, **229**, 787-790.

Maccecchini, M.L., Rudin, Y., Blobel, G. and Schatz, G. (1979) Import of proteins into mitochondria: precursor forms of the extramitochondrially made F1-ATPase subunits in yeast. *Proc Natl Acad Sci USA*, **76**, 343-347.

Maillard, A.P., Lalani, S., Silva, F., Belin, D. and Duong, F. (2007) Deregulation of the SecYEG translocation channel upon removal of the plug domain. *J Biol Chem*, **282**, 1281-1287.

Manting, E.H., van der Does, C., Remigy, H., Engel, A. and Driessen, A.J. (2000) SecYEG assembles into a tetramer to form the active protein translocation channel. *Embo J*, **19**, 852-861.

Matlack, K., Misselwitz, B., Plath, K. and Rapoport, T. (1999) BiP acts as a molecular ratchet during posttranslational transport of prepro-alpha factor across the ER membrane. *Cell*, **97**, 553-564.

Matsumoto, G., Nakatogawa, H., Mori, H. and Ito, K. (2000) Genetic dissection of SecA: suppressor mutations against the secY205 translocase defect. *Genes Cells*, **5**, 991-999.

Matsumoto, G., Yoshihisa, T. and Ito, K. (1997) SecY and SecA interact to allow SecA insertion and protein translocation across the *Escherichia coli* plasma membrane. *Embo J*, **16**, 6384-6393.

Matsuyama, S., Fujita, Y. and Mizushima, S. (1993) SecD Is Involved in the Release of Translocated Secretory Proteins from the Cytoplasmic Membrane of *Escherichia coli*. *Embo J*, **12**, 265-270.

McNew, J.A. and Goodman, J.M. (1994) An oligomeric protein is imported into peroxisomes in vivo. *J Cell Biol*, **127**, 1245-1257.

Menetret, J.F., Hegde, R.S., Heinrich, S.U., Chandramouli, P., Ludtke, S.J., Rapoport, T.A. and Akey, C.W. (2005) Architecture of the ribosome-channel complex derived from native membranes. *J Mol Biol*, **348**, 445-457.

Menetret, J.F., Neuhof, A., Morgan, D.G., Plath, K., Radermacher, M., Rapoport, T.A. and Akey, C.W. (2000) The structure of ribosome-channel complexes engaged in protein translocation. *Mol Cell*, **6**, 1219-1232.

Menz, R.I., Walker, J.E. and Leslie, A.G. (2001) Structure of bovine mitochondrial F(1)-ATPase with nucleotide bound to all three catalytic sites: implications for the mechanism of rotary catalysis. *Cell*, **106**, 331-341.

Miller, A., Wang, L. and Kendall, D.A. (1998) Synthetic signal peptides specifically recognize SecA and stimulate ATPase activity in the absence of preprotein. *J Biol Chem*, **273**, 11409-11412.

Miller, A., Wang, L. and Kendall, D.A. (2002) SecB modulates the nucleotide-bound state of SecA and stimulates ATPase activity. *Biochemistry*, **41**, 5325-5332.

Miller, J.D., Wilhelm, H., Gierasch, L., Gilmore, R. and Walter, P. (1993) GTP Binding and Hydrolysis by the Signal Recognition Particle During Initiation of Protein Translocation. *Nature*, **366**, 351-354.

Milstein, C., Brownlee, G.G., Harrison, T.M. and Mathews, M.B. (1972) A possible precursor of immunoglobulin light chains. *Nature New Biol*, **239**, 117-120.

Miroux, B. and Walker, J. (1996) Over-production of proteins in *Escherichia coli:* mutant hosts that allow synthesis of some membrane proteins and globular proteins at high levels. *J Mol Biol*, **260**, 289-298.

Misselwitz, B., Staeck, O., Matlack, K. and Rapoport, T. (1999) Interaction of BiP with the J-domain of the Sec63p component of the endoplasmic reticulum protein translocation complex. *J Biol Chem*, **274**, 20110-20115.

Mitchell, C. and Oliver, D. (1993) Two Distinct ATP-Binding Domains Are Needed to Promote Protein Export by *Escherichia coli* SecA ATPase. *Mol Microbiol*, **10**, 483-497.

Mitra, K. and Frank, J. (2006) A model for co-translational translocation: ribosome-regulated nascent polypeptide translocation at the protein-conducting channel. *FEBS Lett*, **580**, 3353-3360.

Mitra, K., Schaffitzel, C., Shaikh, T., Tama, F., Jenni, S., Brooks, C.L., 3rd, Ban, N. and Frank, J. (2005) Structure of the *E. coli* protein-conducting channel bound to a translating ribosome. *Nature*, **438**, 318-324.

Monne, M., Gafvelin, G., Nilsson, R. and von Heijne, G. (1999) N-tail translocation in a eukaryotic polytopic membrane protein: synergy between neighboring transmembrane segments. *Eur J Biochem*, **263**, 264-269.

Moore, M., Harrison, M.S., Peterson, E.C. and Henry, R. (2000) Chloroplast Oxa1p homolog albino3 is required for post-translational integration of the light harvesting chlorophyll-binding protein into thylakoid membranes. *J Biol Chem*, **275**, 1529-1532.

Morgan, D.G., Menetret, J.-F., Neuhof, A., Rapoport, T.A. and Akey, C.W. (2002) Structure of the Mammalian Ribosome-Channel Complex at 17 Å Resolution. *J Mol Biol*, **324**, 871-886.

Mori, H. and Ito, K. (2001) An essential amino acid residue in the protein translocation channel revealed by targeted random mutagenesis of SecY. *Proc Natl Acad Sci USA*, **98**, 5128-5133.

Mori, H. and Ito, K. (2003) Biochemical characterization of a mutationally altered protein translocase: proton motive force stimulation of the initiation phase of translocation. *J Bacteriol*, **185**, 405-412.

Mori, H. and Ito, K. (2006) Different modes of SecY-SecA interactions revealed by site-directed in vivo photo-cross-linking. *Proc Natl Acad Sci USA*, **103**, 16159-16164.

Mori, H., Tsukazaki, T., Masui, R., Kuramitsu, S., Yokoyama, S., Johnson, A.E., Kimura, Y., Akiyama, Y. and Ito, K. (2003) Fluorescence resonance energy transfer analysis of protein translocase. SecYE from *Thermus thermopholus* HB8 forms a constitutive oligomer in membranes. *J Biol Chem*, **278**, 14257-14264.

Mould, R.M. and Robinson, C. (1991) A Proton Gradient Is Required for the Transport of Two Lumenal Oxygen-Evolving Proteins Across the Thylakoid Membrane. *J Biol Chem*, **266**, 12189-12193.

Müller, M. and Blobel, G. (1984) In vitro translocation of bacterial proteins across the plasma membrane of *Escherichia coli*. *Proc Natl Acad Sci USA*, **81**, 7421-7425.

Müller, M., Koch, H., Beck, K. and Schafer, U. (2001) Protein traffic in bacteria: multiple routes from the ribosome to and across the membrane. *Prog Nucleic Acid Res Mol Biol*, **66**, 107-157.

Musial-Siwek, M., Rusch, S.L. and Kendall, D.A. (2005) Probing the affinity of SecA for signal peptide in different environments. *Biochemistry*, **44**, 13987-13996.

Musial-Siwek, M., Rusch, S.L. and Kendall, D.A. (2007) Selective Photoaffinity Labeling Identifies the Signal Peptide Binding Domain on SecA. *J Mol Biol*, **365**, 637–648.

Natale, P., Swaving, J., van der Does, C., de Keyzer, J. and Driessen, A.J. (2004) Binding of SecA to the SecYEG complex accelerates the rate of nucleotide exchange on SecA. *J Biol Chem*, **279**, 13769-13777.

Neuhof, A., Rolls, M., Jungnickel, B., Kalies, K. and Rapoport, T. (1998) Binding of signal recognition particle gives ribosome/nascent chain complexes a competitive advantage in endoplasmic reticulum membrane interaction. *Mol Biol Cell*, **9**, 103-115.

Neumann-Haefelin, C., Schafer, U., Muller, M. and Koch, H. (2000) SRP-dependent co-translational targeting and SecA-dependent translocation analyzed as individual steps in the export of a bacterial protein. *Embo J*, **19**, 6419-6426.

Nilsson, I., Witt, S., Kiefer, H., Mingarro, I. and von Heijne, G. (2000) Distant downstream sequence determinants can control N-tail translocation during protein insertion into the endoplasmic reticulum membrane. *J Biol Chem*, **275**, 6207-6213.

Nishiyama, K., Fukuda, A., Morita, K. and Tokuda, H. (1999) Membrane deinsertion of SecA underlying proton motive force-dependent stimulation of protein translocation. *Embo J*, **18**, 1049-1058.

Nishiyama, K., Hanada, M. and Tokuda, H. (1994) Disruption of the gene encoding p12 (SecG) reveals the direct involvement and important function of SecG in the protein translocation of *Escherichia coli* at low temperature. *Embo J*, **13**, 3272-3277.

Nishiyama, K., Mizushima, S. and Tokuda, H. (1993) A Novel Membrane Protein Involved in Protein Translocation Across the Cytoplasmic Membrane of *Escherichia coli*. *Embo J*, **12**, 3409-3415.

Nishiyama, K., Suzuki, T. and Tokuda, H. (1996) Inversion of the membrane topology of SecG coupled with SecA-dependent preprotein translocation. *Cell*, **85**, 71-81.

Nouwen, N., Berrelkamp, G. and Driessen, A.J. (2007) Bacterial Sec-translocase Unfolds and Translocates a Class of Folded Protein Domains. *J Mol Biol*, **372**, 422-433.

Nouwen, N., de Kruijff, B. and Tommassen, J. (1996) Delta mu H^+ dependency of in vitro protein translocation into *Escherichia coli* inner-membrane vesicles varies with the signal-sequence core-region composition. *Mol Microbiol*, **19**, 1205-1214.

Nouwen, N. and Driessen, A.J. (2002) SecDFyajC forms a heterotetrameric complex with YidC. *Mol Microbiol*, **44**, 1397-1405.

Nouwen, N., van der Laan, M. and Driessen, A.J. (2001) SecDFyajC is not required for the maintenance of the proton motive force. *FEBS Lett*, **508**, 103-106.

Okamoto, K., Brinker, A., Paschen, S.A., Moarefi, I., Hayer-Hartl, M., Neupert, W. and Brunner, M. (2002) The protein import motor of mitochondria: a targeted molecular ratchet driving unfolding and translocation. *Embo J*, **21**, 3659-3671.

Oliver, D. and Beckwith, J. (1981) *E. coli* mutant pleiotropically defective in the export of secreted proteins. *Cell*, **25**, 765-772.

Oliver, D. and Beckwith, J. (1982) Identification of a new gene (secA) and gene product involved in the secretion of envelope proteins in *Escherichia coli*. *J Bacteriol*, **150**, 686-691.

Oliver, D.B. and Liss, L.R. (1985) prlA-mediated suppression of signal sequence mutations is modulated by the secA gene product of *Escherichia coli* K-12. *J Bacteriol*, **161**, 817-819.

Or, E., Boyd, D., Gon, S., Beckwith, J. and Rapoport, T. (2005) The bacterial ATPase SecA functions as a monomer in protein translocation. *J Biol Chem*, **280**, 9097-9105.

Or, E., Navon, A. and Rapoport, T.A. (2002) Dissociation of the dimeric SecA ATPase during protein translocation across the bacterial membrane. *Embo J*, **21**, 4470-4479.

Or, E. and Rapoport, T. (2007) Cross-linked SecA dimers are not functional in protein translocation. *FEBS Lett*, **581**, 2616-2620.

Osborne, A.R., Clemons, W.M., Jr. and Rapoport, T.A. (2004) A large conformational change of the translocation ATPase SecA. *Proc Natl Acad Sci USA*, **101**, 10937-10942.

Osborne, A.R. and Rapoport, T.A. (2007) Protein Translocation Is Mediated by Oligomers of the SecY Complex with One SecY Copy Forming the Channel. *Cell*, **129**, 97-110.

Osborne, A.R., Rapoport, T.A. and van den Berg, B. (2005) Protein translocation by the Sec61/SecY channel. *Annu Rev Cell Dev Biol*, **21**, 529-550.

Ossenbuhl, F., Gohre, V., Meurer, J., Krieger-Liszkay, A., Rochaix, J.D. and Eichacker, L.A. (2004) Efficient assembly of photosystem II in *Chlamydomonas reinhardtii* requires Alb3.1p, a homolog of *Arabidopsis* ALBINO3. *Plant Cell*, **16**, 1790-1800.

Paetzel, M., Karla, A., Strynadka, N.C. and Dalbey, R.E. (2002) Signal peptidases. *Chem Rev*, **102**, 4549-4580.

Panzner, S., Dreier, L., Hartmann, E., Kostka, S. and Rapoport, T. (1995) Posttranslational protein transport in yeast reconstituted with a purified complex of Sec proteins and Kar2p. *Cell*, **81**, 561-570.

Papanikolau, Y., Papadovasilaki, M., Ravelli, R.B., McCarthy, A.A., Cusack, S., Economou, A. and Petratos, K. (2007) Structure of Dimeric SecA, the *Escherichia coli* Preprotein Translocase Motor. *J Mol Biol*, **366**, 1545-1557.

Pebay-Peyroula, E., Dahout-Gonzalez, C., Kahn, R., Trezeguet, V., Lauquin, G.J. and Brandolin, G. (2003) Structure of mitochondrial ADP/ATP carrier in complex with carboxyatractyloside. *Nature*, **426**, 39-44.

Pecoraro, V.L., Hermes, J.D. and Cleland, W.W. (1984) Stability constants of Mg^{2+} and Cd^{2+} complexes of adenine nucleotides and thionucleotides and rate constants for formation and dissociation of MgATP and MgADP. *Biochemistry*, **23**, 5262-5271.

Peterson, J.H., Woolhead, C.A. and Bernstein, H.D. (2003) Basic amino acids in a distinct subset of signal peptides promote interaction with the signal recognition particle. *J Biol Chem*, **278**, 46155-46162.

Plath, K., Mothes, W., Wilkinson, B., Stirling, C. and Rapoport, T. (1998) Signal sequence recognition in posttranslational protein transport across the yeast ER membrane. *Cell*, **94**, 795-807.

Pogliano, J. and Beckwith, J. (1994) SecD and SecF facilitate protein export in *Escherichia coli*. *Embo J*, **13**, 554-561.

Pohlschroder, M., Prinz, W., Hartmann, E. and Beckwith, J. (1997) Protein translocation in the three domains of life: variations on a theme. *Cell*, **91**, 563-566.

Qi, H.Y. and Bernstein, H.D. (1999) SecA is required for the insertion of inner membrane proteins targeted by the *Escherichia coli* signal recognition particle. *J Biol Chem*, **274**, 8993-8997.

Ramamurthy, V. and Oliver, D. (1997) Topology of the integral membrane form of *Escherichia coli* SecA protein reveals multiple periplasmically exposed regions and modulation by ATP binding. *J Biol Chem*, **272**, 23239-23246.

Randall, L.L., Crane, J.M., Lilly, A.A., Liu, G., Mao, C., Patel, C.N. and Hardy, S.J. (2005) Asymmetric binding between SecA and SecB two symmetric proteins: implications for function in export. *J Mol Biol*, **348**, 479-489.

Randall, L.L. and Hardy, S.J. (2002) SecB, one small chaperone in the complex milieu of the cell. *Cell Mol Life Sci*, **59**, 1617-1623.

Rapoport, T., Matlack, K., Plath, K., Misselwitz, B. and Staeck, O. (1999) Posttranslational protein translocation across the membrane of the endoplasmic reticulum. *J Biol Chem*, **380**, 1143-1150.

Riggs, P.D., Derman, A.I. and Beckwith, J. (1988) A mutation affecting the regulation of a secA-lacZ fusion defines a new sec gene. *Genetics*, **118**, 571-579.

Robertson, J.D. (1959) The ultrastructure of cell membranes and their derivatives. *Biochem Soc Symp*, **16**, 3-43.

Robson, A. and Collinson, I. (2006) The structure of the Sec complex and the problem of protein translocation. *Embo Rep*, **7**, 1099-1103.

Robson, A., Booth, A.E., Gold, V.A., Clarke, A.R. and Collinson, I. (2007) A Large Conformational Change Couples the ATP Binding Site of SecA to the SecY Protein Channel. *J Mol Biol*, **374**, 965-976.

Römisch, K., Webb, J., Herz, J., Prehn, S., Frank, R., Vingron, M. and Dobberstein, B. (1989) Homology of 54K protein of signal-recognition particle, docking protein and two *E. coli* proteins with putative GTP-binding domains. *Nature*, **340**, 478-482.

Samuelson, J., Chen, M., Jiang, F., Moller, I., Wiedmann, M., Kuhn, A., Phillips, G. and Dalbey, R. (2000) YidC mediates membrane protein insertion in bacteria. *Nature*, **406**, 637-641.

Saparov, S.M., Erlandson, K., Cannon, K., Schaletzky, J., Schulman, S., Rapoport, T.A. and Pohl, P. (2007) Determining the conductance of the SecY protein translocation channel for small molecules. *Mol Cell*, **26**, 501-509.

Saraste, M., Sibbald, P.R. and Wittinghofer, A. (1990) The P-loop--a common motif in ATP- and GTP-binding proteins. *Trends Biochem Sci*, **15**, 430-434.

Scheuring, J., Braun, N., Nothdurft, L., Stumpf, M., Veenendaal, A.K., Kol, S., van der Does, C., Driessen, A.J. and Weinkauf, S. (2005) The oligomeric distribution of SecYEG is altered by SecA and translocation ligands. *J Mol Biol*, **354**, 258-271.

Schiebel, E., Driessen, A.J.M., Hartl, F.-U. and Wickner, W. (1991) $D\mu H^+$ and ATP Function at Different Steps of the Catalytic Cycle of Preprotein Translocase. *Cell*, **64**, 927-939.

Schmidt, M., Ding, H., Ramamurthy, V., Mukerji, I. and Oliver, D. (2000) Nucleotide binding activity of SecA homodimer is conformationally regulated by temperature and altered by prlD and azi mutations. *J Biol Chem*, **275**, 15440-15448.

Serek, J., Bauer-Manz, G., Struhalla, G., van den Berg, L., Kiefer, D., Dalbey, R. and Kuhn, A. (2004) *Escherichia coli* YidC is a membrane insertase for Sec-independent proteins. *Embo J*, **23**, 294-301.

Sharma, V., Arockiasamy, A., Ronning, D.R., Savva, C.G., Holzenburg, A., Braunstein, M., Jacobs, W.R., Jr. and Sacchettini, J.C. (2003) Crystal structure

of Mycobacterium tuberculosis SecA, a preprotein translocating ATPase. *Proc Natl Acad Sci USA*, **100**, 2243-2248.

Shilton, B., Svergun, D., Volkov, V., Koch, M., Cusack, S. and Economou, A. (1998) *Escherichia coli* SecA shape and dimensions. *FEBS Lett*, **436**, 277-282.

Shin, J.Y., Kim, M. and Ahn, T. (2006) Effects of signal peptide and adenylate on the oligomerization and membrane binding of soluble SecA. *J Biochem Mol Biol*, **39**, 319-328.

Shinkai, A., Mei, L.H., Tokuda, H. and Mizushima, S. (1991) The Conformation of SecA, As Revealed by Its Protease Sensitivity, Is Altered upon Interaction with ATP, Presecretory Proteins, Everted Membrane Vesicles, and Phospholipids. *J Biol Chem*, **266**, 5827-5833.

Sianidis, G., Karamanou, S., Vrontou, E., Boulias, K., Repanas, K., Kyrpides, N., Politou, A.S. and Economou, A. (2001) Cross-talk between catalytic and regulatory elements in a DEAD motor domain is essential for SecA function. *Embo J*, **20**, 961-970.

Singer, S.J. and Nicolson, G.L. (1972) The fluid mosaic model of the structure of cell membranes. *Science*, **175**, 720- 731.

Snyders, S., Ramamurthy, V. and Oliver, D. (1997) Identification of a Region of Interaction between *Escherichia coli* SecA and SecY Proteins. *J Biol Chem*, **272**, 11302-11306.

Song, M. and Kim, H. (1997) Stability and solvent accessibility of SecA protein of *Escherichia coli*. *J Biochem (Tokyo)*, **122**, 1010-1018.

Song, W., Raden, D., Mandon, E.C. and Gilmore, R. (2000) Role of Sec61alpha in the regulated transfer of the ribosome-nascent chain complex from the signal recognition particle to the translocation channel. *Cell*, **100**, 333-343.

Soultanas, P. and Wigley, D.B. (2000) DNA helicases: 'inching forward'. *Curr Opin Struct Biol*, **10**, 124-128.

Spelbrink, R.E., Kolkman, A., Slijper, M., Killian, J.A. and de Kruijff, B. (2005) Detection and identification of stable oligomeric protein complexes in *Escherichi coli* inner membranes: a proteomics approach. *J Biol Chem*, **280**, 28742-28748.

Squire, P.G. and Himmel, M.E. (1979) Hydrodynamics and protein hydration. *Arch Biochem Biophys*, **196**, 165-177.

Starling, A.P., Dalton, K.A., East, J.M., Oliver, S. and Lee, A.G. (1996) Effects of phosphatidylethanolamines on the activity of the $Ca^{(2+)}$-ATPase of sarcoplasmic reticulum. *Biochem J*, **320 (Pt 1)**, 309-314.

Story, R.M. and Steitz, T.A. (1992) Structure of the recA protein-ADP complex. *Nature*, **355**, 374-376.

Suzuki, H., Nishiyama, K. and Tokuda, H. (1999) Increases in acidic phospholipid contents specifically restore protein translocation in a cold-sensitive secA or secG null mutant. *J Biol Chem*, **274**, 31020-31024.

Tam, P.C., Maillard, A.P., Chan, K.K. and Duong, F. (2005) Investigating the SecY plug movement at the SecYEG translocation channel. *Embo J*, **24**, 3380-3388.

Taura, T., Akiyama, Y. and Ito, K. (1994) Genetic analysis of SecY: additional export-deficient mutations and factors affecting their phenotypes. *Mol Gen Genet*, **243**, 261-269.

Tomkiewicz, D., Nouwen, N., van Leeuwen, R., Tans, S. and Driessen, A.J. (2006) SecA supports a constant rate of preprotein translocation. *J Biol Chem*, **281**, 15709-15713.

Triplett, T.L., Sgrignoli, A.R., Gao, F.B., Yang, Y.B., Tai, P.C. and Gierasch, L.M. (2001) Functional signal peptides bind a soluble N-terminal fragment of SecA and inhibit its ATPase activity. *J Biol Chem*, **276**, 19648-19655.

Tziatzios, C., Schubert, D., Lotz, M., Gundogan, D., Betz, H., Schagger, H., Haase, W., Duong, F. and Collinson, I. (2004) The bacterial protein-translocation complex: SecYEG dimers associate with one or two SecA molecules. *J Mol Biol*, **340**, 513-524.

Ulbrandt, N., London, E. and Oliver, D. (1992) Deep penetration of a portion of *Escherichia coli* SecA protein into moel membranes is promoted by anionic phospholipids and by partial unfolding. *J Biol Chem*, **267**, 15184-15192.

Unwin, N. and Henderson, R. (1984) The structure of proteins in biological membranes. *Sci Am*, **250**, 78-94.

Valent, Q.A., Scotti, P.A., High, S., de Gier, J.W., von Heijne, G., Lentzen, G., Wintermeyer, W., Oudega, B. and Luirink, J. (1998) The *Escherichia coli* SRP and SecB targeting pathways converge at the translocon. *Embo J*, **17**, 2504-2512.

van Bloois, E., Jan Haan, G., de Gier, J.W., Oudega, B. and Luirink, J. (2004) F(1)F(0) ATP synthase subunit c is targeted by the SRP to YidC in the *E. coli* inner membrane. *FEBS Lett*, **576**, 97-100.

van den Berg, B., Clemons, W.M., Jr., Collinson, I., Modis, Y., Hartmann, E., Harrison, S.C. and Rapoport, T.A. (2004) X-ray structure of a protein-conducting channel. *Nature*, **427**, 36-44.

van der Does, C., den Blaauwen, T., de Wit, J., Manting, E., Groot, N., Fekkes, P. and Driessen, A. (1996) SecA is an intrinsic subunit of the *Escherichia coli* preprotein translocase and exposes its carboxyl terminus to the periplasm. *Mol Microbiol*, **22**, 619-629.

van der Does, C., Swaving, J., van Klompenburg, W. and Driessen, A. (2000) Non-bilayer lipids stimulate the activity of the reconstituted bacterial protein translocase. *J Biol Chem*, **275**, 2472-2478.

van der Sluis, E.O., Nouwen, N., Koch, J., de Keyzer, J., van der Does, C., Tampe, R. and Driessen, A.J. (2006a) Identification of two interaction sites in SecY that are important for the functional interaction with SecA. *J Mol Biol*, **361**, 839-849.

van der Sluis, E.O., van der Vries, E., Berrelkamp, G., Nouwen, N. and Driessen, A.J. (2006b) Topologically fixed SecG is fully functional. *J Bacteriol*, **188**, 1188-1190.

van der Wolk, J., Fekkes, P., Boorsma, A., Huie, J., Silhavy, T. and Driessen, A. (1998) PrlA4 prevents the rejection of signal sequence defective preproteins by stabilizing the SecA-SecY interaction during the initiation of translocation [published erratum appears in *Embo J* 1998 Sep 15; 17(18):5519]. *Embo J*, **17**, 3631-3639.

van der Wolk, J., Klose, M., Breukink, E., Demel, R.A., de Kruijff, B., Freudl, R. and Driessen, A.J.M. (1993) Characterization of a *Bacillus subtilis* SecA Mutant Protein Deficient in Translocation ATPase and Release from the Membrane. *Mol Microbiol*, **8**, 31-42.

van der Wolk, J.P., de Wit, J.G. and Driessen, A.J. (1997) The catalytic cycle of the *Escherichia coli* SecA ATPase comprises two distinct preprotein translocation events. *Embo J*, **16**, 7297-7304.

van der Wolk, J.P., Klose, M., de Wit, J.G., den Blaauwen, T., Freudl, R. and Driessen, A.J. (1995) Identification of the magnesium-binding domain of the

high-affinity ATP-binding site of the *Bacillus subtilis* and *Escherichia coli* SecA protein. *J Biol Chem*, **270**, 18975-18982.

Vassylyev, D.G., Mori, H., Vassylyeva, M.N., Tsukazaki, T., Kimura, Y., Tahirov, T.H. and Ito, K. (2006) Crystal structure of the translocation ATPase SecA from *Thermus thermophilus* reveals a parallel, head-to-head dimer. *J Mol Biol*, **364**, 248-258.

Veenendaal, A., C, v.d.D. and Driessen, A. (2001) Mapping the sites of interaction between SecY and SecE by cysteine scanning mutagenesis. *J Biol Chem*, **276**, 32559-32566.

von Heijne, G. (1985) Signal sequences. The limits of variation. *J Mol Biol*, **184**, 99-105.

Vrontou, E., Karamanou, S., Baud, C., Sianidis, G. and Economou, A. (2004) Global co-ordination of protein translocation by the SecA IRA1 switch. *J Biol Chem*, **279**, 22490-22497.

Walker, J. (1998) ATP synthesis by rotary catalysis (Nobel Lecture). *Angew Chem Int Ed Engl*, **37**, 2309–2319.

Walker, J.E., Saraste, M., Runswick, M.J. and Gay, N.J. (1982) Distantly related sequences in the alpha- and beta-subunits of ATP synthase, myosin, kinases and other ATP-requiring enzymes and a common nucleotide binding fold. *Embo J*, **1**, 945-951.

Walter, P. and Blobel, G. (1981) Translocation of proteins across the endoplasmic reticulum. III. Signal recognition protein (SRP) causes signal sequence and site specific arrest of chain elongation that is released by microsomal membranes. *J.Cell Biol*, **91**, 557-561.

Walter, P., Ibrahimi, I. and Blobel, G. (1981) Translocation of proteins across the endoplasmic reticulum. I. Signal recognition protein (SRP) binds to in vitro assembled polysomes synthesizing secretory protein. *J Cell Biol*, **91**, 545-550.

Walter, P. and Johnson, A.E. (1994) Signal sequence recognition and protein targeting to the endoplasmic reticulum membrane. *Annu Rev Cell Biol*, **10**, 87-119.

Wang, H., Chen, Y., Yang, H., Chen, X., Duan, M., Tai, P. and Sui, S. (2003) Ring-like pore structures of SecA: Implication for bacterial protein-conducting channels. *Proc Natl Acad Sci USA*, **100**, 4221-4226.

Wang, L., Miller, A. and Kendall, D.A. (2000) Signal peptide determinants of SecA binding and stimulation of ATPase activity. *J Biol Chem*, **275**, 10154-10159.

Webb, M.R. (1992) A continuous spectrophotometric assay for inorganic phosphate and for measuring phosphate release kinetics in biological systems. *Proc Natl Acad Sci USA*, **89**, 4884-4887.

Weiss, J., Ray, P. and Bassford, P. (1988) Purified SecB protein of *Escherichia coli* retards folding and promotes membrane translocation of the maltose-binding protein in vivo. *Proc Natl Acad Sci USA*, **85**, 8978-8982.

Wong, J.T. (1975) Kinetics of Enzyme Mechanisms. *Academic Press, London and New York*, 1-298.

Woodbury, R.L., Hardy, S.J. and Randall, L.L. (2002) Complex behavior in solution of homodimeric SecA. *Protein Sci*, **11**, 875-882.

Woodbury, R.L., Topping, T.B., Diamond, D.L., Suciu, D., Kumamoto, C.A., Hardy, S.J. and Randall, L.L. (2000) Complexes between protein export chaperone SecB and SecA. Evidence for separate sites on SecA providing binding energy and regulatory interactions. *J Biol Chem*, **275**, 24191-24198.

Woolhead, C.A., Thompson, S.J., Moore, M., Tissier, C., Mant, A., Rodger, A., Henry, R. and Robinson, C. (2001) Distinct Albino3-dependent and -independent pathways for thylakoid membrane protein insertion. *J Biol Chem*, **276**, 40841-40846.

Xie, K., Kiefer, D., Nagler, G., Dalbey, R.E. and Kuhn, A. (2006) Different regions of the nonconserved large periplasmic domain of *Escherichia coli* YidC are involved in the SecF interaction and membrane insertase activity. *Biochemistry*, **45**, 13401-13408.

Yahr, T. and Wickner, W. (2000) Evaluating the oligomeric state of SecYEG in preprotein translocase. *Embo J*, **19**, 4393-4401.

Yasuda, R., Noji, H., Yoshida, M., Kinosita, K., Jr. and Itoh, H. (2001) Resolution of distinct rotational substeps by submillisecond kinetic analysis of F1-ATPase. *Nature*, **410**, 898-904.

Ye, J., Osborne, A.R., Groll, M. and Rapoport, T.A. (2004) RecA-like motor ATPases - lessons from structures. *Biochim et Biophys Acta*, **1659**, 1-18.

Ye, J.J. and Lin, Z.H. (1990) Specificity of acidic phospholipids (CL & PA) in the activation of mitochondrial F0F1 ATPase by Mg^{2+}. *Biochem Int*, **22**, 219-226.

Yi, L., Celebi, N., Chen, M. and Dalbey, R.E. (2004) Sec/SRP requirements and energetics of membrane insertion of subunits a, b, and c of the *Escherichia coli* F1F0 ATP synthase. *J Biol Chem*, **279**, 39260-39267.

Zhou, J. and Xu, Z. (2003) Structural determinants of SecB recognition by SecA in bacterial protein translocation. *Nat Struct Biol*, **10**, 942-947.

Zimmer, J., Li, W. and Rapoport, T.A. (2006) A novel dimer interface and conformational changes revealed by an X-ray structure of *B. subtilis* SecA. *J Mol Biol*, **364**, 259-265.

Zito, C.R., Antony, E., Hunt, J.F., Oliver, D.B. and Hingorani, M.M. (2005) Role of a conserved glutamate residue in the *Escherichia coli* SecA ATPase mechanism. *J Biol Chem*, **280**, 14611-14619.

Appendix

Publications

Gold, V. A., Robson, A., Clarke, A. R. & Collinson, I. (2007). Allosteric regulation of SecA: magnesium-mediated control of conformation and activity. *J Biol Chem* **282** (24), 17424-32.

Gold, V. A., Duong, F. & Collinson, I. (2007). Structure and function of the bacterial Sec translocon. *Mol Membr Biol* **24** (5-6), 387-94.

Robson, A., Booth, A. E., Gold, V. A., Clarke, A. R. & Collinson, I. (2007). A Large Conformational Change Couples the ATP Binding Site of SecA to the SecY Protein Channel. *J Mol Biol* **374** (4), 965-976.

Some text bound close to the spine.

There have been several observations with respect to magnesium and its effects on the regulation of SecA, which have not been adequately explained. Removal of the cation from a binding site, distinct from the nucleotide binding folds, can result in a 10-fold stimulation of ADP release (30). The activity of SecA and the elevated activity found in a complex of SecA and SecYEG were both stimulated by the removal of Mg^{2+}, which also served to stabilize the latter complex in the presence of ATP (or ATPγS) (5). Mg^{2+} has also been shown to modulate fluorescence anisotropy measurements, as well as the fluorescence observed from intrinsic and extrinsic probes of the enzyme (27, 31, 32).

Despite the fact that the structures of both SecA and SecYEG have been determined, we are still a long way from understanding their concerted mechanism of action. To reach this point, we need to understand the nature and timing of the conformational changes within SecA, and how they are affected by the ATPase cycle. In the light of the conflicting and fragmented accounts of the reaction cycle, we decided to conduct a thorough analysis of the kinetics of the protein translocation process. As a first approach to this characterization we have performed a steady-state analysis of SecA in isolation, together with a study of its oligomeric state by equilibrium and velocity sedimentation using analytical centrifugation. An analysis of the wild-type and proposed monomeric mutant SecA-Δ11/N95 (21) in this way generated some new findings on the oligomeric state of SecA, its ATPase activity, and the influence of magnesium and lipids.

EXPERIMENTAL PROCEDURES

Chemicals and Biochemicals—*Escherichia coli* polar lipid and *E. coli* cardiolipin were purchased from Avanti, and were prepared at 10 mg/ml in 50 mM triethanolamine, pH 7.5, 50 mM KCl. Polyoxyethylene(9)dodecyl ether ($C_{12}E_9$) was purchased from Anatrace, the EnzChek™ kit from Molecular Probes (Invitrogen), Chelating Sepharose fast flow from GE Healthcare, and all other reagents from Sigma.

Overexpression and Purification of SecA and SecA-Δ11/N95—Wild-type SecA was derived from plasmid pT7SecA2 (20) and the SecA mutant Δ11/N95 from the plasmid pET21Δ11N95 (21). They were expressed in *E. coli* host cells BL21.19(λDE3) grown in LB medium with 100 μg/ml ampicillin and induced with 1 mM isopropyl 1-thio-β-D-galactopyranoside at mid-log phase (A_{600} ~ 0.8). After 1.5 h of induction the cells were pelleted by centrifugation, then resuspended in 20 mM Tris-HCl, pH 7.5, 100 mM KCl, 2 mM $MgCl_2$ and ruptured using a cell disruptor (Constant Cell Disruption Systems, Daventry, UK). Membranes and insoluble material were removed by centrifugation (50,000 × *g* for 1 h at 4 °C). Supernatants were applied to a Ni^{2+}-Sepharose column (Chelating Sepharose fast flow), washed in the same buffer with 25 mM imidazole and eluted in 300 mM. Proteins were further purified by anion exchange chromatography (Mono-Q HR 10/10, GE Healthcare) and gel filtration (Superdex 200 HR 26/60, GE Healthcare). Purified concentrated protein was stored in 20 mM Tris-HCl, pH 7.5, 100 mM KCl, 1 mM dithiothreitol at −80 °C.

ATPase Assays—Steady-state ATPase assays were carried out and monitored at 25 °C, either by the linked pyruvate kinase/lactate dehydrogenase assay, or by using the EnzChek™ Kit (Invitrogen), employing a Lambda 25 spectrophotometer (PerkinElmer Life Sciences). The pyruvate kinase/lactate dehydrogenase assay was used to measure extremely slow turnover accurately by virtue of a regenerating system, and the EnzChek™ kit to investigate the effects of Mg^{2+}, where the former would be inappropriate due to the dependence of pyruvate kinase on this cation.

Pyruvate Kinase/Lactate Dehydrogenase Assay—Standard assay components were 1000 units/ml lactate dehydrogenase, 700 units/ml pyruvate kinase, 2 mM phosphoenolpyruvate, and 0.2 mM NADH in TKM buffer (50 mM triethanolamine, pH 7.5, 50 mM KCl, 2 mM $MgCl_2$). 0.3 μM SecA or SecA-Δ11/N95 (monomer concentration) was used in each reaction, and the assays were initiated by addition of ATP.

EnzChek™ Assay—The standard assay components were 0.2 mM 2-amino-6-mercapto-7-methylpurine riboside and 1 unit of purine nucleoside phosphorylase in TK buffer (50 mM triethanolamine, pH 7.5, 50 mM KCl). 0.3 μM SecA or SecA-Δ11/N95 was used (monomer concentration) in each reaction, and ADP, Mg^{2+}, and *E. coli* lipids were added to the concentrations indicated in the text, prior to the initiation of the reaction by addition of ATP.

Determination of Residual Magnesium Concentration—The amount of Mg^{2+} contained within the standard assay conditions (TK buffer) was calculated using inductively coupled plasma-atomic emission spectroscopy, using a Jobin Yvon Horiba Ultima 2 sequential spectrometer fitted with a Bergener Mira Mist Nebulizer and automated with a Jobin Yvon AS421 auto-sampler.

Curve fitting and analysis for all kinetic data, including that of the global fits is shown under supplemental materials.

Analytical Ultracentrifugation—SecA stock solutions of wild-type and SecA-Δ11/N95 were dialyzed extensively against either TK or TKM buffers. These were subjected to sedimentation velocity and sedimentation equilibrium centrifugation experiments using either an XL-A or XL-I centrifuge (Beckman Instruments) equipped with standard Epon centerpieces and an An-60Ti rotor. SecA or SecA-Δ11/N95 (0.4–13 μM) were used and scans were recorded at either 230 or 280 nm. Sedimentation velocity experiments were carried out at 25 °C and 130,000 × *g*. The scans were fitted to a continuous c(s) model, using Ultrascan (34). The data were then extrapolated to zero concentration to yield $s^0_{20,w}$. Equilibrium scans were taken at 16 and 20 h, at speeds of 3,000, 5,800, and 8,000 × *g* at 25 °C. The data were analyzed using a variety of models, the data shown are that of a 1-component ideal species model, which yielded the most appropriate fit using Ultrascan (34). The data were then subjected to a Monte Carlo analysis, to reveal the statistical values for all parameters.

In Vitro Translocation Assays—SecYEG was reconstituted into *E. coli* polar lipid proteoliposomes as described previously (35). Translocation of proOmpA into SecYEG proteoliposomes was assayed essentially as described (36), except that protease-protected proOmpA was detected by Western blot using an antibody raised against proOmpA.

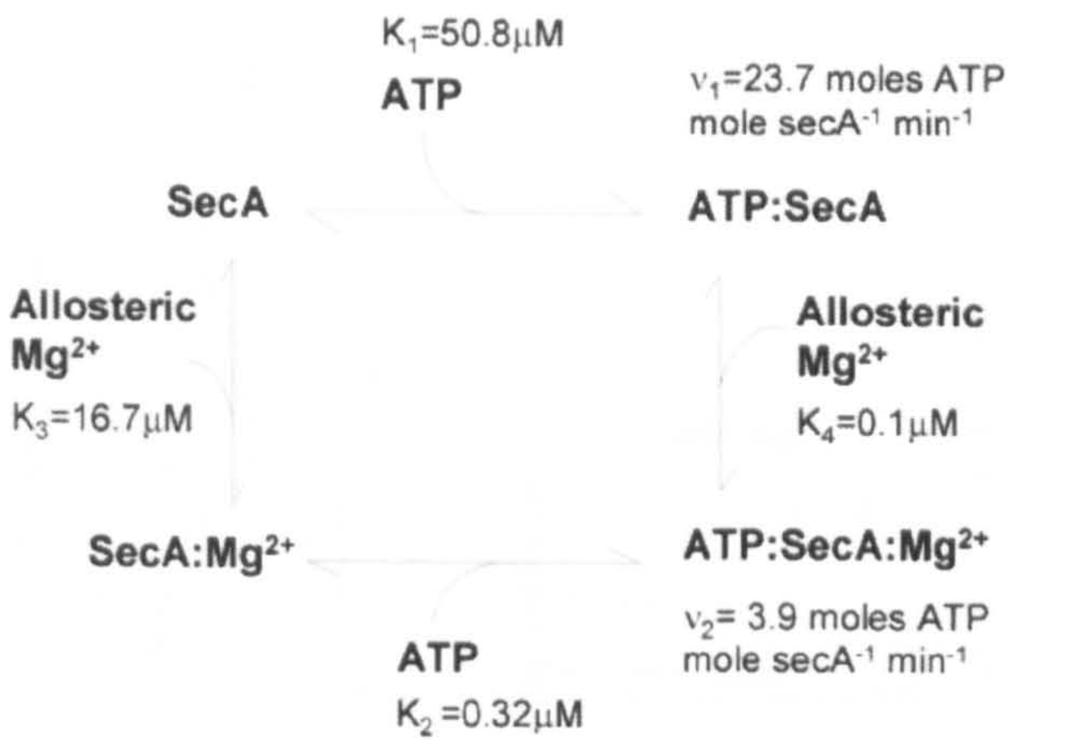

FIGURE 3. **The SecA binding cycle for ATP substrate and the non-catalytic regulatory Mg^{2+}.** The parameters from the global fit shown in Fig. 2*B* were used to construct the kinetic model shown.

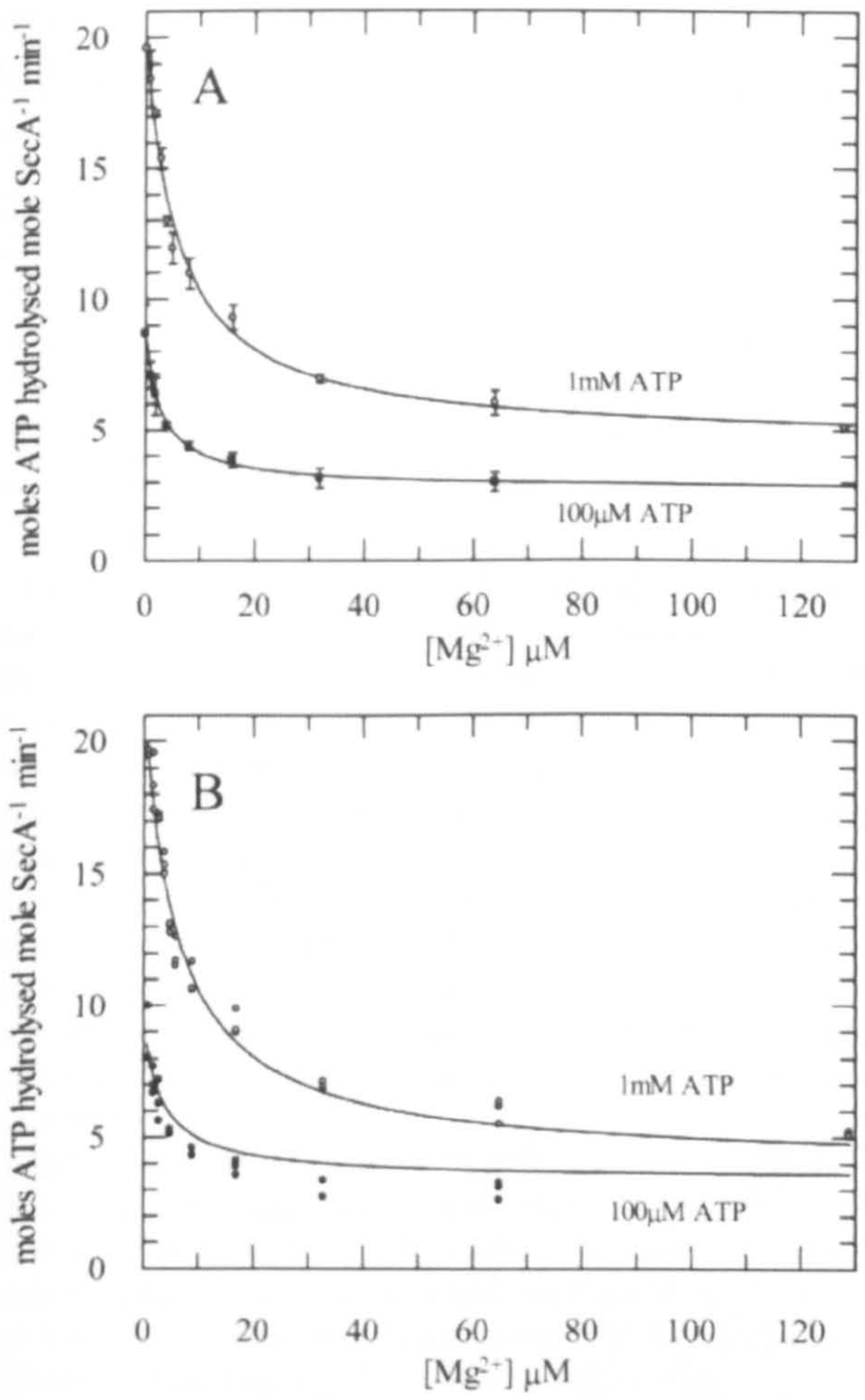

FIGURE 2. **Inhibition of ATP turnover by Mg^{2+}.** The ATPase activity of purified wild-type SecA was measured over a range of Mg^{2+} concentrations, with 1 mM ATP (*open circles*) and 100 μM ATP (*filled circles*), in TK buffer. *A*, the data were fitted to the hyperbolic inhibition function (Equation 1, "supplemental materials") to determine values for $K_{i(app)}[Mg^{2+}]$. *Error bars* represent S.D. from 3 replicates. *B*, the same data sets were fitted globally to Equation 2 under supplemental materials, making an adjustment for the chelation effect of Mg^{2+}-ATP and incorporating the data for both weak and tight binding of ATP by SecA under high and low Mg^{2-} conditions. Data from six different experiments are shown. An allowance of 10% was allowed for enzyme concentration between the two separate data sets in the fit. Calculated values for $K_{i(app)}$ are shown in Table 2.

TABLE 2

Calculated values for the apparent $K_{i(app)}[Mg^{2+}]$ of the ATPase reaction in the presence of 1 mM and 100 μM ATP

The data were collected according to Fig. 2*A*, and fitted to Equation 1 as described under supplemental materials. S.E. from the fitting procedure is shown.

	$K_{i(app)}[Mg^{2+}$, 1 mM ATP]	$K_{i(app)}[Mg^{2+}$, 100 μM ATP]
	μM	
SecA	5.8 ± 0.94	2.97 ± 0.22

which is proposed to be the active form.[3] Cardiolipin is also known to be a chelator of divalent cations (38). In addition, acidic phospholipids have been shown to be important for protein translocation (39). Therefore, we reasoned that the influence of cardiolipin on protein translocation might be an indirect effect mediated by Mg^{2+}, and decided to determine the

[3] F. Duong and I. Collinson, unpublished results.

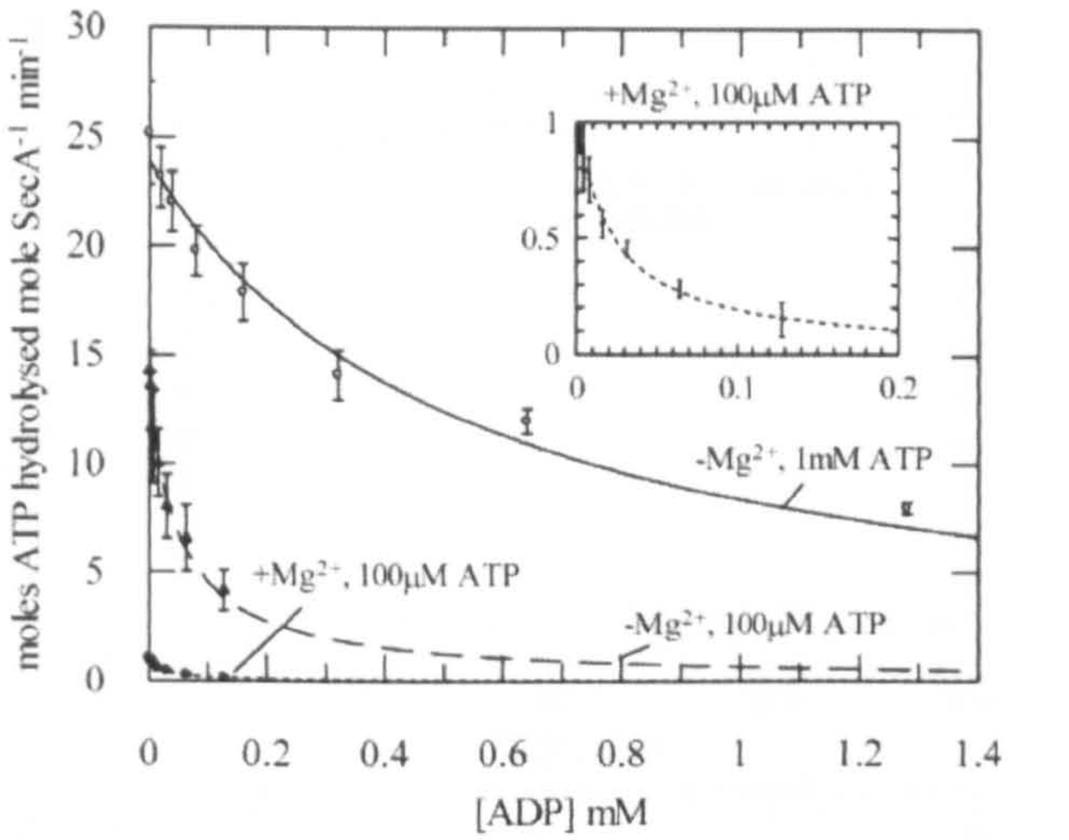

FIGURE 4. **The effect of Mg^{2+} on competitive product inhibition by ADP.** The ATPase activity of purified wild-type SecA was measured with respect to the ADP concentration, with residual Mg^{2+} in TK buffer including both 1 mM ATP (*open circles*, *solid line*) and 100 μM ATP (*filled triangles*, *dashed line*). The experiments were repeated in the presence of 2 mM Mg^{2+} in TKM buffer at 100 μM ATP (*inset*, *filled circles*, *dotted line*). The data were fitted to Equation 3 as shown under supplemental materials. The *inset curve* is an expansion of the data collected at 2 mM Mg^{2+} and 100 μM ATP. *Error bars* represent S.D. from four to five replicates. The calculated values for $K_{i(app)}[ADP]$ and $K_d[ADP]$ are shown in Table 3.

TABLE 3

Calculated values for the $K_{i(app)}[ADP]$ determined with different concentrations of Mg^{2+} and ATP

The data were collected according to Fig. 4, and fitted to Equation 3 under supplemental materials. Actual values for $K_d[ADP]$, taking into account the altered $K_m[ATP]$ at high concentrations of Mg^{2+}, were calculated by fitting the data in Fig. 4 to Equation 4 as described under supplemental materials. S.E. from the fitting procedure is shown.

	$K_{i(app)}[ADP]$	$K_d[ADP]$
	mM	μM
$-Mg^{2+}$, 1 mM ATP	0.54 ± 0.06	26.25 ± 3.09
$-Mg^{2+}$, 100 μM ATP	0.051 ± 0.007	17.08 ± 2.21
$+Mg^{2+}$, 100 μM ATP	0.023 ± 0.001	0.1 ± 0.004

effect of cardiolipin on SecA activity. The experiment was conducted with and without added 2 mM Mg^{2+}; the detergent $C_{12}E_9$ was used to solubilize the lipid, and was shown to change neither the affinity of SecA for ATP nor the turnover rate (Table

TABLE 4

Calculated values of the K_m[ATP] for wild-type SecA in the presence of 2 mM Mg^{2+} and 36 μM solubilized cardiolipin, and $C_{12}E_9$ (control)

These are compared to the values in +/−Mg^{2+} conditions. The data were collected according to Figs. 1, *A* and *B*, and 5*B*, and fitted to the Michaelis-Menten equation as described under supplemental materials. S.E. from the fitting procedure is shown.

	K_m[ATP]	V_{max}
	μM	*mol ATP hydrolyzed mol sA^{-1} min^{-1}*
+Mg^{2+}	0.32 ± 0.03	0.56 ± 0.01
−Mg^{2+}	50.8 ± 3.2	22.36 ± 0.28
+Mg^{2+}; 36 μM cardiolpin	10.4 ± 1.0	11.33 ± 0.26
−Mg^{2+}; +0.64% $C_{12}E_9$ (control)	61.3 ± 6.4	18.07 ± 0.40

4). In low concentrations of Mg^{2+}, cardiolipin was found to inhibit the ATPase activity (Fig. 5*A*), presumably due to chelation of the Mg^{2+} required for the hydrolysis of ATP. At higher concentrations of Mg^{2+} (100 μM) there was a striking increase in activity peaking at ~2.4 μM cardiolipin, followed by a gradual reduction (Fig. 5*A*), indicating that the effect cannot be simply explained by the chelation of Mg^{2+}. The effects of increasing cardiolipin in a yet higher concentration of Mg^{2+} resulted in a less pronounced rise and fall of ATPase activity. The inhibitory phase of cardiolipin in the presence of added Mg^{2+} may have been the result of the aggregation of SecA-lipid complexes, because it cannot be the result of Mg^{2+} chelation at this high a concentration.

Next, we determined the K_m value for ATP binding with high (2 mM) Mg^{2+} and high (36 μM) cardiolipin (*asterisk* in Fig. 5, *A* and *B*, and Table 4); both the K_m and V_{max} were characteristic of conditions having only a low concentration of Mg^{2+}. Therefore, we can infer from this data that cardiolipin counteracts the inhibition caused by Mg^{2+}. Total *E. coli* polar lipids had a less dramatic effect (Fig. 5*C*). An ~10-fold higher concentration was required to reach an equivalent enhancement. Therefore, we assumed that this was a result of the cardiolipin (9.8%, w/w) contained in this fraction.

Magnesium Alters the Conformation of the SecA Dimer, but Not the Oligomeric State—To determine whether the observed change in activity was affected by a change in the oligomeric state of SecA, sedimentation equilibrium and sedimentation velocity experiments were carried out by analytical ultracentrifugation. Sedimentation equilibrium revealed unambiguously that SecA is a dimer within a 0.4–13 μM concentration range in equivalent buffers to those used in the ATPase assays (Fig. 6 and Table 5), and also in the presence of 2 mM EDTA (data not shown). Rather surprisingly, SecA-Δ11/N95, previously reported to be a monomer (21), was found to be a dimer as well. In both cases, the monomers were in such rarity that they could not be detected with sufficient accuracy to determine a dissociation constant, an indication that this value must therefore be in the low nanomolar range.

Subsequently, sedimentation velocity also revealed that there is essentially only a dimeric species present (Fig. 7 and Table 6). However, it could be shown for SecA and SecA-Δ11/N95 that the sedimentation properties, and hence shape, were sensitive to Mg^{2+}. An increase of 0.54 (SecA) and 0.11 (SecA-Δ11/N95) $s^0_{20,w}$ units (the sedimentation coefficient S, expressed in terms of a water solvent at 20 °C and extrapolated to zero concentra-

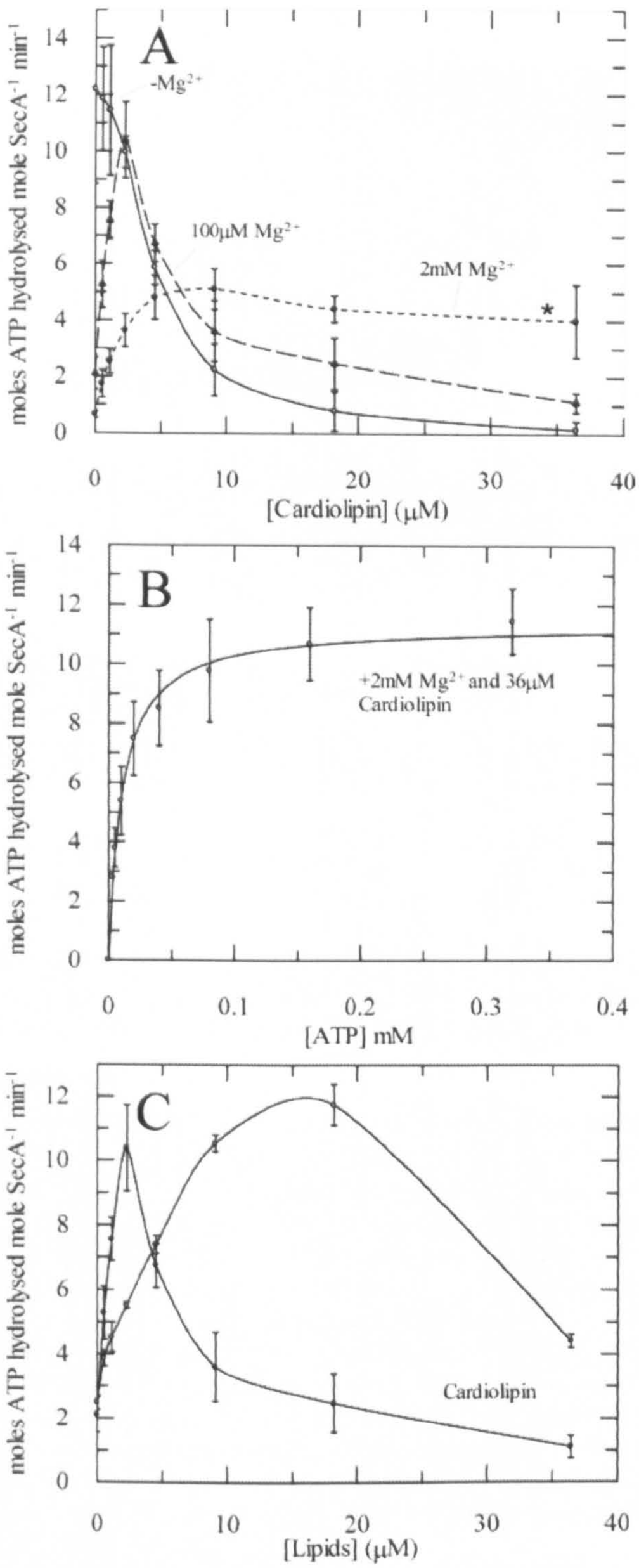

FIGURE 5. **Cardiolipin relieves Mg^{2+} inhibition through the formation of a ternary SecA-Mg^{2+}-cardiolipin complex.** *A*, the ATPase activity of purified wild-type SecA was measured in the presence of 100 μM ATP in TK buffer with residual Mg^{2+} (*open circles, solid line*), 100 μM Mg^{2+} (*filled triangles, dashed line*), or 2 mM Mg2+ (*filled circles, dotted line*), with increasing concentrations of cardiolipin. *B*, the ATPase activity of purified wild-type SecA was measured with 36 μM $C_{12}E_9$-solubilized cardiolipin in TKM buffer (*asterisk* in *A*), over a range of ATP concentrations to determine the Michaelis-Menten parameters. Calculated values of K_m and V_{max} are shown in Table 4. *C*, the ATPase activity wild-type SecA was measured in the presence 100 μM ATP and 100 μM Mg^{2+} with increasing concentrations of cardiolipin and total *E. coli* polar lipids, which contain 9.8% cardiolipin. *Error bars* represent S.D. from four to six replicates.

TABLE 4

Calculated values of the K_m[ATP] for wild-type SecA in the presence of 2 mM Mg^{2+} and 36 μM solubilized cardiolipin, and $C_{12}E_9$ (control)

These are compared to the values in +/−Mg^{2+} conditions. The data were collected according to Figs. 1, *A* and *B*, and 5*B*, and fitted to the Michaelis-Menten equation as described under supplemental materials. S.E. from the fitting procedure is shown.

	K_m[ATP]	V_{max}
	μM	*mol ATP hydrolyzed mol sA^{-1} min^{-1}*
+Mg^{2+}	0.32 ± 0.03	0.56 ± 0.01
−Mg^{2+}	50.8 ± 3.2	22.36 ± 0.28
+Mg^{2+}; 36 μM cardiolipin	10.4 ± 1.0	11.33 ± 0.26
−Mg^{2+}; +0.64% $C_{12}E_9$ (control)	61.3 ± 6.4	18.07 ± 0.40

4). In low concentrations of Mg^{2+}, cardiolipin was found to inhibit the ATPase activity (Fig. 5*A*), presumably due to chelation of the Mg^{2+} required for the hydrolysis of ATP. At higher concentrations of Mg^{2+} (100 μM) there was a striking increase in activity peaking at ~2.4 μM cardiolipin, followed by a gradual reduction (Fig. 5*A*), indicating that the effect cannot be simply explained by the chelation of Mg^{2+}. The effects of increasing cardiolipin in a yet higher concentration of Mg^{2+} resulted in a less pronounced rise and fall of ATPase activity. The inhibitory phase of cardiolipin in the presence of added Mg^{2+} may have been the result of the aggregation of SecA-lipid complexes, because it cannot be the result of Mg^{2+} chelation at this high a concentration.

Next, we determined the K_m value for ATP binding with high (2 mM) Mg^{2+} and high (36 μM) cardiolipin (*asterisk* in Fig. 5, *A* and *B*, and Table 4); both the K_m and V_{max} were characteristic of conditions having only a low concentration of Mg^{2+}. Therefore, we can infer from this data that cardiolipin counteracts the inhibition caused by Mg^{2+}. Total *E. coli* polar lipids had a less dramatic effect (Fig. 5*C*). An ~10-fold higher concentration was required to reach an equivalent enhancement. Therefore, we assumed that this was a result of the cardiolipin (9.8%, w/w) contained in this fraction.

Magnesium Alters the Conformation of the SecA Dimer, but Not the Oligomeric State—To determine whether the observed change in activity was affected by a change in the oligomeric state of SecA, sedimentation equilibrium and sedimentation velocity experiments were carried out by analytical ultracentrifugation. Sedimentation equilibrium revealed unambiguously that SecA is a dimer within a 0.4–13 μM concentration range in equivalent buffers to those used in the ATPase assays (Fig. 6 and Table 5), and also in the presence of 2 mM EDTA (data not shown). Rather surprisingly, SecA-Δ11/N95, previously reported to be a monomer (21), was found to be a dimer as well. In both cases, the monomers were in such rarity that they could not be detected with sufficient accuracy to determine a dissociation constant, an indication that this value must therefore be in the low nanomolar range.

Subsequently, sedimentation velocity also revealed that there is essentially only a dimeric species present (Fig. 7 and Table 6). However, it could be shown for SecA and SecA-Δ11/N95 that the sedimentation properties, and hence shape, were sensitive to Mg^{2+}. An increase of 0.54 (SecA) and 0.11 (SecA-Δ11/N95) $s^0_{20,w}$ units (the sedimentation coefficient S, expressed in terms of a water solvent at 20 °C and extrapolated to zero concentra-

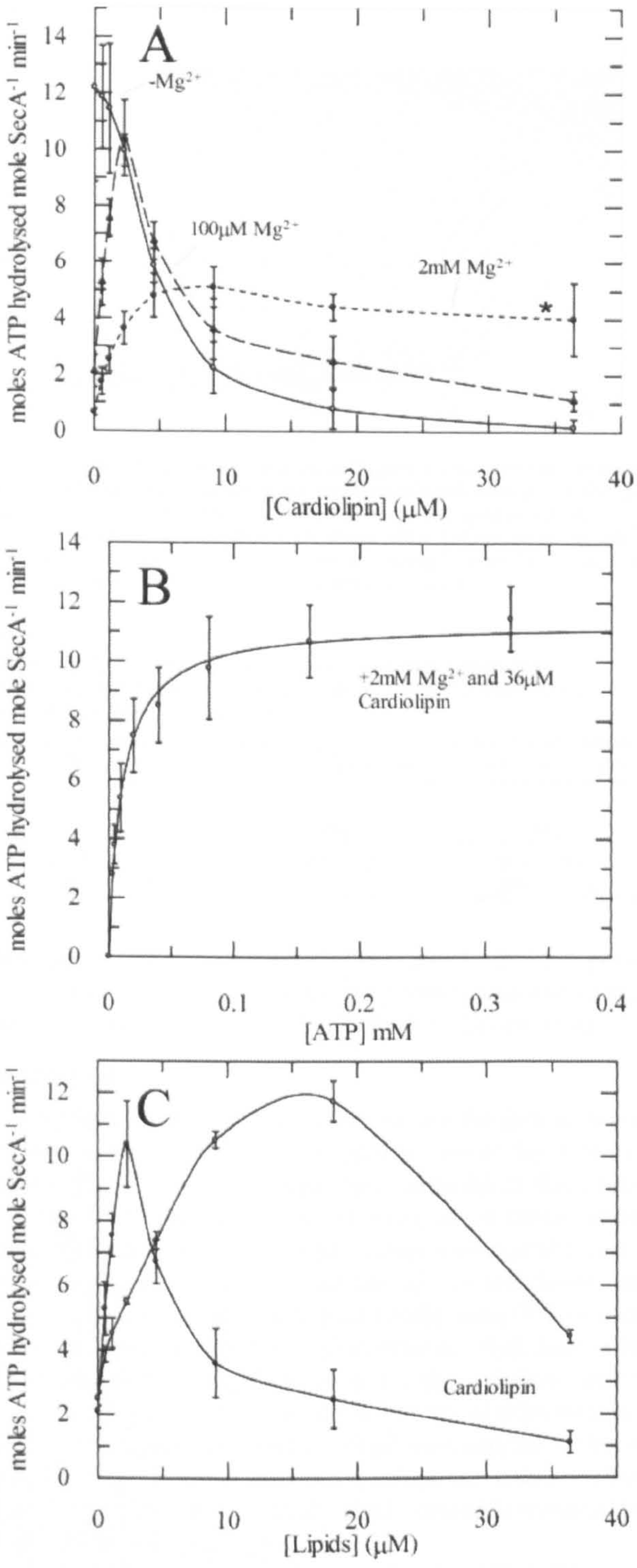

FIGURE 5. **Cardiolipin relieves Mg^{2+} inhibition through the formation of a ternary SecA-Mg^{2+}-cardiolipin complex.** *A*, the ATPase activity of purified wild-type SecA was measured in the presence of 100 μM ATP in TK buffer with residual Mg^{2+} (*open circles*, *solid line*), 100 μM Mg^{2+} (*filled triangles*, *dashed line*), or 2 mM Mg2+ (*filled circles*, *dotted line*), with increasing concentrations of cardiolipin. *B*, the ATPase activity of purified wild-type SecA was measured with 36 μM $C_{12}E_9$-solubilized cardiolipin in TKM buffer (*asterisk* in *A*), over a range of ATP concentrations to determine the Michaelis-Menten parameters. Calculated values of K_m and V_{max} are shown in Table 4. *C*, the ATPase activity wild-type SecA was measured in the presence 100 μM ATP and 100 μM Mg^{2+} with increasing concentrations of cardiolipin and total *E. coli* polar lipids, which contain 9.8% cardiolipin. *Error bars* represent S.D. from four to six replicates.

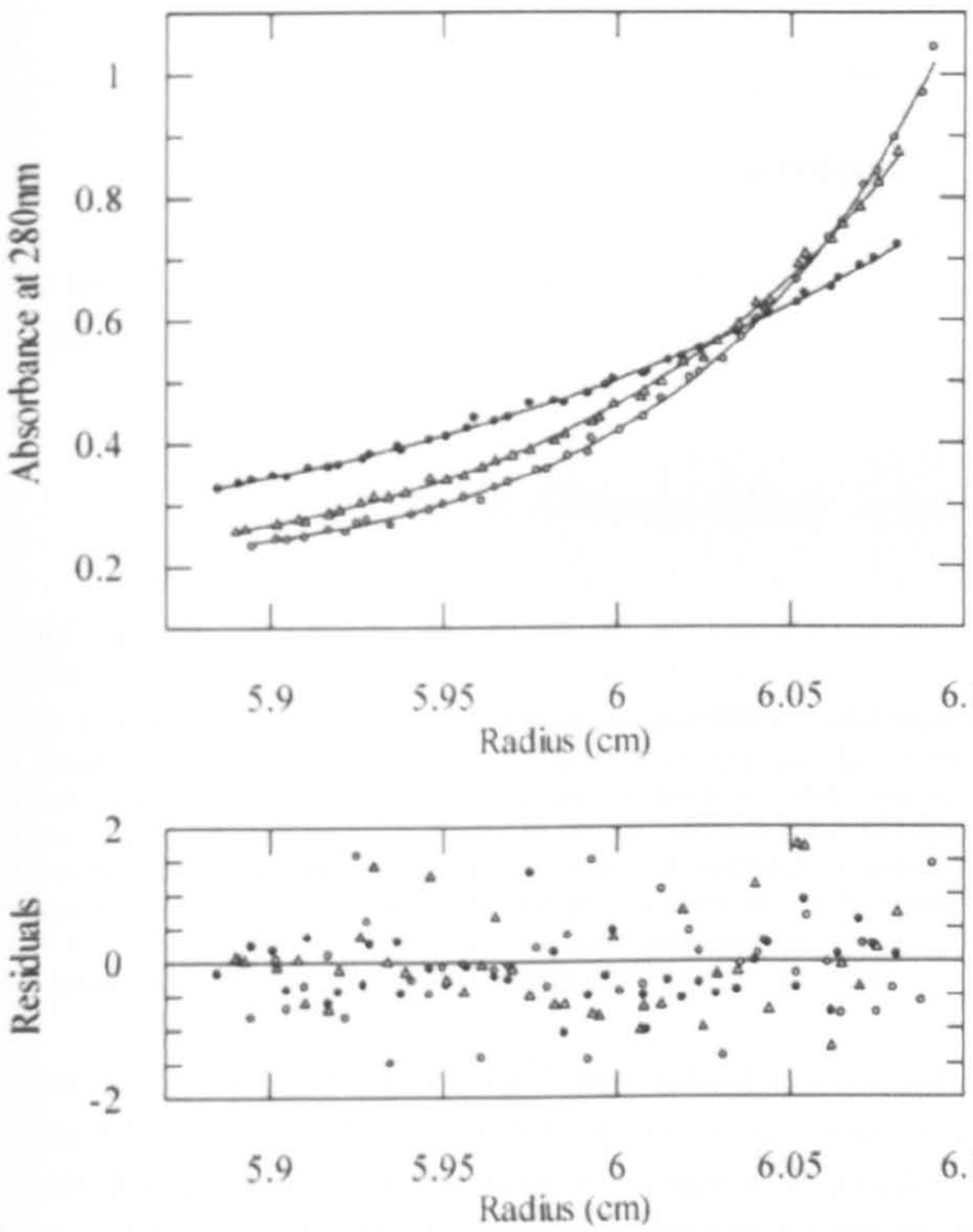

FIGURE 6. **Sedimentation equilibrium centrifugation demonstrates that both SecA and SecA-Δ11/N95 are dimers, irrespective of the Mg^{2+} concentration.** 1–13 μM SecA or SecA-Δ11/N95 were centrifuged at three speeds at 25 °C in either TK or TKM buffers. Equilibrium scans were taken at 16 and 20 h, and the data analyzed using a 1-component ideal species model using ultrascan (34). The data shown are an example fit from an experiment containing 1.5 μM SecA in TK buffer at 3,000 (*filled circles*), 5,800 (*open triangles*), and 8,000 × *g* (*open circles*) and the corresponding residual values. Calculated values for molecular weight are shown in Table 5.

TABLE 5

Molecular weight determined by equilibrium velocity centrifugation for wild-type SecA and SecA-Δ11/N95 with and without added 2 mM Mg^{2+}

The data were collected according to Fig. 6, and fitted to a 1-component ideal species model as described under "Experimental Procedures." The S.D. from the Monte Carlo analysis is shown, following the converged value from the fit. The molecular weight of a monomer of each species, based on the amino acid sequence, is shown in parentheses.

	Molecular mass (kDa)		Oligomeric state	
	$+Mg^{2+}$	$-Mg^{2+}$	$+Mg^{2+}$	$-Mg^{2+}$
SecA (102 kDa)	200.1 ± 7.1	201.6 ± 6.4	Dimer	Dimer
SecA-Δ11/N95 (94 kDa)	184.6 ± 7.1	181.5 ± 8.3	Dimer	Dimer

tion) was observed in the presence of 2 mM Mg^{2+}, compared with residual Mg^{2+}, indicative of a more extended shape.

The Influence of Magnesium Is Countered by Conditions That Promote Protein Translocation—The protein translocation reaction driven by wild-type SecA and SecA-Δ11/N95 through SecYEG were compared and the mutant was found to have a significant proportion of the wild type activity. The amount of proOmpA translocated by wild type and by Δ11/N95 is approximately the same after 5 and 15 min, respectively (Fig. 8*A*). Mg^{2+} was titrated into the protein translocation assay and its effects monitored (Fig. 8*B*). There is a difference in the dependence of Mg^{2+} in translocation compared with the ATPase activity of isolated SecA, indicating that conditions that promote translocation also alleviate the inhibitory effect of Mg^{2+}.

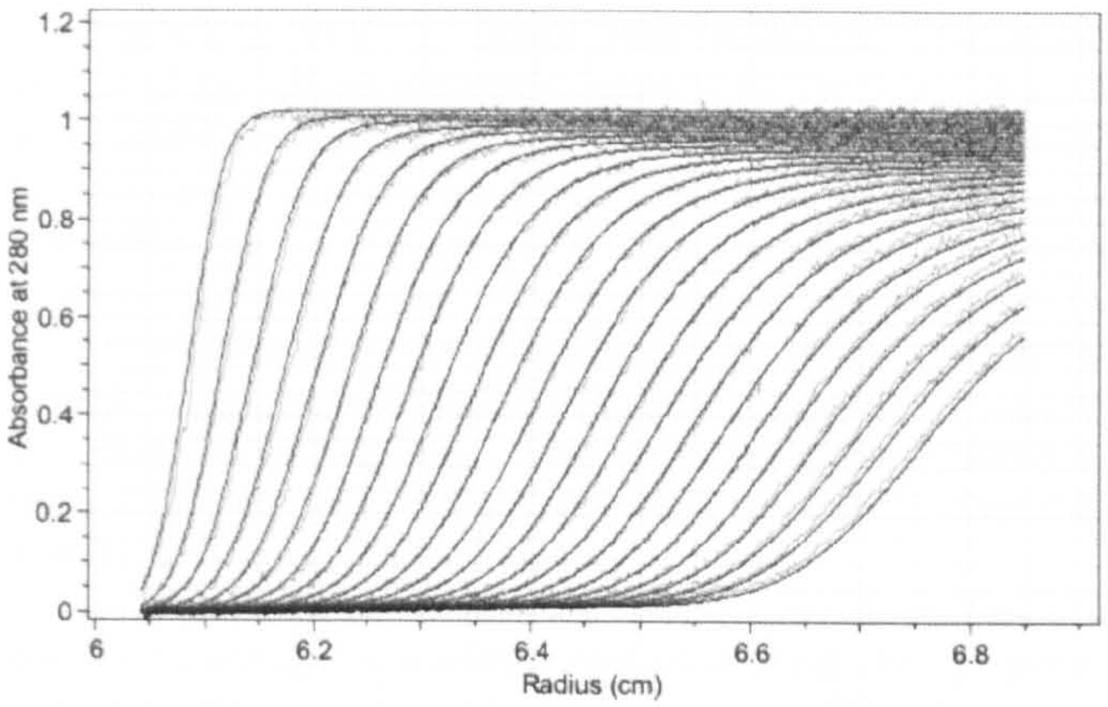

FIGURE 7. **Sedimentation velocity centrifugation experiments show that there is a large Mg^{2+}-dependent conformational change in the SecA dimer.** 1–13 μM SecA or SecA-Δ11/N95 were centrifuged at 130,000 × *g* at 25 °C and analyzed by a continuous c(s) model, fitted using Ultrascan (34). The data shown is an example scan and corresponding fit from 13 μM SecA in TK buffer. Calculated values for $s^0_{20,w}$ are shown in Table 6.

TABLE 6

Values for $s^0_{20,w}$ determined by sedimentation velocity centrifugation for wild-type SecA and SecA-Δ11/N95 with and without added 2 mM Mg^{2+}

The data were collected according to Fig. 7, fitted to a continuous c(s) model and extrapolated to zero concentration as described under "Experimental Procedures."

	$s^0_{20,w}$	
	$+Mg^{2+}$	$-Mg^{2+}$
SecA	9.60 ± 0.16	9.06 ± 0.13
SecA-Δ11/N95	8.17 ± 0.10	8.06 ± 0.12

This may, in part, be due to the influence of cardiolipin present in the SecYEG proteoliposomes, but possibly also due to interactions of SecA with substrate and the SecYEG complex.

DISCUSSION

Our understanding of the molecular mechanism of Sec-dependent translocation and the specific role of SecA is in its infancy. There are now six structures available of this protein, five dimers and one monomer. There is, for instance, no consensus with respect to the active oligomeric form of the protein, the processive nature of the reaction and the stoichiometry of ATP/amino acid translocated (see Introduction). These uncertainties are understandable in view of the fact that there is little data to describe the interactions that occur between SecYEG, SecA, and substrate. There is also a paucity of information on the kinetics and the hydrolytic cycle of SecA and the timing and nature of the reactions that bring about the conformational changes that must ultimately drive the vectorial passage of proteins through the membrane.

The experiments described in this paper address this fundamental aspect of the system, the reaction cycle of SecA. We begin at the simplest level of the system and elucidate the basic ATPase mechanism. We have characterized SecA by steady-state ATPase assays and related the observed kinetics to structural changes by analytical ultracentrifugation.

The divalent metal cation Mg^{2+} was found to have a powerful effect on the binding affinity and turnover of ATP: tight and slow in the presence of high concentrations, loose and fast with trace amounts. The simplest way of explaining this

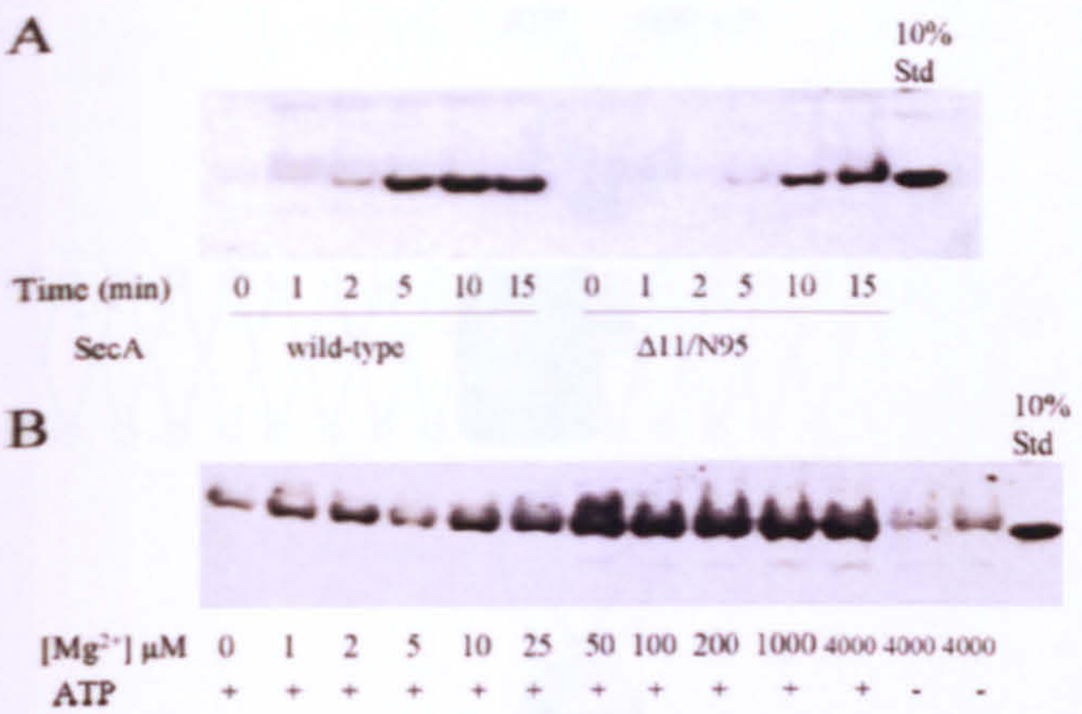

FIGURE 8. **Translocation of proOmpA through SecYEG by wild-type SecA and SecA-Δ11/N95.** *A*, translocation of proOmpA into SecYEG-containing proteoliposomes using 0.2 μM wild-type SecA or SecA-Δ11/N95. Successfully translocated (protease-protected) proOmpA was detected by Western blot. *B*, translocation assays performed with a range of magnesium acetate concentrations, including 1 mM ATP. The sample applied to the far right-hand lane of the blot in both panels had not been protease treated and was loaded as a measure of 10% of the total pro-OmpA used in each reaction.

inhibition is by binding of Mg^{2+} at a site distinct from the nucleotide binding cleft, which leads to an increase in ATP affinity but a decrease in the rate of turnover. This allosteric effect of Mg^{2+} is likely to be mediated by a rearrangement of the SecA dimer, which we have observed by the change in sedimentation behavior described below. In the presence of Mg^{2+}, the affinity for ADP was also found to be increased by about 200-fold, very similar to the effect on the ATP affinity (150-fold increase). This indicates that the binding of ADP is similarly sensitive to this conformational change induced by Mg^{2+} binding.

The fact that Mg^{2+} is both an inhibitor and an essential cofactor to the enzyme has meant that many of the previous results on the activity of SecA have been difficult to interpret. Moreover, the fact that the cation concentration varies according to the concentration of ATP will have added further confusion.

It has been proposed that Zn^{2+} binds to the C-terminal 22 residues of SecA (40) to stabilize the interaction with the molecular chaperone SecB (41). The divalent cation-binding site determined in this study cannot be the same one that co-ordinates Zn^{2+}, as SecA-Δ11/N95 has a 70-amino acid deletion at the C terminus (42), and remains the subject of Mg^{2+} inhibition. IRA elements have been identified as "internal regulators" of ATP hydrolysis (43, 44). Deletion of IRA1 (residues 783–795) results in an elevated rate of ATP turnover (44). These observations may have been due to the disruption of the allosteric site identified in this study.

The observed change in affinity for ATP caused by Mg^{2+} indicates that a conformational change occurs upon binding. This prediction was tested by analytical ultracentrifugation to determine the extent of the rearrangement. In potentially oligomeric proteins, such rearrangements could take the form of changes in the state of assembly, but sedimentation equilibrium data showed that the molecular mass of the protein (200 kDa) was unchanged by Mg^{2+} and was consistent with a dimeric quaternary structure. However, the results of sedimentation velocity reveal that structural rearrangements of the dimer are quite large, with the Mg^{2+}-bound form of the protein having a significantly larger (~6%) Svedberg constant. Interpreted empirically this is equivalent to the difference in sedimentation behavior between bovine carboxypeptidase A and bovine superoxide dismutase (45). These proteins have the same molecular mass and partial specific volumes but the latter is 40% longer in its longest axis (from 50 to 72 Å) (45). Hence, the change in sedimentation coefficient observed in SecA could represent a considerable opening of the structure.

The mutant SecA-Δ11/N95 is also a dimeric species but does not undergo such a large conformational change, probably due in part to its smaller size, and possibly also to the participation of the C terminus in this rearrangement, which has been truncated in the mutant form. This could explain why the mutant behaves in an identical manner in terms of ATPase activity, but has a reduced activity in terms of translocation. One slightly surprising aspect of this analysis was the indication that the predicted monomeric mutant SecA-Δ11/N95 (42) is a dimer, in contrast to previous findings. However, this is not to say that a monomeric form of SecA plays no part in the transport process.

The different structures of SecA all reveal essentially the same nucleotide binding fold. Insofar as we can tell most crystals were grown in the presence of inhibitory Mg^{2+} concentrations. Therefore the activated state of SecA with a dramatically reduced affinity for ATP that we have identified kinetically, may not be represented in the structural data base.

The concentration of free Mg^{2+} in bacterial cells is ~1 mM (46), sufficient to effectively inhibit the reaction and prevent futile ATP consumption by SecA. The curious observation that cardiolipin is able to counteract the Mg^{2+}-induced inhibition might reflect a natural function or regulatory process, important for protein translocation. Conditions that promote protein translocation are insensitive to high concentrations of Mg^{2+}.

SecA is water-soluble, but due to the nature of its activity has an intimate association with the lipid bilayer. It has been reported that acidic lipids and those that do not form lamellae increase SecA ATPase activity (28, 29). Moreover, reports show that acidic phospholipids are required for protein translocation (39). There have also been accounts of lipid binding sites on SecA (33, 47). The ability of lipids such as cardiolipin to chelate divalent cations (38) might indicate that the activation in ATPase activity is not directly affected by the lipid, but by its potential to extract Mg^{2+} from the allosteric binding site. This effect cannot be by a simple bulk chelation of Mg^{2+}, as we observe the activation with only 2.4 μM cardiolipin in the presence of 100 μM Mg^{2+}. Instead, the effect is likely to occur upon the formation of a SecA-Mg^{2+}-cardiolipin ternary complex, in which the Mg^{2+} may be shifted from the allosteric site by local interaction with the cardiolipin. It is tempting to propose that this kind of regulation might be important in the activation of the enzyme as it delivers substrate protein in the vicinity of the membrane and the Sec complex. Preliminary experiments show that cardiolipin stabilizes the dimeric and active form of the SecYEG complex in *E. coli*,[3] raising the possibility that this

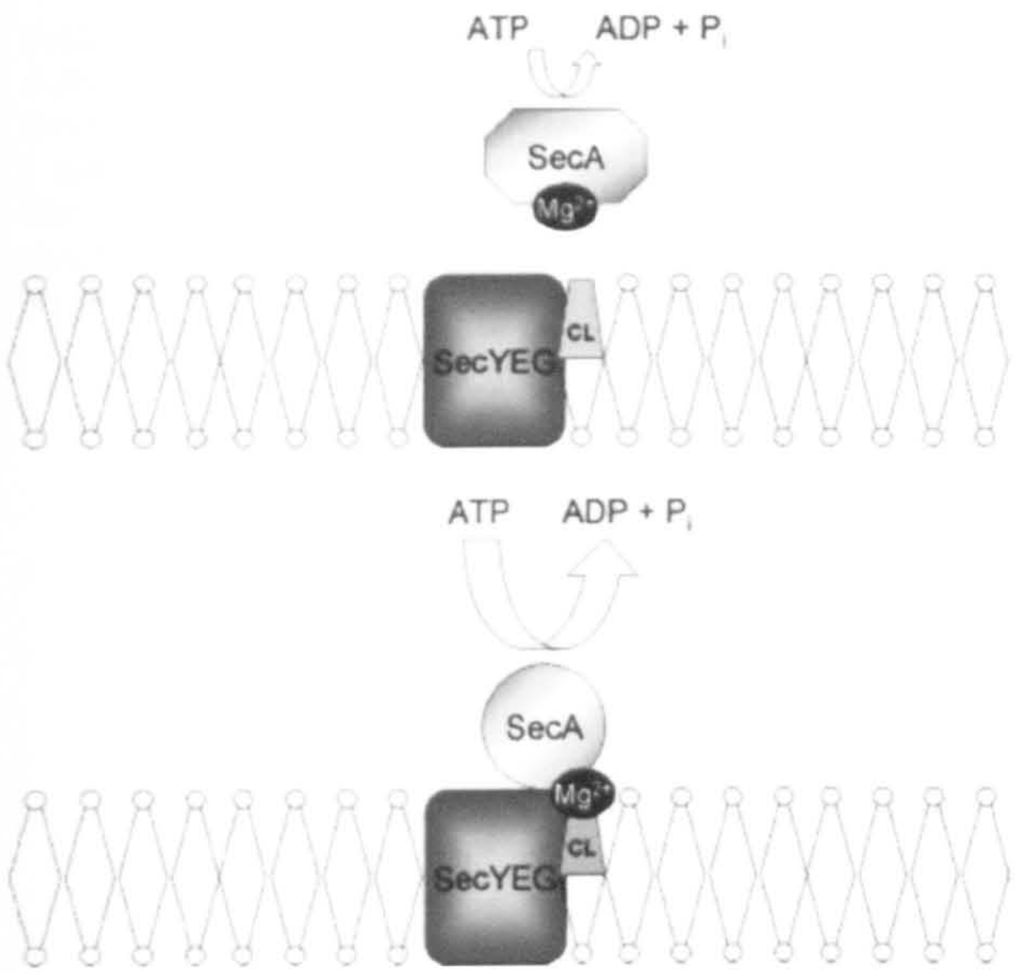

FIGURE 9. **Schematic overview depicting alleviation of Mg^{2+}-induced inhibition, mediated by cardiolipin.** Dimers of SecA and SecYEG are shown as a single object. SecA with Mg^{2+} bound to an allosteric binding site has low catalytic activity, denoted by the *smaller arrow*. When SecA is targeted to the membrane, cardiolipin (*CL*), possibly bound to SecYEG, can alleviate this inhibition, probably by formation of a SecA-Mg^{2+}-cardiolipin complex. In this ternary complex the cardiolipin shifts the Mg^{2+} from the inhibitory site, the resulting species having a lower affinity for ATP and an increase in catalytic activity, denoted by the *larger arrow*. This model does not rule out subsequent dissociation of SecA into monomers, proposed elsewhere (21).

activation could be promoted by a specific cardiolipin encountered only during the initiation of protein translocation (Fig. 9).

The results presented here describe a comprehensive analysis of the steady-state kinetics of the isolated motor domain of the major bacterial protein translocation apparatus. A conformational change in the dimer regulated by Mg^{2+} brings about a large shift in the properties of the nucleotide binding affinity and turnover of the enzyme, and it is likely that these events are coupled to the protein translocation reaction. More detailed mechanistic understanding requires an analysis of the transient kinetics of ATP binding and hydrolysis that can then be extended to include the protein substrate and SecYEG.

Acknowledgments—We express our gratitude to Dr. Mark Dillingham for valuable insights and advice and Prof. Steve Halford, Prof. Dek Woolfson, Dr. Emma Longman, Dr. Lucy Catto, and Dr. Abdenor Soufi for use and essential guidance of the analytical ultracentrifuge. We also thank Dr. Gus Cameron for assistance in global fitting and Lee Roberts for assistance in part of this project. Gifts of plasmids (proOmpA) and host strains thereof were gratefully received from Prof. Tom Rapoport and Dr. Andrew Osborne.

REFERENCES

1. Matlack, K. E., Mothes, W., and Rapoport, T. A. (1998) *Cell* **92,** 381–390
2. van den Berg, L., Clemons, W. M., Jr., Collinson, I., Modis, Y., Hartmann, E., Harrison, S. C., and Rapoport, T. A. (2004) *Nature* **427,** 36–44
3. Breyton, C., Haase, W., Rapoport, T. A., Kühlbrandt, W., and Collinson, I. (2002) *Nature* **418,** 662–665
4. Tam, P. C., Maillard, A. P., Chan, K. K., and Duong, F. (2005) *EMBO J.* **24,** 3380–3388
5. Duong, F. (2003) *EMBO J.* **22,** 4375–4384
6. Mitra, K., Schaffitzel, C., Shaikh, T., Tama, F., Jenni, S., Brooks, C. L., 3rd, Ban, N., and Frank, J. (2005) *Nature* **438,** 318–324
7. Tziatzios, C., Schubert, D., Lotz, M., Gundogan, D., Betz, H., Schagger, H., Haase, W., Duong, F., and Collinson, I. (2004) *J. Mol. Biol.* **340,** 513–524
8. Hartl, F., Lecker, S., Schiebel, E., Hendrick, J., and Wickner, W. (1990) *Cell* **63,** 269–279
9. Arkowitz, R. A., Joly, J. C., and Wickner, W. (1993) *EMBO J.* **12,** 243–253
10. Brundage, L., Hendrick, J. P., Schiebel, E., Driessen, A. J., and Wickner, W. (1990) *Cell* **62,** 649–657
11. Lill, R., Cunningham, K., Brundage, L., Ito, K., Oliver, D., and Wickner, W. (1989) *EMBO J.* **8,** 961–966
12. Economou, A., Pogliano, J., Beckwith, J., Oliver, D., and Wickner, W. (1995) *Cell* **83,** 1171–1181
13. van der Wolk, J. P., de Wit, J. G., and Driessen, A. J. (1997) *EMBO J.* **16,** 7297–7304
14. Tomkiewicz, D., Nouwen, N., van Leeuwen, R., Tans, S., and Driessen, A. J. (2006) *J. Biol. Chem.* **281,** 15709–15713
15. Ding, H., Hunt, J. F., Mukerji, I., and Oliver, D. (2003) *Biochemistry* **42,** 8729–8738
16. Woodbury, R. L., Hardy, S. J., and Randall, L. L. (2002) *Protein Sci.* **11,** 875–882
17. Driessen, A. (1993) *Biochemistry* **32,** 13190–13197
18. de Keyzer, J., van der Sluis, E. O., Spelbrink, R. E., Nijstad, N., de Kruijff, B., Nouwen, N., van der Does, C., and Driessen, A. J. (2005) *J. Biol. Chem.* **280,** 35255–35260
19. Jilaveanu, L. B., and Oliver, D. (2006) *J. Bacteriol.* **188,** 335–338
20. Or, E., Navon, A., and Rapoport, T. A. (2002) *EMBO J.* **21,** 4470–4479
21. Or, E., Boyd, D., Gon, S., Beckwith, J., and Rapoport, T. (2005) *J. Biol. Chem.* **280,** 9097–9105
22. Hunt, J. F., Weinkauf, S., Henry, L., Fak, J. J., McNicholas, P., Oliver, D. B., and Deisenhofer, J. (2002) *Science* **297,** 2018–2026
23. Sharma, V., Arockiasamy, A., Ronning, D. R., Savva, C. G., Holzenburg, A., Braunstein, M., Jacobs, W. R., Jr., and Sacchettini, J. C. (2003) *Proc. Natl. Acad. Sci. U. S. A.* **100,** 2243–2248
24. Zimmer, J., Li, W., and Rapoport, T. A. (2006) *J. Mol. Biol.* **364,** 259–265
25. Vassylyev, D. G., Mori, H., Vassylyeva, M. N., Tsukazaki, T., Kimura, Y., Tahirov, T. H., and Ito, K. (2006) *J. Mol. Biol.* **364,** 248–258
26. Papanikolau, Y., Papadovasilaki, M., Ravelli, R. B., McCarthy, A. A., Cusack, S., Economou, A., and Petratos, K. (2007) *J. Mol. Biol.* **366,** 1545–1557
27. Osborne, A. R., Clemons, W. M., Jr., and Rapoport, T. A. (2004) *Proc. Natl. Acad. Sci. U. S. A.* **101,** 10937–10942
28. Lill, R., Dowhan, W., and Wickner, W. (1990) *Cell* **60,** 271–280
29. Ahn, T., and Kim, H. (1998) *J. Biol. Chem.* **273,** 21692–21698
30. Fak, J. J., Itkin, A., Ciobanu, D. D., Lin, E. C., Song, X. J., Chou, Y. T., Gierasch, L. M., and Hunt, J. F. (2004) *Biochemistry* **43,** 7307–7327
31. den Blaauwen, T., Terpetschnig, E., Lakowicz, J. R., and Driessen, A. J. (1997) *FEBS Lett.* **416,** 35–38
32. van der Wolk, J. P., Klose, M., de Wit, J. G., den Blaauwen, T., Freudl, R., and Driessen, A. J. (1995) *J. Biol. Chem.* **270,** 18975–18982
33. Breukink, E., Keller, R. C. A., and de Kruijff, B. (1993) *FEBS Lett.* **331,** 19–24
34. Demeler, B., Scott, D. J., Harding, S. E., and Rowe, A. J. (2005) in *A Comprehensive Data Analysis Software Package for Analytical Ultracentrifugation Experiments. Modern Analytical Ultracentrifugation: Techniques and Methods* (Scott, D. J., Harding, S. E., and Rowe, A. J., eds) pp. 210–229, Royal Society of Chemistry, United Kingdom
35. Collinson, I., Breyton, C., Duong, F., Tziatzios, C., Schubert, D., Or, E., Rapoport, T. A., and Kühlbrandt, W. (2001) *EMBO J.* **20,** 2462–2471
36. van der Does, C., de Keyzer, J., van der Laan, M., and Driessen, A. J. (2003) *Methods Enzymol.* **372,** 86–98
37. Pecoraro, V. L., Hermes, J. D., and Cleland, W. W. (1984) *Biochemistry* **23,** 5262–5271
38. Brenza, J. M., Neagle, C. E., and Sokolove, P. M. (1985) *Biochem. Pharmacol.* **34,** 4291–4298
39. Hendrick, J. P., and Wickner, W. (1991) *J. Biol. Chem.* **266,** 24596–24600
40. Fekkes, P., de, W. J., Boorsma, A., Friesen, R., and Driessen, A. (1999) *Biochemistry* **38,** 5111–5116

41. Fekkes, P., van der Does, C., and Driessen, A. (1997) *EMBO J.* **16**, 6105–6113
42. Smith, M. A., Clemons, W. M., Jr., DeMars, C. J., and Flower, A. M. (2005) *J. Bacteriol.* **187**, 6454–6465
43. Sianidis, G., Karamanou, S., Vrontou, E., Boulias, K., Repanas, K., Kyrpides, N., Politou, A. S., and Economou, A. (2001) *EMBO J.* **20**, 961–970
44. Karamanou, S., Vrontou, E., Sianidis, G., Baud, C., Roos, T., Kuhn, A., Politou, A. S., and Economou, A. (1999) *Mol. Microbiol.* **34**, 1133–1145
45. Squire, P. G., and Himmel, M. E. (1979) *Arch. Biochem. Biophys.* **196**, 165–177
46. Froschauer, E. M., Kolisek, M., Dieterich, F., Schweigel, M., and Schweyen, R. J. (2004) *FEMS Microbiol. Lett.* **237**, 49–55
47. Breukink, E., Nouwen, N., van Raalte, A., Mizushima, S., Tommassen, J., and de Kruijff, B. (1995) *J. Biol. Chem.* **270**, 7902–7907

Molecular Membrane Biology, September–December 2007; 24(5–6): 387–394

informa
healthcare

Structure and function of the bacterial Sec translocon (Review)

VICKI A. M. GOLD[1], FRANCK DUONG[2], & IAN COLLINSON[1]

[1]*Department of Biochemistry, University of Bristol, Bristol, UK and* [2]*Department of Biochemistry & Molecular Biology, University of British Columbia, Vancouver BC, Canada*

(Received 9 February 2007; and in revised form 30 March 2007)

Abstract

Bacteria and archaea possess a protein complex in the plasma membrane that governs protein secretion and membrane protein insertion. Eukaryotes carry homologues in the endoplasmic reticulum (ER) where they direct the same reaction. A combination of experiments conducted on the systems found in all three domains of life has revealed a great deal about protein translocation. The channel provides a route for proteins to pass through the hydrophobic barrier of the membrane, assisted by various partner proteins which maintain an unfolded state of the substrate, target it to the channel and provide the energy and mechanical drive required for transport. In bacteria, the post-translational reaction utilizes an ATPase that couples the free energy of ATP binding and hydrolysis to move the substrate through the protein pore. This review will draw on genetic, biochemical and structural findings in an account of our current understanding of this mechanism.

Keywords: *Protein translocation, SecY complex, structure & dynamics, energy transduction*

Introduction

Proteins required in extra-cytosolic locations rely on specific targeting and transport apparatus for their localization. This process directs protein secretion and membrane protein insertion, and is therefore essential for cellular biogenesis. There exists a ubiquitous membrane protein complex found in the plasma membrane of bacteria and archaea (SecY), and in the ER of eukaryotic cells (Sec61). Two modes of translocation (co- and post-translational) converge at the Sec complex, which is a versatile and dynamic structure capable of conducting large substrates through the membrane without the loss of small molecules.

Some of the proteins synthesized in the cytosol carry N-terminal signal sequences, which are recognized by factors required for targeting [1]. In the event of co-translational translocation, the ribosome-nascent chain complex is targeted to the membrane courtesy of the signal recognition particle (SRP) and its receptor [2,3]. Subsequent reactions deliver the translating ribosome to the SecY/Sec61 complex and in this state the ribosomal polypeptide exit site is located in close vicinity to the Sec complex [4], enabling protein translocation to be driven by the concomitant chain elongation [5].

Post-translational translocation in eukaryotes and bacteria operate by different mechanisms. In eukaryotes this process relies on BiP, an Hsp70 homologue in the ER lumen which utilises ATP to effectively pull the polypeptide chain in a ratchet-like mechanism [6,7]. Bacteria have adopted a mechanism that pushes proteins across the channel by employing a motor protein ATPase SecA [8,9]. In addition, the reaction requires a cytosolic component SecB to aid targeting to the membrane and to prevent premature protein folding and aggregation, to maintain a translocation competent conformation of the pre-protein [8,10–12].

Elements of the Sec pathway were identified through different genetic screens conducted with *Escherichia coli*. Conditional-lethal mutations associated with a generalized protein-secretion defect facilitated the identification of the genes *secA*, *secB*, *secE* and *secY* [13–15]. The second strategy selected for mutations restoring the periplasmic localization of proteins with secretion-defective signal sequences, where *prlD*, *prlG* and *prlA* were identified as allelic forms of *secA*, *secE* and *secY*, respectively [16–18]. A landmark advance illustrated the requirement for ATP in post-translational translocation [19] and subsequent analysis of the gene products identified three membrane protein components SecY, SecE

Correspondence: Ian Collinson, Department of Biochemistry, University of Bristol, Bristol BS8 1TD, UK. Tel: +44 117 928 9786. E-mail: ian.collinson@bristol.ac.uk

ISSN 0968-7688 print/ISSN 1464-5203 online
DOI: 10.1080/09687680701416570

and SecG of the protein channel, and SecA a soluble ATPase [9,20–22]. Seminal experiments reconstituted the entire translocation reaction *in vitro*, when a Sec dependent substrate could be transported to the interior of vesicles containing SecYEG in the presence of SecA and ATP [9].

The SecY protein channel

Images recorded by electron cryo-microscopy provided the first pictures of the Sec complex and revealed an oligomeric assembly of an estimated 3–4 complexes with an area of low density formed at the interface [23]. This pore aligned with the polypeptide exit channel of the ribosome [24–26]. The first crystal structure determined to a significantly higher resolution was of the membrane bound *E. coli* SecYEG complex. Electron microscopy and image reconstruction revealed all 15 of the predicted trans-membrane (TM) α-helices, [27,28]. The arrangement of the SecYEG protomers seen in the membrane bound state was that of a dimer in a so-called 'back-to-back' arrangement.

The breakthrough came with the solution of a high-resolution X-ray structure of a monomeric and closed archaeal SecY complex, resolved in detergent solution (Figure 1) [29]. The most surprising observation was a hydrophilic restriction point in the centre of the monomer reminiscent of a closed channel or pore. This narrow pore is held closed by a short reinserted loop (the 'plug') and a girdle of hydrophobic side chains. The more conserved residues in SecY line the channel, which is also the site of several *prl* mutations [29]. This putative channel is conveniently located next to the signal sequence binding pocket between TM2 & 7 [30] and has also been shown to form cross-links with translocating pre-protein [31]. The periphery of the monomeric complex is too hydrophobic to form part of a protein channel at the interface of an oligomeric complex.

The structure and oligomeric state of the active channel

The channel pore is formed between two distinct halves of the SecY protein (Figure 1). SecE has been proposed to form a clamp around these domains, in order to maintain the channel closed in the resting state [29]. When perturbed, SecE may relax this grip, enabling the channel to open. This would require the concomitant displacement of the 'plug' domain to a location at the periphery of the complex, in addition to a widening of the central pore to accommodate the substrate protein. These conformational changes are presumably directed by the association of the partner protein and substrate, and the subsequent forces brought to bear by protein synthesis or the hydrolytic cycle of SecA. The separation of the two halves of SecY, comparable to a 'clam-shell' also offers an escape route to the membrane. Therefore, the structure is compatible with the ability of the complex to facilitate the passage of proteins both through and into the membrane.

There are a few clues with respect to how the channel might open. The 'plug' has been shown to cross-link to the C-terminus of SecE, approximately 20 Å away from its position in the structure [32,33], identifying a potential pocket which it can inhabit during protein translocation. The formation of this cross-link, as well as the deletion of the plug resulted in enhanced protein translocation [32], indicating that the complex may be held in a partially open state. The removal of the plug domain was however not lethal [34] indicating that this domain is not the only determinant for channel regulation. The Hsp70 homologue BiP involved in the eukaryotic post-translational translocation reaction is thought to contribute to the seal formed by the channel [35]. However, prokaryotes lack this component, indicating that other mechanisms can be adopted to provide a barrier to small molecules. A careful comparison of the membrane bound dimer [28] and the detergent solubilized monomer [29], indicates that in the former the plug has moved about 6 Å towards the outside, and the lateral gate for membrane protein insertion has opened slightly (Figure 2) [36]. In this context, although closed, the dimer of SecYEG appears to be primed for protein translocation.

One puzzling aspect of the structure is the fact that the monomer appears to provide all of the components for translocation: the signal sequence binding site, the protein-pore, exposed cytosolic loops for partner protein interaction and a lateral and traversal exit site. Several studies from independent laboratories have observed the bacterial channel in a dimeric form [28,33,37–40]. The reasons for the presence of high oligomeric states are not entirely clear. The complex may exist as an oligomer with multiple independent active sites as many other soluble and membrane proteins do. Alternatively, the larger assemblies might be required to provide a large enough platform for the association of the more sizable partners. Specific inter-subunit interactions might also be required for activation or to support a dynamic process required for the reaction. Finally, the mechanism might rely on the partner proteins or substrate to introduce an asymmetric element important for the reaction, to generate a singly active protomer. A recent study

has shown that protein translocation occurs through only one copy of the two that are present in the active complex (and not through a consolidated channel) [Osborne & Rapoport (2007) Cell, 129, 97–110].

The 'back-to-back' orientation observed of the membrane bound form has also been detected biochemically. In this particular form TM3 of SecE is located at the interface and the lateral gate for membrane protein insertion (between TM2 & TM7 of SecY; Figure 3) point in opposite directions and toward the lipid bilayer [28,29,36]. Cysteine mutagenesis experiments identified residues in SecE that were close to the equivalent helix in the neighbouring monomer [41,42]. These observations were enhanced by conditions that promote a productive association of the partner protein SecA [41]. Moreover, the cross-linked dimer retained the capacity to tightly bind and activate SecA, but had lost the ability to couple ATP hydrolysis to the work of translocation [41]. A careful inspection of the position of the respective side chains reveal that, although close, they point away from each another (Figure 3). The association of SecA may have perturbed them and brought them closer together, and thus more amenable to cross-linking. The formation of a disulphide in this position would bring about a considerable distortion of the two helices. It is conceivable that this imposed distortion and restriction on the motility at the dimer interface may have had a minor affect on the association with SecA, but a disastrous one for the energy coupling process.

Another study by electron cryo-microscopy has revealed two SecYEG dimers with a ribosome-nascent chain complex (one bound close to the exit channel and the other to mRNA) [39]. The map was of insufficient detail to resolve clear and individual TM domains, but could be used to fit the high-resolution structure into the density. On the basis of normal mode-based flexible fitting the 'back-to-back' SecYEG structure was rejected in favour of a new 'front-to-front' model. This arrangement places the same TM domain of SecE on the opposite side of the membrane complex, and the two lateral gates close to each other at the dimer interface. This proposal has been used as a foundation for a model of translocation incorporating both monomers of SecYEG in a single translocation cycle; in this context it has been suggested that the channels open at the dimer interface to form a consolidated environment for protein transport [39,43,44]. However, disulfide cross-linking shows that the contacts the translocating pre-protein makes with SecY are within the strict confides of the channel, and not, as might be expected from such an arrangement, in the teeth of the 'clam-shell' [31].

The structure and domain organization of SecA

Like other molecular motors SecA must undergo large ATP-dependent conformational changes and couple them to the domain movements required for function. The key step for energy transduction in SecA must be the conformational change regulated by ATP binding and product release in the nucleotide-binding fold (NBF). It is how these movements are relayed through the enzyme and to their partners, which provides the power stroke, and holds the key to understanding the reaction mechanism.

SecA is a soluble protein of 102 kDa and exists in solution in a monomer-dimer equilibrium, predominantly dimeric [45,46]. Of the six published SecA crystal structures [47–52], five of them are dimeric and one monomeric (Figure 4). The protomers of each dimer all have a similar structure, the major differences between them being at the dimer interface. Interestingly, the structure from *Thermus thermophilus* is in a parallel conformation [47], in contrast to all of the other structures which are packed in an anti-parallel manner [48,50–52]. It is not clear which of these structures is the correct physiological state, as it is possible that the oligomeric arrangement observed in X-ray structures is a consequence of the extreme crystallization conditions or the lattice contacts. The parallel and two anti-parallel forms have however been shown to exist in solution by directed cysteine mutagenesis and cross-linking [47,50] suggesting that in the absence of other translocation partners and pre-protein there may be different conformational states of the enzyme.

Within each protomer there are five major domains, from N- to C-terminus these are: nucleotide binding fold 1 (NBF1), pre-protein cross-linking domain (PPXD) [53,54], nucleotide binding fold 2 (NBF2), helical scaffold domain (HSD) and helical wing domain (HWD) [51]. In the monomeric crystal, movements of the HWD, HSD and PPXD domains results in opening of a groove that may be the polypeptide binding site [49,55] (Figure 4). In all of the apo- and nucleotide-bound structures, there are essentially no major changes in the structure of the NBFs [48,51,56]. This means that there are missing active states of the complex. The constraints of the crystallization process or the transient nature of these states may mean that they are difficult to characterise structurally.

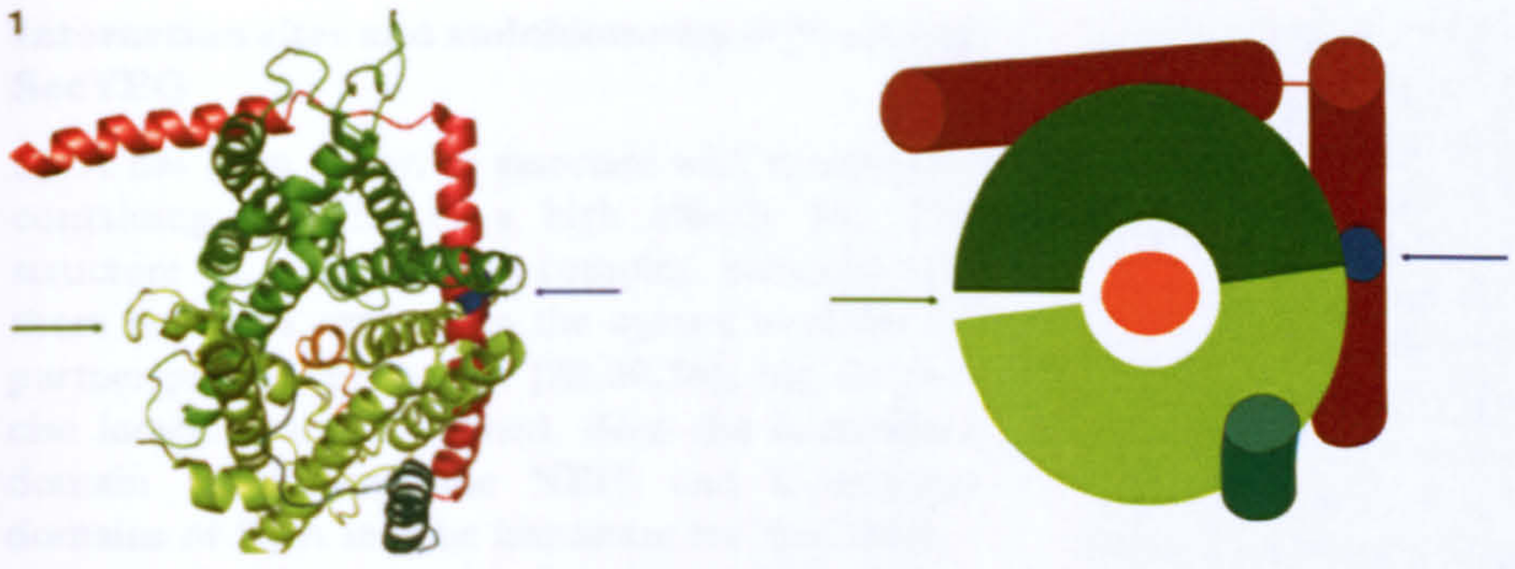

Figure 1. Ribbon and schematic representation of the detergent solubilized monomeric *Methanococcus jannaschii* SecYEβ complex viewed from the cytosolic face [29]. Transmembrane helices 1–5 are coloured in light green, helices 6–10 dark green, the 'plug' orange, SecE red and Secβ (SecG) is shown in sea green. The equivalent *E. coli* cysteine cross-link (*L106C*) is indicated in blue, close to the blue arrow. The green arrow denotes the position of the lateral gate.

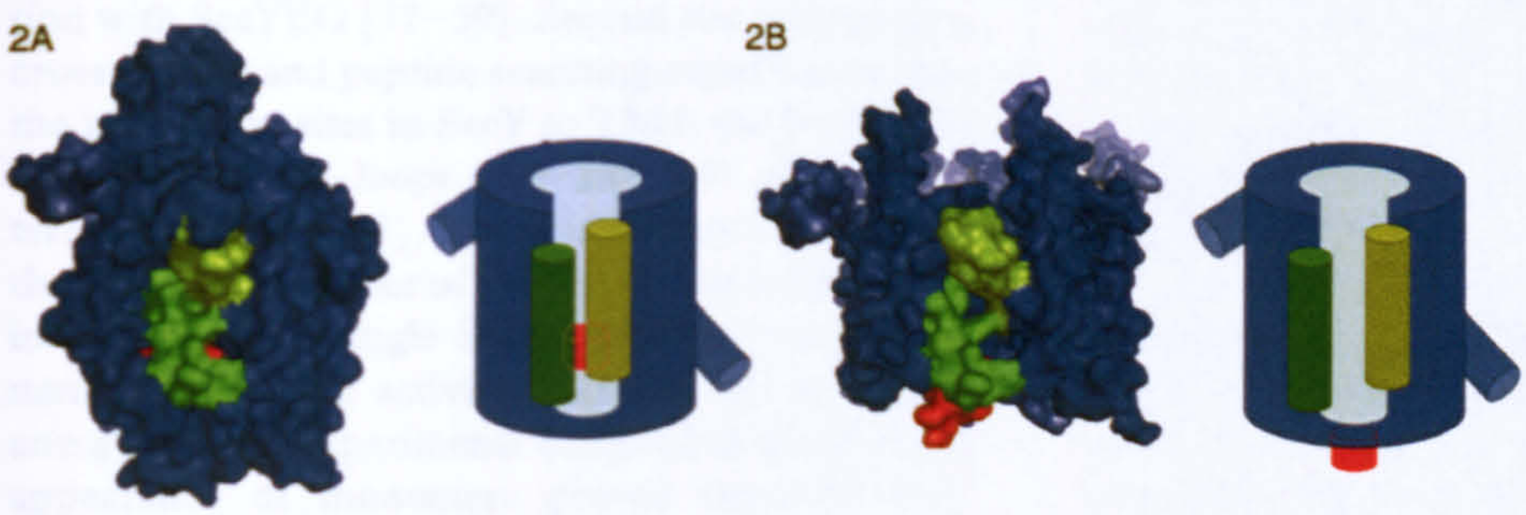

Figure 2. (A) Homology model of *E. coli* SecYEG based on the detergent solubilized SecYEβ monomer. (B) Model fitted according to the membrane bound dimer [36]. Both are side views with the cytosolic face uppermost; the latter shows only the membrane sector, as the loops were not resolved sufficiently. TM2b (olive) and TM7 (green) form the signal sequence-binding site and have parted slightly in the dimer. The 'plug' (red) is obscured in (A) and is about 6.5 Å higher. For purposes of clarity schematic representations have been drawn on the right hand sides.

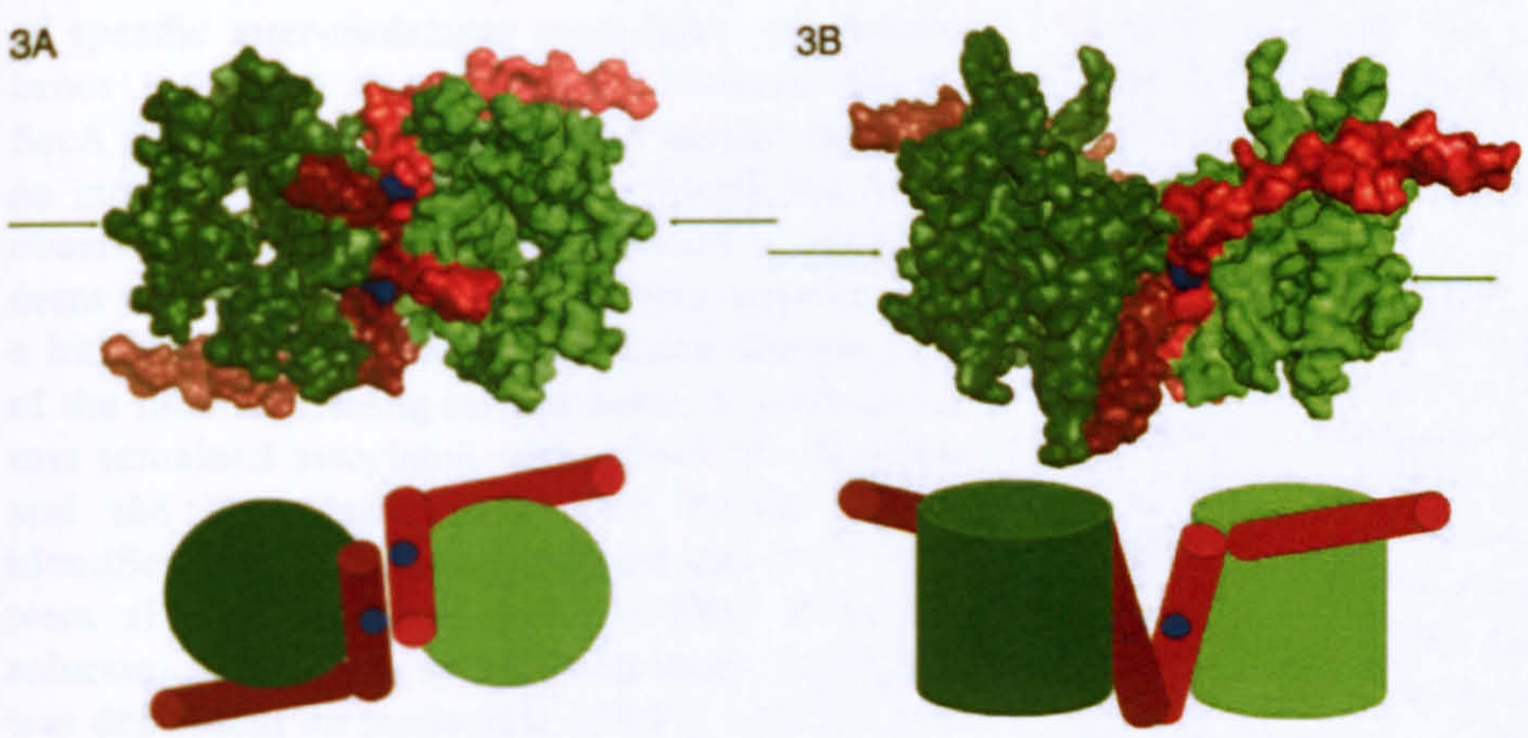

Figure 3. Space filling representation of the dimeric membrane-bound *E. coli* atomic model [36]. SecY and SecE are coloured green and red, respectively. The green arrows denote the position of the lateral gate. The *E. coli* cysteine cross-link (L106C) is shown in blue. The distance between the two cysteines is 18.5 Å, contrasting to the 2.05Å disulphide bond length. (A) View from the periplasmic face of the membrane. (B) View from the side of the membrane. Simplified views have been drawn underneath; the open blue circle (B) denotes that the cysteine is on the other side of TM3 of SecE.

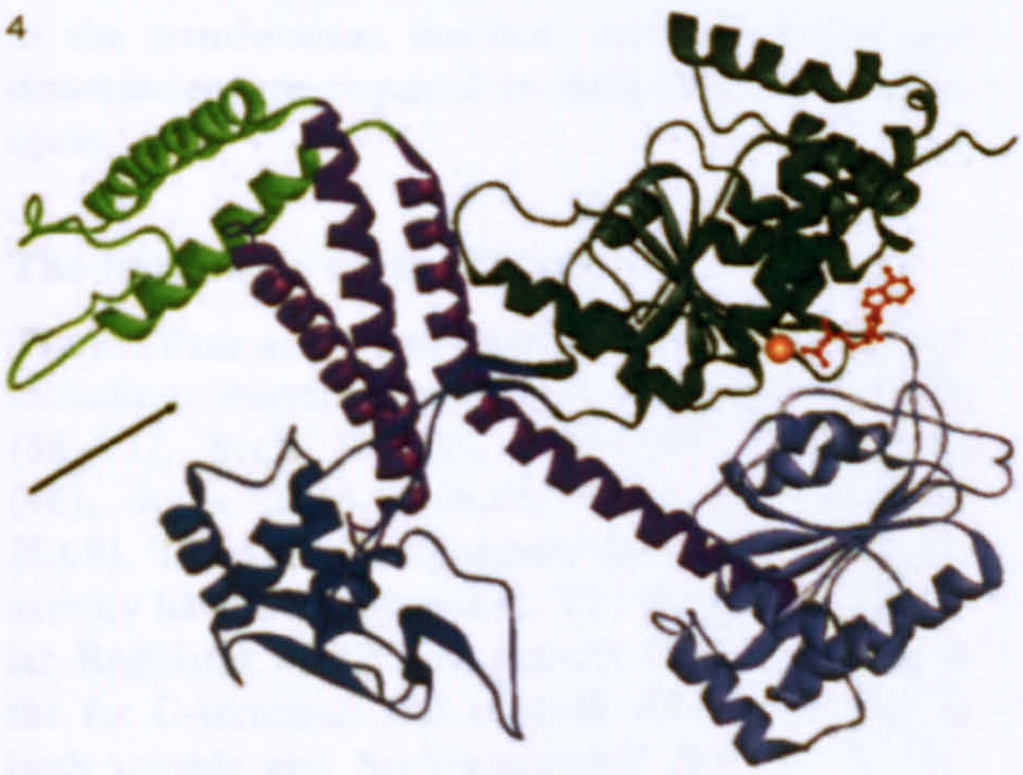

Figure 4. Ribbon representation of the monomeric SecA structure [49]. NBF1 is shown in dark green, NBF2 pale blue, HSD purple, HWD bright green, PPXD in dark blue and Mg^{2+}-ADP in orange/red. The arrow denotes the position of the putative polypeptide-binding site.

Interaction sites and stoichiometry of SecA and SecYEG

SecA has been shown to associate with membranes containing SecYEG to a high affinity [8]. The structure of the SecYEG complex indicates that there are loops exposed to the cytosol available for partner protein interaction [28,29,36], but the precise locations are ill defined. Both the N-terminal domain (comprising the NBF) and C-terminal domains of SecA may be important for the interaction with SecYEG [57–59]. Second site suppressors, cross-linking and peptide scanning experiments map the interaction sites in SecY to TM4, the fourth and fifth cytoplasmic loops (C4 and C5) and the C-terminal tail [60–63]. There is evidence to support the fact that the dimer of SecA is an active form. The inactivation of a single SecA protomer has a dominant effect on the activity of dimer and resonance energy transfer experiments designed to monitor the appearance of monomers proved negative [64]. However, recent reports have challenged this view. The fact that one of the structures of SecA is a monomer led to suggestion that the dimer might dissociate when activated [49,50]. The observed loss of specific inter-molecular cross-links and fluorescence resonance energy transfer between dimeric SecA on exposure to translocation specific ligands is an indication of monomerization [49,65,66]. These observations may also be the result of a rearrangement to form one of the other dimeric structures, or a hitherto uncharacterized and active dimeric form of the protein. During translocation, a SecA monomer remained associated with a SecYEG protomer and the pre-protein [67]. Two further studies identified that both monomers and dimers of SecA were able to associate with SecYEG dimers in solution, and that the specific oligomeric association was dependent on nucleotide [37,67]. Perhaps both monomers and dimers of SecA play important roles in the translocation reaction, and association and dissociation are required to complete the reaction cycle.

The hydrolytic cycle of SecA

The ATPase activity of SecA is sensitive to ligands, including: mature proteins [68], signal peptides [68–71], SecB [72,73], ADP [46], magnesium [46], lipids [8,46,65,66,68,74–76] and SecYEG [8,68]. Two specific regulatory domains for ATPase activity have been proposed. The first Intramolecular Regulator of ATPase activity (IRA1) resides at the far C-terminus and controls ATP hydrolysis in both soluble and SecY-associated SecA [77]. The second, IRA2 (NBF2) controls the nucleotide binding and release occurring at NBF1 [78].

The ATP bound state of SecA has been shown to be in an extended conformation [79], whereas the ADP bound form is more compact [51,77–81], the release of which is thought to be the rate limiting step of the steady-state reaction cycle [80]. The non-hydrolysable ATP analogue AMP-PNP stabilises the association of SecA and SecYEG and promotes the 'inserted' state of a substrate protein [37,82]. Experiments employing surface plasmon resonance and cross-linking show that ATP induces the release of SecA from SecYEG [67,83].

The divalent cation magnesium exerts a strong inhibitory effect upon SecA, affecting both the dimeric conformation (but not oligomeric state) and the affinity for ATP; it does this by acting on an allosteric binding site distinct from the catalytic one [46]. This inhibition could be overcome by the acidic phospholipid cardiolipin, which had a stimulatory role only in the presence of magnesium. Lipid binding sites have been found on SecA [84,85], and acidic phospholipids are required for translocation [86]. This suggests that the 'lipid-ATPase' activity reported may in fact be related to a counteraction of magnesium inhibition by cardiolipin-SecA interactions [46]. This inhibition presumably prevents the futile hydrolysis of ATP during moments of inactivity, and is released as a result of intimate exposure to the membrane.

The catalytic cycle has been proposed to proceed by a multi-step mechanism for translocation via SecA insertion and de-insertion events [82]. The evidence is based upon the protease protection of a large domain of SecA while bound by SecY, which is dependent on ATP and pre-protein [82,87]. This protection is the result of a necessary and uncharacterized large conformational change of the peripherally associated protein and not necessarily the result of a deep penetration of the enzyme. The thermodynamics of this reaction have also not been well characterized; one study proposes that one ATP drives the passage of 40 amino acids, and another determines that each amino acid requires 5 molecules of ATP [88,89].

Concluding comments

This is an extremely complicated field of membra ne biology and our comprehension of it is thanks to a generation of research on the related eukaryotic, bacterial and archaeal systems. In spite of the recent progress there are several disputed and unanswer ed aspects of the reaction mechanism. These outstanding problems will need to be addressed by detailed structural determination of an active state of

the translocation complex with pre-protein, and by further biophysical studies aimed to comprehend the dynamics of the reaction. Understanding details both on the nature and timing of the conformational changes that derive from the release of chemical energy, and of specific protein-protein interactions holds the key to understanding how they are coupled to protein transport.

References

[1] Walter P, Blobel G. 1981. Translocation of proteins across the endoplasmic reticulum. III. Signal recognition protein (SRP) causes signal sequence and site specific arrest of chain elongation that is released by microsomal membranes. J Cell Biol 91:557–561.

[2] Walter P, Ibrahimi I, Blobel G. 1981. Translocation of proteins across the endoplasmic reticulum. I. Signal recognition protein (SRP) binds to *in vitro* assembled polysomes synthesizing secretory protein. J Cell Biol 91:545–550.

[3] Gilmore R, Blobel G. 1983. Transient involvement of signal recognition particle and its receptor in the microsomal membrane prior to protein translocation. Cell 35:677–685.

[4] Beckmann R, Spahn C, Eswar N, Helmers J, Penczek P, Sali A, Frank J, Blobel G. 2001. Architecture of the protein-conducting channel associated with the translating 80S ribosome. Cell 107:361–372.

[5] Görlich D, Prehn S, Hartmann E, Kalies K, Rapoport T. 1992. A mammalian homolog of SEC61p and SECYp is associated with ribosomes and nascent polypeptides during translocation. Cell 71:489–503.

[6] Misselwitz B, Staeck O, Matlack K, Rapoport T. 1999. Interaction of BiP with the J-domain of the Sec63p component of the endoplasmic reticulum protein translocation complex. J Biol Chem 274:20110–20115.

[7] Matlack K, Misselwitz B, Plath K, Rapoport T. 1999. BiP acts as a molecular ratchet during posttranslational transport of prepro-alpha factor across the ER membrane. Cell 97:553–564.

[8] Hartl F, Lecker S, Schiebel E, Hendrick J, Wickner W. 1990. The binding cascade of SecB to SecA to SecY/E mediates preprotein targeting to the *E. coli* plasma membrane. Cell 63:269–279.

[9] Brundage L, Hendrick JP, Schiebel E, Driessen AJM, Wickner W. 1990. The purified *E. Coli* integral membrane protein SecY/E is sufficient for reconstitution of SecA-dependent precursor protein translocation. Cell 62:649–657.

[10] Weiss J, Ray P, Bassford P. 1988. Purified SecB protein of *Escherichia coli* retards folding and promotes membrane translocation of the maltose-binding protein *in vivo*. Proc Natl Acad Sci USA 85:8978–8982.

[11] Kusters R, de Vrije T, Breukink E, de Kruijff B. 1989. SecB protein stabilizes a translocation-competent state of purified PrePhoe protein. J Biol Chem 264:20827–20830.

[12] de Keyzer J, van der Does C, Driessen AJ. 2002. Kinetic analysis of the translocation of fluorescent precursor proteins into *Escherichia coli* membrane vesicles. J Biol Chem 277:46059–46065.

[13] Kumamoto CA, Beckwith J. 1983. Mutations in a new gene, secB, cause defective protein localization in *Escherichia coli*. J Bacteriol 154:253–260.

[14] Oliver D, Beckwith J. 1981. *E. coli* mutant pleiotropically defective in the export of secreted proteins. Cell 25:765–772.

[15] Oliver D, Beckwith J. 1982. Identification of a new gene (secA) and gene product involved in the secretion of envelope proteins in *Escherichia coli*. J Bacteriol 150:686–691.

[16] Emr SD, Hanley-Way S, Silhavy T. 1981. Suppressor mutations that restore export of a protein with a defective signal sequence. Cell 23:79–88.

[17] Brickman E, Oliver D, Garwin J, Kumamoto C, Beckwith J. 1984. The use of extragenic suppressors to define genes involved in protein export in *Escherichia coli*. Mol Gen Genet 196:24–27.

[18] Oliver DB, Liss LR. 1985. prlA-mediated suppression of signal sequence mutations is modulated by the secA gene product of *Escherichia coli* K-12. J Bacteriol 161:817–819.

[19] Chen L, Tai PC. 1985. ATP is essential for protein translocation into *Escherichia coli* membrane vesicles. Proc Natl Acad Sci USA 82:4384–4388.

[20] Lill R, Cunningham K, Brundage L, Ito K, Oliver D, Wickner W. 1989. SecA protein hydrolyzes ATP and is an essential component of the protein translocation ATPase of *Escherichia coli*. EMBO J 8:961–966.

[21] Bieker KL, Silhavy TJ. 1990. PrlA (SecY) and PrlG (SecE) Interact directly and function sequentially during protein translocation in *E. Coli*. Cell 61:833–842.

[22] Hanada M, Nishiyama K, Mizushima S, Tokuda H. 1994. Reconstitution of an efficient protein translocation machinery comprising SecA and the three membrane proteins, SecY, SecE, and SecG (p12). J Biol Chem 269: 23625–23631.

[23] Hanein D, Matlack K, Jungnickel B, Plath K, Kalies K, Miller K, Rapoport T, Akey C. 1996. Oligomeric rings of the Sec61p complex induced by ligands required for protein translocation. Cell 87:721–732.

[24] Beckmann R, Bubeck D, Grassucci R, Penczek P, Verschoor A, Blobel G, Frank J. 1997. Alignment of conduits for the nascent polypeptide chain in the ribosome-Sec61 complex. Science 278:2123–2126.

[25] Menetret J, Neuhof A, Morgan D, Plath K, Radermacher M, Rapoport T, Akey C. 2000. The structure of ribosome-channel complexes engaged in protein translocation. Mol Cell 6:1219–1232.

[26] Morgan DG, Menetret J-F, Neuhof A, Rapoport TA, Akey CW. 2002. Structure of the mammalian Ribosome-Channel complex at 17 Å resolution. J Mol Biol 324:871–886.

[27] Collinson I, Breyton C, Duong F, Tziatzios C, Schubert D, Or E, Rapoport T, Kuhlbrandt W. 2001. Projection structure and oligomeric properties of a bacterial core protein translocase. EMBO J 20:2462–2471.

[28] Breyton C, Haase W, Rapoport TA, Kuhlbrandt W, Collinson I. 2002. Three-dimensional structure of the bacterial protein-translocation complex SecYEG. Nature 418:662–665.

[29] van den Berg B, Clemons WM Jr, Collinson I, Modis Y, Hartmann E, Harrison SC, Rapoport TA. 2004. X-ray structure of a protein-conducting channel. Nature 427: 36–44.

[30] Plath K, Mothes W, Wilkinson B, Stirling C, Rapoport T. 1998. Signal sequence recognition in posttranslational protein transport across the yeast ER membrane. Cell 94:795–807.

[31] Cannon KS, Or E, Clemons WM Jr, Shibata Y, Rapoport TA. 2005. Disulfide bridge formation between SecY and a translocating polypeptide localizes the translocation pore to the center of SecY. J Cell Biol 169:219–225.

[32] Harris CR, Silhavy TJ. 1999. Mapping an interface of SecY (PrlA) and SecE (PrlG) by using synthetic phenotypes and in vivo cross-linking. J Bacteriol 181:3438–3444.

[33] Tam PC, Maillard AP, Chan KK, Duong F. 2005. Investigating the SecY plug movement at the SecYEG translocation channel. EMBO J 24:3380–3388.
[34] Maillard AP, Lalani S, Silva F, Belin D, Duong F. 2007. Deregulation of the SecYEG translocation channel upon removal of the plug domain. J Biol Chem 282:1281–1287.
[35] Alder NN, Shen Y, Brodsky JL, Hendershot LM, Johnson AE. 2005. The molecular mechanisms underlying BiP-mediated gating of the Sec61 translocon of the endoplasmic reticulum. J Cell Biol 168:389–399.
[36] Bostina M, Mohsin B, Kuhlbrandt W, Collinson I. 2005. Atomic model of the *E. coli* membrane-bound protein translocation complex SecYEG. J Mol Biol 352:1035–1043.
[37] Tziatzios C, Schubert D, Lotz M, Gundogan D, Betz H, Schagger H, Haase W, Duong F, Collinson I. 2004. The bacterial protein-translocation complex: SecYEG dimers associate with one or two SecA molecules. J Mol Biol 340:513–524.
[38] Bessonneau P, Besson V, Collinson I, Duong F. 2002. The SecYEG preprotein translocation channel is a conformationally dynamic and dimeric structure. EMBO J 21:995–1003.
[39] Mitra K, Schaffitzel C, Shaikh T, Tama F, Jenni S, Brooks CL 3rd, Ban N, Frank J. 2005. Structure of the *E. coli* protein-conducting channel bound to a translating ribosome. Nature 438:318–324.
[40] Scheuring J, Braun N, Nothdurft L, Stumpf M, Veenendaal AK, Kol S, van der Does C, Driessen AJ, Weinkauf S. 2005. The oligomeric distribution of SecYEG is altered by SecA and translocation ligands. J Mol Biol 354:258–271.
[41] Kaufmann A, Manting EH, Veenendaal AK, Driessen AJ, van der Does C. 1999. Cysteine-directed cross-linking demonstrates that helix 3 of SecE is close to helix 2 of SecY and helix 3 of a neighboring SecE. Biochemistry 38:9115–9125.
[42] Veenendaal A, van der Does C, Driessen A. 2001. Mapping the sites of interaction between SecY and SecE by cysteine scanning mutagenesis. J Biol Chem 276:32559–32566.
[43] Mitra K, Frank J. 2006. A model for co-translational translocation: Ribosome-regulated nascent polypeptide translocation at the protein-conducting channel. FEBS Lett 580:3353–3360.
[44] Mitra K, Frank J, Driessen A. 2006. Co- and post-translational translocation through the protein-conducting channel: analogous mechanisms at work? Nat Struct Mol Biol 13:957–964.
[45] Woodbury RL, Hardy SJS, Randall LL. 2002. Complex behavior in solution of homodimeric SecA. Protein Sci 11:875–882.
[46] Gold VAM, Robson A, Clarke AR, Collinson I. 2007. Allosteric regulation of SecA: magnesium-mediated control of conformation and activity. J Biol Chem (in press).
[47] Vassylyev DG, Mori H, Vassylyeva MN, Tsukazaki T, Kimura Y, Tahirov TH, Ito K. 2006. Crystal structure of the translocation ATPase SecA from *Thermus thermophilus* reveals a parallel, head-to-head dimer. J Mol Biol 364:248–258.
[48] Papanikolau Y, Papadovasilaki M, Ravelli RB, McCarthy AA, Cusack S, Economou A, Petratos K. 2006. Structure of dimeric SecA, the *Escherichia coli* preprotein translocase motor. J Mol Biol 366:1545–1557.
[49] Osborne AR, Clemons WMJr, Rapoport TA. 2004. A large conformational change of the translocation ATPase SecA. Proc Natl Acad Sci USA 101:10937–10942.
[50] Zimmer J, Li W, Rapoport TA. 2006. A novel dimer interface and conformational changes revealed by an X-ray structure of *B. subtilis* SecA. J Mol Biol 364:259–265.
[51] Hunt JF, Weinkauf S, Henry L, Fak JJ, McNicholas P, Oliver DB, Deisenhofer J. 2002. Nucleotide control of interdomain interactions in the conformational reaction cycle of SecA. Science 297:2018–2026.
[52] Sharma V, Arockiasamy A, Ronning DR, Savva CG, Holzenburg A, Braunstein M, Jacobs WR Jr, Sacchettini JC. 2003. Crystal structure of Mycobacterium tuberculosis SecA, a preprotein translocating ATPase. Proc Natl Acad Sci USA 100:2243–2248.
[53] Kimura E, Akita M, Matsuyama S, Mizushima S. 1991. Determination of a region in SecA that interacts with presecretory proteins in *Escherichia coli*. J Biol Chem 266:6600–6606.
[54] Kourtz L, Oliver D. 2000. Tyr-326 plays a critical role in controlling SecA-preprotein interaction. Mol Microbiol 37:1342–1356.
[55] Musial-Siwek M, Rusch SL, Kendall DA. 2007. Selective photoaffinity labeling identifies the signal peptide binding domain on SecA. J Mol Biol 365:637–648.
[56] Osborne AR, Rapoport TA, van den Berg B. 2005. Protein translocation by the Sec61/SecY channel. Annu Rev Cell Dev Biol 21:529–550.
[57] Vrontou E, Karamanou S, Baud C, Sianidis G, Economou A. 2004. Global co-ordination of protein translocation by the SecA IRA1 switch. J Biol Chem 279:22490–22497.
[58] Matsumoto G, Nakatogawa H, Mori H, Ito K. 2000. Genetic dissection of SecA: suppressor mutations against the secY205 translocase defect. Genes Cells 5:991–999.
[59] Snyders S, Ramamurthy V, Oliver D. 1997. Identification of a region of interaction between *Escherichia coli* SecA and SecY proteins. J Biol Chem 272:11302–11306.
[60] Taura T, Akiyama Y, Ito K. 1994. Genetic analysis of SecY: additional export-deficient mutations and factors affecting their phenotypes. Mol Gen Genet 243:261–269.
[61] Mori H, Ito K. 2003. Biochemical characterization of a mutationally altered protein translocase: proton motive force stimulation of the initiation phase of translocation. J Bacteriol 185:405–412.
[62] van der Sluis EO, Nouwen N, Koch J, de Keyzer J, van der Does C, Tampe R, Driessen AJ. 2006. Identification of two interaction sites in SecY that are important for the functional interaction with SecA. J Mol Biol 361:839–849.
[63] Mori H, Ito K. 2006. Different modes of SecY-SecA interactions revealed by site-directed *in vivo* photo-cross-linking. Proc Natl Acad Sci USA 103:16159–16164.
[64] Driessen A. 1993. SecA, the peripheral subunit of the *Escherichia coli* precursor protein translocase, is functional as a dimer. Biochemistry 32:13190–13197.
[65] Or E, Navon A, Rapoport TA. 2002. Dissociation of the dimeric SecA ATPase during protein translocation across the bacterial membrane. EMBO J 21:4470–4479.
[66] Or E, Boyd D, Gon S, Beckwith J, Rapoport T. 2005. The bacterial ATPase SecA functions as a monomer in protein translocation. J Biol Chem 280:9097–9105.
[67] Duong F. 2003. Binding, activation and dissociation of the dimeric SecA ATPase at the dimeric SecYEG translocase. EMBO J 22:4375–4384.
[68] Lill R, Dowhan W, Wickner W. 1990. The ATPase activity of SecA is regulated by acidic phospholipids, SecY, and the leader and mature domains of precursor proteins. Cell 60:271–280.
[69] Wang L, Miller A, Kendall DA. 2000. Signal peptide determinants of SecA binding and stimulation of ATPase activity. J Biol Chem 275:10154–10159.
[70] Triplett TL, Sgrignoli AR, Gao FB, Yang YB, Tai PC, Gierasch LM. 2001. Functional signal peptides bind a

soluble N-terminal fragment of SecA and inhibit its ATPase activity. J Biol Chem 276:19648–19655.
[71] Miller A, Wang L, Kendall DA. 1998. Synthetic signal peptides specifically recognize SecA and stimulate ATPase activity in the absence of preprotein. J Biol Chem 273:11409–11412.
[72] Miller A, Wang L, Kendall DA. 2002. SecB modulates the nucleotide-bound state of SecA and stimulates ATPase activity. Biochemistry 41:5325–5332.
[73] Kim J, Miller A, Wang L, Muller JP, Kendall DA. 2001. Evidence that SecB enhances the activity of SecA. Biochemistry 40:3674–3680.
[74] Benach J, Chou Y-T, Fak JJ, Itkin A, Nicolae DD, Smith PC, Wittrock G, Floyd DL, Golsaz CM, Gierasch LM, Hunt JF. 2003. Phospholipid-induced monomerization and signal-peptide-induced oligomerization of SecA. J Biol Chem 278:3628–3638.
[75] Bu Z, Wang L, Kendall DA. 2003. Nucleotide binding induces changes in the oligomeric state and conformation of SecA in a lipid environment: A small-angle neutron-scattering study. J Mol Biol 332:23–30.
[76] Ahn T, Kim H. 1998. Effects of nonlamellar-prone lipids on the ATPase activity of SecA bound to model membranes. J Biol Chem 273:21692–21698.
[77] Karamanou S, Vrontou E, Sianidis G, Baud C, Roos T, Kuhn A, Politou AS, Economou A. 1999. A molecular switch in SecA protein couples ATP hydrolysis to protein translocation. Mol Microbiol 34:1133–1145.
[78] Sianidis G, Karamanou S, Vrontou E, Boulias K, Repanas K, Kyrpides N, Politou AS, Economou A. 2001. Cross-talk between catalytic and regulatory elements in a DEAD motor domain is essential for SecA function. EMBO J 20:961–970.
[79] den Blaauwen T, Fekkes P, de Wit JG, Kuiper W, Driessen AJ. 1996. Domain interactions of the peripheral preprotein Translocase subunit SecA. Biochemistry 35:11994–12004.
[80] Fak JJ, Itkin A, Ciobanu DD, Lin EC, Song XJ, Chou YT, Gierasch LM, Hunt JF. 2004. Nucleotide exchange from the high-affinity ATP-binding site in SecA is the rate-limiting step in the ATPase cycle of the soluble enzyme and occurs through a specialized conformational state. Biochemistry 43:7307–7327.
[81] Kim J, Ahn T, Ko J, Park C, Kim H. 2001. Effect of divalent cations on the ATPase activity of *Escherichia coli* SecA. FEBS Lett 493:12–16.
[82] Economou A, Wickner W. 1994. SecA promotes preprotein translocation by undergoing ATP-driven cycles of membrane insertion and deinsertion. Cell 78:835–843.
[83] de Keyzer J, van der Does C, Kloosterman TG, Driessen AJ M. 2003. Direct demonstration of ATP-dependent release of SecA from a translocating preprotein by surface plasmon resonance. J Biol Chem 278:29581–29586.
[84] Breukink E, Nouwen N, van Raalte A, Mizushima S, Tommassen J, de Kruijff B. 1995. The C terminus of SecA is involved in both lipid binding and SecB binding. J Biol Chem 270:7902–7907.
[85] Breukink E, Keller RCA, de Kruijff B. 1993. Nucleotide and negatively charged lipid-dependent vesicle aggregation caused by SecA. Evidence that SecA contains two lipid-binding sites. FEBS Lett 331:19–24.
[86] Hendrick JP, Wickner W. 1991. SecA protein needs both acidic phospholipids and SecY/E protein for functional high-affinity binding to the *Escherichia coli* plasma membrane. J Biol Chem 266:24596–24600.
[87] Jilaveanu LB, Oliver DB. 2007. *In vivo* membrane topology of *Escherichia coli* SecA ATPase reveals extensive periplasmic exposure of multiple functionally important domains clustering on one face of SecA. J Biol Chem 282:4661–4668.
[88] Tomkiewicz D, Nouwen N, van Leeuwen R, Tans S, Driessen AJ. 2006. SecA supports a constant rate of preprotein translocation. J Biol Chem 281:15709–15713.
[89] van der Wolk J, de Wit J, Driessen A. 1997. The catalytic cycle of the *Escherichia coli* SecA ATPase comprises two distinct preprotein translocation events. EMBO J 16:7297–7304.

This paper was first published online on iFirst on 8 June 2007.

doi:10.1016/j.jmb.2007.09.086 J. Mol. Biol. (2007) 374, 965–976

JMB

Available online at www.sciencedirect.com

ScienceDirect

ELSEVIER

A Large Conformational Change Couples the ATP Binding Site of SecA to the SecY Protein Channel

Alice Robson, Antonia E. G. Booth, Vicki A. M. Gold Anthony R. Clarke and Ian Collinson*

Department of Biochemistry University of Bristol, University Walk, Bristol, BS8 1TD, UK

Received 1 August 2007; received in revised form 26 September 2007; accepted 27 September 2007
Available online 4 October 2007

In bacteria, the SecYEG protein translocation complex employs the cytosolic ATPase SecA to couple the energy of ATP binding and hydrolysis to the mechanical force required to push polypeptides through the membrane. The molecular basis of this energy transducing reaction is not well understood. A peptide-binding array has been employed to identify sites on SecYEG that interact with SecA. These results along with fluorescence spectroscopy have been exploited to characterise a long-distance conformational change that connects the nucleotide-binding fold of SecA to the transmembrane polypeptide channel in SecY. These movements are driven by binding of non-hydrolysable ATP analogues to a monomer of SecA in association with the SecYEG complex. We also determine that interaction with SecYEG simultaneously decreases the affinity of SecA for ATP and inhibitory magnesium, favouring a previously identified active state of the ATPase. Mutants of SecA capable of binding but not hydrolysing ATP do not elicit this conformationally active state, implicating residues of the Walker B motif in the early chain of events that couple ATP binding to the mobility of the channel.

Keywords: ATPase; conformational changes; membrane transport; protein-translocation

Edited by I. B. Holland

Introduction

Proteins rely on specific translocation machines if they are to cross or enter the lipid bilayer. Protein secretion and membrane insertion usually occurs through the ubiquitous SecYEG/Sec61 protein conducting complex.[1] In bacteria, proteins can be translocated during or after they have been fully translated; in the latter case they are maintained in an unfolded conformation by the action of chaperones such as SecB.[2] A heterotrimeric membrane-bound complex SecYEG and a soluble protein factor SecA are necessary and sufficient for this reaction to proceed.[3] The free energy released during the ATP hydrolytic cycle by SecA is used to push the translocating polypeptide substrate through SecYEG.[4–6]

Important advances in our knowledge have begun to provide clues about the mechanics of this complicated reaction. The high-resolution structure of an archael homologue of the channel revealed the site of the signal sequence binding pocket, the protein-conducting pore and the cytosolic loops responsible for the interaction with partner proteins.[7] Whilst the X-ray structure was crystallised in monomeric form, the SecYEG complex is known to form dimers in the membrane and when active.[8–11] Proteins are translocated through one of the two protein channels that are formed by a dimer, one at the centre of each protomer.[7,12] Low-resolution structures of the active and inactive forms of the complex indicate that it must undergo large conformational changes during transport.[11]

The SecA partner protein is a large soluble protein of 102 kDa, which is primarily dimeric in solution.[13–17] However, monomers have also been implicated as the active species.[12,18–21] Complexes containing either one or two SecA molecules bound to a SecYEG dimer, depending on the nucleotide present, have been observed by analytical ultracentrifugation and blue native gel electrophoresis.[8,22]

Several different high-resolution structures of SecA have been determined. Most of them are dimers[23–27] and one of them is a monomer.[28] Despite

*Corresponding author. E-mail address: ian.collinson@bristol.ac.uk.

Abbreviations used: NBF, nucleotide-binding fold; TM, trans-membrane helix; DDM, *n*-dodecyl-β-D-maltoside.

0022-2836/$ - see front matter

the differences in quaternary structures, the form of the protomer in most is essentially the same, apart from an opening of the cleft forming a putative preprotein binding site.[27,28] This might be one of the conformational changes involved during the reaction cycle, although it is not dependent on nucleotide. Surprisingly, the structure of the nucleotide-binding fold (NBF) of SecA appears to be the same irrespective of the presence or type of nucleotide bound there. The protein appears to have crystallised in a form which is not hydrolytically active.[27] This phenomenon is not unique to SecA, since other ATPases have been found to crystallise in a single form independent of the occupancy of the nucleotide binding site (for example GroEL).[29–31] Clearly, ATP driven energy transducing machines rely on large conformational changes at the NBF that drive the domain movements required for their function.[29,32,33] Unfortunately it appears as though some of the key conformations adopted by SecA through the reaction cycle are not represented by any of the structures.

Conditions that promote translocation of preprotein through vesicles containing SecYEG stimulate the ATPase activity of SecA.[34] A concomitant conformational change has been characterised by the formation of a protease-resistant 30 kDa fragment of SecA; in this respect, the non-hydrolysable analogue AMPPNP alleviates the need for the preprotein.[5,35] This state can also be promoted by SecYEG in detergent solution.[36] Studies based on kinetics and analytical ultracentrifugation have recognised a large conformational change, regulated by an allosteric magnesium binding site and lipids, that has a profound effect on the affinity for nucleotide and the rate of hydrolysis.[17]

The nature of the reaction and the observations recounted above mean that SecA and SecYEG must combine and cooperate to undergo conformational changes that drive protein locomotion. This transduction of energy constitutes a hitherto uncharacterised dynamic process communicating the nucleotide-binding cleft of SecA to the protein channel formed in the centre of SecY. Here we describe our efforts to identify and measure these movements. The major findings of this study rely on the incorporation of an extrinsic fluorescent probe, fluorescein, fixed near the entrance of the protein channel in SecYEG. The results shed light on the magnesium and nucleotide dependence of these events, and in this context the nature and stoichiometry of the interaction between the two partners.

Results

SecA undergoes a large conformational change upon binding to the cytosolic face of SecYEG

To probe for possible conformational changes induced by the interaction of SecA with SecYEG, limited proteolysis was performed on the individual partners and a complex of the two (Figure 1). SecA alone is relatively resistant to proteolysis by trypsin and largely remained intact in the conditions employed (Figure 1); whereas, SecY is rapidly cleaved, resulting in the appearance of a band between SecY and SecE, due to cleavage at residue R255 located in the cytosolic loop between trans-membrane helices (TM) 6 and 7.[3] The monoclonal antibody (10A4) stabilises SecYEG dimers and promotes the tight binding of SecA such that it can be isolated by gel-filtration chromatography.[22] When it was bound to the antibody SecYEG had the same proteolytic degradation profile (Figure 1). However, when SecA was also bound, SecY was protected and SecA became considerably more sensitive to degradation (Figure 1). These observations were independent of nucleotide (data not shown). Therefore, this association occludes the 6–7 cytoplasmic loop of SecY and SecA adopts a more open, proteolytically sensitive conformation.

SecA binds to the two large cytosolic loops of SecY and the amphipathic helix of SecE

In order to identify potential interaction sites of SecA and SecYEG, a synthetic peptide array based on the cytosolic regions of SecY and SecE was prepared and tested for SecA binding (Figure 2(a)

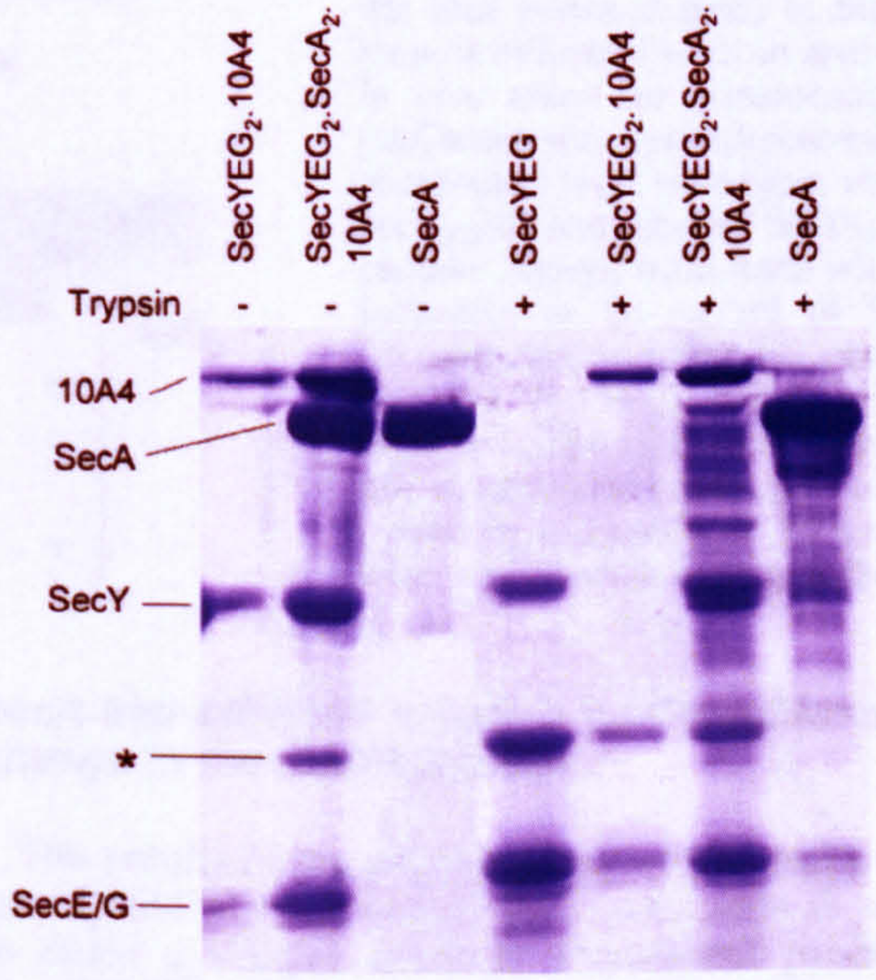

Figure 1. Limited proteolysis of SecA, SecYEG and SecA–SecYEG–antibody complexes. SecYEG, SecA, $SecYEG_2$.10A4 (two SecYEG bound to one monoclonal antibody 10A4) and $SecYEG_2.SecA_2$.10A4 (two SecYEG bound to two SecA and one monoclonal antibody 10A4) were subjected to proteolysis by trypsin as described in Materials and Methods. Proteins were subsequently separated by SDS–PAGE and visualised by Coomassie blue staining. Positions of the different polypeptides are indicated; the asterisk denotes the predominant proteolytic fragment of SecY, the result of cleavage at the 6–7 loop.[3]

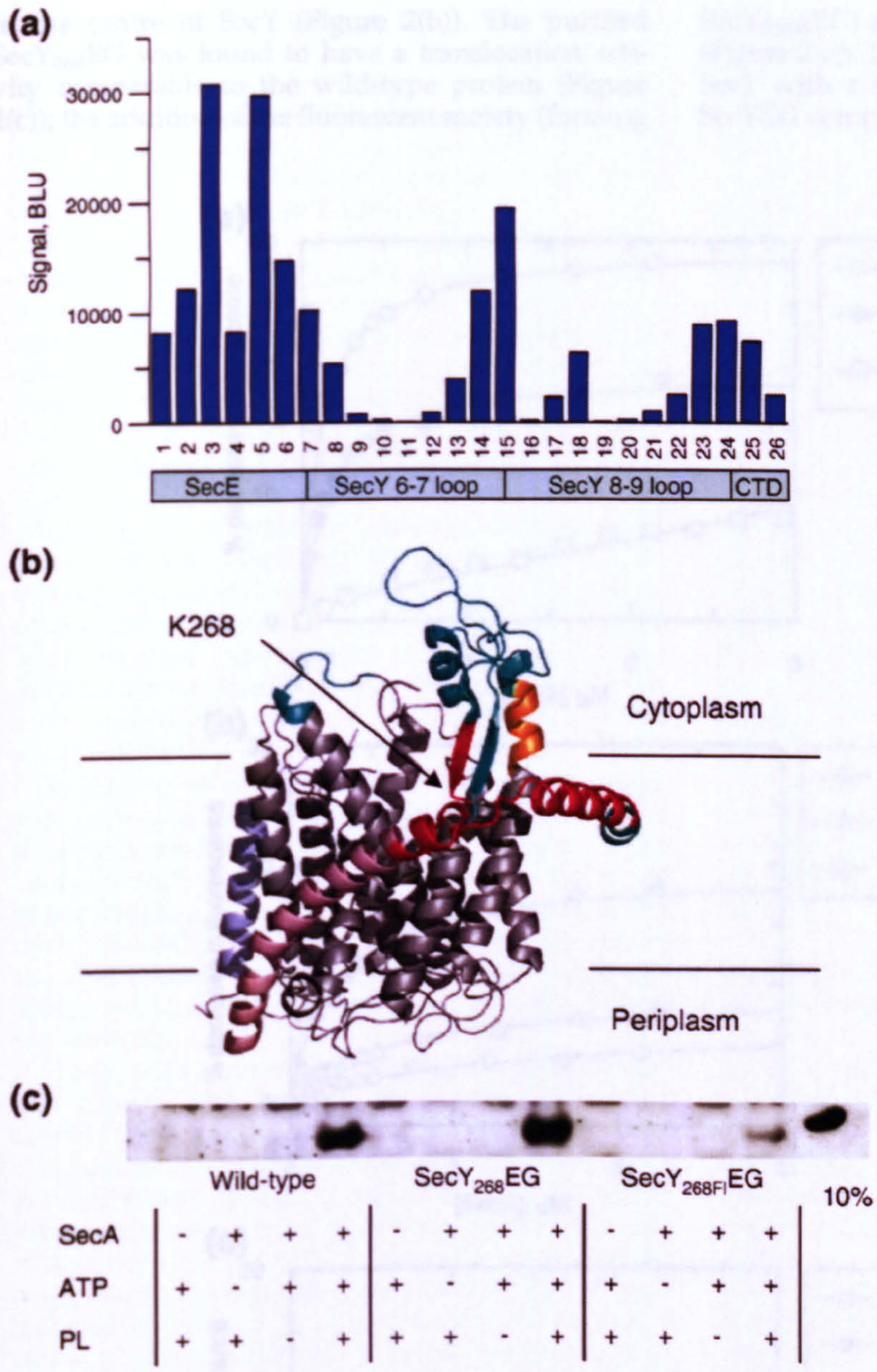

Figure 2. Binding analysis of SecA to a peptide array of the cytoplasmic regions of SecYEG. (a) Relative binding efficiencies of peptides in the array binding to SecA, expressed in Boehringer Light Units (BLU). Peptides were derived from the amphipathic helix of SecE, the two large cytoplasmic loops of SecY and the C-terminal domain (CTD) of SecY as shown. Peptide sequences are defined in Supplementary Data, Table 1. (b) Homology model of the structure of the *E. coli* SecYEG based on the *M. jannaschii* structure.[48] The regions identified with high and medium binding efficiency in (a) are shown in red and orange, respectively. Regions included in the peptide array, which did not bind SecA are in cyan and the rest of the complex, which was not assayed, is in grey (SecY), pink (SecE) and light blue (SecG). Residue K268, at the end of the first β-strand (red) in the 6–7 loop, is indicated with an arrow. (c) *In vitro* assay for translocation of proOmpA into proteoliposomes reconstituted with wild-type, mutant $SecY_{268}EG$ and labelled $SecY_{268Fl}EG$ protein. Assays were done with the inclusion of 20 μg/ml of SecA, 2.5 mM ATP and SecYEG proteoliposomes (PL; 34 μg/ml of SecYEG) as shown. The right-hand lane was not subjected to proteolysis and is loaded as a measure of 10% of the total proOmpA in each reaction.

and (b); Supplementary Data, Table 1). The highest affinity binding hotspots were measured to be one to three orders of magnitude over and above the background and were located on the 6–7 loop of SecY and the amphipathic helix of SecE (coloured red in Figure 2(b)). Significant but weaker binding was also found on the 8–9 loop at the N-terminal end of TM 9 of SecY (orange in Figure 2(b)).

Table 1. Binding parameters for SecA binding to $SecY_{268Fl}EG$ from the fitted curves of Figure 3

Conditions	K_d for SecA (μM)	B_{max} (% change)
AMPPNP + Mg^{2+}	0.108±0.0024	29.5±0.2
ATPγS + Mg^{2+}	0.153±0.0082	19.5±0.3
AMPPNP − Mg^{2+}	0.248±0.027	19.4±0.7

SecA and AMPPNP induce a conformational change in the SecYEG dimer

The results of the peptide array screen were used as a guide to engineer mutant constructs in order to place a unique extrinsic fluorescent probe on SecYEG. The fluorescence properties of fluorescein are very sensitive to its environment, and often act as a useful reporter of its immediate surroundings. Changes in its environment resulting as a consequence of structural rearrangement of the protein can therefore be potentially monitored optically. A lysine residue on SecY, K268, in the centre of the SecA binding hotspot (Figure 2(b)) was selected and mutated to cysteine, in an otherwise cysteine-less background (hereinafter referred to as $SecY_{268}EG$). This residue is reasonably well buried in the structure and sits at the edge of the protein channel

in the centre of SecY (Figure 2(b)). The purified $SecY_{268}EG$ was found to have a translocation activity comparable to the wild-type protein (Figure 2(c)); the addition of the fluorescent moiety (forming $SecY_{268Fl}EG$) retained but diminished this activity (Figure 2(c)). The protein was labelled specifically on SecY with a stoichiometry of one fluorescein per SecYEG complex (see Materials and Methods).

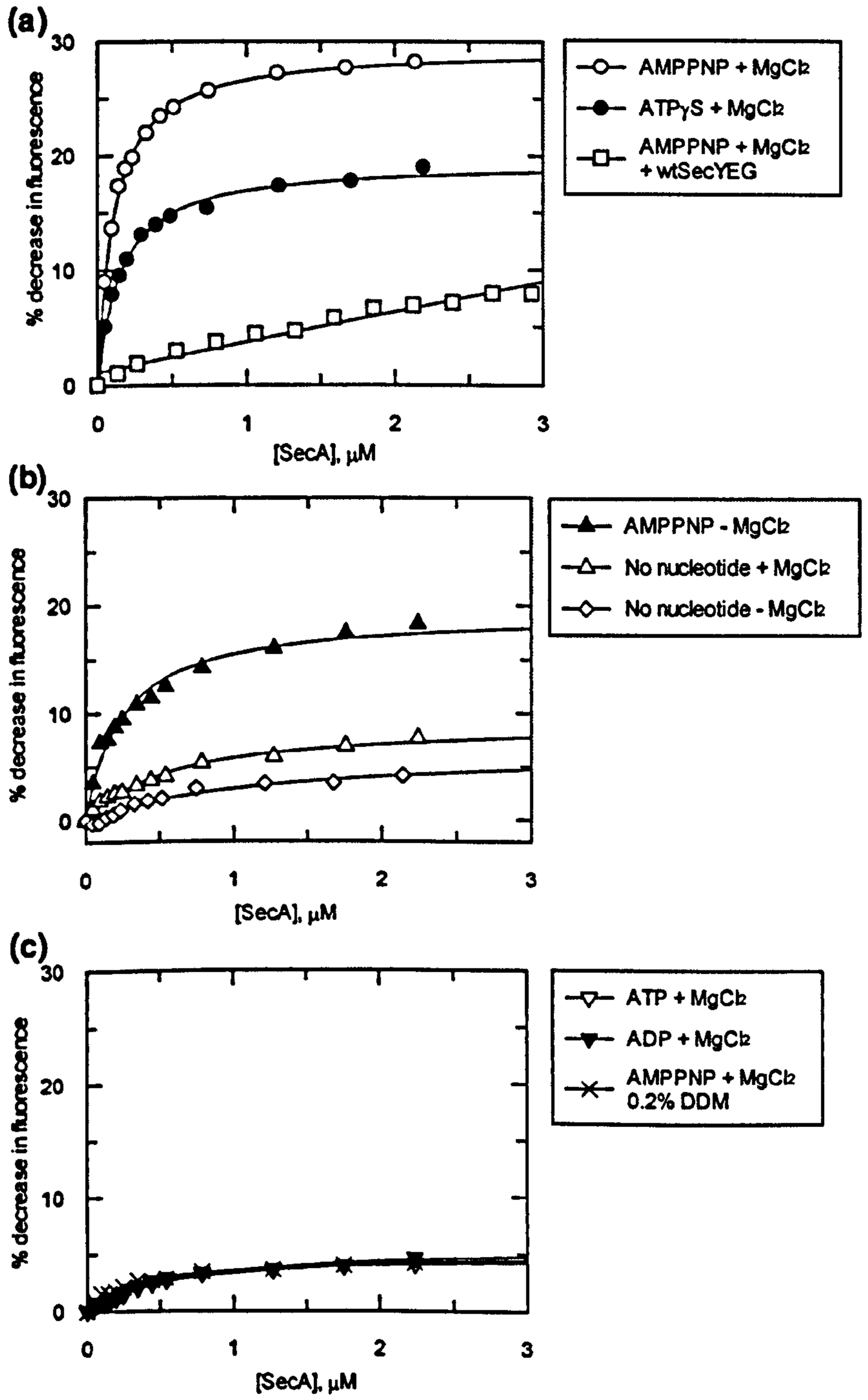

Figure 3. Binding of SecA to $SecY_{268Fl}EG$ causes nucleotide and magnesium-dependent reduction in fluorescence. (a) SecA was titrated into a solution containing 30 nM $SecY_{268Fl}EG$ in SecYEG buffer with 0.02% DDM. The quench in fluorescence was expressed as a percentage fluorescence change and plotted against the concentration of SecA. The titrations were performed in the presence of 2 mM $MgCl_2$ and 1 mM AMPPNP or ATPγS as shown. These were fitted to a one-site binding equation (see Materials and Methods) and the parameters are shown in Table 1. The titration with the inclusion of excess wild-type SecYEG (2 μM) could not be saturated and was fitted to a straight line. (b) SecA titrations were performed as in (a) except with the exclusion of nucleotides or $MgCl_2$, and fitted as described for (a). (c) SecA titrations were performed with the inclusion of different nucleotides and detergent concentrations and fitted as described in (a).

A large, rapid and saturable quenching of the fluorescence intensity from the detergent-solubilised $SecY_{268Fl}EG$ was observed upon addition of SecA in the presence of AMPPNP and magnesium (Figure 3); a signal indicative of an association that has propagated a conformational change to the inner face of the channel (see Discussion).

A titration of SecA into solutions containing low concentrations of $SecY_{268Fl}EG$ generated data that could be perfectly fitted to a one-site weak-binding equation (K_d=0.11 μM; Figure 3(a) and Table 1; see also Materials and Methods). A similar result was observed when ATPγS replaced AMPPNP, except that the total fluorescence change was slightly reduced (Figure 3(a) and Table 1). Crucially, the signal could be fully competed to a non-saturable background by the inclusion of a 60-fold molar excess of wild-type, unlabelled SecYEG, confirming that this binding was specific and that the labelled protein is equivalent to wild-type in this behaviour (Figure 3(a)). Similar experiments conducted with the SecYEG dimer stabilised with the monoclonal antibody (employed above)[22] generated exactly the same results (not shown).

To further test the specificity of this signal change the same probe has been incorporated onto a position known to be much further away from the SecA interaction site on the other side of the membrane ($SecY_{63Fl}EG$). As expected, this fluorescent derivative exhibited a reduced saturable quench in the fluorescence upon interaction with SecA (5% compared to around 30% with $SecY_{268Fl}EG$; results not shown).

Previous experiments conducted on SecA identified a second binding site for magnesium that is distinct from the ATP hydrolysis site. The removal of magnesium from this allosteric site promotes a large conformational change, a reduction in ATP binding affinity and an increase in ATPase activity.[17] When magnesium was omitted from the fluorescence experiments the total fluorescence intensity change induced by SecA in $SecY_{268Fl}EG$ and the apparent binding affinity were both reduced (Figure 3(b) and Table 1). When ATP, ADP or no nucleotide was included in the experiment (with or without added magnesium) the signal change was reduced close to the level of the background (Figure 3(b) and (c)). Increasing the *n*-dodecyl-β-D-maltoside (DDM) detergent concentration in the solution abolished the fluorescence change (Figure 3(c)). This effect is not simply due to the dissociation of the SecYEG complex into monomers under these conditions,[37] since a similar result was observed in the presence of a monoclonal antibody that stabilises SecYEG dimers[22] (results not shown).

The inhibitory potency of magnesium for SecA is alleviated by SecYEG

To further define the dependence of the conformational change on nucleotides, AMPPNP was titrated into a solution containing $SecY_{268Fl}EG$ pre-saturated with SecA, in the presence and absence of added magnesium (Figure 4(a)). As $SecY_{268Fl}EG$ elicits the signal, the results reflect the binding affinity of nucleotide to SecA when it is bound to SecYEG. The total fluorescence change was greater in the presence of magnesium, consistent with the experiments varying the SecA concentration (above). The affinity for nucleotides was higher in the presence of added magnesium (Table 2), a trend reflected by the affinity of the SecA dimer alone for ATP.[17] However, the magnitude of this effect is only sixfold when SecA is bound to SecYEG, compared to 160-fold for the enzyme alone, demonstrating that the presence of SecYEG significantly reduces the inhibitory potential magnesium has for SecA.

The affinity of SecYEG-bound SecA for magnesium binding to the allosteric site on SecA was similarly determined, with and without AMPPNP (Figure 4(b) and Table 3). Whilst the total fluorescence change was greater in the presence of AMPPNP, as expected, the apparent binding affinity ($K_{d(app)}$) was very similar in the presence or absence of AMPPNP. However, once an adjustment was applied for the effect of magnesium chelation by AMPPNP (K_d=34 μM, see also Materials and Methods),[38] the actual affinity of magnesium for SecYEG-SecA is about 35 times higher in the presence of AMPPNP (Table 3), compared to an increase of 160-fold in the K_M of SecA for ATP without SecYEG.[17]

The SecA mutations D209N and E210Q abolish the conformational coupling with SecYEG

Since AMPPNP, but not ATP, confers the ability of SecA to induce the fluorescence change in $SecY_{268Fl}EG$, mutants of SecA that can bind, but not hydrolyse ATP were investigated. $SecA_{D209N}$ and $SecA_{E210Q}$ have defective Walker B motifs in the NBF and are incapable of hydrolysis (data not shown). $SecA_{D209N}$ was found to bind to fluorescent *N*-methylanthraniloyl derivatives of both ATP and ADP with a K_d<1 μM, in the presence of 2 mM magnesium (data not shown). Neither $SecA_{E210Q}$ nor $SecA_{D209N}$ could induce the nucleotide-dependent conformational change in $SecY_{268Fl}EG$ (Figure 5).

The complex that undergoes the conformational change contains one SecA and a dimer of SecYEG

In order to measure the stoichiometry of the interaction that evokes this long-range conformational effect, SecA was titrated into solutions containing concentrations of $SecY_{268Fl}EG$ above the K_d value (Figure 6) and the data were fitted to a one-site tight-binding equation (Table 4; see Materials and Methods). Experiments employing two different concentrations of $SecY_{268Fl}EG$ determined the ratio of SecA binding to SecYEG to be 0.67 and 0.58. The accuracy of these values is dependent on the protein quantification, which was carried out by amino acid analysis, giving values for the extinction coefficient of SecA of 99,000 (±1980) $M^{-1}cm^{-1}$ and SecYEG of

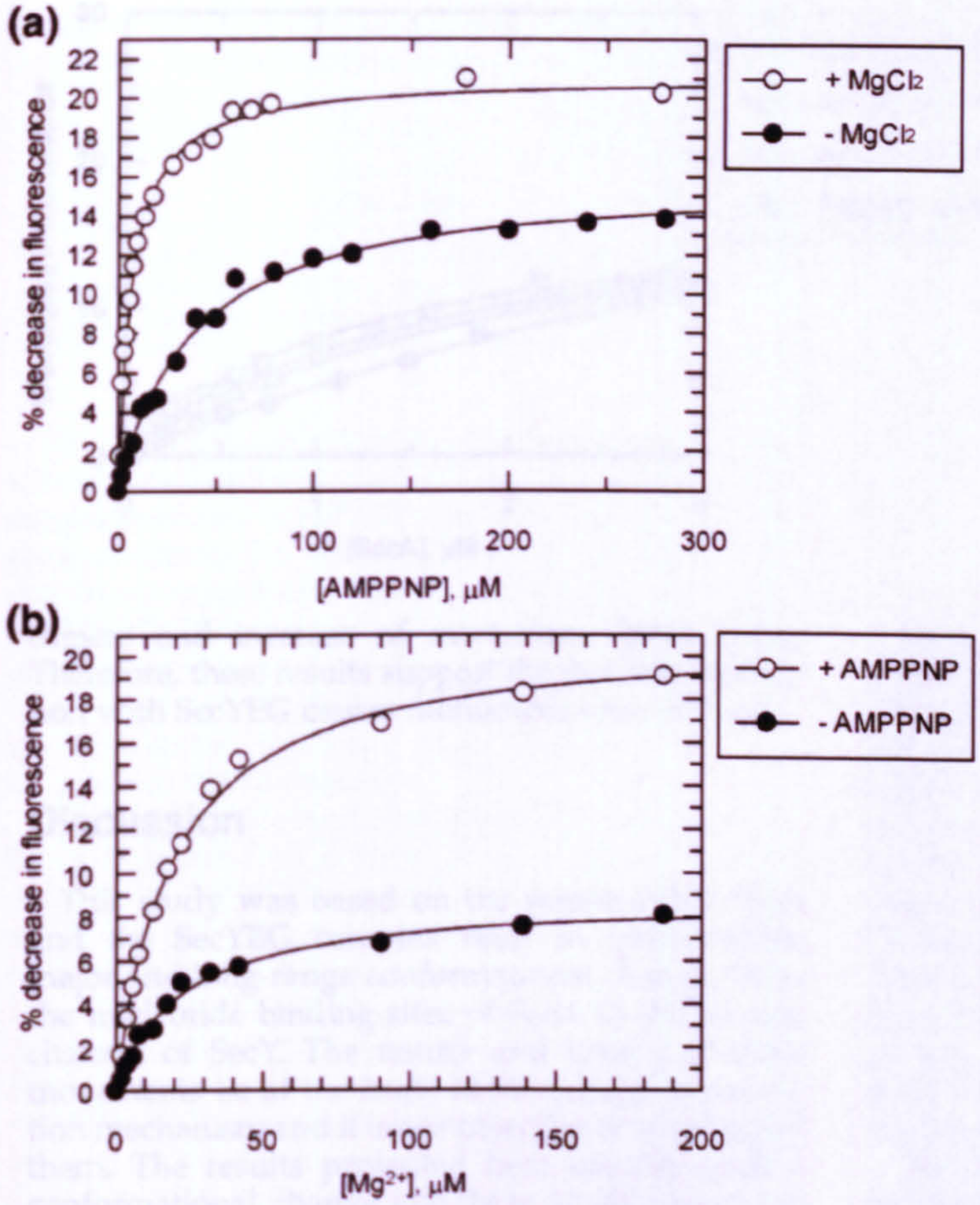

Figure 4. Affinity of SecYEG-bound SecA for AMPPNP and magnesium. (a) AMPPNP was titrated into a solution of 30 nM $SecY_{268Fl}EG$ and 3 μM SecA in SecYEG buffer containing 0.02% DDM, in the presence or absence of 2 mM $MgCl_2$. The percentage fluorescence decrease was plotted against the concentration of AMPPNP and fitted to a one-site binding equation (Materials and Methods). The fitted parameters are shown in Table 2. (b) $MgCl_2$ was titrated into a solution of SecA-saturated $SecY_{268Fl}EG$ under the conditions described for (a) in the presence or absence of AMPPNP. Data were fitted as described in the same way and the fitted parameters are shown in Table 3.

139,000 (±23,350) $M^{-1}cm^{-1}$. Therefore, these observations suggest that a complex of one SecA bound to a SecYEG dimer brings about this conformational change.

SecYEG promotes the monomerisation of SecA

Another experimental approach utilising photo-induced cross-linking of unmodified proteins (PICUP)[39] was used to investigate the stoichiometry of SecA and SecYEG (Figure 7). Wild-type SecYEG and SecA were cross-linked either individually or together, in the presence of magnesium and AMPPNP. The products of the reaction were visualised by SDS–PAGE (Figure 7) and the composition of the bands was confirmed by Western blotting with antibodies specific to SecY, SecE and SecG (not shown). Complexes containing YE, YG and YEG could be identified in experiments including only SecYEG (Figure 7, lanes 2–5). Analysis of SecA alone (lanes 6 and 13) after cross-linking revealed two bands with molecular mass substantially below 200 kDa and hence both monomers. One of them ran slightly higher than expected (labelled A*), presumably because of different intra-molecular cross-links. The corresponding dimer is also evident (A_2*). When SecA and SecYEG were cross-linked together, a series of new bands migrated above the SecA monomer and contained SecA together with different combinations of SecY, SecE and SecG (lanes 7–12). These complexes can only contain one copy of SecA, as they are smaller than the SecA dimer. Moreover, in these conditions there is a concomitant decrease in the relative quantities SecA dimer and an increase in the monomer (compare lanes 12 and 13). As the SecYEG sample is titrated into a fixed quantity of SecA, there is a simultaneous and proportional loss of SecA

Table 2. Binding parameters for AMPPNP binding to SecA–$SecY_{268Fl}EG$ from the fitted curves in Figure 4(a)

Conditions	K_d for AMPPNP (μM)	B_{max} for AMPPNP (%)
+ Mg^{2+}	6.81±0.33	21.1±0.2
− Mg^{2+}	38.4±2.7	16.1±0.4

Table 3. Binding parameters for magnesium binding to the allosteric site of SecA bound to $SecY_{268Fl}EG$ from the fitted curves in Figure 4(b)

Conditions	$K_{d(app)}$ for Mg^{2+} (μM)	K_d for Mg^{2+} (μM)	B_{max} for Mg^{2+} (%)
+ AMPPNP	18.8±0.92	0.618	21.0±0.3
− AMPPNP	22.2±1.9	22.2	8.81±0.26

The K_d value for magnesium was calculated from the $K_{d(app)}$, taking into account its chelation by AMPPNP, according to equation (3) (Materials and Methods).

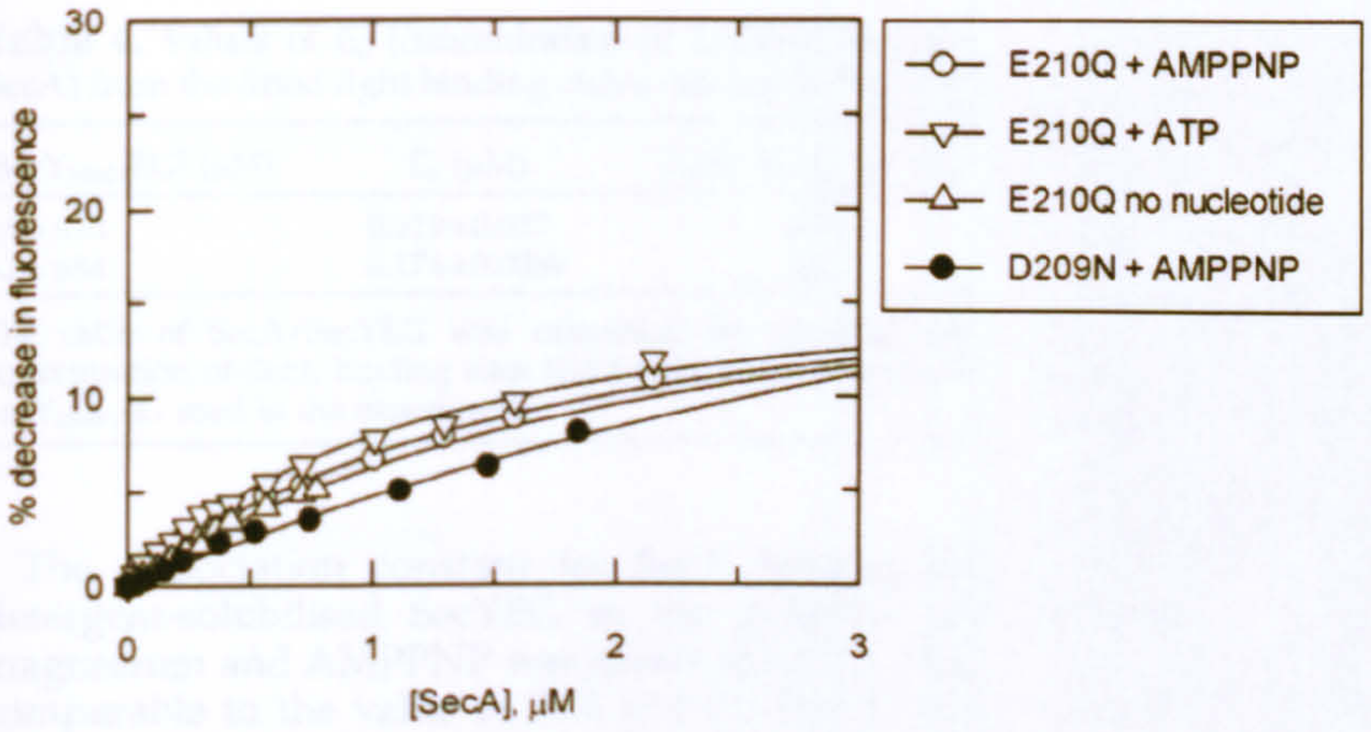

Figure 5. Binding of SecA mutants E210Q and D209N to $SecY_{268Fl}EG$ does not produce a nucleotide-dependent fluorescence change. SecA mutants were titrated into $SecY_{268Fl}EG$, in the presence of 2 mM $MgCl_2$, and the data fitted in the manner described for Figure 3.

dimers and increase of monomers (lanes 7–10). Therefore, these results support the fact that association with SecYEG causes monomerisation of SecA.

Discussion

This study was based on the premise that SecA and the SecYEG complex need to communicate major and long-range conformational changes from the nucleotide binding sites of SecA to the protein channel of SecY. The nature and timing of these movements lie at the heart of the energy transduction mechanism and it is our objective to understand them. The results presented here identify such a conformational change and help to illuminate the nature of the interplay between the two partners.

Previous studies have shown that SecA and SecYEG interact with one another, even in the absence of substrate, both in lipid vesicles[2] and in detergent solution.[8,22,36,40] Here we find that the consequences of this interaction include the nucleotide-independent formation of a protease-sensitive state of SecA consistent with the formation of an open-like form and the structural identification of a large conformational change, also nucleotide independent, that opens a deep putative polypeptide binding groove.[28] In addition, there is a concomitant protease-protection of the loop between TM6 and 7 of SecY.

Peptide array experiments were employed to refine this analysis and they recognised sites on SecYEG that interact with SecA. Interestingly, the hot spots identified in this study are all fairly well buried on the cytosolic face of SecYEG (Figure 2). A previous and similar screen identified another site on the cytosolic end of SecY TM4, also found in a deep cytosolic location.[41] One of the sites identified in our screen is located on the 6–7 loop of SecY, in the vestibule close to the opening of the translocation pore. Incorporation of an extrinsic fluorescent probe on this position (fluorescein; Figure 2) provided us with an extremely useful tool to probe the interaction and dynamics of the two partner proteins.

The fluorescence properties of fluorescein are particularly sensitive to changes in its local environment.[42] Therefore, in this position on SecYEG, as expected, it was very sensitive to perturbation by SecA. In contrast, an alternative position on the other side of the membrane was largely insensitive. The fluorescence change was only elicited in the presence of AMPPNP or ATPγS, even though a complex can be formed between SecY and SecA without nucleotides (see above).[8,22,40,43] This means that the change in fluorescence we observe is not merely a consequence of the initial encounter complex formation, but the result of an additional downstream conformational change dependent on ATP binding and relayed all the way from the NBF of SecA to the central region of SecY forming the protein channel.

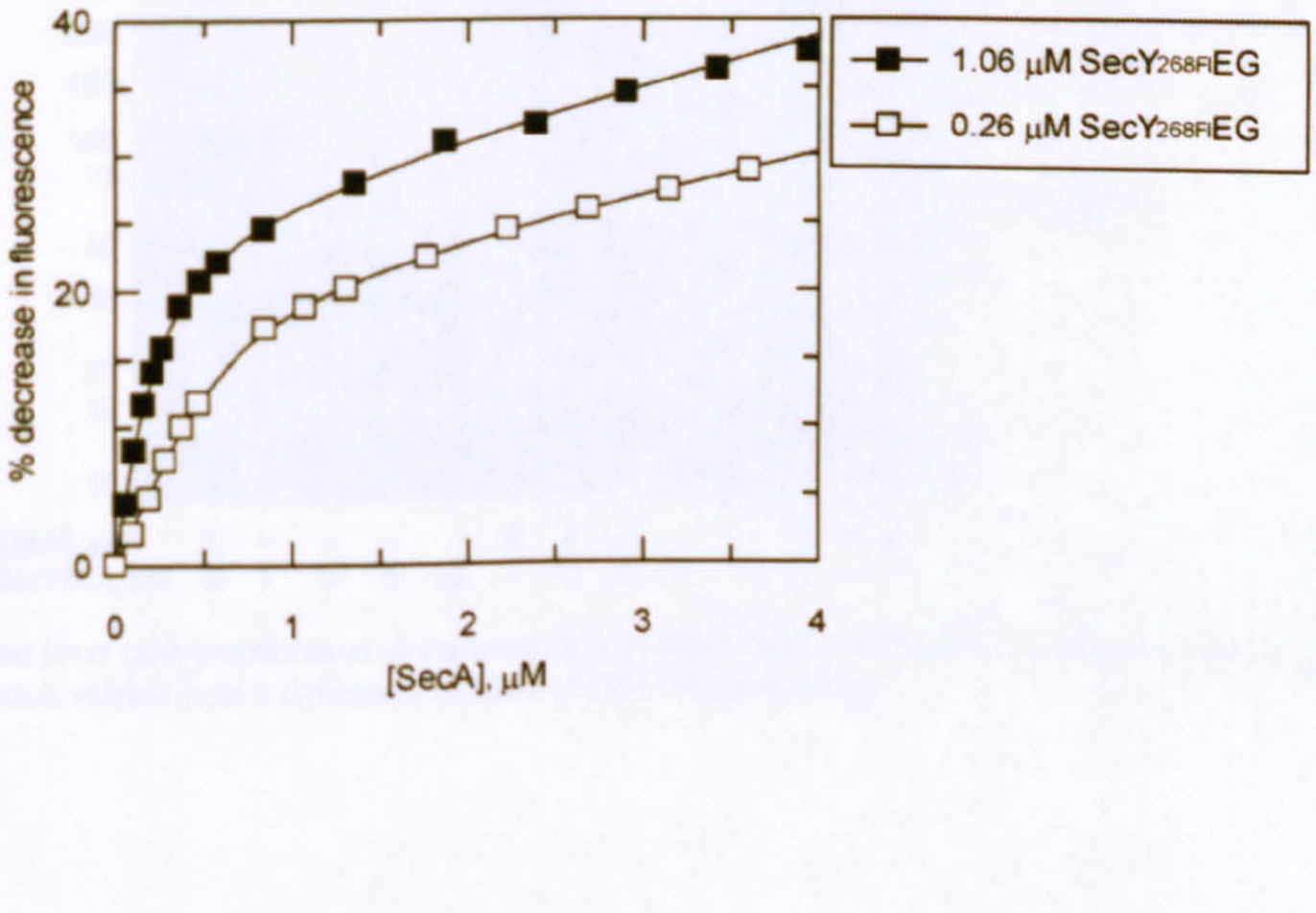

Figure 6. Stoichiometry of SecA–$SecY_{268Fl}EG$ complex responsible for the large change in fluorescence. SecA was titrated into a solution of $SecY_{268Fl}EG$ at concentrations of either 1.06 μM or 0.26 μM, in the presence of 1 mM AMPPNP and 2 mM $MgCl_2$. The data were fitted to a tight-binding equation with a linear increase due to a non-specific interaction (see Materials and Methods). The fitted parameters are shown in Table 4.

Table 4. Values of E_0 (concentration of binding sites for SecA) from the fitted tight binding curves shown in Figure 6

[$SecY_{268Fl}EG$] (μM)	E_0 (μM)	Ratio SecA/SecYEG
1.06 μM	0.619±0.027	0.58
0.26 μM	0.174±0.0089	0.67

The ratio of SecA/SecYEG was calculated by dividing the concentration of SecA binding sites (E_0) by the concentration of $SecY_{268Fl}EG$ used in the experiment.

The dissociation constant for SecA binding to detergent-solubilised SecYEG in the presence of magnesium and AMPPNP was found to be 0.1 μM, comparable to the value of 0.04 μM for *Escherichia coli* inner membrane vesicles containing enriched SecYEG.[2] This interaction was abolished in the presence of dimeric SecYEG and high concentrations of detergent, probably due to the depletion of bound phospholipids (V.A.M.G., A.R., M. Sun, A.R.C. & I.C., unpublished results).

The binding of magnesium to the allosteric site of SecA increases the affinity of SecA for ATP and reduces its hydrolysis rate,[17] but has only a minor effect on the induced rearrangement of SecYEG, measured by the fluorescence reporter in the channel. The signal reflecting this movement has also been used to measure the affinity of the SecYEG–SecA complex for the regulatory magnesium and for AMPPNP. The results have been compared with the affinity of the hydrolysing steady-state species of SecA for ATP and magnesium as measured by K_M (Figure 8).[17] At low magnesium concentrations, the affinity of SecA for AMPPNP is very similar to that for ATP (V.A.M.G. & I.C., unpublished results; Figure 8). The major differences resulting from the presence of SecYEG are the reduction of the affinity of SecA for allosteric magnesium in the presence of nucleotide (K_4) and the magnitude of the associated increase in ATP (AMPNP) affinity (K_2). Therefore, the loss of the inhibitory potency of magnesium in the presence of SecYEG helps to explain the loss of inhibition by magnesium experienced in conditions that promote protein translocation.[17]

The measurement of an optical signal change as one protein is titrated against the other is a worthwhile, but temperamental method to determine the stoichiometry of an association. Our experiments using carefully quantified protein samples obtained a result of one SecA to two SecYEG. To complement this tentative stoichiometry, cross-linking experiments were performed, showing that association with SecYEG and AMPPNP increases monomerisation propensity of SecA. These results are consistent with other recent reports stating SecYEG functions as a dimer,[8,9,11] and that SecA may monomerize on interaction with the SecYEG.[12,18,21] Our observations, taken together with work published elsewhere[8,9,12,18–22,28] strongly suggest that there is a key conformational change activating or priming the channel for translocation propagated by the binding of ATP to a complex formed by one SecA and two SecYEG.

The presentation of SecA with ATP does not elicit the fluorescent change in $SecY_{268Fl}EG$ because ATP hydrolysis is much faster than product (ADP) release[44,45] (A.R., V.A.M.G., S.R.W. Bellamy, A.R. & I.C., unpublished results). Therefore, the steady-state species during ATP turnover is a SecA:ADP complex, so the negative results mirror those we see for ADP. In an attempt to trap the SecA in an ATP-bound state, we made use of the mutants $SecA_{D209N}$ and $SecA_{E210Q}$. Both D209 and E210 are part of the DEAD-box sequence of the Walker B motif located in the NBF1 domain. The equivalent amino acids in *Bacillus subtilis* SecA, D207 and E208, form contacts with the catalytic magnesium and water molecules, respectively (Figure 9).[23] E210 provides the catalytic base for ATP hydrolysis[45] and removal of the negative charge abolishes this function, while retaining its ability to bind ATP. Surprisingly, the mutants uncouple the nucleotide-dependent conformational change in SecYEG. This shows that these residues in SecA are important for transmitting downstream nucleotide-dependent conformational information to the channel.

Interestingly, another study also identifies an activated form of SecA by the appearance of a 30 kDa

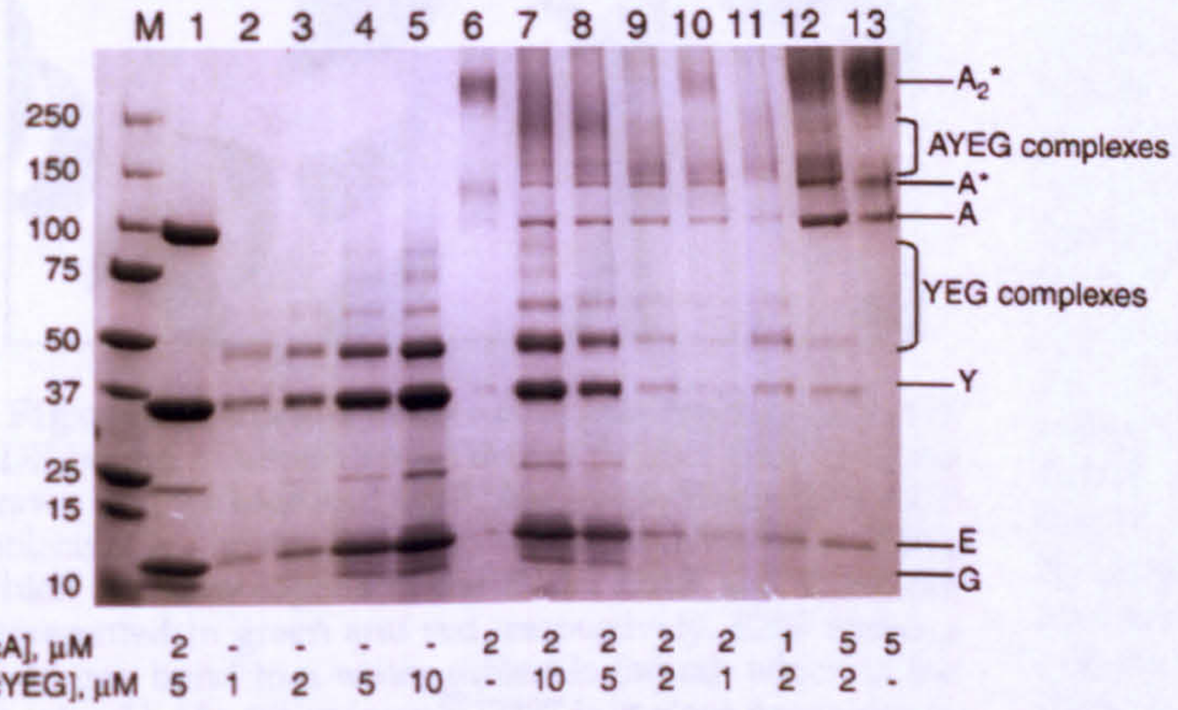

Figure 7. Cross-linking SecA to SecYEG with photo-induced cross-linking of unmodified proteins (PICUP). The proteins were mixed together at the concentrations indicated and cross-linked by addition of Tris-bipyridylruthenium(II) and ammonium persulphate and exposure to light (Materials and Methods). Proteins were subsequently separated by SDS–PAGE and visualised by Coomassie staining. Lane M shows molecular mass markers with the sizes in kDa indicated. Lane 1 is a control where no cross-linker was added. The position of the four polypeptides and various complexes were confirmed by Western blotting for SecY, E and G. A* is a monomer of SecA which has a different mobility after cross-linking.

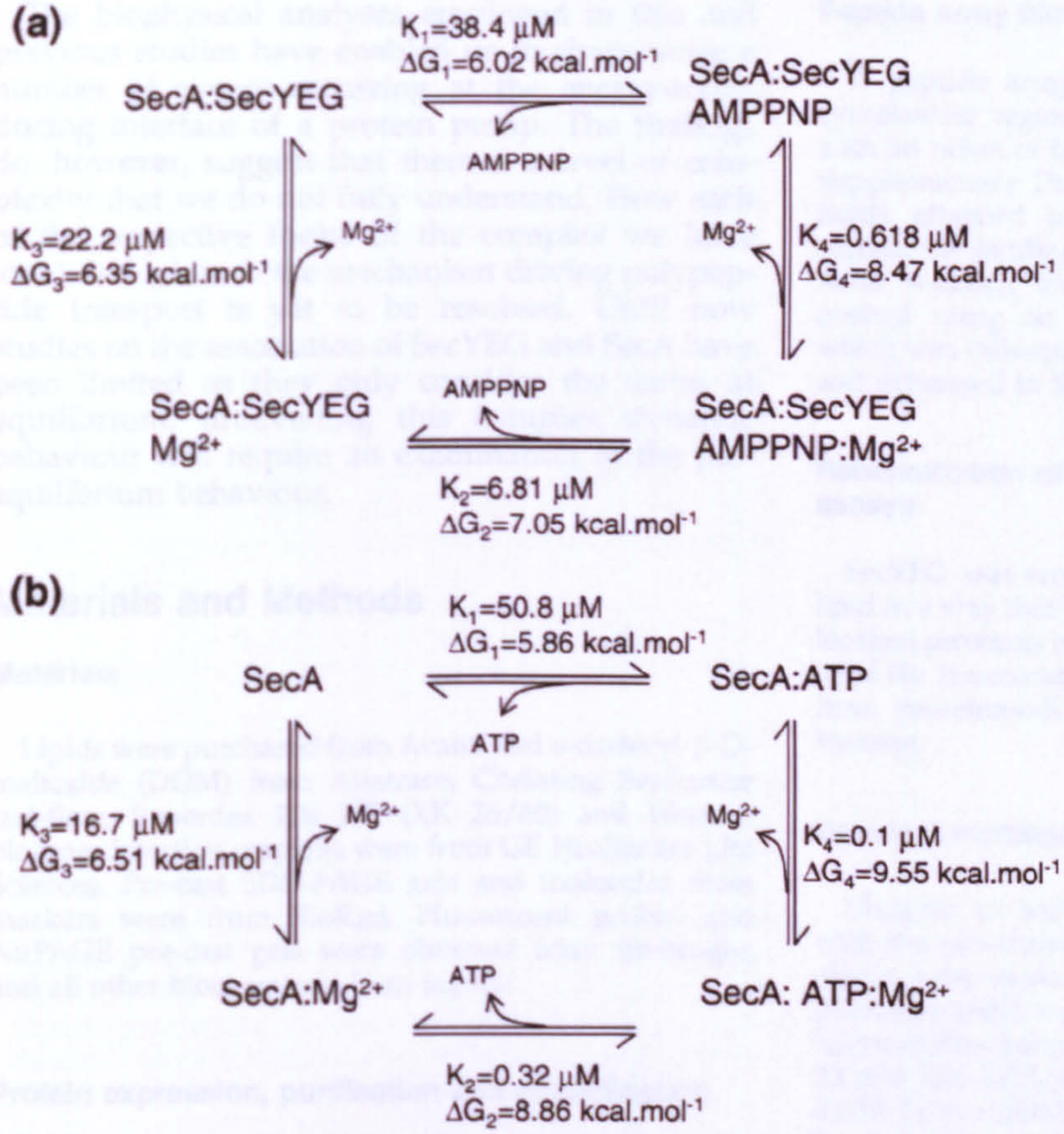

Figure 8. A thermodynamic cycle for binding of allosteric magnesium and AMPPNP to SecA alone and bound to SecYEG. (a) The affinities of the SecA–SecYEG complex for magnesium and AMPPNP are expressed as dissociation constants (K_d) and ΔG for the dissociation reaction from the data shown in Figure 4, Table 2 and Table 3. (b) Affinities for SecA alone, derived from K_M values from steady-state ATPase assays, as reported.[17]

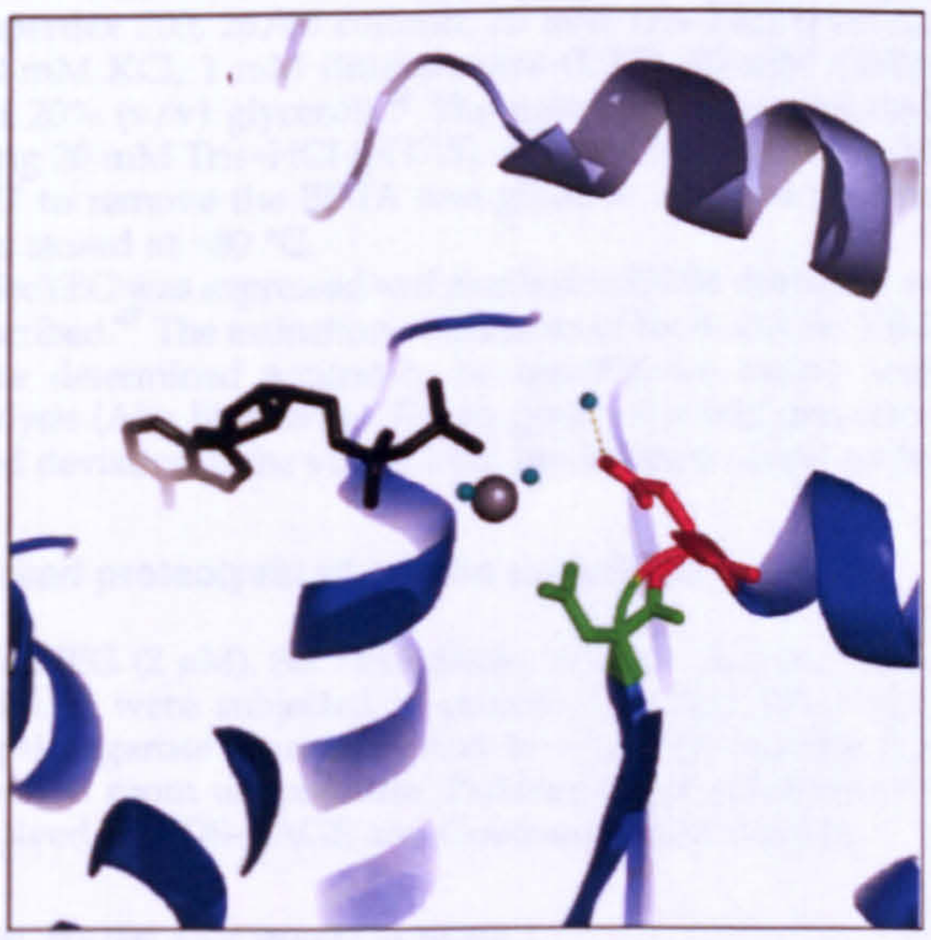

Figure 9. Structure of the nucleotide-binding pocket of ADP-bound *B. subtilis* SecA (1M74).[23] NBF1 and NBF2 are drawn in dark blue and light blue, respectively. The ADP molecule is shown in black. Residues D207 and E208, which are homologous of the *E. coli* D209 and E210, are represented in green and red, respectively. E208 forms a hydrogen bond to a water molecule (aqua), which is the proposed hydrolytic water.[23] D207 is in close proximity to the catalytic magnesium (grey sphere) coordinated by two water molecules (aqua).

proteinase-protected fragment, promoted by membrane-bound SecYEG, pro-OmpA and ATP; AMPPNP alleviates the need for substrate.[5,35] In this and our case, the maintenance of the ATP bound state (by AMPPNP) may account for the detection of a pseudo-active conformation, in the absence of substrate that would otherwise be short-lived. However, the states that generate the fluorescent change and the 30 kDa protected fragment appear to be different on account that only the latter can be promoted by $SecA_{D209N}$.[35]

Another apparently distinct complex, containing two SecYEG, two SecA, AMPPNP and a stabilising monoclonal antibody, has been detected by gel filtration, analytical ultracentrifugation and native PAGE. In the absence of AMPPNP only one SecA associates.[22] The methodologies employed here only have the capacity to measure very stable and tight binding interactions, made possible by the antibody.[22] Our fluorescent analysis has enabled the characterisation of weaker binding events that do not depend on the antibody. The results of the different studies are not incompatible, but each of them identifies components that would be undetected in the other. It may also be that the antibody has stabilised a complex that is otherwise short-lived and normally invisible to experiments conducted at equilibrium. The fact that there appear to be several different forms and stoichiometries of the associated channel and motor domain is not particularly surprising given the complexity of the reaction.

The biophysical analyses employed in this and previous studies have enabled us to characterise a number of events occurring at the energy-transducing interface of a protein pump. The findings do, however, suggest that there is a level of complexity that we do not fully understand. How each of the respective forms of the complex we have identified relate to the mechanism driving polypeptide transport is yet to be resolved. Until now studies on the association of SecYEG and SecA have been limited as they only consider the states at equilibrium; unravelling this complex dynamic behaviour will require an examination of the pre-equilibrium behaviour.

Materials and Methods

Materials

Lipids were purchased from Avanti and *n*-dodecyl-β-D-maltoside (DDM) from Anatrace. Chelating Sepharose fast-flow, Superdex 200 HR (XK 26/60) and Western blotting detection reagents were from GE Healthcare Life Sciences. Pre-cast SDS–PAGE gels and molecular mass markers were from BioRad. Fluorescent probes and NuPAGE pre-cast gels were obtained from Invitrogen and all other biochemicals from Sigma.

Protein expression, purification and quantification

SecA was expressed and purified in a manner described.[17] An extra purification step was added to remove bound nucleotides and magnesium by gel filtration (Superdex 200, 26/60 column; 20 mM Tris–HCl (pH7.5), 100 mM KCl, 1 mM dithiothreitol (DTT), 50 mM EDTA and 20% (v/v) glycerol).[46] The procedure was repeated using 20 mM Tris–HCl (pH7.5), 100 mM KCl and 0.2 mM DTT to remove the EDTA and glycerol. Purified protein was stored at −80 °C.

SecYEG was expressed and purified in DDM detergent as described.[47] The extinction coefficients of SecA and SecYEG were determined accurately by quantitative amino acid analysis (Alta Bioscience). Errors given represent one standard deviation of the values from the different amino acids.

Limited proteolysis of protein complexes

SecYEG (2 μM), $SecYEG_2.SecA_2.10A4$ (5 μM) and SecA (2.5 μM) were subjected to proteolysis using 20 μl of a trypsin-agarose slurry (Sigma) in a 100 μl reaction for 1 min at room temperature. Products were subsequently resolved by SDS–PAGE and Coomassie blue staining.

SDS–PAGE and Western blots

SDS–PAGE was performed using Ready gels or NuPAGE precast gels according to the manufacturer's protocols. Gels were either stained by Coomassie blue staining or subjected to Western blot after transferring onto nitrocellulose membranes. Monoclonal antibodies against SecY, SecE and SecG were made by Cocalico Biologicals, Inc. (PA, USA). Horseradish peroxidase (HRP)-linked secondary antibodies were subsequently visualised using Western blotting detection reagents.

Peptide array binding assays

A peptide array was made up of sequences of the cytoplasmic regions of SecYEG using 15mer peptides, with an offset of five amino acids between peptides (see Supplementary Data, Table 1). The peptides were covalently attached to cellulose membranes, which were probed for binding to SecA using 20 μg/ml of protein. After washing the membranes, the bound SecA was probed using an HRP-linked hexa-histidine antibody, which was subsequently visualised by chemiluminescence and expressed in Boehringer Light Units (BLU).

Reconstitution of SecYEG and *in vitro* translocation assays

SecYEG was reconstituted into vesicles of *E. coli* polar lipid in a way that has been described.[47] The *in vitro* translocation protocols have been documented elsewhere.[12] Successfully translocated proOmpA substrate was protected from proteinase-K digestion and detected by Western blotting.

Covalent modification of SecYEG with fluorescein

Mutants of SecYEG, $SecY_{K268C}EG$ and $SecY_{M63FI}EG$, with the two native cysteine residues in SecY mutated to serine, were made and purified as described above. The purified protein was incubated for 1 h on ice with a five-fold molar excess of 5-iodoacetamidofluorescein (5-IAF) in 20 mM Tris–HCl (pH 8), 130 mM NaCl, 10% glycerol and 0.02% (w/v) DDM (SecYEG buffer). The labelled protein was separated from excess label by gel filtration (Superose 6) eluted in the same buffer. SDS–PAGE analysis showed that only the SecY band was fluorescent (not shown). The efficiency of labelling was calculated by absorbance spectroscopy: the extinction coefficient of 5-IAF (78,000 $M^{-1}cm^{-1}$) following thiol-derivatisation (after complete reaction with DTT) was determined to be 71,023 $M^{-1}cm^{-1}$. A spectrum of the labelled protein showed the ratio of fluorophore to SecYEG to be 1.1:1.

Fluorescence spectroscopy

Fluorescence was measured with a Jobin Yvon (Horiba) Fluorolog, exciting at 498 nm and collecting emission at 515 nm. Excitation and emission band pass widths were 3 nm and the photomultiplier tube was set to 950 V. Assays were performed in a 1 ml cuvette with a stirrer bar, in SecYEG buffer unless otherwise indicated. The fluorescence emission was monitored over time and the signal was allowed to equilibrate after each addition for 150 s.

Cross-linking using PICUP

SecA and SecYEG were cross-linked either individually or together using the PICUP method.[39] The proteins were mixed together in a total volume of 10 μl in SecYEG buffer in the presence of 1 mM AMPPNP and 2 mM $MgCl_2$. In a dimly lit laboratory, 2 mM ammonium persulphate and 0.1 mM Tris-bipyridylruthenium(II) were added to the mixture and the proteins were cross-linked by irradiation for 2 s with a 250 W slide projector lamp at a distance of 20 cm. The reaction was quenched by addition of 100 mM DTT and the samples were analysed by SDS–PAGE, visualising the proteins by Coomassie staining.

Data analysis

Data were analysed using Grafit (Erithacus) software. Titrations conducted in conditions of weak binding (where the concentration of $SecY_{268Fl}EG$ was 30 nM and therefore significantly below the K_d) were fitted to a one-site weak binding equation according to equation (1):

$$B = \frac{B_{max}.L}{K_d + L} \quad (1)$$

where L is the total concentration of ligand (SecA) and B is the signal change. B_{max} is the maximum signal change and K_d is the dissociation constant. Titrations conducted in tight binding conditions (where the concentration of $SecY_{268Fl}EG$ was greater than the K_d) were fitted to a tight-binding equation with a linear increase according to equation (2):

$$B = B_{max}.\frac{L + E_0 + K_d - \sqrt{(L + E + K_d)^2 - 4E.L}}{2.E_0} + m.L \quad (2)$$

where E_0 is the concentration of binding sites for SecA and m is a linear gradient (a result of a non-saturable background component). To obtain more accurate values of E_0 the K_d was fixed at 0.11 μM (Table 1).

To calculate the K_d for magnesium in the presence of AMPPNP, the effect of chelation of the ion by the nucleotide was taken into account using the dissociation constant for magnesium binding to AMPPNP ($K_{d[AMPPNP]}$) of 34 μM.[38] The effect of this chelation on the free concentration of magnesium is defined by:

$$[M] = [M_0]\left(1 - \frac{[A_0]}{[A_0] + K_{d[AMPPNP]}}\right) = \frac{[M_0]}{1 + \frac{[A_0]}{K_{d[AMPPNP]}}}$$

where $[M]$ is the free concentration of magnesium, $[M_0]$ is the total concentration of magnesium and $[A_0]$ is the total concentration of AMPPNP.[17] The K_d for magnesium binding to SecA in this context can therefore be calculated from the apparent dissociation constant ($K_{d(app)}$) using equation (3):

$$K_d = \frac{K_{d(app)}}{1 + \frac{[A_0]}{K_{d[AMPPNP]}}} \quad (3)$$

Values of Gibbs free energy, ΔG, were calculated from dissociation constants according to equation (4):

$$\Delta G = -RT\ln K_d \quad (4)$$

Acknowledgements

I.C. and A.R. are supported from a grant awarded by the Biotechnology and Biological Sciences Research Council (BBSRC), UK (BB/C503538/1). V.A.M.G. is supported by a BBSRC studentship.

Supplementary Data

Supplementary data associated with this article can be found, in the online version, at doi:10.1016/j.jmb.2007.09.086

References

1. Robson, A. & Collinson, I. (2006). The structure of the Sec complex and the problem of protein translocation. *EMBO Rep.* **7**, 1099–1103.
2. Hartl, F., Lecker, S., Schiebel, E., Hendrick, J. & Wickner, W. (1990). The binding cascade of SecB to SecA to SecY/E mediates preprotein targeting to the E. coli plasma membrane. *Cell*, **63**, 269–279.
3. Brundage, L., Hendrick, J. P., Schiebel, E., Driessen, A. J. M. & Wickner, W. (1990). The purified *E. coli* integral membrane protein SecY/E is sufficient for reconstitution of SecA-dependent precursor protein translocation. *Cell*, **62**, 649–657.
4. Lill, R., Cunningham, K., Brundage, L., Ito, K., Oliver, D. & Wickner, W. (1989). SecA protein hydrolyzes ATP and is an essential component of the protein translocation ATPase of *Escherichia coli*. *EMBO J.* **8**, 961–966.
5. Economou, A. & Wickner, W. (1994). SecA promotes preprotein translocation by undergoing ATP-driven cycles of membrane insertion and deinsertion. *Cell*, **78**, 835–843.
6. Schiebel, E., Driessen, A., Hartl, F. & Wickner, W. (1991). Delta mu H+ and ATP function at different steps of the catalytic cycle of preprotein translocase. *Cell*, **64**, 927–939.
7. van den Berg, L., Clemons, W. M. J., Collinson, I., Modis, Y., Hartmann, E., Harrison, S. C. & Rapoport, T. A. (2004). X-ray structure of a protein-conducting channel. *Nature*, **427**, 36–44.
8. Duong, F. (2003). Binding, activation and dissociation of the dimeric SecA ATPase at the dimeric SecYEG translocase. *EMBO J.* **22**, 4375–4384.
9. Breyton, C., Haase, W., Rapoport, T. A., Kühlbrandt, W. & Collinson, I. (2002). Three-dimensional structure of the bacterial protein-translocation complex SecYEG. *Nature*, **418**, 662–665.
10. Veenendaal, A., van der Does, C. & Driessen, A. (2001). Mapping the sites of interaction between SecY and SecE by cysteine scanning mutagenesis. *J. Biol. Chem.* **276**, 32559–32566.
11. Mitra, K., Schaffitzel, C., Shaikh, T., Tama, F., Jenni, S., Brooks, C. L., 3rd *et al.* (2005). Structure of the *E. coli* protein-conducting channel bound to a translating ribosome. *Nature*, **438**, 318–324.
12. Osborne, A. R. & Rapoport, T. A. (2007). Protein translocation is mediated by oligomers of the SecY complex with one SecY copy forming the channel. *Cell*, **129**, 97–110.
13. de Keyzer, J., van der Sluis, E. O., Spelbrink, R. E., Nijstad, N., de Kruijff, B., Nouwen, N. *et al.* (2005). Covalently dimerized SecA is functional in protein translocation. *J. Biol. Chem.* **280**, 35255–35260.
14. Jilaveanu, L. B. & Oliver, D. (2006). SecA dimer cross-linked at its subunit interface is functional for protein translocation. *J. Bacteriol.* **188**, 335–338.
15. Ding, H., Hunt, J. F., Mukerji, I. & Oliver, D. (2003). *Bacillus subtilis* SecA ATPase exists as an antiparallel dimer in solution. *Biochemistry*, **42**, 8729–8738.
16. Woodbury, R. L., Hardy, S. J. S. & Randall, L. L. (2002). Complex behavior in solution of homodimeric SecA. *Protein Sci.* **11**, 875–882.
17. Gold, V. A. M., Robson, A., Clarke, A. R. & Collinson, I. (2007). Allosteric regulation of SecA: Magnesium-mediated control of conformation and activity. *J. Biol. Chem.* **282**, 17424–17432.
18. Or, E., Navon, A. & Rapoport, T. A. (2002). Dissociation of the dimeric SecA ATPase during protein